CRUISE REPORTS

RV LIVONIA Cruise 92, Kiel-Kiel, 21.8.-17.9.1992
GLORIA Studies of the East Greenland Continental Margin between 70° and 80°N

RV POSEIDON PO200/10, Lisbon-Brest-Bremerhaven, 7.-23.8.1993
European North Atlantic Margin: Sediment Pathways, Processes and Fluxes

RV AKADEMIK ALEKSANDR KARPINSKIY, Kiel-Tromsø, 5.-25.7.1994
Gas Hydrates on the Northern European Continental Margin

Edited by Jürgen Mienert

GEOMAR
Forschungszentrum
für marine Geowissenschaften
der Christian-Albrechts-Universität
zu Kiel

Kiel 1994

GEOMAR REPORT 30

GEOMAR
Research Center
for Marine Geosciences
Christian Albrechts University
in Kiel

Redaktion der Serie: Gerhard Haass
Umschlag: Kerstin Kreis, Harald Gross, GEOMAR Technologie GmbH

Managing Editor: Gerhard Haass
Cover: Kerstin Kreis, Harald Gross, GEOMAR Technologie GmbH

GEOMAR REPORT
ISSN 0936 - 5788

GEOMAR REPORT
ISSN 0936 - 5788

GEOMAR
Forschungszentrum
für marine Geowissenschaften
D-24148 Kiel
Wischhofstr. 1-3
Telefon (0431) 7202-0
Telefax (0431) 72 53 91, 7 20 22 93, 72 56 50

GEOMAR
Research Center
for Marine Geosciences
D-24148 Kiel / Germany
Wischhofstr. 1-3
Telephone (49) 431 / 7202-0
Telefax (49) 431 / 72 53 91, 7 20 22 93, 72 56 50

Contents

GLORIA STUDIES OF THE EAST GREENLAND CONTINENTAL MARGIN BETWEEN 70° AND 80° NORTH

Kiel-Kiel

21 August -17 September 1992

IOS

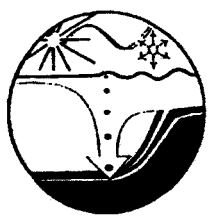

SFB 313

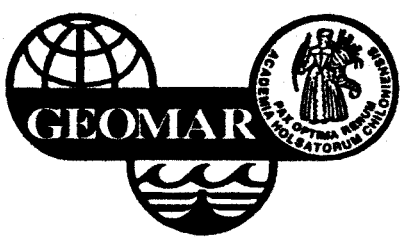

Jürgen Mienert [1,2]
and shipboard scientific party

[1] GEOMAR, Forschungszentrum für marine Geowissenschaften der Christian-Albrechts-Universität zu Kiel, Wischhofstr. 1-3, 24148 Kiel, F.R.G.

[2] Sonderforschungsbereich 313 (SFB 313) der Christian-Albrechts-Universität zu Kiel, Olshausenstr. 40-60, 24108 Kiel, F.R.G.

IOS, Institute of Oceanographic Sciences, Brook Road, Wormley, Godalming, Surrey, GU8 5UB, U.K.

RV LIVONIA CRUISE 92, KIEL-KIEL, 21 August - 17 September 1992

GLORIA STUDIES OF THE EAST GREENLAND CONTINENTAL MARGIN BETWEEN 70° AND 80° NORTH

Table of Contents

1. Abstract

GLORIA, the I.O.S. (Institute of Ocean Sciences) long range side-scan sonar, has been used in 1992 on a RV Livonia cruise to map large-scale changes in sedimentary patterns along the East Greenland continental margin. The working area (Figure 1) is permanently hindered by sea ice apart from the period from August to September when sea ice starts to melt and retreats from the Greenland basin to the shelf edge. During this period GLORIA made its first survey to the polar regions of the East Greenland margin and reached its most northern working area at the ice edge of the Arctic Ocean at 79° N.

The overall objective of this cruise was to determine the variety of large-scale sea floor processes in order to improve our understanding of the interaction between ice sheets, current regimes and sedimentary processes along polar margins. Along the East Greenland continental margin southward flowing currents such as the East Greenland current (EGC) and the Arctic Intermediate Waters (AIW) are carrying cold water masses from the Arctic Ocean through the Fram Strait and Denmark Strait into the North Atlantic. While these currents may cause a vigorous along-slope transport of sediments the calving of glaciers from the East Greenland ice sheet and melt water may entrain large amounts of sediments and transport them across the shelf and finally to the deep-sea basin by gravity flows.

In the co-operation with the Institute of Oceanographic Sciences, Wormley (U.K.) a 28 day cruise produced a high quality of sea floor data.

2. Introduction

The RV LIVONIA left the GEOMAR pier in Kiel at 07:00 am on 21 August 1992 and returned to Kiel on 17 September 1992 after a 12 000 km (6400 nm) long cruise. The major part of the cruise was carried out in the Greenland Basin and close to the Greenland shelf and north of 78° N, where sea ice conditions allowed. During this part of the cruise five 1000 km long and 50 km wide track lines and four 500 km long track lines produced an impressive side-scan sonar coverage of the complete Greenland Basin and margin to a total area of about 250,000 km^2.

Since one of the key locations of our survey is in areas where cold water cascades possibly occur on the margin, we anticipated that this research project would add crucial information to the debate about the role of cold water cascades in the downslope transport of sediments. In this context one of our interests is to determine and to understand to what extent the present East Greenland margin provides a realistic analog for a glaciated European margin during the last

glacial. Moreover, we intended to find out what differences, if any, can be detected between the present "warm house coast" of Norway versus the "ice house coast" of East Greenland. The scientific efforts will allow comparisons with other studies, for example the southern East Greenland margin (Andrews et al., 1989; Mienert et al., 1992) and the European PONAM (Polar North Atlantic Margins) project. Finally, it will contribute to the specific site selection for the scheduled Ocean Drilling Program Leg 151 in 1993.

3. Research area

The research area (Figures 1 and 2) encompassed from north to south, the Fram Strait, the Boreas Basin, the Greenland Basin and a small basin just north of the Jan Mayen fracture zone. The overall basin development is determined by the large fracture zones. In the Greenland Basin one large isolated seamount, which is barely covered by sediments and therefore appears to be young in age, is called Vesteris Bank. The survey was undertaken in such a way that all the major morphological changes in the area from north (Hovgaard fracture zone) to south (Jan Mayen fracture zone) were studied. In the east we started close to the Mid Ocean Ridge and in the west the sea ice created a natural limit to our survey. Also in some places close to the sea ice edge the GLORIA sonographs became distorted. This is caused by the meltwater inflow that influences the water stratification which in turn causes refraction of the acoustic beam pattern. These changes in the acoustic pattern of the water column made it difficult or impossible to identify the sea floor. Thus close to the ice boundary the records became less reliable for a sound geological interpretation. Three areas in particular were very close to the ice edge, i.e. within a few hundred meters, as can also be seen in the temperature records (Figure 3). The GLORIA sonographs from these sites will need to be interpreted with caution.

A total of 6602 km of GLORIA sonograph lines were obtained (Table 1). Details of the various patterns will be published in international journals.

4. Sea floor features along the East Greenland margin: preliminary sonograph interpretations (J. Mienert, N. Kenyon and F.-J. Hollender)

The primary purpose of this data discussion is to provide a preliminary overview of the sonograph interpretations of an area covering most of the East Greenland margin. This interpretation has two components: first we present field observations and based on this we attempt to deduce the sedimentary processes shaping the margin and basins.

Two copies of a mosaic of the GLORIA data were made at a scale of 1:375,000 and one copy was made at a scale of 1:250,000. The base maps were prepared by hand with a Polar Stereographic Projection having a standard parallel of 71 degrees. This is an equal area projection that proved to be well suited to lay down the sonographs and has the additional advantage of being identical to the projection of the bathymetric map. The sonograph recording paper was found to fade readily on exposure to light thus the mosaics had to be kept covered.

Oceanic basement transform ridges

In general, the East Greenland Basin structure is linked to major fracture zones and ridges (Vogt, 1986). The transform ridges divide the area between Fram Strait and Jan Mayen into three basins. These are from north to south: the small NW-SE oriented 3200 m deep Boreas Basin, the large NE-SW aligned 3600 m deep East Greenland Basin, and the small E-W oriented 2400 m deep basin just north of Jan Mayen. On the ridges there are flat sedimented tops in part of the ridge to the north of the Jan Mayen fracture zone and in part of the Hovgaard Fracture Zone Ridge. These plateaus are at respective depths of about 500 to 1000 m and 1400 m. It is presumed that the plateaus were planed off near sea level. Such a scenario could be explained by either a continuous subsidence from the mid-ocean ridge to the basin or tectonic movements which caused the ridges to uplift close to the sea surface followed by a subsidence. The steep sides of the ridges are gullied and the gullies are to be seen especially well around these submarine plateaus. They are almost parallel and north-south directed in the direction of the currents. Clearly, these ridges cause barriers to the southward flowing Arctic water masses and have an influence on the pathways of the deep-water flow.

Oceanic basins sedimentary features

The three basins are one of the keys to the understanding of the glacially influenced margins. Sedimentary features of the three basins give them a strikingly different appearance.

The Boreas basin has a very uniform, medium to low level backscatter apart from a single, weakly backscattering feature that looks like a channel. This channel is discontinuous and is thus believed to be inactive and perhaps filled by a fine-grained abandonment facies. There is an outstanding acoustic artefact on all of the sonographs across this basin. It is believed to be interference fringes due to multiple paths taken through the uppermost layers of soft sediment. This implies that there is acoustic penetration into the sea floor and that the sediment layers have different acoustic properties and are fine-grained. The separation of the interference fringes

increases progressively nearer to the Greenland margin. This is believed to indicate an increase in layer thickness away from the margin (Huggett et al., 1992). At the margin characteristic circular patches of high backscatter are present, including some with positive relief. The patches are equidimensional and up to half a kilometre across. The suggested origin is that they are indicative of gas venting and show some kind of gas venting feature such as pockmarks, diapirisms and hard grounds.

The East Greenland Basin, the largest and deepest basin along the East Greenland continental margin, shows a variety of backscattering where the overall backscatter level is much higher than that of the Boreas Basin. The only extensive area of the basin with a low level of uniform backscatter is in the southeastern part where there is sea floor that is presently isolated from any downslope gravity driven sedimentation. Clearly, the basin is dominated by systems that feed in from the margin. In the south there are four channel systems whereas in the north there is an area with a contrasting pattern of non-channelised features.

The non-channelised pattern is in front of a very long cross shelf trough known as Belgica Strath. The shelf here is at its widest and is believed to have been built out over a long period by sedimentation through the glacier system that possibly occupied the cross shelf trough. On the continental slope we encountered changes from very high backscatter at the upper slope to intermediate backscatter at a possible sediment wave field to low backscatter at the base of the slope. This zonation of backscatter shows downslope trending stripes on the steeper slopes. These give way near the foot of the slope to a pattern that resembles regular bedforms with both transverse and longitudinal elements and below to a uniform and weakly backscattering zone. In the deepest regions the backscattering strength increases and covers most of the sea floor. Downslope changes in the depositional-erosional regime are implied by this zonation. The stripe feature is in keeping with the size of downslope trending features on the Norwegian margin that have been attributed to cold water cascades (e.g. Vorren et al., 1989).

The characteristic channel systems in the south resemble each other in most respects. Only the uppermost part of the slope was not seen because of ice cover and distortions due to water stratifications which limit the range of the sonar. Below the steepest part of the slope there is a well-developed tributary pattern of channels with a high order of branching. The branches join at obtuse, small angles and the channels are shallow and narrow. Below the junction of the tributaries there are single channels that turn to the north and run towards the deepest part of the basin. They are narrow, up to about 2 km and fairly straight. One sinuous channel is to be seen in Figure 4. To the side of the channels there are regularly spaced bands of contrasting backscatter that are believed to be sediment waves with a wavelength of 2-3 km. This kind of feature is common in deep-sea channelised systems and is usually attributed to moulding of the muddy overbank sediments by a process of flow stripping of the uppermost part of the channelised

turbidity flows. The distal part of the channel systems has patterns that have been attributed elsewhere (Belderson et al., 1984) to the deposition of sandy lobes. There is a braid-like pattern consisting of higher backscattering, lozenge shaped, elongate features that are pointed at either end. They are separated by narrow, low backscattering features that are probably very shallow channels. The style of these channelised depositional systems is similar to those of the glaciated margin in the Gulf of Alaska as mapped by GLORIA side-scan sonar. Whether this downslope sedimentation is currently active needs to be determined by sea floor sampling.

The non-channelised and more uniform southern basin is the smallest basin and connects the large East Greenland Basin to the Denmark Strait in the south, one of the most important oceanographic gateways of the North Atlantic deep water flow. This basin, like the Boreas Basin, shows no obvious pattern of sediment input from the shelf. Surprisingly, there are only few signs on the long-range sonographs of along-slope processes apart from some possible mud waves near to the ridge north of the Jan Mayen fracture zone.

What is the reason for the major differences in sedimentation along this glaciated margin? The initial explanation suggested here is that the Boreas Basin is dominated by vertical settling through the water column and deep current processes rather than by downslope sedimentation, because it has presumably permanently been sea ice covered at the margin where downslope entrainment would take place. The large body of sediment, with its characteristic patterns, in front of the major cross shelf trough is deposited by the bulldozer effect of the glacier that drains a large area of the Greenland ice cap and feeds the eroded material to a near point source on the shelf slope. This contrasts with the linear source feeding the channelised systems. In our interpretations we have to consider that the GLORIA system will see through a thin veneer of fine-grained material but is sensitive to sand size sediments that are more likely to be deposited from downslope processes (Kenyon, 1992).

Based on the preliminary interpretation of the GLORIA sonographs we may conclude that:

(1) little direct evidence for along-slope transport of sediments have been found along the East Greenland margin and basin investigated,

(2) in contrast, strong evidence exists for downslope transport processes in the East Greenland Basin,

(3) sediment wave fields may indicate the processes of bottom water current or turbidity current activity at specific site locations,

(4) circular high backscatter regions give hints of large areas of gas venting which needs to be ground truthed by coring and seismic studies,

(5) there exists a large contrast to the Norwegian margin in that the wide areas of sediment slide complexes, a characteristic feature of the Norwegian margin, were not observed on the East Greenland margin. This suggests that distinct differences exist in the sediment stability (instability) of the two margins.

5. Physical oceanography: surface-water temperature distribution of the East Greenland Sea (K. Heidemann, C. Berndt, J. Fest, B. Krämer, F. Nitsche)

During this cruise the surface water temperatures were measured every hour from September 1st until 12th.

From these data a general trend of decreasing water temperatures from the east to the west, i.e. from the basin to the shelf of Greenland, was found. The maximum of 5° C was near Spitsbergen. The isotherms show three minima (Figure 3): at the Jan Mayen and Hovgaard fracture zone ridge and near the northern ice margin.

There was a steep temperature gradient found every time we approached the ice margin due to the cold melt water. There were also local minima when we passed drifting sea ice.

The observed distribution fits quite well with the data trends of Koltermann and Lüthje (1989), apart from the fact that our measured temperatures are about two degrees higher. The reason for this might be that our measurements were carried out two months later than the measurements documented by Koltermann and Lüthje (1989).

The decrease of temperature near the shelf is caused by the melting of sea ice which permanently covers the northern shelf waters. The temperature maximum towards Spitsbergen is probably caused by the northward flowing Spitsbergen current. In contrast, we recognized no direct evidence for the southward flowing cold East Greenland current, which normally shows a temperature of -1.5° C. This indicates that the main current probably flows closer to the shelf and was not detectable during our measurements.

6. GLORIA system technical report (J. Campell, A. Gray, A. Harris)

The GLORIA system was installed on the RV Livonia in Kiel over the period 17th-20th August. The system used consisted of a towfish, launching gantry and hydraulic power pack belonging to Marconi Underwater Systems Ltd (MUSL), together with the IOS Mk 2 power amplifiers and electronic systems. The installation went smoothly apart from a dimensioning error in the IOS drawings of the gantry fixing pads. This resulted in the 2 forward fixing pads (and their associated under deck strengthening) being 1m too far forward. After discussions with the dockyard it was decided to weld extension pieces to the front of the gantry rather than re-position the pads, and this proved satisfactory.

The towfish was deployed 4 days after sailing at 1100Z on day 238. All the Pulse Power Amplifiers (PPAs) were tested and the anticipated matching problem with the titanium transducers in the MUSL towfish did not materialise, although the output current was 20% higher than for the aluminium transducers in the Mk2 towfish. Some problems were encountered in getting the battery charger to charge at a sufficiently high rate from the ship's 220v supply, but these were surmounted by altering the transformer tappings on the supply to the charger control card. Once the charger was functioning properly, data logging was commenced some 6 hours before the start of the first survey line.

Bad weather was encountered during the first few days of the survey which caused some damage to the smallest of the electrical conductors in the tow cable. As these only carry the sensor signals, they are not an essential part of the system and fortunately the weather improved before any more serious damage occurred. The towfish sensors (measuring pitch, roll, temperature, heading and depth) were in fact giving erroneous readings from the beginning because the IOS sensor electronics was not calibrated for use with the MUSL towfish. The towfish heading is the only one of these that is logged and this was reading around 20° higher than the ship's magnetic compass. Throughout the survey, faint bands of noise were occasionally present at far range on the port side. These were less severe than on the previous Mk 2 survey cruise, but remained something of a mystery. The spacing of the bands coincides with the steps in the TVG attenuator which suggests that the noise is originating at a very early stage in the system. The port side TVG control board was replaced shortly after the start of the survey but this made no difference to the problem. The PPAs performed admirably, despite their considerable age. One of the starboard ones failed gradually at around 0800Z on day 248 and was replaced with a spare. Another of the starboard ones tripped its protection circuit at 0745 on day 252 resulting in a few minutes of reduced power on the starboard side.

The only other hiccup in the smooth running of the system occurred at 1800Z on day 253, when the logger cartridge recorder suffered a glitch that resulted in the loss of 3 lines of data and

the absence of a pass 61 from the sequence of passes.

The on-line data display system (which is still under development) proved to be very sensitive to electrical interference from the ship's HF radio transmissions which frequently caused the PC to crash. This radio interference was also faintly visible on the sonar records, appearing as dark "cross-hatching" over periods of a few minutes.

Off-line data processing

This survey presented a number of novel problems in the production of a GLORIA mosaic, necessitating a considerable amount of software development. For the first time, prints were produced on a thermal linescan recorder rather than by the traditional wet photography. This greatly increased the speed, simplicity and consistency of the image production process, but required some software development to get the images correctly scaled.

Another problem was the absence of a deep water echo-sounder to provide the bathymetry necessary to correct the images for slant range distortion. A mobile deep echo sounder was not brought on board because it did not fit into the hydrographic pool and it was impossible to tow it at a cruising speed of 9 knts. This problem was overcome by developing a program to automatically track the bottom return in the GLORIA data itself, and hence derive an estimate of the depth. This proved to be a fairly challenging task, particularly on steep gradients and in areas where the bottom return was masked by spurious reflections from ice or planktonic organisms in the water column. An additional complication was that the local oscillator frequency in the transceiver drifts slightly, causing the port and starboard time zero points to shift in opposite directions by a few pixels. This means that the port and starboard bottom returns are no longer coincident. A method of detecting and compensating for this drift was developed and incorporated into the bottom tracking program.

The GLORIA images also need to be corrected for variations in speed over the ground, using navigation data. The ship's position was recorded every 20 seconds or so using a GPS system provided by GEOMAR. Two programs were developed to process the data files from this system into the format required by the GLORIA along-track correction program. The first of these parses the GPS file, correcting an error in the date change and removing any non-valid readings. The second extracts 2 minute positions and re-formats them into the "dx-fmt" format used at I.O.S.

In the absence of any kind of bathymetry profile, another program was developed from the bottom tracking routine to print out an expanded bottom profile on the thermal recorder at the

same scale as the mosaic prints. This record is produced by adding the port and starboard data together (after correcting for local oscillator drift) and then repeating each pixel 5 times to exaggerate any gradients in the bottom profile. Range marks were added at 1000m intervals, though without some means of calibrating the GLORIA bottom returns, the accuracy of these marks is unlikely to exceed 150 m (approx. 3 pixels).

GLORIA data tapes

The usual data storage and transfer medium is standard 9-track tape. These are written at 1600 bpi on a Digi-Data 2000 tape deck connected to a PC via an ODI interface card.

File/block structure

GLORIA data is logged in 6 hour chunks referred to as "passes", that contain 720 "lines" of data at the usual 30 second pulse repetition period. Each line consists of a 1024 byte record that contains the port and starboard returns from a single ping as well as header information. These records are written to tape in blocks of 60 (i.e. a 60KB block size). Each pass ends with a file mark and the last pass on a tape ends with a normal End Of Tape mark.

Record structure.

Raw data records.

Each raw data record comprises of:

496 port data samples
496 starboard data samples
26 bytes of header information
6 marker bytes

To see how this information is arranged within a record, consider an example having the following values:

Pass number	56
Line number	692
Slant Range correction code	26
Pulse Repetition Period	30 seconds
Vehicle heading	271 degrees (magnetic)
Year	1991
Day number	048

Time 1546:32

For this example the record contents will be:

Byte Val.	Contents	ASCII Char.	Hex
0	Pass number high byte	*	00
1	Pass number low byte	*	38
2	Line number high byte	*	02
3	Line number low byte	*	64
4	Hour mark flag (set to 1 on the hour)	*	00
5	Slant Range correction code	*	1A
6	Not used	*	00
7	PRP code (1,2,3 or 4 in ASCII)	'3'	33
8	Vehicle Heading (hundreds)	'2'	32
9	Vehicle Heading (tens)	'7'	37
10	Vehicle Heading (units)	'1'	31
11	Year (tens)	'9'	39
12	Year (units)	'1'	31
13	Port Far Range edge mark	*	FF
14	Port Far Range edge mark	*	FF
15	496th Port data sample (far range)	*	data
16	495th Port data sample	*	data
509	2nd Port data sample	*	data
510	1st Port data sample (near range)	*	data
511	Ship's track centre mark	*	FF
512	Ship's track centre mark	*	FF
513	1st Starboard data sample (near range)	*	data
514	2nd Starboard data sample	*	data
1008	496th Starboard data sample (far range)	*	data
1009	Starboard Far Range edge mark	*	FF
1010	Starboard Far Range edge mark	*	FF
1011	Julian Day number (hundreds)	'0'	30
1012	Julian Day number (tens)	'4'	34
1013	Julian Day number (units)	'8'	38
1014	GMT hours (tens)	'1'	31
1015	GMT hours (units)	'5'	35
1016	GMT minutes (tens)	'4'	34
1017	GMT minutes (units)	'6'	36
1018	GMT seconds (tens)	'3'	33
1019	GMT seconds (tens)	'2'	32

1020	Checksum	*	*
1021	Checksum	*	*
1022	Not used	*	00
1023	Not used	*	00

Some notes on the header contents

Slant Range Correction code. This is an octal code entered by the watchstander to correct the real-time LSR record and is therefore not very accurate.

Vehicle Heading: This is an instantaneous reading from the magnetic compass in the tail of the vehicle, taken just after the pulse has been transmitted. Because of imperfections in the compass response the reading is only accurate to within a few degrees, especially in rough weather.

Time: The time is the GMT "time zero" point for the pulse that produced the data in the record. This corresponds to the end of the pulse.

Sonar Data: The sonar data is logged as 12-bit samples and then compressed to 8-bits using a Bell-255 logarithmic compression. The algorithm for expanding an 8-bit value to 12-bits is:

val_12 = (4095/255)*(exp(log(256) * val_8 / 255) - 1)

Since most image display systems incorporate some form of contrast stretching, it is not normally necessary to perform this expansion.

Processed data records

Processed data means data that has been slant range corrected and may also have undergone other processing such as filtering or shading. This data is also in 1024 byte records and is arranged in much the same way as the raw data, with the important exception that the records contain no header information. Instead, each "pass" has 8 lines of annotation added at the beginning and 9 at the end, giving an overall file size of (17 + 720) * 1024 bytes. This annotation gives the cruise title, pass number and start and end times. It is designed to be displayed as part of the image and is therefore not easily decoded by software.

The layout of the data within a record is as follows:

Bytes 0 to 12 are zero unless there is an hour mark in which case they are set to hex FF.
Bytes 13 and 14 are the Port far range edge mark and are always hex FF.

Byte 15 is the Port far range sample and so on up to byte 510 which is the Port near range sample (after slant range correction).
Bytes 511 and 512 mark the ship's track and are always set to zero.
Byte 513 is the Starboard near range sample and so on up to byte 1008 which is the Starboard far range sample.
Bytes 1009 and 1010 are the Starboard far range mark and are always hex FF.
Bytes 1011 to 1022 are zero or FF depending on whether or not there's an hour mark.
Byte 1023 is a binary number corresponding to the number of times that line should be drawn to produce a correctly scaled image on an IOS Laser Filmwriter. In other words, this allows the display device to perform the required along-track correction for variations in the ship's speed. To produce correctly scaled images on a different recorder, it is necessary to multiply the contents of byte 1023 by a constant "fix-it" factor to determine how many times to repeat that scan line on the new recorder.

7. Cruise schedule

Friday 21 August 1992

The research vessel LIVONIA left Kiel (GEOMAR pier) at 07:15 on a rainy and slightly foggy day. At 08:30 the pilot left and the ship headed at a speed of 13 knots towards Skagerrak. The scientific crew had a first briefing by the chief scientist about the science programme. After the scientific crew had tied down their equipment, the Captain and his officers introduced the scientists to the safety regulations on board. During the afternoon the wind increased to Beaufort scale 7-8 and most of the scientists retreated to their cabins.

Saturday 22 August 1992

Under a cloudy sky we passed the visible Norwegian coastline and crossed the Norwegian Trough at a speed of 13 knots. All the scientists were well and the preparation for the GLORIA operation continued. At 2 pm a life boat drill took place to get the scientists familiar with the ship's safety procedure. The weather cleared up and we continued towards our working area under a clear sky on a sunny afternoon.

Sunday 23 August 1992

Livonia crossed through the oilfields northeast of the Shetland Islands at 11 am. Massive oil rigs were clearly to be seen and the large gas flames looked like giant candles. At about 2 pm the

shelf break was left behind us, and the water depth steadily increased to greater than 1000 m. We left the shallow water and started to cross the Norwegian basin towards the area of Jan Mayen.

Monday 24 August 1992

Fog accompanied us most of the day. The sea was relatively calm when we crossed the Arctic circle at about 2 pm. During the afternoon Neil Kenyon gave a talk about GLORIA imagery in the world ocean and its application and limits for determining sedimentary processes.

Tuesday 25 August 1992

Sea state Beaufort 6-7 and water temperatures of about 4° C marked the fifth day of our transit. Jan Mayen, the last island on our way to the Greenland margin and basin came into sight at 9 am GMT. The island was covered by snow and large glaciers were to be seen, which had steep fronted ice masses that are entrained directly into the ocean. At 11 am (GMT) the GLORIA fish was smoothly launched at a ship's speed of about 5 knots. The fish entered the water and trailed astern from the ship. The fish was towed on 400 m of cable at a ship's speed of 8 knots. This allowed a towing depth of about 45 m beneath the sea surface.

Wednesday 26 August 1992

Sea state Beaufort 8-9 (wind speed about 20m/s) made the work on board difficult because of the ship's rolling. GLORIA was towed along the Jan Mayen fracture zone without any problems and we reached the starting point of profile 1 at ca. 2 am at night. The area until Vesteris Bank was an essentially flat sea floor with few structures. Further north steep slopes and fan-like structures characterized the sea floor.

Thursday 27 August 1992

The sea was relatively calm and GLORIA was towed at a speed of 9 knots across the eastern part of the Greenland Basin. We saw some large-scale features which presumably relate to the distal parts of turbidity channel systems. The second fracture zone was crossed at about 4 pm.

Friday 28 August 1992

A calm sea and partly sunny weather provided ideal conditions for the survey. The ship was running at 9 knots. Water temperature was 5.4° C indicating that we were not within the East

Greenland current. Profile 1 ended at 1:45 am (GMT) just south of the Molloy deep at 78° 51.215 N, 3° 2.355 E. Surface water temperature dropped from 5.4° C in the ice-free zone to -0.3° C close to the ice edge. The ice edge created a sharp boundary that blocked any further sailing towards the north. Patches of sea ice in open waters showed a variety of sculptural shapes that floated around the ship and passed the GLORIA vehicle, which was towed with care.

Profile 2 started at 12:26 pm at 78° 47.072 N 1° 27.889 E with 9 knots ship's speed and a course of 200°. The weather was partly sunny and the sea was calm. Fortunately, Eve (our stewardess), who was seasick during our first profile, quickly recovered and came to the bridge with a big smile on her face.

At about 22:00 pm we crossed an east-west trending patchy icefield at 77° 25.275 N 00°14.051 W, which was about 2 km wide. The ship towed GLORIA through it without misshape.

Saturday 29 August 1992

Another partly sunny day with a calm sea and water temperatures of about 4.2° C at the surface. The ship's speed was 9 knots and the ship's course 213°.

Sunday 30 August 1992

Water temperatures dropped to 2.3° C while air temperature was -0.3° C. The end of profile 2 was reached at 15:07 pm at 72° 1.886 N 13° 05.816 W and the start of profile 3 at 17:00 pm at 72° 7.966W 13° 46.415 W. A strong north-westward directed surface current of about 1.6 knots delayed our course change.

Monday 31 August 1992

We sailed north in sea state Beaufort 5 on a course of 33° under a cloudy sky. Water temperatures varied between 2 and 4° C. A large sediment wave field was encountered at about 22:00 pm at 75° 53.640 N 04° 56.301 W.

Tuesday 1 September 1992

At 6:42 am water temperatures dropped to 1° C and patches of about 2-3 m thick sea ice were seen. The decrease in water temperature goes most likely in parallel with an increase in sea ice melting, which in turn may cause increased water stratification. This may cause a distinct acoustic interference pattern on the GLORIA record which occurred in places where water temperature came close to 0° C. Such a pattern developed very strongly for example at 7:31 am at 77° 4,386

N 1°4,42 W when water temperatures decreased to - 0.3° C. During the afternoon the sun came out and we continued our programme under a blue sky with a blue and calm sea. At 22:00 pm we reached the area close to the ice edge where the temperature decreased rapidly from -0.3° C to -1.1° C. North of 79° 02.00 N a continuous ice boundary apparently blocked the Fram Strait. Thus the end of profile 3 was reached at 79° 02.479 N 00° 23.379 E due to the ice edge. Profile 4 started at 22:38 pm at 79° 01.356 N 00° 20.472 E at a water temperature of -1.1°C. The course was southeast at 238°. However, we soon encountered ice and were forced to change our course to 190°. We towed GLORIA through a large icefield without any problems at a speed of 9 knots.

Wednesday 2 September 1992

The large icefield, with iceplates that were about 3-4 m thick and 2-10 m wide, continued until 0:54 am at position 78° 43.709 N 1° 10.436 W. Therefore, profile 4 started at 78° 42.899 N 1° 11.164 W on a course of 191°. Water temperatures, measured only a few miles away from the icefield, increased to 1.1° C. At 2 pm a large icefield, elongated from west to east, seemed to hinder any further direct route to the south totally. However, as we came closer to the ice we encountered a passage and went through it. The icefield had an extension of about 8 miles with small icebergs drifting towards the east. At the icefield which almost parallels a topographic height, temperatures dropped from 2.5 to -0.3° C. The ice extended from 76° 51.311 N 3° 28.444 W to 76° 36.682 N 4° 20.456 W. It is important to note that on all the occasions where we encountered ice some dirty ice occurred, which was almost completely covered by sediment particles from unknown sources.

Thursday 3 September 1992

Sunshine and a calm sea (Beaufort 2) provided ideal conditions for the GLORIA studies. The fish was towed at a depth of approximately 50 metres below the sea surface at a speed of 8.5 knots across the Greenland Basin.

Friday 4 September 1992

Profile 4 ended at 03:00 am near the westward end of the Jan Mayen fracture zone at 72° 14.91 N 14° 35.002 W. There was a calm sea and water temperatures reached 1.3° C. Profile 5, the first profile near the continental slope, started at 72° 22.154 W 15° 09.631 W at 05:21 am. The ship was steaming northward against a strong southward flowing current of up to 1.5 knots.

Saturday 5 September 1992

A high pressure cell stationed above Greenland provided the adjacent sea with a calm ocean surface and a sunny sky. The ship was running northward at a constant speed of 8.5 knots. The GLORIA records showed sporadic patterns of interference due to a well-stratified water column at the southward flowing cold East Greenland current. Here, low temperatures of about -1.5° C prevailed. At 11:44 am we had a complete power failure on the ship which lasted for about 5 minutes. Fortunately, there were no icebergs or sea ice close by and the sea was calm. A dense bank of fog and floating sea ice hindered our northward journey from 1 to 2:30 pm at 76° 17.208 N 6° 10.452 W. Water temperatures during this profile varied between 1.3 and 2.1° C. At 6 pm we reached the ice edge of East Greenland at 76° 45.920 N 5° 2.240 W, which extended like a nose into the open sea at one of the major transform faults that separate the East Greenland basins. We changed our course to 23°, sailed for half an hour parallel to the ice edge of the rugged and about 1 m thick sea ice and then turned on to profile 6 at 7:23 pm. Profile 6 started at 76° 43.996 N 5° 20.680 W on a course of 211°. Due to encountering a decrease in the quality of the record attributed to well-stratified water masses and the refraction of the GLORIA acoustic beam pattern we ran our profile track lines at a distance of 10 instead of 14 miles. However, we soon discovered that the record quality was so poor that the change in distance did not improve the overlay of the records. Therefore, we returned to our 14 miles distance between track lines.

Sunday 6 September 1992

The records remained distorted due to the stratified water column close to or within the East Greenland current. Water temperatures were in the order of -1.5° C, indicating the presence of the southward flowing cold water masses. We attempted to lower the fish by reducing the ship's speed from 8.5 to 6 knts. No improvement of the record was recognized and we returned to our cruise speed of 8.5 knots. The ship continuously sailed parallel to the East Greenland sea ice margin, which started to bend closer to the shelf at about 6 am at a position of 75° 31.517 N 9° 11.766 W. The ice margin was recorded by the vertical GLORIA beam and showed up as a sharp grey boundary on the record. Even at tens of miles distance from the ice edge the records still showed the ice.

Monday 7 September 1992

The weather remained calm but water temperatures increased to about 2° C as the distance from the East Greenland sea ice edge and current increased. The end of profile 6 was reached at 07:32 am at 72°23,640 N 16° 01.726 W and we turned on to our westernmost profile located close to the ice edge. Profile 7 started at 09:28 am at 72° 33.711 N and 16° 38.127 W. Water temperatures decreased to about -1.6° C. At 09:50 we encountered dense fog banks and soon afterwards ice. Several meters wide and 2 m thick iceplates were floating towards the east. It was

too late to change the course and we attempted to crash through the ice with a speed of 6.5 knots. After 30 minutes of a highly problematical towing operation we passed the ice barrier and continued the profile in the fog. Profile 7 ended close to another sea ice boundary at 05:29 pm at 73° 24.589 N 14° 36.296 W. The transit time to profile 8 was about 12 hours.

Tuesday 8 September 1992.

Profile 8 started at 05:00 am at 71° 56.294 N 12° 22.9 W in surface water temperatures of 2.4° C. A low pressure front in the area from Greenland to Norway caused sea states of 9 to 11. Fortunately, GLORIA worked well even under these weather conditions.

Wednesday 9 September 1992

The low pressure front continued to cause Beaufort 9 and only improved in the area of Fram Strait. However, the GLORIA records remained of a high quality.

Thursday 10 September 1992

End of profile 8 was reached at 09:00 am at 79° 07.608 N 03° 02.908 E. This time no sea ice was encountered within a radius of 8 miles indicating that the sea ice had decayed considerably and retreated northward during our survey. Profile 9 started at 01:00 pm in calmer weather conditions at a speed of 8.0 knots and a position of 78° 43.509 N 04° 31.438 E.

Friday 11 September 1992

Our cruising speed was 9.5 knots despite the fog and increasing wind speeds. We attempted to finish this last profile in time but with a good quality of the sonar records. As the sonographs proved to be good we continued our line at high speed. In the late afternoon (08:00 pm) the fog bank disappeared and gave rise to a clear sky.

Saturday 12 September 1992

Profile 9 continued at Beaufort scale 3-4 until 07:10 pm. The last profile of the voyage ended at position 71° 46.271 N 10° 57.348 W.

GLORIA was safely recovered and brought on deck at 07: 54. Afterwards we started to sail home.

Sunday 13 September to Thursday 17 1992

The transit from the working area to Kiel took place under variable weather conditions from a calm sea to a storm with Beaufort scale 9. We crossed the Arctic circle at 07:00 am on Monday and passed the Norwegian Greenland Sea until Tuesday. The ship entered the area of the Norwegian trench on Tuesday at 09:00 am and continued to sail to the Baltic Sea.

8. Shipboard scientific party

Jürgen Mienert, (chief scientist)	GEOMAR, Research Center for Marine Geosciences Wischhofstr. 1-3, Bldg. 4, D-24148 Kiel, F.R.G. and SFB 313, Christian-Albrechts-University of Kiel, Olshausenstr. 40-60, D-24118 Kiel, F.R.G.
Christian Berndt	SFB 313, Christian-Albrechts-University of Kiel, Olshausenstr. 40-60, D-24118 Kiel, F.R.G.
Jon Campbell	Institute of Oceanographic Sciences, Brook Road, Wormley, Godalming, Surrey, GU8 5UB, U.K.
Janine Fest	SFB 313, Christian-Albrechts-University of Kiel, Olshausenstr. 40-60, D-24118 Kiel, F.R.G.
Alan Gray	Institute of Oceanographic Sciences, Brook Road, Wormley, Godalming, Surrey, GU8 5UB, U.K.
Andrew Harris	Institute of Oceanographic Sciences, Brook Road, Wormley, Godalming, Surrey, GU8 5UB, U.K.
Kerstin Heidemann	GEOMAR, Research Center for Marine Geosciences Wischhofstr. 1-3, Bldg. 4, D-24148 Kiel, F.R.G.
Franz-Josef Hollender	SFB 313, Christian-Albrechts-University of Kiel, Olshausenstr. 40-60, D-24118 Kiel, F.R.G.
Neil Kenyon	Institute of Oceanographic Sciences, Brook Road, Wormley, Godalming, Surrey, GU8 5UB, U.K.
Babette Krämer	GEOMAR, Research Center for Marine Geosciences Wischhofstr. 1-3, Bldg. 4, D-24148 Kiel, F.R.G.
Frank Nitsche	GEOMAR, Research Center for Marine Geosciences Wischhofstr. 1-3, Bldg. 4, D-24148 Kiel, F.R.G.

The co-ordinated project was financed by the Deutsche Forschungsgemeinschaft (Project B1, SFB 313 Christian-Albrechts-University of Kiel) and supported by GEOMAR, who provided funds for the ship time. This report is for interested scientific parties and funding agencies and to comply with Danish regulations.

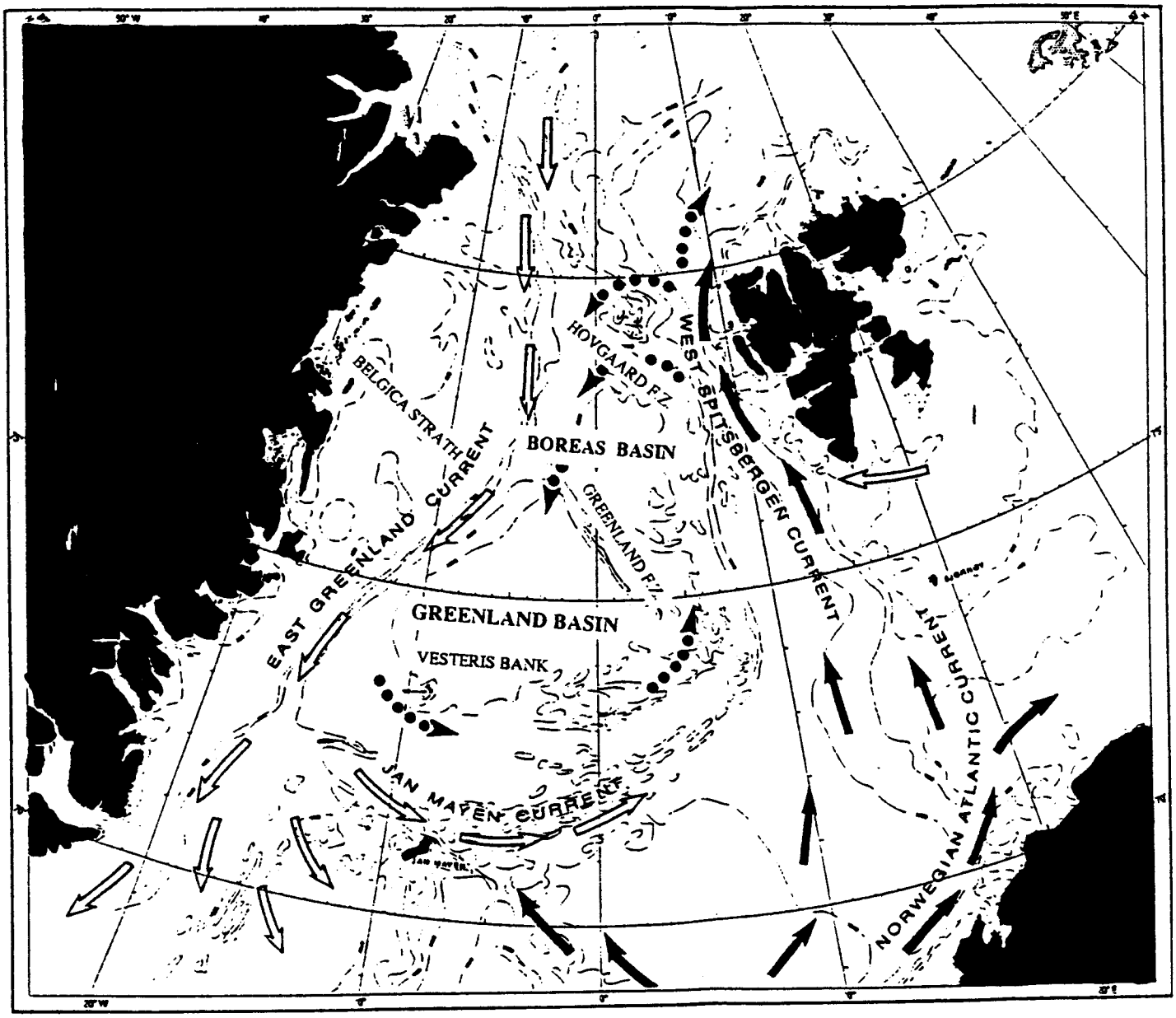

Figure 1: The working area off the East Greenland margin includes the major basins and fracture zones. Schematic circulation patterns in the Norwegian Greenland Sea are indicated by solid arrows (relatively warm surface currents, dotted = warm sub-surface currents) and open arrows (cold surface currents).

9. References

Andrews, J.T., Williams, K.M., Milliman, J., and Weiner, N., 1989. Late Quaternary marine geology of the Kangerdlugssuaq trough, East Greenland shelf. Geol. Soc. Am., Abstract, 21, A331.

Belderson, R.H., Kenyon, N.H., Stride, A.H., and Pelton, C.D., 1984. A braided distributary system on the Orinoco deep-sea fan. Mar. Geol., 56, 195-206.

Huggett, Q.J., Cooper, A.K., Somers, M.L. and Stubles, A.R., 1992. Interference fringes on GLORIA side-scan sonar images from the Bering Sea and their implications. Mar. Geophys. Res., 14, 47-63.

Kenyon, N., 1992. Speculations on the geological causes of backscatter variation on GLORIA sonographs from the Mississipi and de Soto fans, Gulf of Mexico. Geo-Marine Letters, 12, 24-32.

Koltermann, K. P. and Lüthje, H., 1989. Hydrographischer Atlas der Grönland- und nördlichen Norwegischen See, Deutsches Hydrographisches Institut, Hamburg, 274 p.

Mienert, J., Andrews, J.T., and Milliman, J.D., 1992. The East Greenland Continental Margin (65° N) since the last deglaciation: Changes in sea floor properties and ocean circulation. Mar. Geol., 106, 217-238.

Vogt, P.R., 1986. Seafloor topography, sediments, and paleoenvironments. In: Hurdle, B.G. (ed.), The Nordic Seas, 287-386.

Vorren, T.O., Lebesbye, E., Andreassen, K., and Larsen, K.-B.,1989. Glacigenic sediments on a passive continental margin as exemplified by the Barents Sea. Mar. Geol., 85, 251-272.

10. Acknowledgement

We thank Captain Jaan Koit and his crew of the research vessel LIVONIA from Tallinn (Estonia) for their good seamanship and excellent assistance. Although various languages ranging from Estonian, Russian, English to German were used in the day to day communication, there was always good humor and unfailing co-operation on board. The ship proved to be ideally suited for sea ice going operations in the vicinity of the Arctic and East Greenland sea ice margin. Permission to work within Greenland waters was granted by the Ministry of Foreign Affairs of Denmark and the permission to operate in Norwegian waters by the Royal Norwegian Embassy in Tallinn. The chief scientist thankfully acknowledges funding for this co-operative work by the Deutsche Forschungsgemeinschaft (Project B1, SFB 313 of the Christian-Albrechts-University of Kiel, FRG) and the financial support by GEOMAR for ship time.

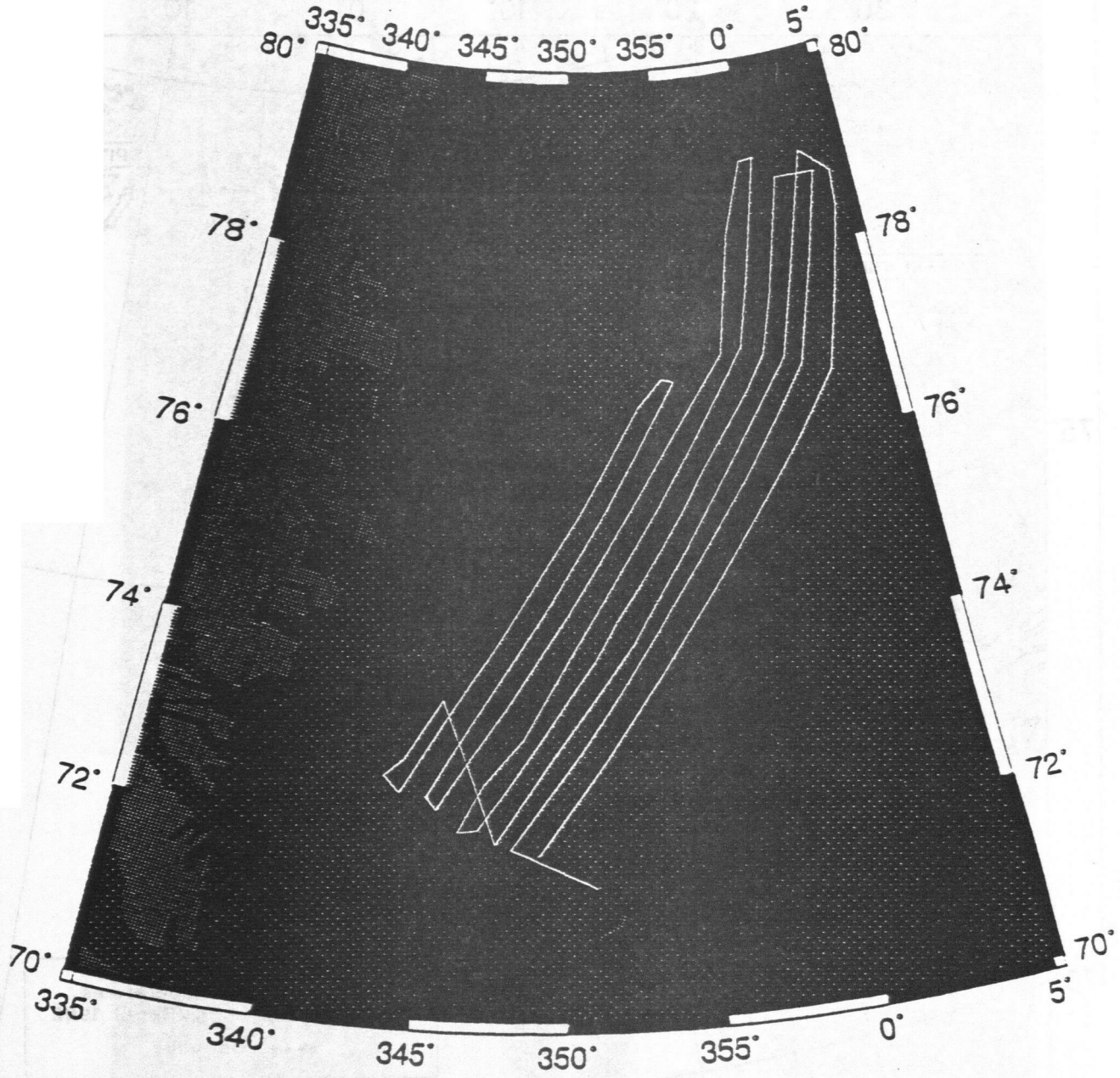

Figure 2: Profile tracks of GLORIA sonographs along the East Greenland margin.

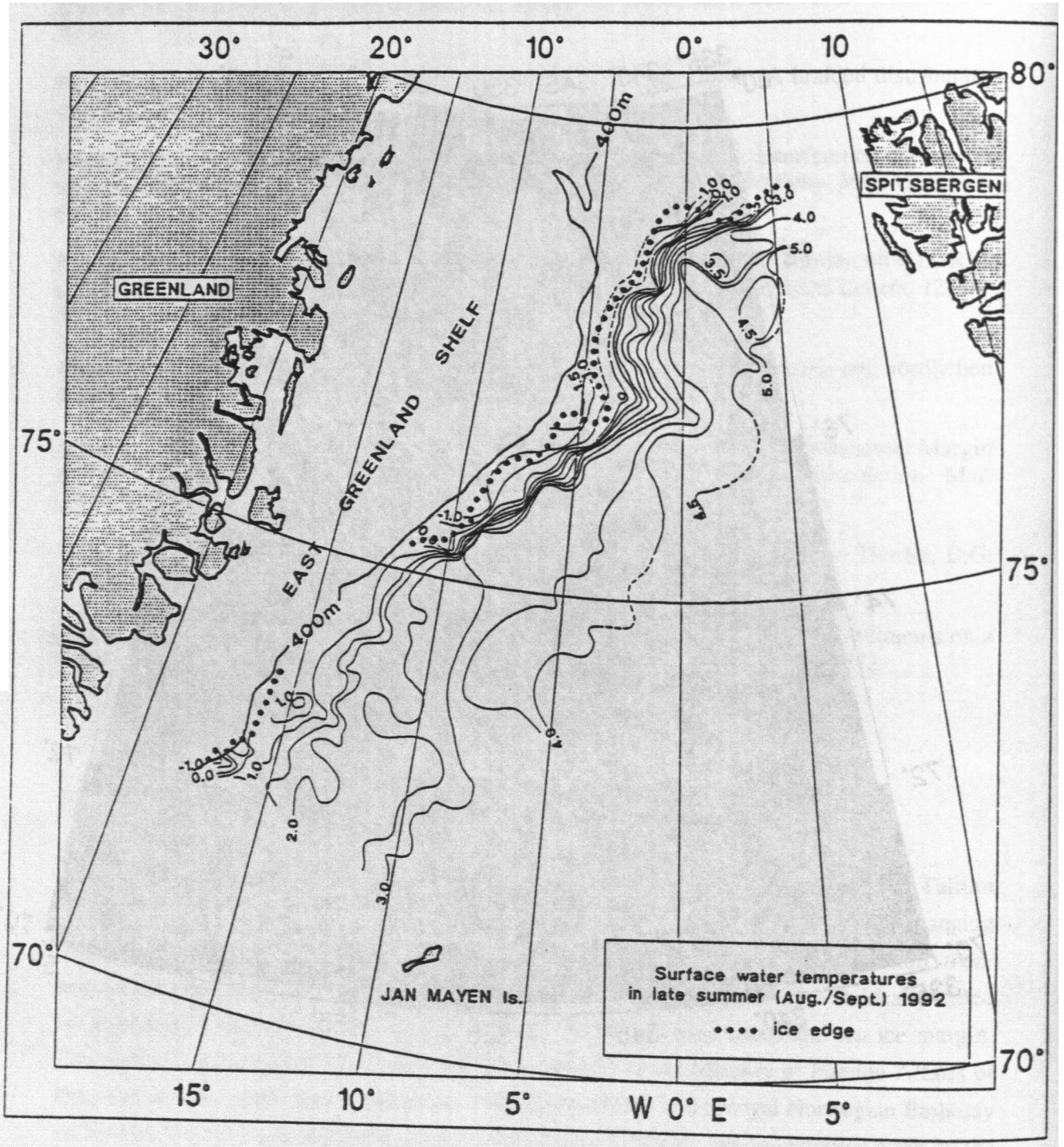

Figure 3: Surface water temperature changes along the East Greenland continental margin. The black dots mark the sea ice edge.

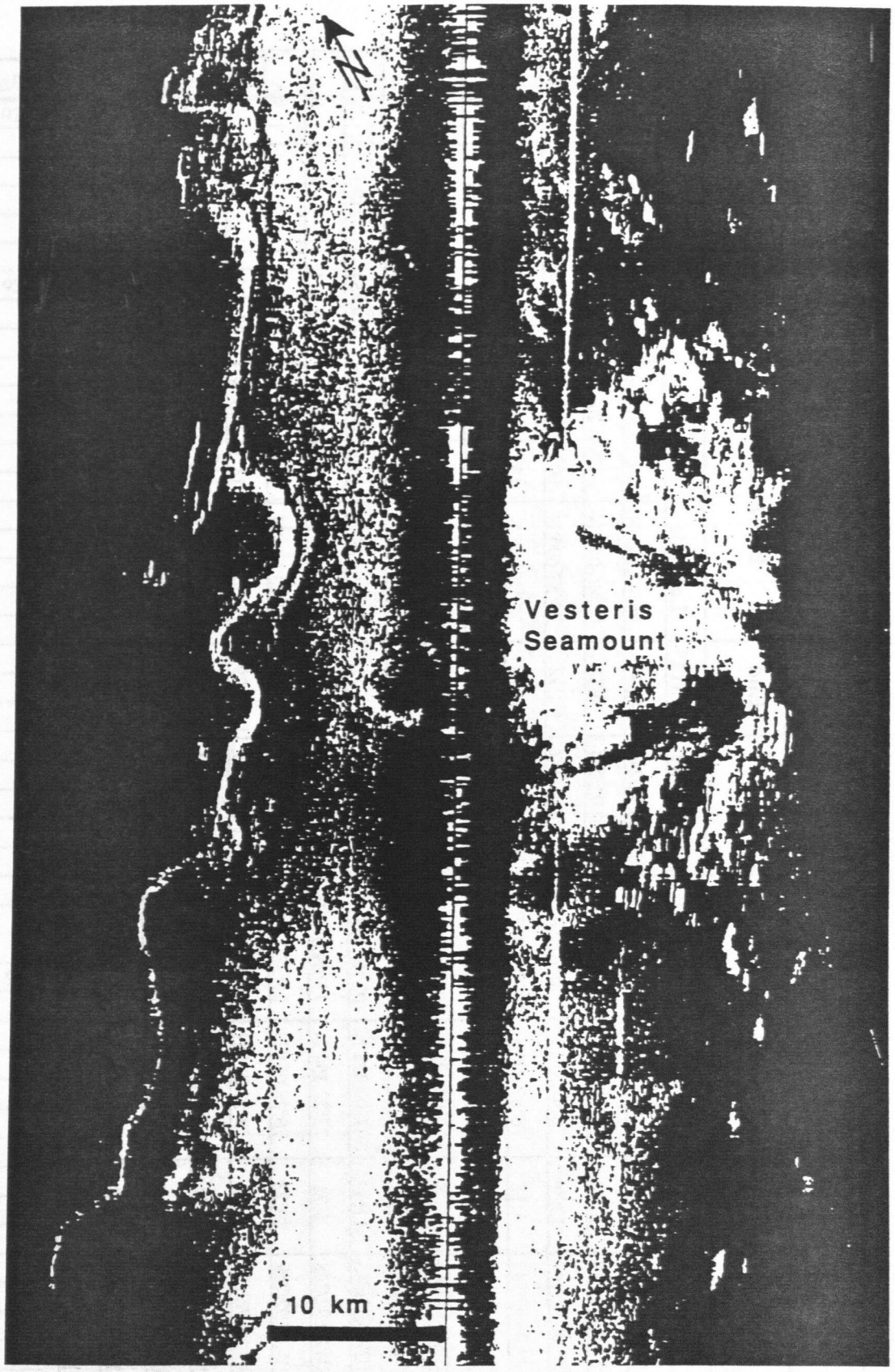

Figure 4: Example of a GLORIA sonograph that shows the Vesteris Seamount and a sinuous channel just northwest of it. The channel runs towards the northeast, i.e. towards the deepest part fo the Greenland basin.

Table 1: GLORIA sonograph lines along the East-Greenland margin

Profile		Start Time	Start Position			End Time	End Position		Distance	Bearing	Ship Speed
	Date/Day	(GMT)	Latitude	Longitude	Date/Day	(GMT)	Latitude	Longitude	(sm)		(knts)
1a	26.08.92/239	2:00	71°50,163`N	11°55,283`W	27.08.92/240	20:36	76°47,105`N	01°02,524`E	362.17	35	8.5
1b	27.08.92/240	20:36	76°47,105`N	01°02,524`E	28.08.92/241	9:51	78°46,049`N	03°36,278`E	123,325	15	9.3
2a	28.08.92/241	12:36	78°47,072`N	01°27,889`E	29.08.92/242	1:12	76°57,690`N	00°40,867`W	112.714	193.5	9
2b	29.08.92/242	1:12	76°57,690`N	00°40,867`W	30.08.92/243	15:07	72°01,806`N	13°05,816`W	355,103	213.5	9.4
3a	30.08.92/243	16:55	72°07,339`N	13°47,850`W	01.09.92/245	7:28	77°03,921`N	01°41,133`W	352,378	33	9.1
3b	01.09.92/245	7:28	77°03,921`N	01°41,133`W	01.09.92/245	21:33	79°02,479`N	00°23,379`E	121.311	12	8.6
4a	01.09.92/245	22:38	79°01,356`N	00°23,631`W	02.09.92/246	11:35	77°09,825`N	02°40,504`W	115.037	191	8.9
4b	02.09.92/246	11:35	77°09,825`N	02°40,504`W	04.09.92/248	3:07	72°14,170`N	14°36,646`W	349,451	212.5	8.8
5	04.09.92/248	5:21	72°22,154`N	15°09,631`W	05.09.92/249	18:00	76°45,920`N	05°02,240`W	308,411	31.4	8.4
6	05.09.92/249	19:23	76°48,651`N	05°33,130`W	07.09.92/251	7:32	72°23,640`N	16°01,726`W	312.19	211	8.6
7	07.09.92/251	9:28	72°33,711`N	16°38,127`W	07.09.92/251	17:29	73°24,589`N	14°36,296`W	62.123	29	7.8
8a	08.09.92/252	4:41	71°53,743`N	12°28,307`W	09.09.92/253	17:48	76°53,240`N	00°15,212`E	361,488	34.5	9.7
8b	09.09.92/253	17:48	76°53,240`N	00°15,212`E	10.09.92/254	9:00	79°07,608`N	03°02,908`E	138.805	15	9.1
9a	10.09.92/254	13:00	78°43,509`N	04°31,438`E	11.09.92/255	3:38	76°38,919`N	02°21,829`E	127,567	194.5	8.7
9b	11.09.92/255	3:38	76°38,919`N	02°21,829`E	12.09.92/256	19:10	71°46,271`N	10°57,348`W	362,852	216.4	9.2

Date/Day	Time/GMT	Latitude	Longitude	Profile
25.8.92/238	18:00	71°25,361`N	08°58,588`W	
	19:00	71°27,840`N	09°19,740`W	
	20:00	71°30,554`N	09°41,799`W	
	21:00	71°33,607`N	10°05,097`W	
	22:00	71°36,474`N	10°29,379`W	
	23:00	71°39,885`N	10°52,317`W	
26.8.92/239	0:00	71°43,578`N	11°15,641`W	
	1:00	71°46,863`N	11°40,144`W	
	2:00	71°50,163`N	11°55,283`W	1a
	3:00	71°57,381`N	11°38,119`W	
	4:00	72°04,835`N	11°21,721`W	
	5:00	72°12,230`N	11°04,750`W	
	6:00	72°19,656`N	10°47,424`W	
	7:00	72°26,572`N	10°30,747`W	
	8:00	72°33,212`N	10°14,733`W	
	9:00	72°38,942`N	09°59,912`W	
	10:00	72°44,472`N	09°46,157`W	
	11:00	72°50,231`N	09°33,070`W	
	12:00	72°55,857`N	09°20,065`W	
	13:00	73°01,107`N	09°07,933`W	
	14:00	73°06,268`N	08°56,074`W	
	15:00	73°11,552`N	08°44,403`W	
	16:00	73°17,313`N	08°31,383`W	
	17:00	73°22,671`N	08°19,584`W	
	18:00	73°28,265`N	08°07,031`W	
	19:00	73°34,110`N	07°54,106`W	
	20:00	73°39,872`N	07°39,323`W	
	21:00	73°45,830`N	07°23,536`W	
	22:00	73°51,910`N	07°06,759`W	
	23:00	73°58,635`N	06°48,008`W	
27.8.92/240	0:00	74°05,629`N	06°28,304`W	
	1:00	74°13,314`N	06°08,040`W	
	2:00	74°21,043`N	05°48,803`W	
	3:00	74°28,993`N	05°27,945`W	
	4:00	74°37,188`N	05°07,379`W	
	5:00	74°45,134`N	04°47,407`W	
	6:00	74°53,078`N	04°27,102`W	
	7:00	75°00,483`N	04°05,411`W	
	8:00	75°08,215`N	03°43,481`W	
	9:00	75°15,949`N	03°21,279`W	
	10:00	75°23,667`N	03°00,587`W	
	11:00	75°31,438`N	02°37,110`W	
	12:00	75°39,619`N	02°16,220`W	
	13:00	75°47,751`N	01°53,314`W	
	14:00	75°55,561`N	01°30,411`W	
	15:00	76°03,570`N	01°06,680`W	
	16:00	76°11,580`N	00°44,036`W	
	17:00	76°19,587`N	00°21,670`W	

Table 2: Position data of profiles

Date/Day	Time/GMT	Latitude	Longitude	Profile
	18:00	76°27,206`N	00°01,591`E	
	19:00	76°34,765`N	00°24,603`E	
	20:00	76°42,182`N	00°48,594`E	
	20:36	76°47,105`N	01°02,524`E	1b
	21:00	76°49,488`N	01°06,133`E	
	22:00	76°58,011`N	01°16,906`E	
	23:00	77°06,402`N	01°29,116`E	
28.8.92/241	0:00	77°15.323`N	01°39.945`E	
	1:00	77°24.366`N	01°50.440`E	
	2:00	77°33.591`N	02°00.600`E	
	3:00	77°42.069`N	02°10.771`E	
	4:00	77°51.748`N	02°24.805`E	
	5:00	78°01.370`N	02°37.819`E	
	6:00	78°10.878`N	02°48.601`E	
	7:00	78°20.094`N	03°01.747`E	
	8:00	78°28.751`N	03°14.386`E	
	9:00	78°37.989`N	03°26.474`E	
	9:51	78°46.049`N	03°36.278`E	Ende 1b
	10:00	78°47.485`N	03°33.675`E	
	11:00	78°31.809`N	02°44.406`E	
	12:00	78°49.300`N	02°56,157`E	
	12:36	78°47.072`N	01°27.889`E	2a
	13:00	78°44.206`N	01°21.046`E	
	14:00	78°35.496`N	01°09.603`E	
	15:00	78°26,690`N	00°59.640`E	
	16:00	78°17.888`N	00°48.977`E	
	17:00	78°09.021`N	00°39.120`E	
	18:00	78°00.245`N	00°29.681`E	
	19:00	77°51.395`N	00°19.574`E	
	20:00	77°34.024`N	00°07.260`E	
	21:00	77°34.022`N	00°04.999`E	
	22:00	77°25.275`N	00°14.051`E	
	23:00	77°16.355`N	00°19.092`W	
29.8.92/242	0:00	77°07.875`N	00°28.851`W	
	1:00	76°59.217`N	00°37.384`W	
	1:12	76°57,690`N	00°40,867`W	2b
	2:00	76°51.346`N	00°58.293`W	
	3:00	76°43.469`N	01°19.117`W	
	4:00	76°35.389`N	01°41.008`W	
	5:00	76°27.476`N	02°03.675`W	
	6:00	76°19,859`N	02°27,347`W	
	7:00	76°12,392`N	02°53,277`W	
	8:00	76°04,513`N	03°16,438`W	
	9:00	75°56,638`N	03°39,117`W	
	10:00	75°48,969`N	04°01,645`W	
	11.04	75°40,711`N	04°23,670`W	
	12:00	75°33,203`N	04°41,419`W	
	13:00	75°25,046`N	04°59,863`W	

Table 2: Position data of profiles

Date/Day	Time/GMT	Latitude	Longitude	Profile
	14:00	75°17,199`N	05°19,532`W	
	15:00	75°09,337`N	05°39,886`W	
	16:00	75°01,625`N	05°59,805`W	
	17:00	74°54,023`N	06°19,919`W	
	18:00	74°46,054`N	06°40,342`W	
	19:00	74°38,138`N	07°01,625`W	
	20:00	74°30,397`N	07°22,399`W	
	21:00	74°22,956`N	07°42,215`W	
	22:00	74°15,271`N	08°02,223`W	
	23:00	74°07,187`N	08°37,196`W	
30.8.92/243	0:00	73°59,246`N	08°37,196`W	
	1:00	73°51,173`N	08°54,623`W	
	2:00	73°43,649`N	09°12,347`W	
	3:00	73°36,351`N	09°32,441`W	
	4:00	73°28,448`N	09°50,872`W	
	5:00	73°20,386`N	10°09,443`W	
	6:00	73°12,485`N	10°27,574`W	
	7:00	73°04,584`N	10°46,305`W	
	8:00	72°56,964`N	11°04,468`W	
	9:00	72°49,359`N	11°21,814`W	
	10:00	72°41,353`N	11°39,055`W	
	11:00	72°34,359`N	11°53,975`W	
	12:00	72°26,740`N	12°11,132`W	
	13:00	72°18,901`N	12,28,385`W	
	14:00	72°10,718`N	12°45,732`W	
	15:00	72°02,892`N	13°03,641`W	
	15:07	72°01,806`N	13°05,816`W	Ende 2b
	16:00	72°04,503`N	13°28,846`W	
	16:55	72°07,339`N	13°47,850`W	3a
	17:00	72°07,966`N	13°46,415`W	
	18:00	72°15.576`N	13°30,452`W	
	19:00	72°23,275`N	13°13,851`W	
	20:00	72°31,128`N	12°56,878`W	
	21:00	72°38.908`N	12°39,712`W	
	22:00	72°46,405`N	12°23,738`W	
	23:00	72°54,236`N	12°08,070`W	
31.8.92/244	0:00	73°01,826`N	11°51,668`W	
	1:00	73°09,322`N	11°34,838`W	
	2:00	73°14,899`N	11°17,113`W	
	3:00	73°24,478`N	10°58,702`W	
	4:00	73°32,726`N	10°38,706`W	
	5:00	73°40,941`N	10°21,256`W	
	6:00	73°49,075`N	10°03,642`W	
	7:00	73°57,470`N	09°43,706`W	
	8:00	74°05,606`N	09°22,702`W	
	9:00	74°13,510`N	09°04,092`W	
	10:00	74°21,054`N	08°44,946`W	
	11:00	74°29,120`N	08°28,604`W	

Table 2: Position data of profiles

Date/Day	Time/GMT	Latitude	Longitude	Profile
	12:00	74°37,441`N	08°11,287`W	
	13:00	74°45,551`N	07°51,660`W	
	14:00	74°53,107`N	07°31,369`W	
	15:14	75°02.190`N	07°08,709`W	
	16:00	75°07,747`N	06°53,940`W	
	17:00	75°15,405`N	06°34.498`W	
	18:00	75°22,794`N	06°15,777`W	
	19:00	75°30,196`N	05°56,630`W	
	20:00	75°38,033`N	05°37,481`W	
	21:00	75°45,791`N	05°17,352`W	
	22:00	75°53,640`N	04°56,301`W	
	23:00	76°01,197`N	04°35,821`W	
1.9.92/245	0:00	76°08,829`N	04°15,428`W	
	1:00	76°16,256`N	03°55,005`W	
	2:00	76°23,589`N	3°35,061`W	
	3:00	76°31,305 `N	03°13,181`W	
	4:00	76°38,840`N	02°52,552`W	
	5:00	76°46,048`N	02°32,004`W	
	6:00	76°53,079`N	02°12,189`W	
	6:42	76°58,279`N	01°57,130`W	
	6:50	76°59,270`N	01°54,597`W	
	7:00	77°00,381`N	01°51,550`W	
	7:28:00	77°03,921`N	01°41,133`W	3b
	7:31:00	77°04,386`N	01°40,420`W	
	8:00	77°08,402`N	01°36,075`W	
	9:00	77°16,816`N	01°27,006`W	
	10:00	77°25,021`N	01°18,287`W	
	11:00	77°33,542`N	01°09,252`W	
	12:00	77°42,048`N	01°00,745`W	
	13:00	77°50,408`N	00°52,680`W	
	14:00	77°58,609`N	00°44,052`W	
	15:00	78°16,021`N	00°35,250`W	
	16:00	78°16,090`N	00°26,205`W	
	17:00	78°25,277`N	00°16,791`W	
	18:00	78°33,010`N	00°09,056`W	
	19:00	78°41,445`N	00°00,551`E	
	20:00	78°49,657`N	00°10,254`E	
	21:00	78°57,900`N	00°18,370`E	
	21:33	79°02,479`N	00°23,379`E	Ende 3b
	22:00	79°03,784`N	00°07,670`E	
	22:38	79°01,356`N	00°20,472`W	4a
	22:43	79°00,900`N	00°23,631`W	
	23:00	78°58,419`N	00°27,249`W	
2.9.92/246	0:00	78°50,339`N	00°49,426`W	
	0:54	78°43,709`N	01°10,436`W	
	1:00	78°42,899`N	01°11,164`W	
	2:00	78°34,479`N	01°19,825`W	
	3:00	78°25,432`N	01°28,712`W	

Table 2: Position data of profiles

Date/Day	Time/GMT	Latitude	Longitude	Profile
	4:00	78°16,636`N	01°37,906`W	
	5:00	78°07,577`N	01°45,929`W	
	6:00	77°59,073`N	01°54,492`W	
	7:00	77°50,421`N	02°02,000`W	
	8:00	77°41,842`N	02°10,911`W	
	9:00	77°32,993`N	02°19,921`W	
	10:00	77°23,780`N	02°27,550`W	
	11:00	77°15,181`N	02°35,329`W	
	11:35	77°09,825`N	02°40,504`W	4b
	12:00	77°06,645`N	02°47,281`W	
	13:00	76°58,908`N	03°06,737`W	
	14:00	76°51,311`N	03°28,444`W	
	15:00	76°42,015`N	03°55,111`W	
	16:00	76°36,682`N	04°20,456`W	
	17:00	76°28,054`N	04°37,893`E	
	18:00	76°20,010`N	04°57,951`W	
	19:00	76°12,314`N	05°18,620`W	
	20:00	76°04,659`N	05°40,058`W	
	21:00	75°56,926`N	06°00,324`W	
	22:00	75°49,539`N	06°19,187`W	
	23:00	75°41,555`N	06°36,842`W	
3.9.92/247	0:00	75°33,981`N	06°55,900`W	
	1:00	75°26,550`N	07°15,021`W	
	2:00	75°19,015`N	07°33,238`W	
	3:00	75°11,842`N	07°52,974`W	
	4:00	75°04,312`N	08°11,801`W	
	5:00	74°56,472`N	08°30,955`W	
	6:00	74°48,846`N	08°49,292`W	
	7:00	74°41,489`N	09°07,310`W	
	8:00	74°34,345`N	09°24,474`W	
	9:00	74°27,272`N	09°41,232`W	
	10:00	74°19,933`N	09°59,006`W	
	11:00	74°12,734`N	10°16,204`W	
	12:00	74°05,401`N	10°32,325`W	
	13:00	73°57,927`N	10°48,705`W	
	14:00	73° 50,538`N	11° 06,539`W	
	14:30	73°47,070`N	11°14,495`W	
	15:00	73°43,165`N	11°23,503`W	
	16:00	73°35,727`N	11°40,407`W	
	17:00	73°28,079`N	11°56,063`W	
	18:00	73°20,585`N	12°14,463^W	
	19:00	73°13,042`N	12°31,736^W	
	20:00	73°05,340`N	12°46,458`W	
	21:00	72°58,330`N	13°02,824`W	
	21:29	72°54,868`N	13°10,564`W	
	22:00	72°51,134`N	13°18,606`W	
	23:00	72°43,674`N	13°34,112`W	
4.9.92/248	0:00	72°36,363`N	13°50,106`W	

Table 2: Position data of profiles

Date/Day	Time/GMT	Latitude	Longitude	Profile
	1:00	72°29,022`N	14°05,736`W	
	2:00	72°21,838`N	14°20,674`W	
	3:00	72°14,900`N	14°35,092`W	
	3:07	72°14,170`N	14°36,646`W	Ende 4b
	4:00	73°13,797`N	15°00,809`W	
	5:00	72°22,154`N	15°11,209`W	
	5:21	72°22,154`N	15°09,631`W	5
	6:00	72°26,753`N	15°00,523`W	
	7:00	72°33,876`N	14°46,140`W	
	8:00	72°41,099^N	14°30,645^W	
	9:00	72°48,405`N	14°14,716`W	
	10:00	72°55,774`N	13°59,024`W	
	11:00	73°03,033`N	13°44,019`W	
	12:00	73°10,376`N	13°29,023`W	
	13:00	73°17,562`N	13°13,506`W	
	14:00	73°24,99`N	12°58,564`W	
	15:00	73°`32,158`N	12°04,303`W	
	16:00	73°39,506`N	12°27,449`W	
	17:00	73°46,825`N	12°10,775`W	
	18:00	73°54,194`N	11°54,480`W	
	19:00	74°01,510`N	11°38,453`W	
	20:00	74°08,536`N	11°22,403`W	
	21:00	74°15,972`N	11°05,699`W	
	22:00	74°23,283`N	10°49,156`W	
	23:00	74°30,609`N	10°33,086`W	
5.9.92/249	0:00	74°37,910`N	10°16,681`W	
	1:00	74°45,157`N	10°00,169`W	
	2:00	74°52,362`N	09°43,105`W	
	3:00	74°59,735`N	09°27,126`W	
	4:00	75°07,293`N	09°09,417`W	
	5:00	75°14,726`N	08°51,314`W	
	6:00	75°22,075`N	08°33,058`W	
	7:00	75°29,164`N	08°16,481`W	
	8:00	75°36,174 N	07°58,146 W	
	9:00	75°43,331`N	07°40,982`W	
	10:00	75°50,338`N	07°23,014`W	
	11:00	75°57,497`N	07°05,950`W	
	11:50	76°03,012`N	06°52,768`W	
	11:55	76°03,379`N	06°51,710`W	
	12:00	76°03,940`N	06°49,945`W	
	13:00	76°10,481`N	06°28,651`W	
	14:00	76°17,188`N	06°10,481`W	
	15:00	76°24,584`N	05°55,702`W	
	16:00	76°31,830`N	05°37,177`W	
	17:00	76°38,758`N	05°19,074`W	
	17:47	76°44,008`N	05°05,346`W	
	18:00	76°45,920`N	05°02,240`W	Ende 5
	19:00	76°49,893`N	05°20,680`W	

Table 2: Position data of profiles

Date/Day	Time/GMT	Latitude	Longitude	Profile
	19:23	76°48,651`N	05°33,930`W	6
	20:00	76°43,996`N	05°46,611`W	
	21:00	76°36,454`N	06°05,647`W	
	21:30	76°32,833`N	06°15,552`W	
	21:52	76°32,043`N	06°27,577`W	
	22:00	76°31,470`N	06°32,092`W	
	22:23	76°31,071`N	06°46,042`W	
	22:36	76°29,712`N	06°49,708`W	
	23:00	76°26,727`N	06°56,836`W	
6.9.92/250	0:00	76°18,981`N	07°13,927`W	
	1:00	76°12,258`N	07°38,458`W	
	2:00	76°03,764`N	07°57,261`W	
	3:00	75°55,469`N	08°14,701`W	
	4:00	75° 47,751`N	08°33,593`W	
	5:00	75°39,409`N	08°53,122`W	
	6:00	75°31,517`N	09°11,766`W	
	7:00	75°24,109`N	09°29,934`W	
	8:00	75°16,372`N	09°46,788`W	
	9:00	75°09,250`N	10°02,724`W	
	10:00	75°02,399`N	10°18,980`W	
	11:00	74°54,784`N	10°35,902`W	
	12:00	74°47,965`N	10°50,223`W	
	13:00	74°40,744`N	10°09,244`W	
	14:00	74°33,246`N	11°26,825`W	
	15:00	74° 25,706 N	11°44,228`W	
	16:00	74°18,498`N	12°00,390`W	
	17:00	74°11,025`N	12°17,141`W	
	18:00	74°03,810`N	12°32,857`W	
	19:00	73°56,806`N	12°49,188`W	
	20:00	73°49,264`N	13°04,745`W	
	21:00	73°41,979`N	13°20,026`W	
	22:00	73°34,570`N	13°35,789` W	
	23:00	73°27,520`N	13°51,274` W	
7.9.92/251	0:00	73°20,335`N	14°05,975` W	
	1:00	73°13,250`N	14°20,563` W	
	2:00	73°05,932`N	14°35,955` W	
	3:00	72°58,361`N	10°51,520` W	
	4:00	72° 50,822`N	15°06,457`W	
	5:00	72°42,823`N	15° 23,321`N	
	6:00	72°35,157`N	15°38,727`W	
	7:00	72°27,658`N	15°53,644`W	
	7:32	72°23,640`N	16°01,726`W	Ende 6
	8:00	72°24,646`N	16°11,780`W	
	9:00	72°30,538`N	16°29,625`W	
	9:28	72°33,711`N	16°38,127`W	7
	9:50	72°36,348`N	16°35,318`W	
	10:00	72°36,724`N	16°31,778`W	
	10:40	72°38,589`N	16°19,099`W	

Table 2: Position data of profiles

Date/Day	Time/GMT	Latitude	Longitude	Profile
	11:00	72°39,526`N	16°12,286`W	
	11:30	72°42,412`N	16°03,144`W	
	12:00	72°45,625`N	15°55,987`W	
	13:00	72°52,864`N	15°41,664`W	
	14:00	73°00,146`N	15°26,650`W	
	15:00	73°07,409`N	15°12,095`W	
	16:00	73°14,501`N	14°57,673`W	
	17:00	73°21,358`N	14°43,298`W	
	17:29	73°24,589`N	14°36,296`W	Ende 7
	17:53	73°22,890`N	14°29,172`W	
	18:00	73°21,820`N	14°27,941`W	
	19:00	73°12,885`N	14°15,403`W	
	20:00	73°03,801`N	14°04,661`W	
	21:00	72°54,641`N	13°51,074`W	
	22:00	72°45,823`N	13°36,400`W	
	23:00	72°37,036`N	13°25,161`W	
8.9.92/252	0:00	72°28,658`N	13°13,922`W	
	1:00	72°20,800`N	13°03,520`W	
	2:00	72°13,125`N	12°53,201`W	
	3:00	72°05,579`N	12°43,016`W	
	4:00	71°56,791`N	12°38,487`W	
	4:41	71°53,743`N	12°28,307`W	8a
	5:00	71°56,294`N	12°22,900`W	
	6:00	72°03,728`N	12°06,807`W	
	7:00	72°11,899`N	11°50,049`W	
	8:00	72°19,928`N	11°33,224`W	
	9:00	72°27,489`N	11°14,757`W	
	10:00	72°34,876`N	10°56,411`W	
	11:00	72°43,178`N	10°38,626`W	
	12:00	72°52,102`N	10°22,202`W	
	13:00	73°00,975`N	10°04,913`W	
	14:00	73°09,148`N	09°45,528`W	
	15:00	73°16,822`N	09°25,302`W	
	16:00	73°24,740`N	09°04,743`W	
	17:00	73°32,848`N	08°45,786`W	
	18:00	73°40,336`N	08°28,064`W	
	19:00	73°48,659`N	08°07,747`W	
	20:00	73°57,317`N	07°45,915`W	
	21:00	74°06,598`N	07°23,195`W	
	22:00	74°15,890`N	07°05,055`W	
	23:00	74°24,284`N	06°50,383`W	
9.9.92/253	0:00	74°31,361`N	06°29,623`W	
	1:00	74°36,886`N	06°03,650`W	
	2:00	74°43,605`N	05°40,912`W	
	3:00	74°51,124`N	05°21,331`W	
	4:00	74°58,851`N	05°03,282`W	
	5:00	75°07,205`N	04°43,882`W	
	6:00	75°14,913`N	04°24,063`W	

Table 2: Position data of profiles

Date/Day	Time/GMT	Latitude	Longitude	Profile
	7:00	75°22,758`N	04°03,257`W	
	8:00	75°31,164`N	03°41,524`W	
	8:00	75°31,164`N	03°41,524`W	
	9:00	75°39,341`N	03°19,027`W	
	10:00	75°46,838`N	02°56,596`W	
	11:00	75°55,183`N	02°36,293`W	
	12:00	76°05,981`N	02°12,623`W	
	13:00	76°15,852`N	01°45,123`W	
	14:00	76°24,819`N	01°21,324`W	
	15:00	76°32,641`N	00°58,123`W	
	16:00	76°40,294`N	00°34,066`W	
	17:00	76°47,576`N	00°06,676`W	
	17:48	76°53,240`N	00°15,212`E	8b
	18:00	76°54,934`N	00°18,687`E	
	19:00	77°03,554`N	00°30,003`E	
	20:00	77°12,667`N	00°38,741`E	
	21:00	77°21,685`N	00°46,418`E	
	22:00	77°30,836`N	00°54,278`E	
	23:00	77°39,858`N	01°06,393`E	
10.9.92/254	0:00	77°48,379`N	01°21,828`E	
	1:00	77°56,854`N	01°36,689`E	
	2:00	78°06,094`N	01°49,129`E	
	3:00	78°15,626`N	01°57,097`E	
	4:00	78°24,728`N	02°05,728`E	
	5:00	78°33,754`N	02°19,541`E	
	6:00	78°42,622`N	02°31,372`E	
	7:00	78°51,086`N	02°37,346`E	
	8:00	78°59,321`N	02°48,158`E	
	9:00	79°07,608`N	03°02,908`E	Ende 8b
	10:00	79°03,348`N	03°27,117`E	
	11:00	78°56,272`N	03°44,272`E	
	12:00	78°49,848`N	04°04,475`E	
	13:00	78°43,509`N	04°31,438`E	9a
	14:00	78°36,795`N	04°43,954`E	
	15:00	78°28,361`N	04°33,055`E	
	15:40	78°22,675`N	04°26,147`E	
	16:00	78°20,121`N	04°22,649`E	
	17:00	78°11,343`N	04°12,112`E	
	18:00	78°02,589`N	04°00,967`E	
	19:00	77°53,860`N	03°49,799`E	
	20:00	77°45,266`N	03°40,369`E	
	21:00	77°36,712`N	03°27,298`E	
	22:00	77°28,006`N	03°19,660`E	
	23:00	77°19,477`N	03°08,066`E	
11.9.92/255	0:00	77°10,670`N	02°58,541`E	
	1:00	77°01,980`N	02°48,477`E	
	2:00	76°53,299`N	02°38,022`E	
	3:00	76°44,439`N	02°28,478`E	

Table 2: Position data of profiles

Date/Day	Time/GMT	Latitude	Longitude	Profile
	3:38	76°38,919`N	02°21,821`E	9b
	4:00	76°36,188`N	02°12,702`E	
	5:00	76°28,539`N	01°48,230`E	
	6:00	76°20,838`N	01°25,229`E	
	7:00	76°13,293`N	01°02,943`E	
	7:55	76°06,741`N	00°41,921`E	
	8:00	76°06,122`N	00°39,862`E	
	9:00	75°59,313`N	00°17,389`E	
	10:00	75°52,071`N	00°05,098`W	
	11:00	75°45,937`N	00°31,382`W	
	12:00	75°38,923`N	00°53,140`W	
	13:00	75°31,758`N	01°13,530`W	
	14:00	75°24,321`N	01°34,818`W	
	15:00	75°16,853`N	01°55,627`W	
	16:00	75°09,452`N	02°17,245`W	
	17:00	75°01,658`N	02°39,155`W	
	18:00	74°54,293`N	02°59,764`W	
	19:00	74°46,985`N	03°21,600`W	
	20:00	74°39,631`N	03°42,824`W	
	21:00	74°32,075`N	04°02,550`W	
	22:00	74°24,417`N	04°21,670`W	
	23:00	74°17,071`N	04°41,029`W	
12.9.92/256	0:00	74°09,937`N	05°01,455`W	
	1:00	74°02,529`N	05°20,625`W	
	2:00	73°55,069`N	05°39,751`W	
	3:00	73°44,508`N	05°59,951`W	
	4:00	73°39,805`N	06°19,772`W	
	5:00	73°32,302`N	06°38,876`W	
	6:00	73°24,660`N	06°58,059`W	
	7:00	73°17,159`N	07°17,511`W	
	8:00	73°09,732`N	07°36,839`W	
	9:00	73°02,247`N	07°53,566`W	
	10:00	72°55,366`N	08°12,563`W	
	11:00	72°48,049`N	08°29,834`W	
	12:00	72°40,576`N	08°48,450`W	
	13:00	72°32,640`N	09°07,659`W	
	14:00	72°25,029`N	09°26,070`W	
	15:00	72°17,592`N	09°43,653`W	
	16:00	72°09,925`N	10°01,751`W	
	17:00	72°02,272`N	10°19,830`W	
	18:00	71°54,895`N	10°37,435`W	
	19:00	71°47,478`N	10°54,552`W	
	19:10	71°46,271`N	10°57,348`W	

Table 2: Position data of profiles

Date / Day	Time / GMT	Position		
		Latitude	Longitude	air
1.9.92/245	17:00	78°25,277`N	00°16,791`W	
	18:00	78°33,010`N	00°09,056`W	
	19:00	78°41,445`N	00°00,551`E	
	20:00	78°49,657`N	00°10,254`E	
	21:00	78°57,900`N	00°18,370`E	
	21:33	79°02,479`N	00°23,379`E	
	22:00	79°03,784`N	00°07,670`E	
	22:38	79°01,356`N	00°20,472`W	
	22:43	79°00,900`N	00°23,631`W	
	23:00	78°58,419`N	00°27,249`W	
2.9.92/246	0:00	78°50,339`N	00°49,426`W	
	0:54	78°43,709`N	01°10,436`W	
	1:00	78°42,899`N	01°11,164`W	
	2:00	78°34,479`N	01°19,825`W	
	3:00	78°25,432`N	01°28,712`W	
	4:00	78°16,636`N	01°37,906`W	
	5:00	78°07,577`N	01°45,929`W	
	6:00	77°59,073`N	01°54,492`W	
	7:00	77°50,421`N	02°02,000`W	
	8:00	77°41,842`N	02°10,911`W	
	9:00	77°32,993`N	02°19,921`W	
	10:00	77°23,780`N	02°27,550`W	
	11:00	77°15,181`N	02°35,329`W	
	11:35	77°09,825`N	02°40,504`W	
	12:00	77°06,645`N	02°47,281`W	
	13:00	76°58,908`N	03°06,737`W	
	14:00	76°51,311`N	03°28,444`W	
	15:00	76°42,015`N	03°55,111`W	-1.3
	16:00	76°36,682`N	04°20,456`W	-1.4
	17:00	76°28,054`N	04°37,893`W	-1.1
	18:00	76°20,010`N	04°57,951`W	-1
	19:00	76°12,314`N	05°18,620`W	-1.1
	20:00	76°04,659`N	05°40,058`W	-1.3
	21:00	75°56,926`N	06°00,324`W	-0.8
	22:00	75°49,539`N	06°19,187`W	-0.5
	23:00	75°41,555`N	06°36,842`W	-0.4
3.9.92/247	0:00	75°33,981`N	06°55,900`W	-0.5
	1:00	75°26,550`N	07°15,021`W	-0.5
	2:00	75°19,015`N	07°33,238`W	-0.8
	3:00	75°11,842`N	07°52,974`W	-0.5
	4:00	75°04,312`N	08°11,801`W	-0.3
	5:00	74°56,472`N	08°30,955`W	-0.1
	6:00	74°48,846`N	08°49,292`W	0.2
	7:00	74°41,489`N	09°07,310`W	0.4
	8:00	74°34,345`N	09°24,474`W	0.6
	9:00	74°27,272`N	09°41,232`W	1
	10:00	74°19,933`N	09°59,006`W	1

Table 3: Surface Temperatures

Date / Day	Time / GMT	Position		
		Latitude	Longitude	air
	11:00	74°12,734`N	10°16,204`W	1
	12:00	74°05,401`N	10°32,325`W	0.9
	13:00	73°57,927`N	10°48,705`W	1
	14:00	73° 50,538`N	11° 06,539`W	1.1
	15:00	73°43,165`N	11°23,503`W	1.1
	16:00	73°35,727`N	11°40,407`W	1.1
	17:00	73°28,079`N	11°56,063`W	1
	18:00	73°20,585`N	12°14,463^W	1.1
	19:00	73°13,042`N	12°31,736^W	1
	20:00	73°05,340`N	12°46,458`W	0.5
	21:00	72°58,330`N	13°02,824`W	0.5
	22:00	72°51,134`N	13°18,606`W	0.2
	23:00	72°43,674`N	13°34,112`W	-0.1
4.9.92/248	0:00	72°36,363`N	13°50,106`W	0.1
	1:00	72°29,022`N	14°05,736`W	0.3
	2:00	72°21,838`N	14°20,674`W	0.5
	3:00	72°14,170`N	14°36,646`W	1
	4:00	73°13,797`N	15°11,209`W	0.8
	5:00	72°22,154`N	15°09,631`W	0.7
	6:00	72°26,753`N	15°00,523`W	0.5
	7:00	72°33,876`N	14°46,140`W	0.4
	8:00	72°41,099^N	14°30,645^W	0.1
	9:00	72°48,405`N	14°14,716`W	0.1
	10:00	72°55,774`N	13°59,024`W	-0.1
	11:00	73°03,033`N	13°44,019`W	-0.1
	12:00	73°10,376`N	13°29,023`W	-0.1
	13:00	73°17,562`N	13°13,506`W	0.1
	14:00	73°24,99`N	12°58,564`W	0.5
	15:00	73°32,158`N	12°04,303`W	0.8
	16:00	73°39,506`N	12°27,449`W	0.6
	17:00	73°46,825N	12°10,775`W	0.3
	18:00	73°54,194`N	11°54,480`W	0.8
	19:00	74°01,510`N	11°38,453`W	1
	20:00	74°08,536`N	11°22,403`W	0.7
	21:00	74°15,972`N	11°05,699`W	0.6
	22:00	74°23,283`N	10°49,156`W	0.6
	23:00	74°30,609`N	10°33,086`W	0.5
5.9.92/249	0:00	74°37,910`N	10°16,681`W	0
	1:00	74°45,157`N	10°00,169`W	-0.9
	2:00	74°52,362`N	09°43,105`W	-1.2
	3:00	74°59,735`N	09°27,126`W	-0.4
	4:00	75°07,293`N	09°09,417`W	0.5
	5:00	75°14,726`N	08°51,314`W	1
	6:00	75°22,075`N	08°33,058`W	0.6
	7:00	75°29,164`N	08°16,481`W	1.3
	8:00	75°36,174 N	07°58,146 W	1
	9:00	75°43,331`N	07°40,982`W	0.5

Table 3: Surface Temperatures

Date / Day	Time / GMT	Position		
		Latitude	Longitude	air
	10:00	75°50,338`N	07°23,014`W	-0.7
	11:00	75°57,497`N	07°05,950`W	-2.8
	12:00	76°03,940`N	06°49,945`W	-3.2
	13:00	76°10,481`N	06°28,651`W	-3.2
	14:00	76°17,188`N	06°10,481`W	-3.2
	15:00	76°24,584`N	05°53,702`W	-1.7
	16:00	76°31,830`N	05°37,177`W	-1.4
	17:00	76°38,758`N	05°19,074`W	-1.1
	18:00	76°45,920`N	05°02,240`W	-1.5
	19:00	76°49,893`N	05°20,680`W	-1.5
	20:00	76°43,996`N	05°46,611`W	-1.9
	21:00	76°36,454`N	06°05,647`W	-1.8
	22:00	76°31,470`N	06°32,092`W	-2
	23:00	76°26,727`N	06°56,836`W	-2.1
6.9.92/250	0:00	76°18,981`N	07°13,927`W	-1.8
	1:00	76°12,258`N	07°38,458`W	-1.7
	2:00	76°03,764`N	07°57,261`W	-2.2
	3:00	75°55,469`N	08°14,701`W	-1.9
	4:00	75° 47,751`N	08°33,593`W	-0.7
	5:00	75°39,409`N	08°53,122`W	-1
	6:00	75°31,517`N	09°11,766`W	-0.6
	7:00	75°24,109`N	09°29,934`W	-0.2
	8:00	75°16,372`N	09°46,788`W	0.6
	9:00	75°09,250`N	10°02,724`W	0.8
	10:00	75°02,399`N	10°18,980`W	0.4
	11:00	74°54,784`N	10°35,902`W	0.6
	12:00	74°47,965`N	10°50,223`W	0.5
	13:00	74°40,744`N	10°09,244`W	0.1
	14:00	74°33,246`N	11°26,825`W	-0.4
	15:00	74° 25,706 N	11°44,228`W	-0.8
	16:00	74°18,498`N	12°00,390`W	-1.2
	17:00	74°11,025`N	12°17,141`W	-1
	18:00	74°03,810`N	12°32,857`W	-1.4
	19:00	73°56,806`N	12°49,188`W	-1.1
	20:00	73°49,264`N	13°04,745`W	-0.9
	21:00	73°41,979`N	13°20,026`W	-1.2
	22:00	73°34,570`N	13°35,789` W	-1.1
	23:00	73°27,520`N	13°51,274` W	-0.6
7.9.92/251	0:00	73°20,335`N	14°05,975` W	-0.5
	1:00	73°13,250`N	14°20,563` W	-1
	2:00	73°05,932`N	14°35,955` W	-0.9
	3:00	72°58,361`N	10° 51,520` W	-1.1
	4:00	72° 50,822`N	15° 06,457` W	-0.8
	5:00	72°42,823`N	15° 23,321`N	-1
	6:00	72°35,157`N	15°38,727`W	-0.9
	7:00	72°27,658`N	15°53,644`W	-1.1
	8:00	72°24,646`N	16°11,780`W	-1.2

Table 3: Surface Temperatures

Date / Day	Time / GMT	Position		
		Latitude	Longitude	air
	9:00	72°30,538`N	16°29,625`W	-1.6
	10:00	72°36,724`N	16°31,778`W	-2.2
	10:40	72°38,589`N	16°19,099`W	-1.6
	11:00	72°39,526`N	16°12,286`W	-1.1
	11:30	72°42,412`N	16°03,144`W	-0.7
	12:00	72°45,625`N	15°55,987`W	-0.3
	13:00	72°52,864`N	15°41,664`W	-0.3
	14:00	73°00,146`N	15°26,650`W	-0.2
	15:00	73°07,409`N	15°12,095`W	0.4
	16:00	73°14,501`N	14°57,673`W	1.3
	17:00	73°21,358`N	14°43,298`W	2.1
	18:00	73°21,820`N	14°27,941`W	2
	19:00	73°12,885`N	14°15,403`W	2.3
	20:00	73°03,801`N	14°04,661`W	2.3
	21:00	72°54,641`N	13°51,074`W	3
	22:00	72°45,823`N	13°36,400`W	3.1
	23:00	72°37,036`N	13°25,161`W	3
8.9.92/252	0:00	72°28,658`N	13°13,922`W	2.8
	1:00	72°20,800`N	13°03,520`W	3.2
	2:00	72°13,125`N	12°53,201`W	3.2
	3:00	72°05,579`N	12°43,016`W	3.4
	4:00	71°56,791`N	12°38,487`W	3.5
	5:00	71°56,294`N	12°22,900`W	3.7
	6:00	72°03,728`N	12°06,807`W	3.7
	7:00	72°11,899`N	11°50,049`W	3.7
	8:00	72°19,928`N	11°33,224`W	3.6
	9:00	72°27,489`N	11°14,757`W	3.6
	10:00	72°34,876`N	10°56,411`W	3.7
	11:00	72°43,178`N	10°38,626`W	3.6
	12:00	72°52,102`N	10°22,202`W	3.5
	13:00	73°00,975`N	10°04,913`W	3.7
	14:00	73°09,148`N	09°45,528`W	3.7
	15:00	73°16,822`N	09°25,302`W	4,0C
	16:00	73°24,740`N	09°04,743`W	4.1
	17:00	73°32,848`N	08°45,786`W	4
	18:00	73°40,336`N	08°28,064`W	4.2
	19:00	73°48,659`N	08°07,747`W	4.2
	20:00	73°57,317`N	07°45,915`W	4
	21:00	74°06,598`N	07°23,195`W	4.1
	22:00	74°15,890`N	07°05,055`W	4.2
	23:00	74°24,284`N	06°50,383`W	4.4
9.9.92/253	0:00	74°31,361`N	06°29,623`W	4.4
	1:00	74°36,886`N	06°03,650`W	4.2
	2:00	74°43,605`N	05°40,912`W	4.3
	3:00	74°51,124`N	05°21,331`W	4.3
	4:00	74°58,851`N	05°03,282`W	4.4
	5:00	75°07,205`N	04°43,882`W	4.4

Table 3: Surface Temperatures

Date / Day	Time / GMT	Position		
		Latitude	Longitude	air
	6:00	75°14,913`N	04°24,063`W	4
	7:00	75°22,758`N	04°03,257`W	3.8
	8:00	75°31,164`N	03°41,524`W	3.7
	9:00	75°39,341`N	03°19,027`W	4
	10:00	75°46,838`N	02°56,596`W	4.7
	11:00	75°55,183`N	02°36,293`W	5.2
	12:00	76°05,981`N	02°12,623`W	5.5
	13:00	76°15,852`N	01°45,123`W	5.5
	14:00	76°24,819`N	01°21,324`W	5.3
	15:00	76°32,641`N	00°58,123`W	5.3
	16:00	76°40,294`N	00°34,066`W	5
	17:00	76°47,576`N	00°06,676`W	4.7
	18:00	76°54,934`N	00°18,687`E	4.9
	19:00	77°03,554`N	00°30,003`E	5.2
	20:00	77°12,667`N	00°38,741`E	5
	21:00	77°21,685`N	00°46,418`E	5.4
	22:00	77°30,836`N	00°54,278`E	5.1
	23:00	77°39,858`N	01°06,393`E	5.4
10.9.92/254	0:00	77°48,379`N	01°21,828`E	5.2
	1:00	77°56,854`N	01°36,689`E	4.8
	2:00	78°06,094`N	01°49,129`E	4.8
	3:00	78°15,626`N	01°57,097`E	5.1
	4:00	78°24,728`N	02°05,728`E	4.8
	5:00	78°33,754`N	02°19,541`E	4.7
	6:00	78°42,622`N	02°31,372`E	4.7
	7:00	78°51,086`N	02°37,346`E	4.5
	8:00	78°59,321`N	02°48,158`E	4.8
	9:00	79°07,608`N	03°02,908`E	4.4
	10:00	79°03,232`N	03°27,476`E	3.7
	11:00	78°56,272`N	03°44,272`E	4.4
	12:00	78°49,848`N	04°04,475`E	4.4
	13:00	78°43,509`N	04°31,438`E	4.5
	14:00	78°36,795`N	04°43,954`E	4.6
	15:00	78°28,361`N	04°33,055`E	4.5
	16:00	78°20,121`N	04°22,649`E	5.4
	17:00	78°11,343`N	04°12,112`E	5.1
	18:00	78°02,589`N	04°00,967`E	4.9
	19:00	77°53,860`N	03°49,799`E	4.9
	20:00	77°45,266`N	03°40,369`E	4.9
	21:00	77°36,712`N	03°27,298`E	4.9
	22:00	77°28,006`N	03°19,660`E	5.2
	23:00	77°19,477`N	03°08,066`E	4.9
	0:00	77°10,670`N	02°58,541`E	4.9
11.9.92/255	1:00	77°01,980`N	02°48,477`E	4.8
	2:00	76°53,299`N	02°38,022`E	4.8
	3:00	76°44,439`N	02°28,478`E	4.6
	4:00	76°36,188`N	02°12,702`E	4.6

Table 3: Surface Temperatures

Date / Day	Time / GMT	Position		
		Latitude	Longitude	air
	5:00	76°28,539`N	01°48,230`E	4.5
	6:00	76°20,838`N	01°25,229`E	4.5
	7:00	76°13,293`N	01°02,943`E	4.4
	8:00	76°06,122`N	00°39,862`E	4.5
	9:00	75°59,313`N	00°17,389`E	4.6
	10:00	75°52,071`N	00°05,098`W	4.6
	11:00	75°45,937`N	00°31,382`W	4.5
	12:00	75°38,923`N	00°53,140`W	4.5
	13:00	75°31,758`N	01°13,530`W	4.3
	14:00	75°24,321`N	01°34,818`W	4.2
	15:00	75°16,853`N	01°55,627`W	4.2
	16:00	75°09,452`N	02°17,245`W	4.2
	17:00	75°01,658`N	02°39,155`W	4.2
	18:00	74°54,293`N	02°59,764`W	4
	19:00	74°46,985`N	03°21,600`W	3.8
	20:00	74°39,631`N	03°42,824`W	3.9
	21:00	74°32,075`N	04°02,550`W	4
	22:00	74°24,417`N	04°21,670`W	4
	23:00	74°17,071`N	04°41,029`W	4
12.9.92/256	0:00	74°09,937`N	05°01,455`W	4
	1:00	74°02,529`N	05°20,625`W	3.8
	2:00	73°55,069`N	05°39,751`W	3.2
	3:00	73°44,508`N	05°59,951`W	2.8
	4:00	73°39,805`N	06°19,772`W	2.4
	5:00	73°32,302`N	06°38,876`W	2.6
	6:00	73°24,660`N	06°58,059`W	2.4
	7:00	73°17,159`N	07°17,511`W	2.4
	8:00	73°09,732`N	07°36,839`W	2.9
	9:00	73°02,247`N	07°53,566`W	2.6
	10:00	72°55,366`N	08°12,563`W	2.7
	11:00	72°48,049`N	08°29,834`W	2.5
	12:00	72°40,576`N	08°48,450`W	2.4
	13:00	72°32,640`N	09°07,659`W	2.5
	14:00	72°25,029`N	09°26,070`W	2.6
	15:00	72°17,592`N	09°43,653`W	2.9
	16:00	72°09,925`N	10°01,751`W	3
	17:00	72°02,272`N	10°19,830`W	3.2
	18:00	71°54,895`N	10°37,435`W	3.3
	19:00	71°47,478`N	10°54,552`W	3.3

Table 3: Surface Temperatures

PORTUGUESE MARGIN

LISBON-BREST-BREMERHAVEN

7 - 23 August 1993

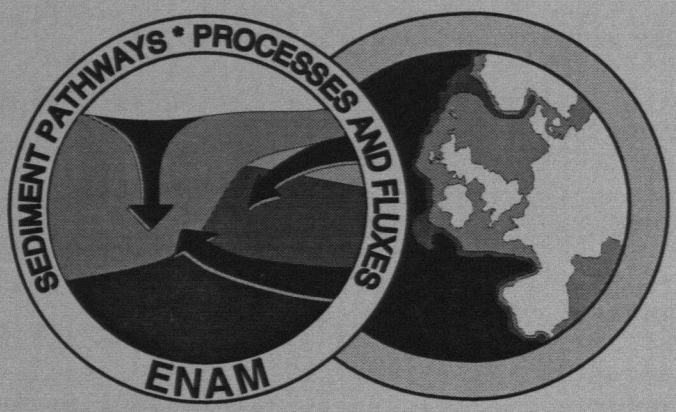

Jürgen Mienert[1]
and shipboard scientific party

[1] GEOMAR, Forschungszentrum für marine Geowissenschaften der Christian-Albrechts-Universität zu Kiel, Wischhofstr. 1-3, 24148 Kiel, F.R.G.

Instituto Geologico e Minero, Rua da Academica das Ciencas 19-28, 1200 Lisboa, PORTUGAL

Aarhus University, AMS Laboratory, Department of Physics, Aarhus, DENMARK

RV POSEIDON PO200/10, LISBON-BREST-BREMERHAVEN, 7 - 23 AUGUST 1993

EUROPEAN NORTH ATLANTIC MARGIN: SEDIMENT PATHWAYS, PROCESSES AND FLUXES

Table of Contents

1. Introduction

The RV POSEIDON cruise 200/10 started the research activities of the **ENAM** programme on the southern margin off Portugal on August 7th, 1993. The European margin research programme called **ENAM** - European North Atlantic Margin: Sediment Pathways, Processes and Fluxes - is funded by the EC under MAST II. **ENAM** is an interdisciplinary research initiative to investigate past changes in thermohaline circulation along the margin and their role in the transport and fluxes of sediments. Various sedimentary processes can occur on the margin which are highly dynamic. Mass wasting processes can remove large (km^3) amounts of sediments downslope, having a profound influence on the margin destruction. Current activities can cause winnowing, sediment transport or complete erosion of sediments. How these sedimentary processes act on the margin in response to climatic changes, is one of the key questions that are to be addressed in the project. The overall goal is to determine European margin developments during glacial and interglacial times which are so complex that a better understanding can only be achieved by merging expertise and resources internationally.

Today's hydrography of the Portuguese margin is mainly influenced by the Mediterranean outflow, which causes highly saline waters to flow north along the margin (Reid, 1979). This situation may have been different during glacial times due to the southward migration of the North Atlantic polar front (Thiede, 1977). The front separated warm subtropical surface waters in the south from cold subpolar surface waters in the north, and it may have determined the role of thermohaline circulation along the Portuguese margin.

We used sedimentological, biological and geochemical properties, measured on sediment cores, to monitor these changes. The cores were taken at five depth transects that range in water depth from 300 m to 2500 m (Figure 1; Table 1). Each transect comprises 4 to 15 site locations which are separated by water depth intervals of 200 m to 500 m (Figures 2-22). The dense sampling interval allows a reconstruction of changes in past water masses.

2. Portuguese margin

After the compression in the Eocene that resulted in the rejuvenation of the rifted margin morphology with the uplift of the Galicia bank and other marginal seamounts (Porto and Vigo), a progressive regional subsidence with minor tilting of the western Iberian margin took place. This allowed the accumulation of hemipelagic sediments at selected locations on the continental slope and rise. The segmentation of the margin by submarine canyons and uplifted areas conditioned the site selection to locations where the sediment accumulation took place.

Sedimentary processes at the margin are dominated by bottom current activity as reflected in the occurrence of contourite drifts, that have developed since the Eocene. The drifts buildup is in direct relationship with the bottom current activity driven by the Atlantic thermohaline circulation. The Mediterranean Outflow Water (MOW) along the slope is particularly important for the sediment transport at water depths ranging from 500m - 1500m. Ice-rafted debris, which may be related to the southern extent of the polar front during glacial times, has been identified (Heinrich, 1988).

The identification of sources of sediment in different drainage basins along the margin may help to distinguish local processes from more regional sediment transport patterns. It allows to determine climatic changes that have affected the circulation as well as the transport and fluxes of particles on the Portuguese margin.

Site selections

A compilation of formerly collected data was made from the Instituto Geologico e Minero files. The area surveyed was divided into 3 major regions and detailed bathymetric charts were prepared as follows:

(1) A map for the margin offshore Sines from 37° 20'N to 38° 20'N for the transect I (Figure 1). The pre-cruise sites for transect I were selected by compiling seismic data (SINFAR , METEOR 67 , ATLANTIS II EACM, HESPERIDES 76). Previous samples from SINFAR, LIVRA and preliminary results of PALEOCINAT II (cores 24, 25, 26, 27, 28), SONNE SO 75-3 (cores 2, 3, 4, 6, 7,1 0, 12, 14, 23, 26, 31, 32, 34, 35) as well as the results of the FAEGAS V (cores 20, 21, 22, 23, 24, 25,2 6) were taken into account for the site selections.

(2) A map of the margin off the Mondego River from 39° 40'N to 40° 40'N was used for pre-locating sites in transects II, III and IV (Figure 1). The margin between the canyons of Aveiro and Nazaré has a complex geological structure with steep slopes and faulted blocks, which have affected sediment accumulation. Exposures of basement rocks are apparent on 1978 GLORIA images. Existing seismic data were used to identify thick sediment sequences (LUSITANIE, HESPERIDES 78 and FLORENCE OC102 and 103). Sediment data for this area are less abundant than for the transect I area. Only data from the FAEGAS V results were used (cores 11, 12, 14,16, 17, 18, 19). Cores 11 and 12 were quantitatively studied for primary productivity changes during the Quaternary and revealed a coherent record of oscillations related to changes in upwelling intensity during the glacial/interglacial changes (Abrantes, pers. comm.).

(3) A map of the margin north off Porto from 41°N to 42°N was used for pre-locating sites in transect V (Figure 1). For this area less information is available about slope sedimentary features and processes than for the areas mentioned above. Only seismic data from FLORENCE OC103 and OC 104 were available. Sediment cores from FAEGAS V (cores 6, 7, 8, 9) provided information about sedimentary records.

3. Scientific objectives

For the achievement of the overall objectives, several specific objectives are to be accomplished on the Portuguese margin:

1. The identification and mapping of features of the surface and subsurface that are associated with sediment instability and/or transport of sediments.

2. The determination of an event chronology for temporal and lateral magnitudes of material fluxes and environmental changes.

3. The delineation of the role of various sedimentary processes in the progradation of the shelf interglacial/glacial cycles during the last m.y.

The Portuguese margin studies provide the southernmost transects in our programme. More specifically there are to be established:

(i) A ^{14}C stratigraphy and chronology for the last 40,000 years to determine the depositional history and the existence and extend of meltwater pulses along the European margin;

(ii) A relationship between the present hydrography and the distribution of benthic and planktic foraminifera to understand the environmental development in the Holocene;

(iii) An oxygen isotope record transect along the Portuguese margin to improve our knowledge about changes in water masses in relationship to climate changes.

These studies contribute to a better understanding of sediment transport processes during glacial/interglacial times and help to identify the relative importance of along-slope and downslope transport during climatic changes.

3.1. ^{14}C dating by accelerator mass spectrometry
(AMS-Laboratory, Aarhus University)

From the cores of the 5 transects (Figure 1), samples of foraminifera, macrofossils and organic matter will be selected for ^{14}C dating. The limited amount of sample material necessitates the use of the relatively new AMS method, which allows ^{14}C datings of samples 1000 times smaller than those required for conventional ^{14}C dating.

^{14}C dating is based on measurement of the content of the radioactive carbon isotope ^{14}C (halflife approx. 5,700yrs) relative to the stable isotope ^{12}C in organisms which have derived their carbon content, directly or indirectly, through the food chain. When the carbon uptake stops with the death of the organism, the $^{14}C/^{12}C$ ratio decays with the halflife of ^{14}C and the age may be calculated from the measured ratio.

In the conventional method, the ^{14}C content is obtained by measuring the radiation from the decay of ^{14}C in the sample, for example by means of a proportional counter. Due to the relative long halflife of ^{14}C, the radiation intensity is low and a large sample of 1g of carbon has to be measured to give 1% counting statistics in 1-2 days.

In contrast to this, AMS uses advanced forms of mass spectrometric methods to isolate and count the ^{14}C atoms individually rather than to detect the radiation from their decay. For this purpose a so-called electrostatic tandem accelerator, operated by the Van de Graff charging principle at a terminal voltage of 3 million volts, is used. Single carbon ions from a graphitized sample are accelerated to a high velocity, which allows separation in several stages by magnetic fields of the ^{14}C atoms, which are isolated free of interference from molecular ions and identified individually in a particle detector. The extremely low abundance of ^{14}C of 10^{-12} for a modern sample puts a very high demand on selectivity in the separation. Since the "sorting" of the carbon atoms can be done more efficiently in a short time instead of waiting for the decay of the ^{14}C atoms, 1mg samples of carbon can be measured in 0.5-1 hour to better than 1% statistical uncertainty depending on the age of the sample.

Thus about 10mg of carbonate (i.e. 1.2mg of carbon) from e.g. 400-1200 foraminifera is sufficient for both AMS ^{14}C dating and high precision ^{13}C and ^{18}O measurements by conventional mass spectrometry.

Foraminifera are the main sample type for ^{14}C dating because of their normally high abundances. Since the small foram shells are prone to redeposition, it is proposed to perform comparative dating on some of the sporadically occuring and less easily transported macrofossil

shells to serve as an indicator of possible deposition of microfossils.

3.2. Impact of the Mediterranean outflow on benthic foraminiferal assemblages (Instituto Geologico e Minero, University of Bergen, GEOMAR)

Benthic foraminiferal assemblages react very sensitively to environmental changes. The distribution pattern of certain benthic foraminiferal species is often similar to the areal extent of distinct sediment facies, oceanographic conditions or coastal upwelling. Their community settings provide an oceanographic tool to deliniate present areas of specific environmental conditions. It also allows to estimate paleoceanographic conditions by studying ^{14}C-dated sediment cores.

The main topic of this study is to describe the spreading of the MOW along the Portuguese margin by using the occurrence pattern of benthic foraminifera. Living species or assemblages have to be assessed with an occurrence pattern matching the present MOW distribution. Their ecological environment should be largely influenced by the MOW, e.g. by water turbulence, suspension load, boundary layers. Biotic interactions and colonisation structures may reveal the dominance of these factors for MOW-indicative species. Potential hard substrates and other free-standing organisms, e.g. bryozoans and sponges, have to be examined carefully. Species with elevated habitat preferences have to be determined and their population density in different heights above the sea floor has to be evaluated. Independent evidence for the intensity of MOW-current activity has to be obtained from the grain size distribution of surface and subsurface sediments.

Previous work on RV Sonne cruise SO-75 (1991) and SO-83 (1992) between the C. de Sines and C. de San Vincente provided some surface samples (Kudrass, 1993) from the southernmost Portuguese margin close to our transect Io (Figure 1). They comprise a rather coarse grid and most of the stations extend along a traverse perpendicular to the continental slope at 36° 50'N. Benthic foraminifers, grain size data and surface structures reveal that current strength has its maximum near the upper level of the MOW and that the intensity decreases northwards. *Planulina ariminensis* and other elevated, epibenthic suspension feeders, are abundant in sand-rich samples near the upper MOW level. The existing distribution of samples allows only very limited interpretations and is, therefore, unsuitable to determine the faunal distribution along the margin and their relationship to the hydrography. Our additional samples allow to fill these gaps.

3.3. Are there gassy sediments on the Portuguese margin? (Danish Geological Survey)

In the event of considerable amounts of gas in the sediments, samples of gas for chemical and isotopic analysis are to be collected from gravity cores for chemical and isotopic analysis. This study will allow to determine the changes in gas composition, if any gas is present, between the northern and the southern European margin. The following procedure has been applied: a 4 mm hole is drilled into the capped liner and the tip of a 60 ml syringe is placed in the hole as quickly as possible. It may take 30 minutes or even more for the gas to migrate out of the sediment. After sampling, the gas is transferred into a 15 ml Vacutainers (serum test tubes). We did not encounter traceable amounts of gas in our transects.

3.4. Sediment architecture and sediment fluxes on the Portuguese margin (Instituto Geologico e Minero, Danish Geological Survey, University of Bergen, GEOMAR)

The field and laboratory contribution of Instituto Geologico e Minero to ENAM is to obtain high resolution stratigraphic profiles and sedimentary records of changes in organic productivity. This includes :

(1) Analysis of existing seismic and core data of the Portuguese margin in order to evaluate the coring sites where accumulation rates are high and undisturbed records of the coastal climatic changes are expected to be preserved.

(2) Participation in the evaluation of downslope core transects from 200 to 2000 metres off the Portuguese margin (37° to 42° N).

(3) Production of high resolution stratigraphic profiles from selected box and gravity cores from the continental slope off Portugal. For this purpose faunal studies of foraminifera, oxygen isotope stratigraphy, AMS C-14, Pb-210 and Cs-137 dating are to be conducted on selected samples in co-operation with the Danish Geological Survey, Aarhus University and GEOMAR.

(4) From cores with a detailed stratigraphic control, high resolution records of productivity changes that resulted from changes in coastal upwelling throughout the Quaternary are to be produced, based on productivity indicators such as diatoms and organic carbon.

4. Field operations

4.1. Weather conditions

During the cruise, the weather was mostly sunny, partly foggy, and the sea state (< Bft 5) provided ideal conditions for our research activities.

RV POSEIDON embarked from Lisbon on August 7th, 1993 at 08:15h. After 20hrs of steam time, we started our coring programme on the shelf and continued downslope of the Portuguese margin. We finished our five coring transects (Figure 1) on August 15th, left the northern working area at 01:00h, and sailed towards Brest, which was reached on August 19th. The ship docked in Brest and left the port on the same day. It reached Bremerhaven on August 23th, 1993.

4.2. Sediment sampling

We collected 67 sediment cores using an up to 50 cm long box corer and an up to 600 cm long gravity corer (Figures 2-15, and Figures 16 - 23; Table 1). The gravity cores were taken with a liner (Ø 12.5 cm) in a core barrel using a core weight of 1.3 tons.

Unfortunately, the EPC-recorder of the 3.5 kHz sediment subbottom profiler failed at the beginning of the cruise and we therefore had a lack of pre-site information. However, existing seismic profiler records gave us some background information for the selection of possible coring sites. Nonetheless, only a very restricted pre-examination of the sea floor was possible and the deployment of coring devices was at a higher risk.

The following damages and losses occurred during the coring operations:

09/08	11:18h	station 8	total loss of the box corer
10/08	14:19h	station 11	distorted core barrel
11/08	11:10h	station 17	distorted core barrel
11/08	17:17h	station 20	distorted core barrel
12/08	13:58h	station 24	distorted core barrel
13/08	23:05h	station 33	distorted core barrel
14/08	04:27h	station 34	distorted core barrel
14/08	17:44h	station 42	distorted core barrel

Two core catchers were damaged after touching a stone and two have completely been bent. The cutting of the damaged core barrels provided two short 2.5 m gravity corers and two core catchers were suitably arranged to improve the deployment of gravity corers in this environment of highly variable sediment stiffness. The short barrels provided information about upper sea floor sediment stiffness. Six meter long core barrels were used in soft sediments only, to avoid a further bending.

Box cores

The box cores provided undisturbed sea floor samples. Both the sediment surface and one side of the core were photographed. Afterwards, the surface macro-biota was described briefly. If the surface showed meio-benthos such as shells, bryozoa, and tubeworms, we removed and conserved it in alcohol for onshore studies. The 50 x 50 cm box core surface was devided into four quadrants. The first quadrant was subsampled for present day fauna assemblages. A rectangular sampler with a size of 20 x 20 x 2 cm was pushed into the sediment and, with a spatula, the sediment was scraped off and put into an 1 l plastic jar. A concentration of "rose bengal" in alcohol was added and mixed well with the sample to preserve biota and to differentiate living from dead biota (Lutze and Altenbach, 1991). The second quadrant was subsampled for analysis of organic matter. A 12.5 cm diameter PVC tube was pushed into the sediment of the box core. The tube was removed and capped at the base and the top. Sediment cores which are to be analysed for organic matter were stored upright in a freezer at a temperature of -20° C. The third quadrant was subsampled for lithologic/stratigraphic analysis using another 12.5 cm diameter PVC tube. The fourth quadrant was subsampled for geochemical analysis and dating (Cs-137). The procedure was the same as for the second and third quadrant.

Gravity cores

Liner of sediment cores were processed from the bottom to the top. A line on a liner marked the core orientation, a necessity for paleomagnetic measurements. One meter sections were labelled in a sequential way (from bottom to top) using roman numbers on both sides of the core (example Core Po200/10-1 section I 0-50 cm). Arrows point towards the core top in each section. Selected cores were opened and cut into halves. One half was put immediately aside in a plastic liner and closed at both ends. The second half was photographed and described using ODP references.

Sampling of the working half of cores was done in the following way: At the top of the core and at every 10 cm downward two samples were taken; one for lithological (L) and oxygen

isotope (I) analysis and one for diatom (D) analysis. For the diatom analysis, we collected 2 cc with a 5 cc syringe labelled with the core number, section and sample depth. For the lithological and oxygen isotope analysis a 60 cc syringe was used. In between (5, 15, 25 cm etc.) subsamples with a known volume of about 20 cc were taken to study the foram assemblages. For organic analysis, 1 cm slices at 10 cm intervals were cut off the sediment, wrapped in aluminium foil, put in plastic bags and stored in a freezer at -20° C.

Gas sampling took place at intervals of 100 cm. A 4 mm hole was drilled into the liner and a 60 cc syringe was inserted. After 30 minutes the syringe was removed. In the cores sampled no gas has been observed.

5. Preliminary cruise results

Surface and subsurface observations made on sediment cores onboard RV POSEIDON document the impact of the MOW on the sediments. With the exception of core PO 200/10-1, ripples and irregular surface undulations of up to 8 cm height have only been observed in the MOW water-depth interval from 600 to 1500 m (Figure 24). The highest amplitudes occur in the upper part of the MOW. As the observation range is confined to the size of the box corer, these values may be lower than the true surface roughness. A photographic survey of the sea floor in water depths between 1000 and 1200 m, carried out on RV SONNE cruise SO75, shows mud ripples with a height of a few centimetres and wavelengths of approximately 30 cm (Kudrass et al., 1993) which confirms the above results.

Tubular suspension-feeding foraminifers, *e.g. Saccorhiza ramosa* and *Rhizammina abyssorum*, are more abundant within the MOW depth-interval than above and below (Figure 24). They are more frequent in the southern part of the study area. At stations with a high surface morphology, however, these fragile organisms are less abundant and mostly concentrated in depressions.

Pteropod shells on the sediment surface have only been observed in box-cores from the lower part of the MOW and waterdepths below. The highest abundances have been recognized near the lower MOW limit.

The surface observations confirm the results on MOW activity as obtained from grain-size data (Schönfeld, 1993). Ripples and surface undulations indicate active sediment transport and redeposition in the MOW depth-interval with the highest current activity in the upper part. Pteropod shells are kept in turbulence in the upper part of the MOW and accumulate near the

base of the MOW where the turbulence decreases. Higher abundances of tubular suspension-feeding foraminifers also display current activity in the MOW depth-interval. From their higher abundances in the southern part may be concluded,that the suspension concentration, and thus the current velocity, decreases northwards.

Macrofauna

Macro invertebrates collected from the sediment surface and determined by Dr. A. Brand, Institute of Polar Ecology Kiel, show a wide variety of organisms which are given for each box core as follows:

PO 200/10-1-1 (246 m waterdepth):

1 ophiurid: *Ophiura albida*

1 fragment of a regular echinoid with attached epibenthic foraminifers: *Textularia pseudogramen* and *Hanzawaia concentrica*

PO 200/10-1-2 (247 m waterdepth):

4 crinoids: *Leptometra phalangium*

1 amphipod belonging to the suborder Gammerioidea

2 ophiurids: *Ophiura albida* and *Ophiotrix fragilis*

1 little bivalve

1 colony of polychaets, overgrown with serpulids and hydroids

1 holoturid

1 priapolid

PO 200/10-2-2 (368 m waterdepth):

1 polychaet worm in a chitineous tube

1 ophiurid

1 amphipod belonging to the family Lysianassidae

2 large arenaceous foraminifers: *Spiculosiphon* sp.

PO 200/10-3-1 (819 m waterdepth):

2 different polychaet tubes

1 piece of ship clinker overgrown with serpulides and hydroids

1 sponge: *Pheronema* sp.

PO 200/10-4-1 (1265 m waterdepth):

1 siliceous sponge, 3 cm in diameter, with long spines where numerous

epibenthic foraminifers, among others *Epistominella exigua*, are attached.
1 polychaet tube

PO 200/10-5-1 (550 m waterdepth):
1 green polychaet worm in a chitineous tube which is also squatterd by a nematod
1 bivalve: *Astarte* sp.

PO 200/10-6-1 (1103 m waterdepth):
1 crinoid with a stem of 7 cm length: *Ptilocrinus pinnatus.*
Only a few foraminifers are attached to the stem.
1 sponge, 1 cm in diameter.

PO 200/10-7-1 (1471 m waterdepth):
1 polychaet tube
3 pebbles with attached serpulides and foraminifers: mostly *Cibicides lobatulus.*

PO 200/10-10 (227 m water depth):
many corals: *Cariophyllia smithi*

5.1. Core logging records of Portuguese margin sediment cores: sedimentary processes

Core logging

On board of the RV Poseidon magnetic susceptibility was determined for some gravity cores and box cores. About half of these cores were subsequently opened for macroscopic description. The remaining half was processed with a core logger onshore at GEOMAR before being opened in the sediment laboratory. The core logger measures magnetic susceptibility, changes in p-wave amplitudes and velocities, and bulk density of sediments (Figures 3-15).

Magnetic susceptibility

The magnetic susceptibility data collected on board and at GEOMAR show similar trends. However, the absolute values are different, due to the different measurement techniques. Background susceptibility values are about 20 for cores processed at GEOMAR. Increasing and

decreasing susceptibility values occur on different length scales indicating changes in the sedimentary environment. Susceptibility peaks (up to 50) occur in several cores. They may correspond to ice-rafted material, i.e. the Heinrich layers. At first sight, no significant correlation exists between adjacent cores. However, it should be emphasized that at this point, the cores were not compared in detail and no correlation statistics was done.

Bulk density and P-wave velocity

Bulk density mainly varies between 1.5 g/cm^3 and 2.2 g/cm^3. Bulk density usually increases from top to bottom in cores, as expected in normally consolidating sediments. High and low density values are present and may denote differences in mineralogical composition and/or water content.

The propagation velocity of P-waves through the sediment mainly varies between 1500 m/s and 1600 m/s. In longer cores, a positive correlation between bulk density and sound wave velocity is apparent. Hence, acoustic impedances, calculated by the product of density and velocity, enhance existing peaks in the data sets. Therefore, synthetic seismograms will be made shortly, as they may allow to correlate acoustically between sediment cores.

6. Cruise participants

Tim Bergmann	Geophysics	GEOMAR-Forschungszentrum für marine Geowissenschaften, Wischhofstr. 1-3, 24148 Kiel, Germany
Christian Berndt	Geophysics	GEOMAR-Forschungszentrum für marine Geowissenschaften, Wischhofstr. 1-3, 24148 Kiel, Germany
Janine Fest	Geophysics	GEOMAR-Forschungszentrum für marine Geowissenschaften, Wischhofstr. 1-3, 24148 Kiel, Germany
Foster Harps	Technician	GEOMAR- Technology GmbH, Wischhofstr. 1-3 , 24148 Kiel, Germany
Dr. Jan Heinemeier	Physics	Aarhus University, AMS Laboratory, Department of Physics, Aarhus, Denmark
Dr. Jürgen Mienert	Chief scientist	GEOMAR-Forschungszentrum für marine Geowissenschaften, Wischhofstr. 1-3, 24148 Kiel, Germany
Dr. Jose Monteiro	Sedimentology	Instituto Gelogico e Minero, Rua da Academica das Ciencas 19-28, 1200 Lisboa, Portugal
Joao Moreno	Micropaleontology	Instituto Gelogico e Minero, Rua da Academica das Ciencas 19-28, 1200 Lisboa, Portugal
Anja Wersinski	Sedimentology	GEOMAR-Forschungszentrum für marine Geowissenschaften, Wischhofstr. 1-3, 24148 Kiel, Germany
Manon Wilken	Sedimentology	GEOMAR-Forschungszentrum für marine Geowissenschaften, Wischhofstr. 1-3, 24148 Kiel, Germany
Dietmar Wilkens	Coring/Geophysics	GEOMAR-Forschungszentrum für marine Geowissenschaften, Wischhofstr. 1-3, 24148 Kiel, Germany

7. References

Heinrich, H. (1988): Origin and Consequences of Cyclic Ice Rafting in the Northeast Atlantic Ocean during the past 130,000 years. Quaternary Res., 29: 142-152.

Kudrass, H.R. (1993): Photographic survey of the sea floor. - In: Kudrass H.R. (Ed.): SONNE CRUISE SO-75-3 1991. Survey and Sampling of the Southwestern Portuguese Continental Slope: 60-63; Hannover (Rept., Bundesanst. für Geowiss. und Rohstoffe).

Lutze, G.F. & Altenbach, A.V. (1991): Technik und Signifikanz der Lebendfärbung benthischer Foraminiferen mit Bengalrot. - Geol.Jb., A128: 251-265.

Reid, J. L. (1979): On the contribution of the Mediterranean Sea outflow to the Norwegian-Greenland Sea. Deep-Sea Res., 26: 1199-1223.

Schönfeld, J. (1993): Sedimentological studies: preliminary results on lithofacies, grain-size distribution and carbonate content. - In: Kudrass, H.R. (Ed.): SONNE CRUISE SO-75-3 1991. Survey and Sampling of the Southwestern Portuguese Continental Slope: 67-96; Hannover (Rept., Bundesanst. Geowiss. und Rohstoffe).

Thiede, J. (1977): Aspects of the variability of the glacial and interglacial North Atlantic boundary current (last 150,000 years). "Meteor" Forsch. Ergebn., 28C, 1-36.

8. Acknowledgments

We thank Captain Andresen and his crew of the research vessel POSEIDON for their good co-operation and excellent assistance during the research programme. We thank Drs. Joachim Schönfeld and Jaco H. Baas for their contribution to the preliminary cruise results, and Dipl. Phys. Martin Rahlfs for the logging of sediment cores. Permission to work within Portuguese waters was granted by the Ministerio dos Negocios Estrangeiros of Portugal. The chief scientist thankfully acknowledges funding for this co-operative European research by the EC under MAST II in Brussels; the support for ship time by the BMFT and DFG in Bonn, and the logistic support by the Institute of Meereskunde in Kiel.

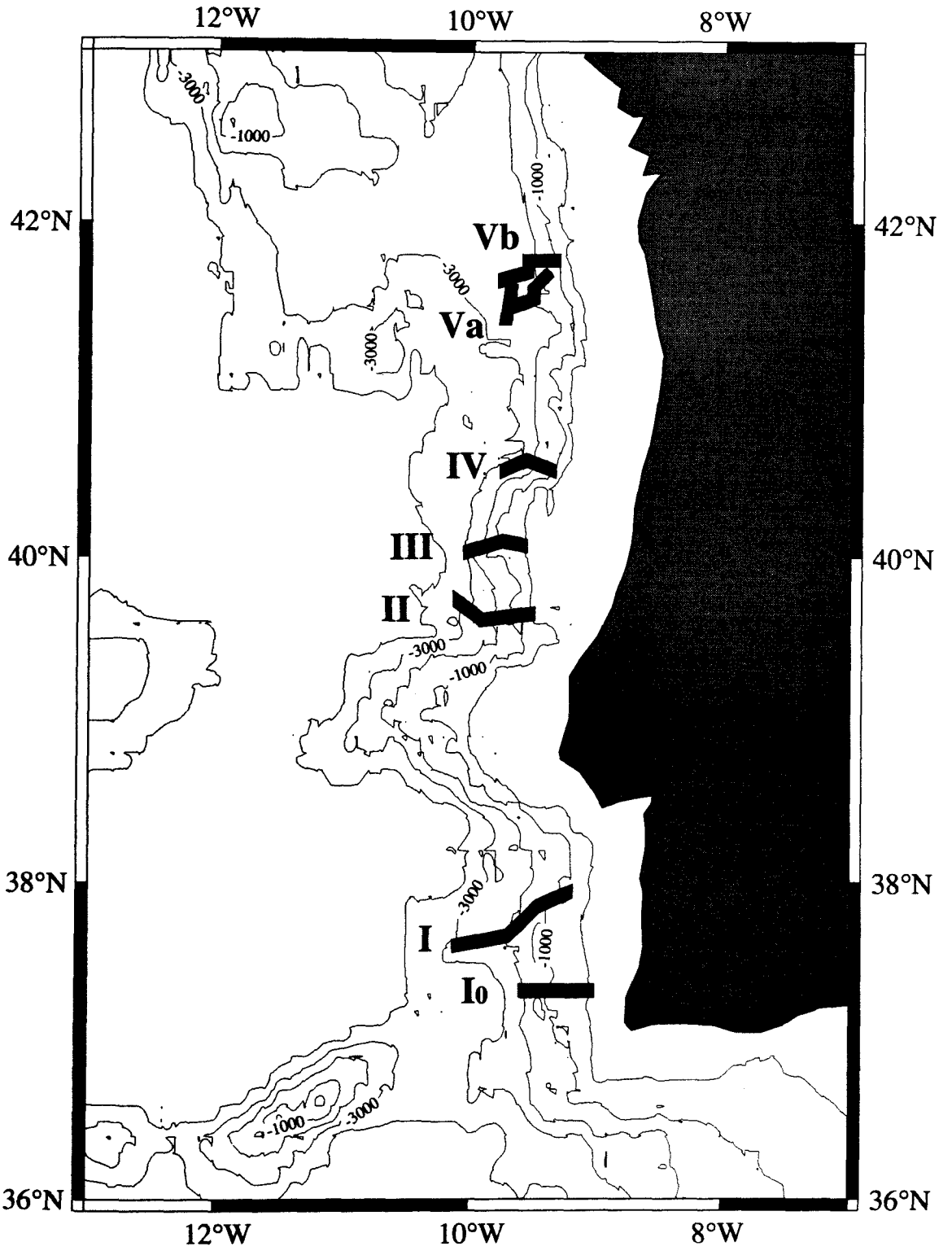

Figure 1a. Bathymetry map of the Portuguese margin showing PO 200/10 transects Io to Vb

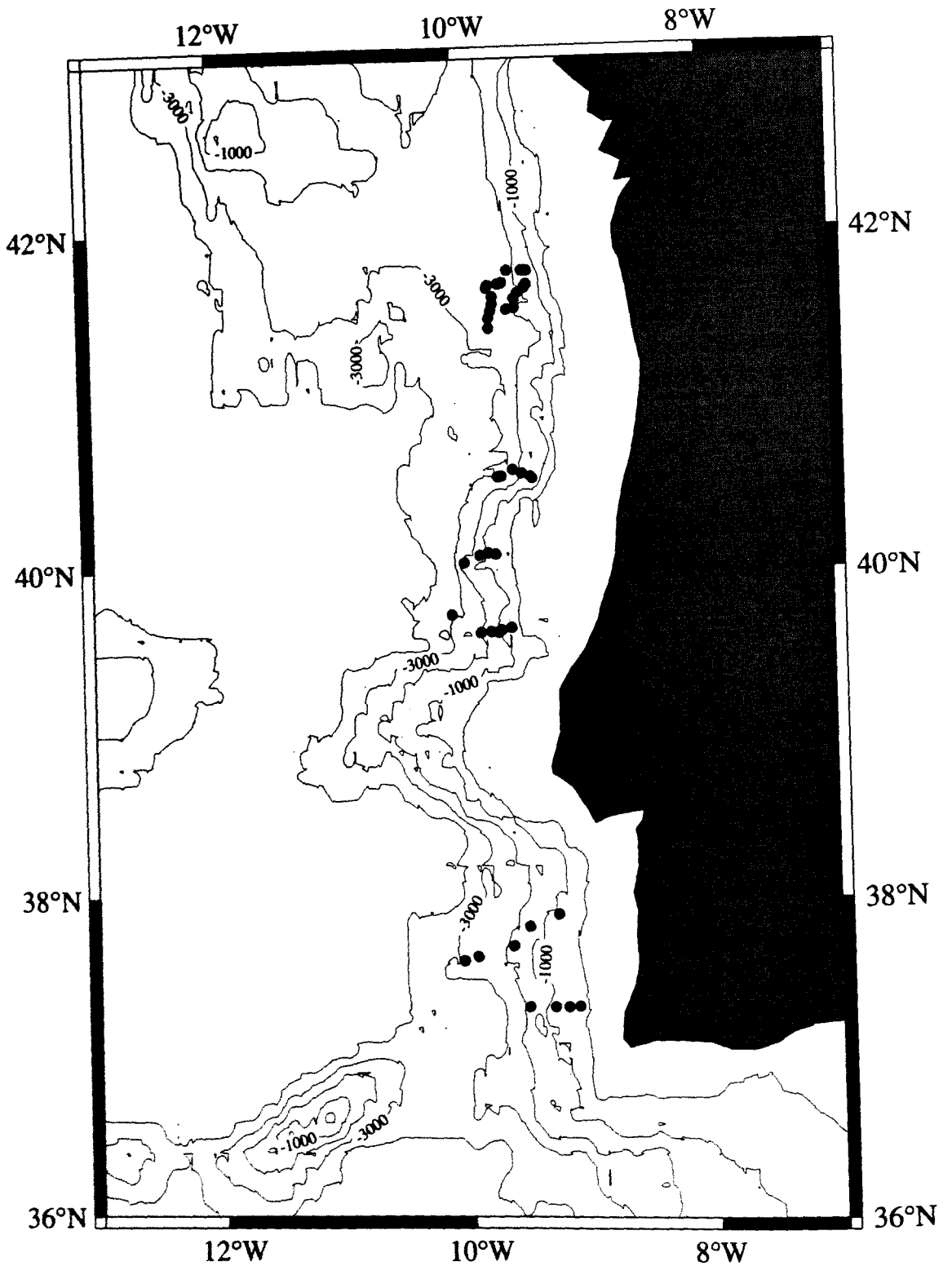

Figure 1b. Poseidon 200/10 core stations on the Portuguese margin

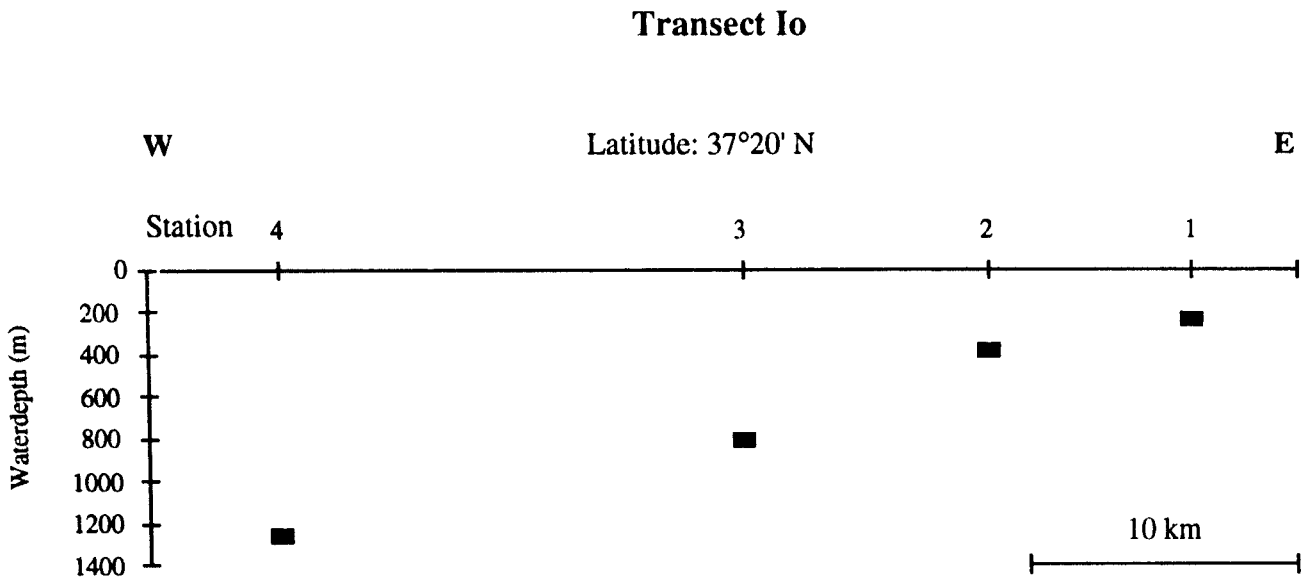

Figure 2. Core stations on southernmost transect Io, showing waterdepth of core positions projected on 37°20' N Latitude

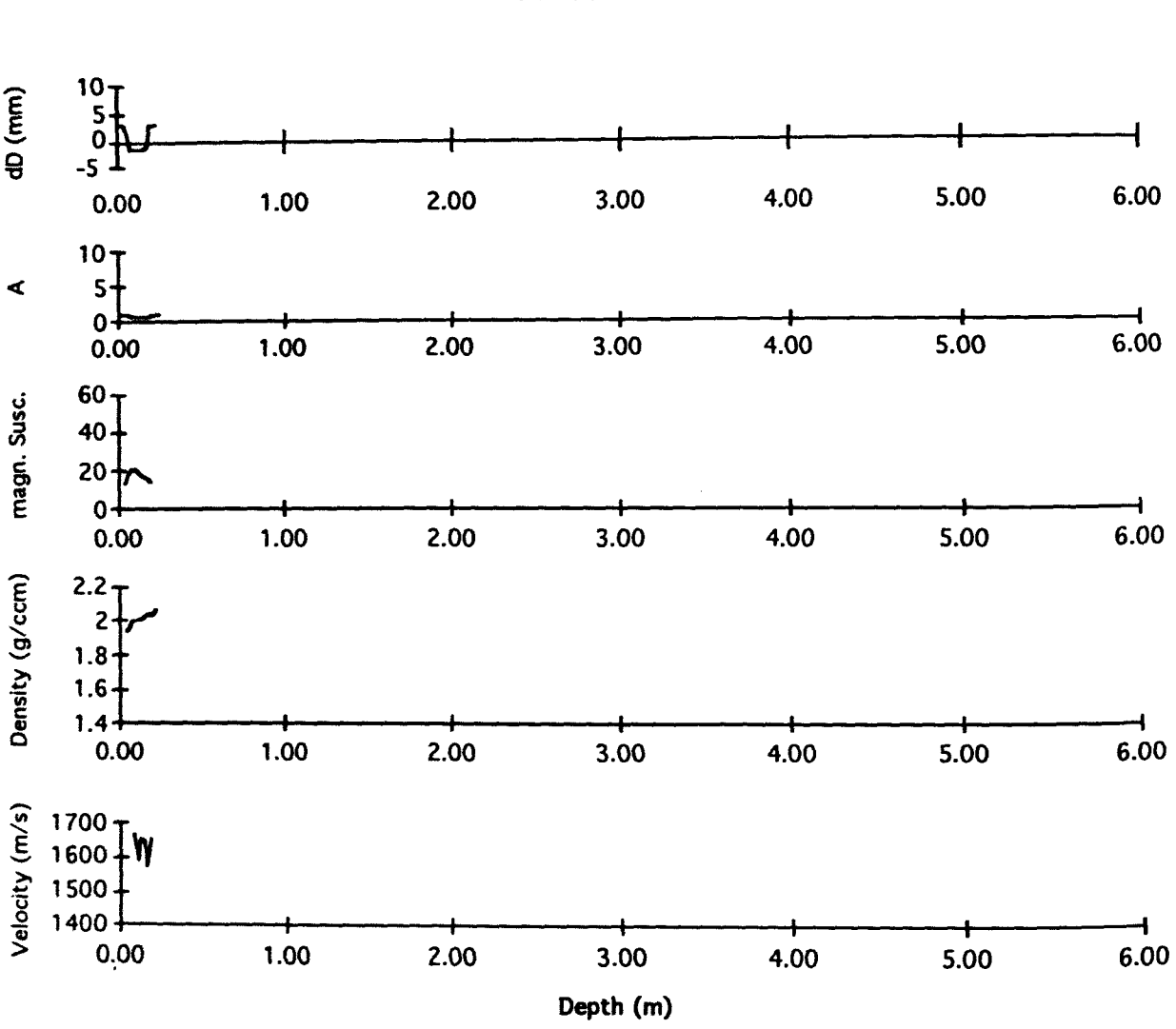

Figure 3a. Physical properties of core 1-2 derived from continous logging. From top to bottom are shown: deviation from standard core diameter, changes in wave amplitude, magnetic suszeptibility (cgs), density (g/cc) and velocity (m/s).

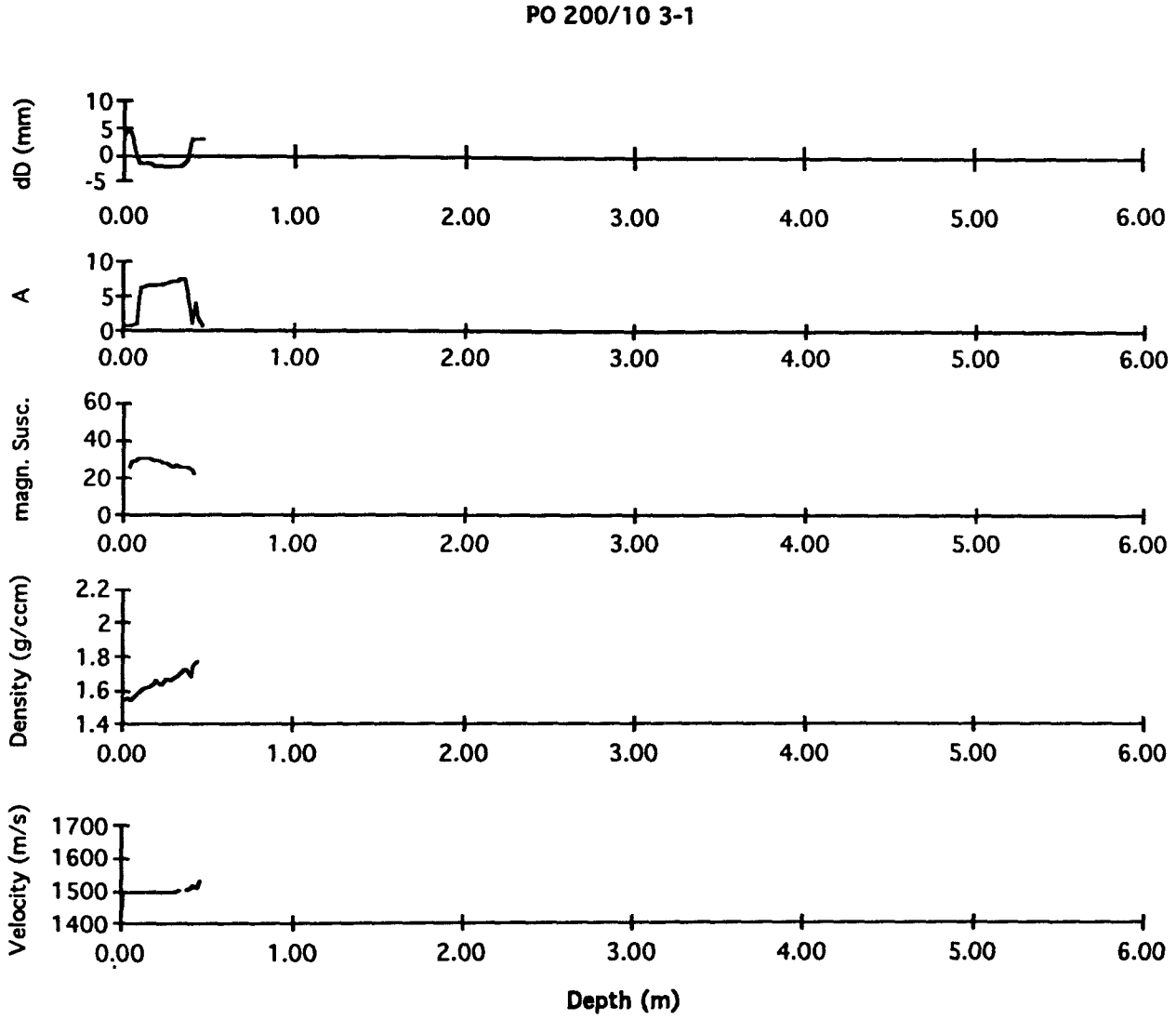

Figure 3b. Physical properties of core 3-1 derived from continous logging. From top to bottom are shown: deviation from standard core diameter, changes in wave amplitude, magnetic suszeptibility (cgs), density (g/cc) and velocity (m/s).

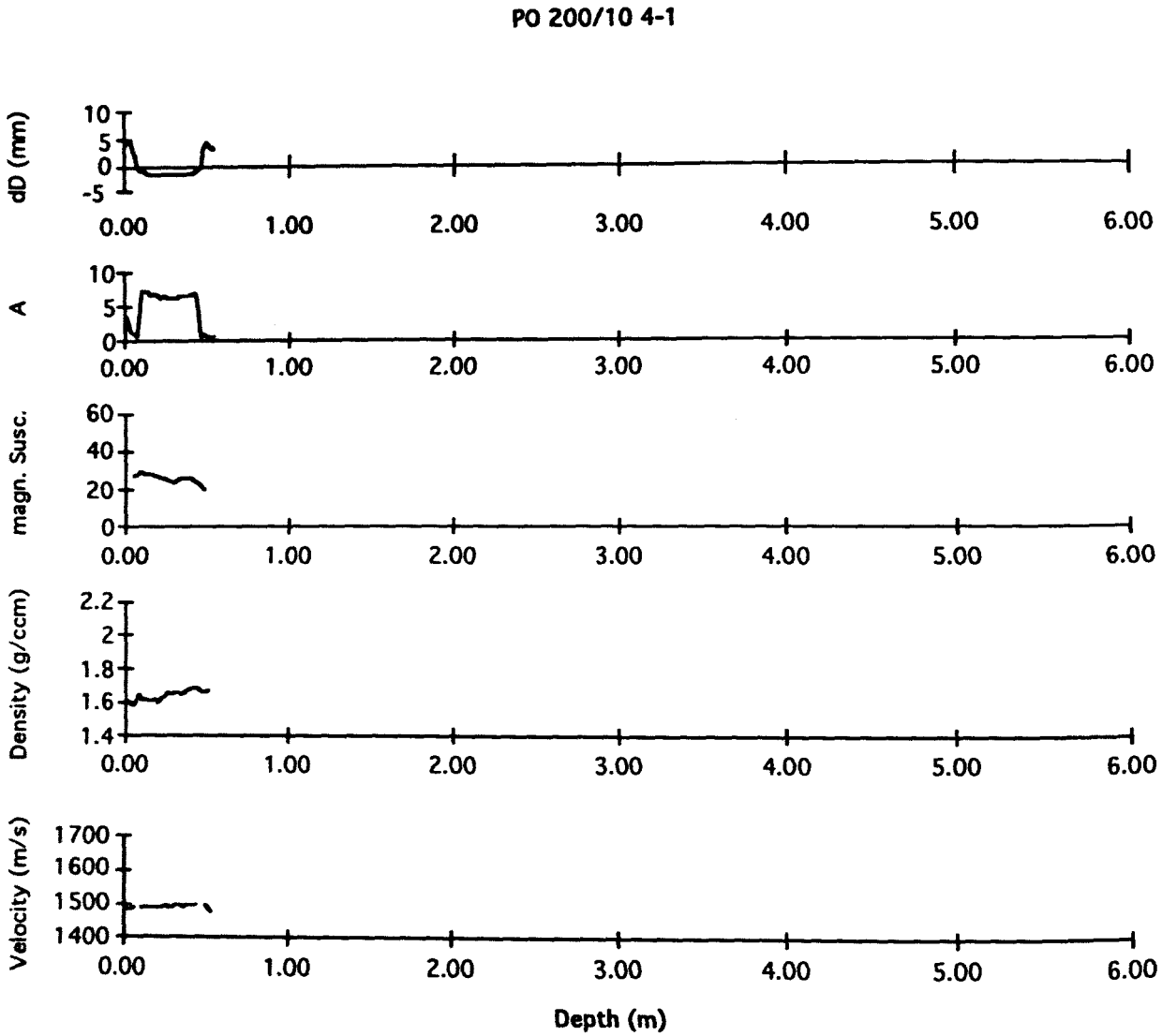

Figure 3c. Physical properties of core 4-1 derived from continous logging. From top to bottom are shown: deviation from standard core diameter, changes in wave amplitude, magnetic suszeptibility (cgs), density (g/cc) and velocity (m/s).

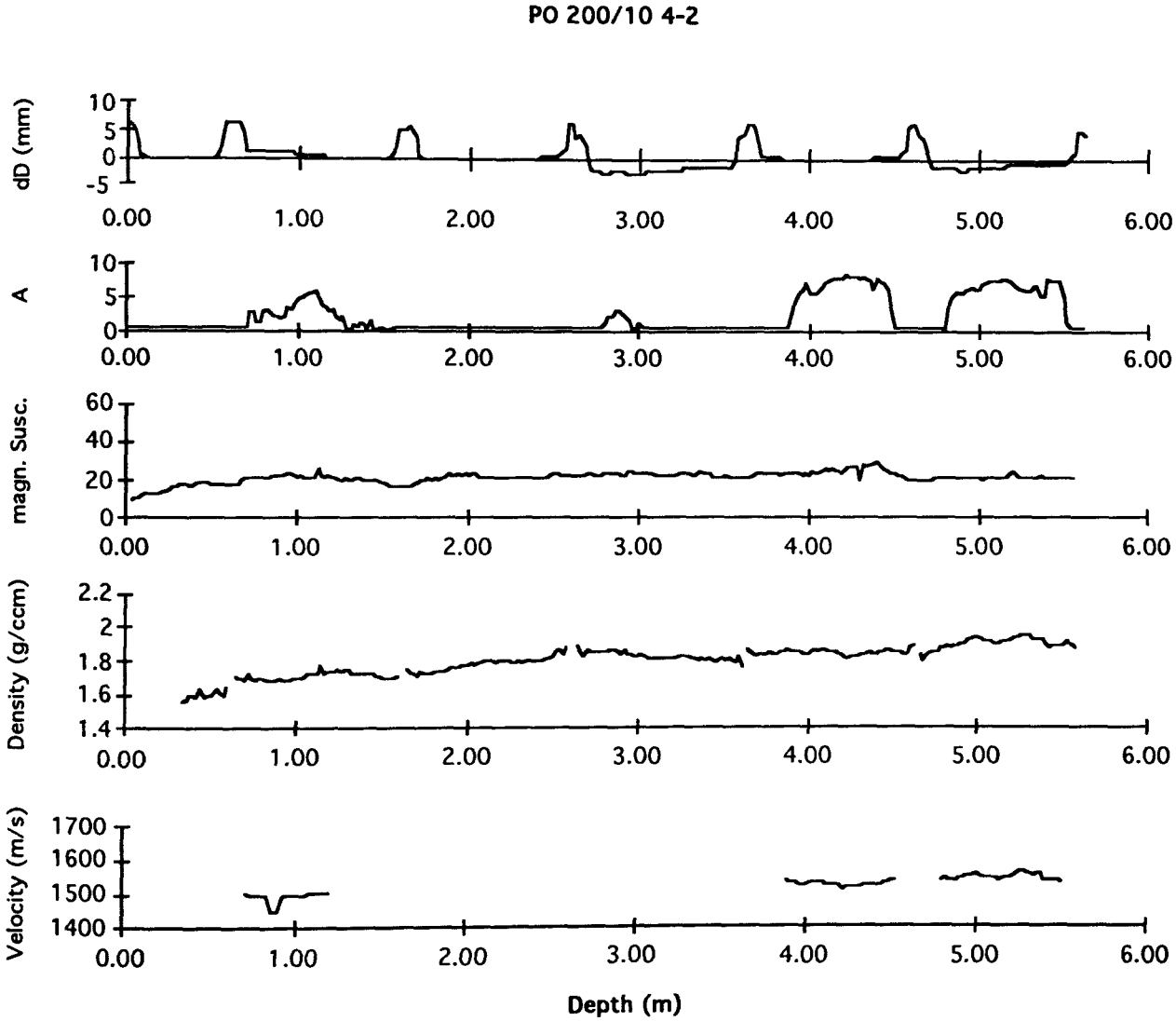

Figure 3d. Physical properties of core 4-2 derived from continous logging. From top to bottom are shown: deviation from standard core diameter, changes in wave amplitude, magnetic suszeptibility (cgs), density (g/cc) and velocity (m/s).

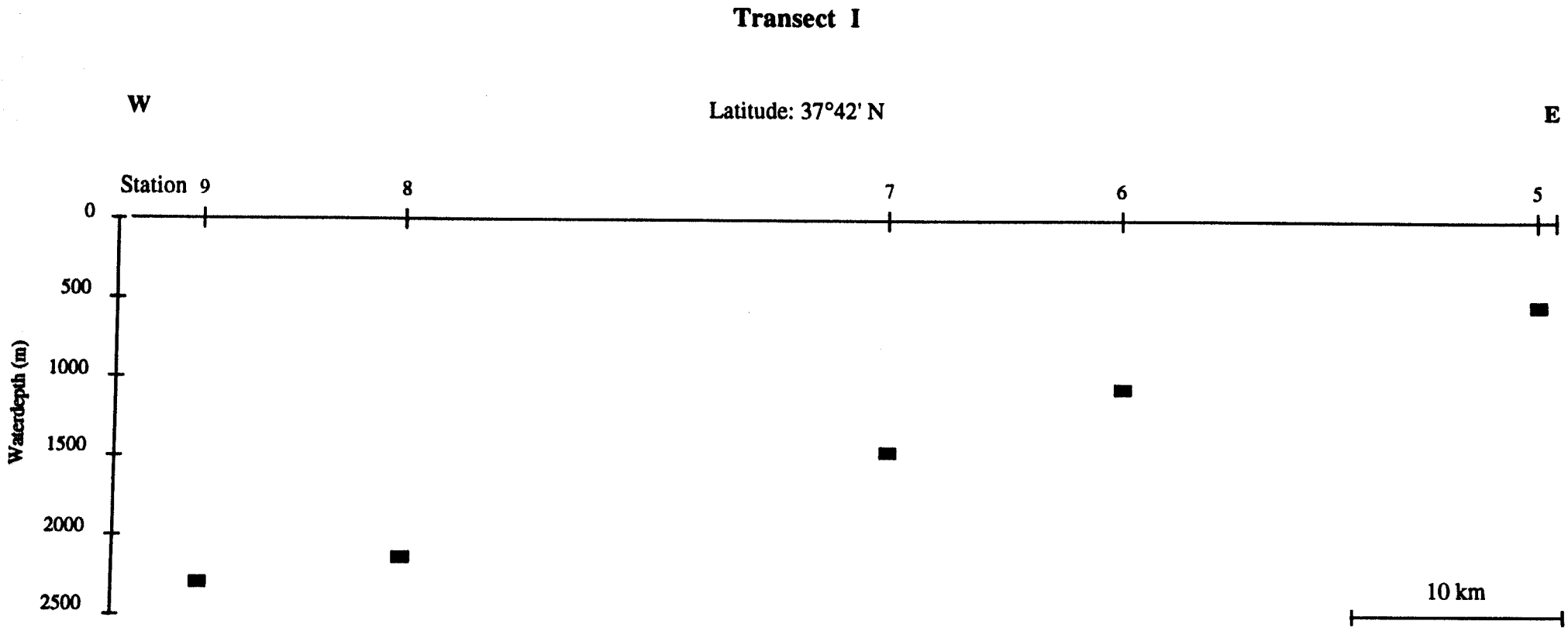

Figure 4. Core stations on transect I, showing waterdepth of core positions projected on 37°42' N Latitude

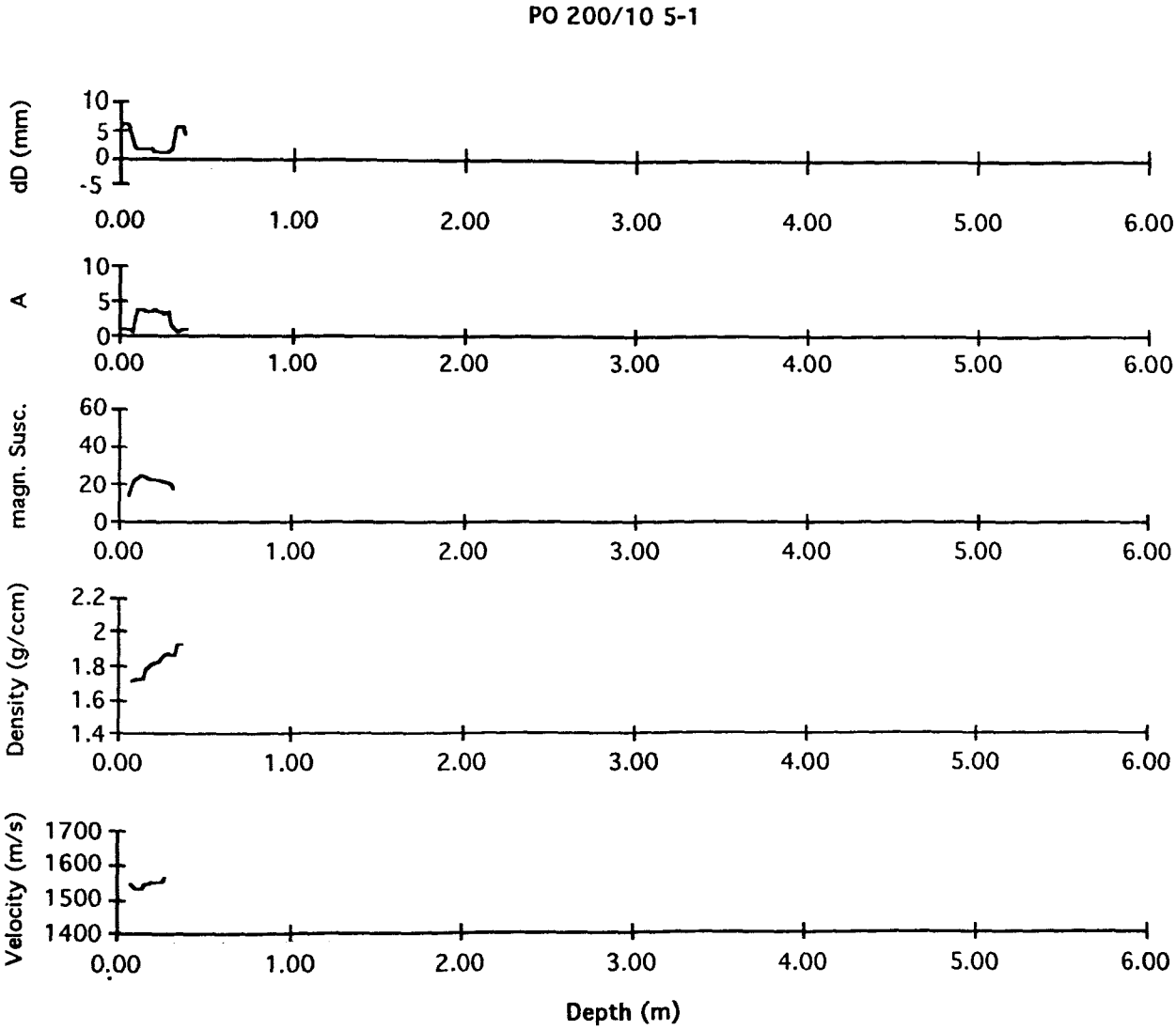

Figure 5a. Physical properties of core 5-1 derived from continous logging. From top to bottom are shown: deviation from standard core diameter, changes in wave amplitude, magnetic suszeptibility (cgs), density (g/cc) and velocity (m/s).

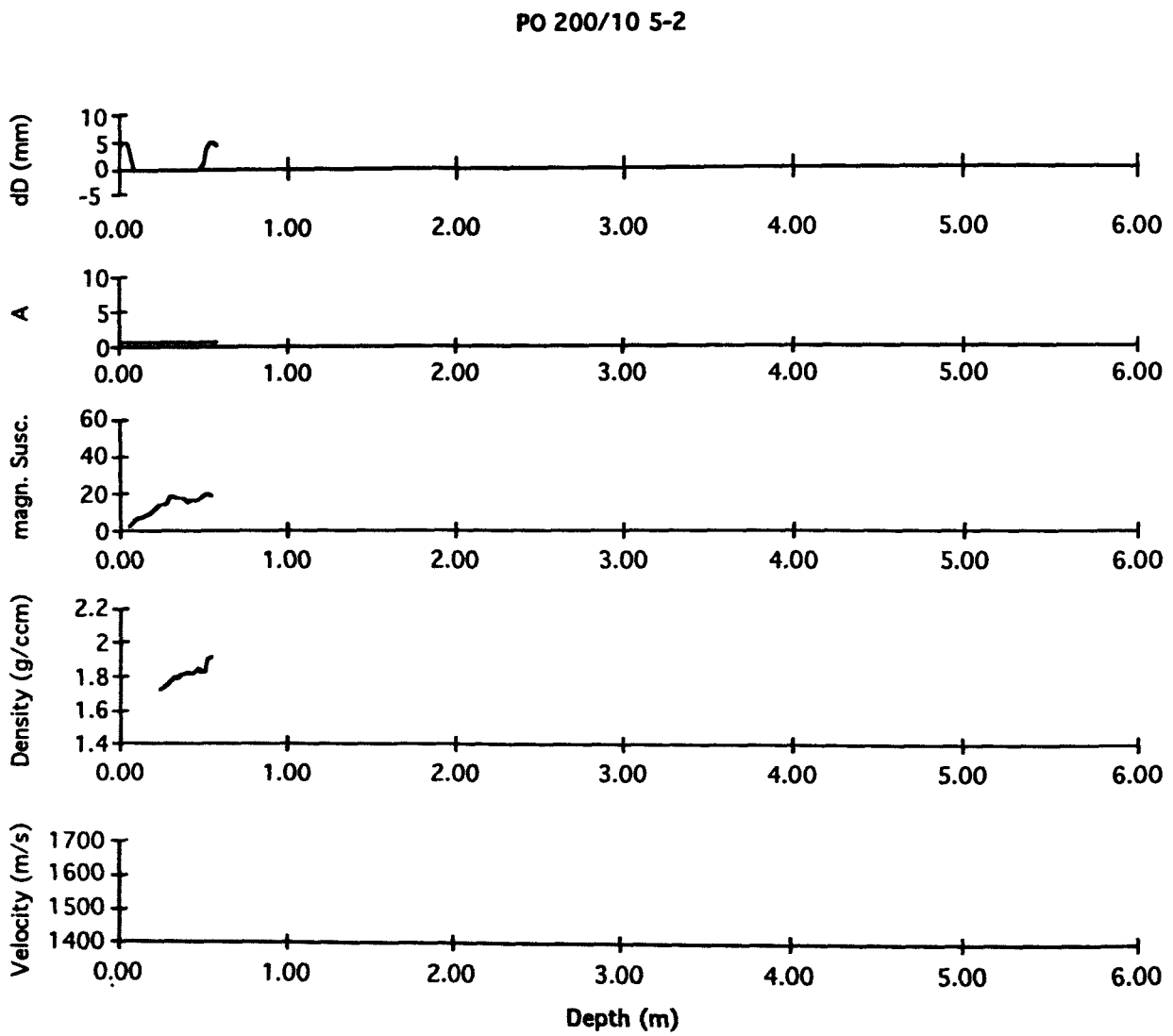

Figure 5b. Physical properties of core 5-2 derived from continous logging. From top to bottom are shown: deviation from standard core diameter, changes in wave amplitude, magnetic suszeptibility (cgs), density (g/cc) and velocity (m/s).

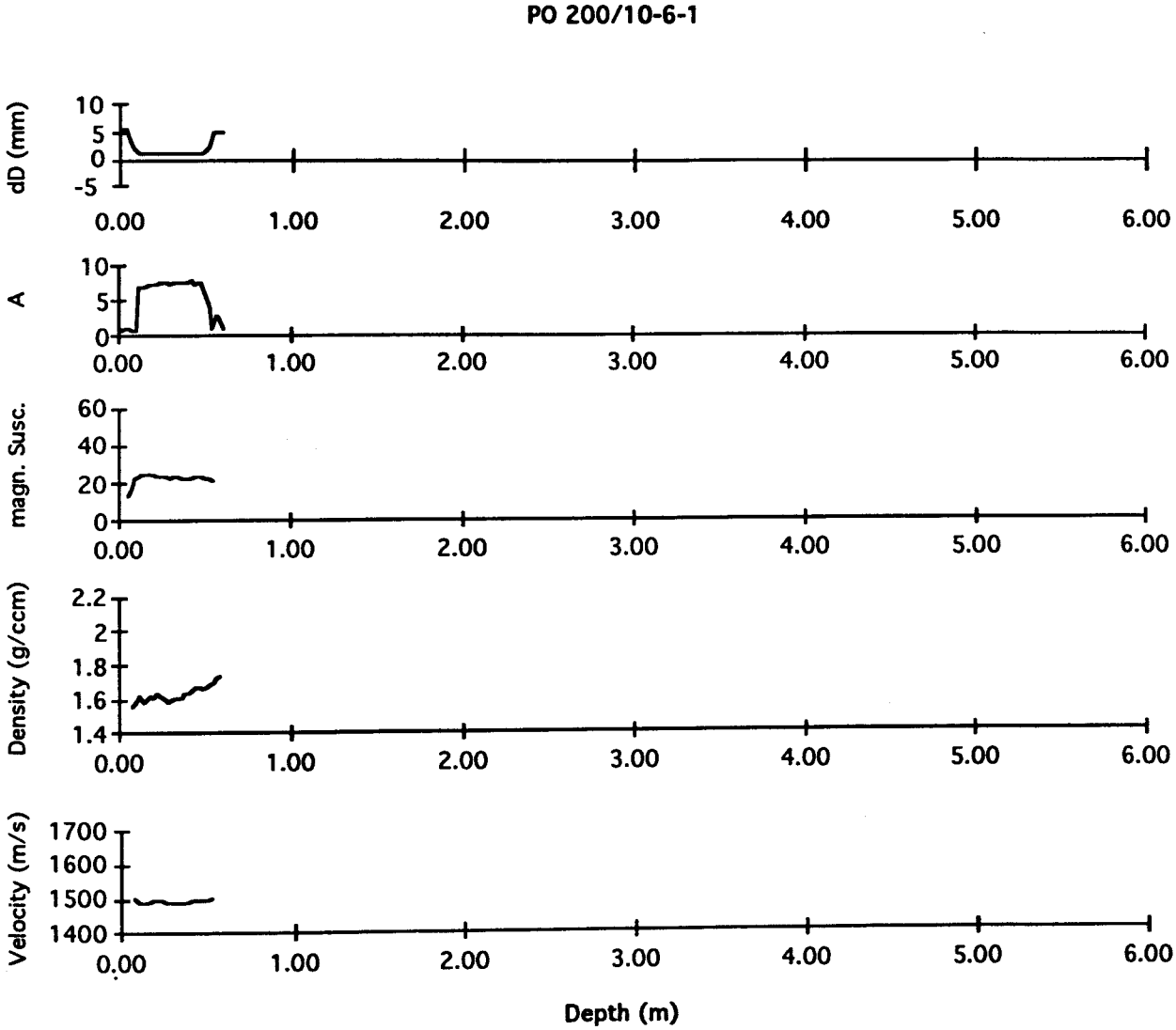

Figure 5c. Physical properties of core 6-1 derived from continous logging. From top to bottom are shown: deviation from standard core diameter, changes in wave amplitude, magnetic suszeptibility (cgs), density (g/cc) and velocity (m/s).

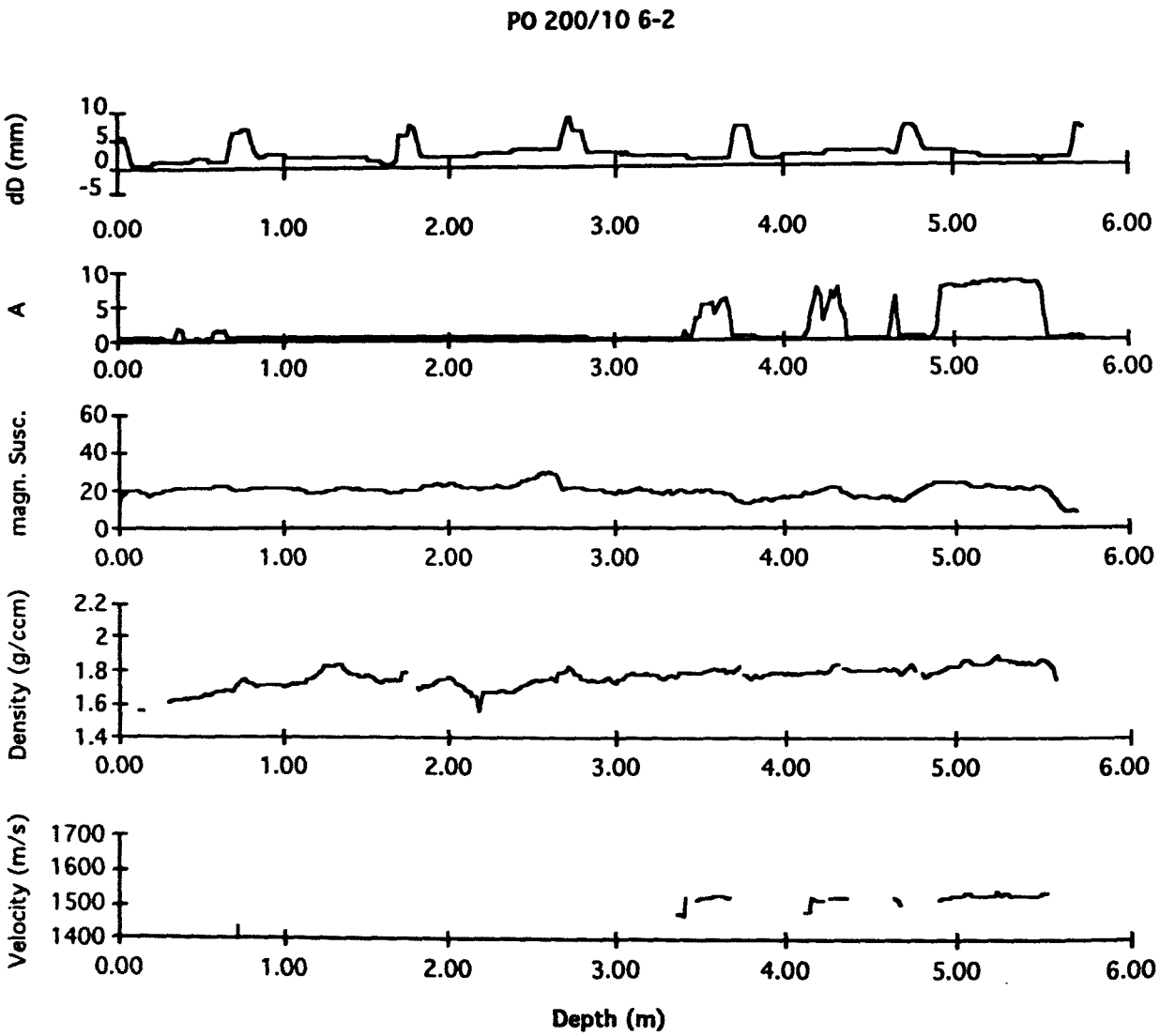

Figure 5d. Physical properties of core 6-2 derived from continous logging. From top to bottom are shown: deviation from standard core diameter, changes in wave amplitude, magnetic suszeptibility (cgs), density (g/cc) and velocity (m/s).

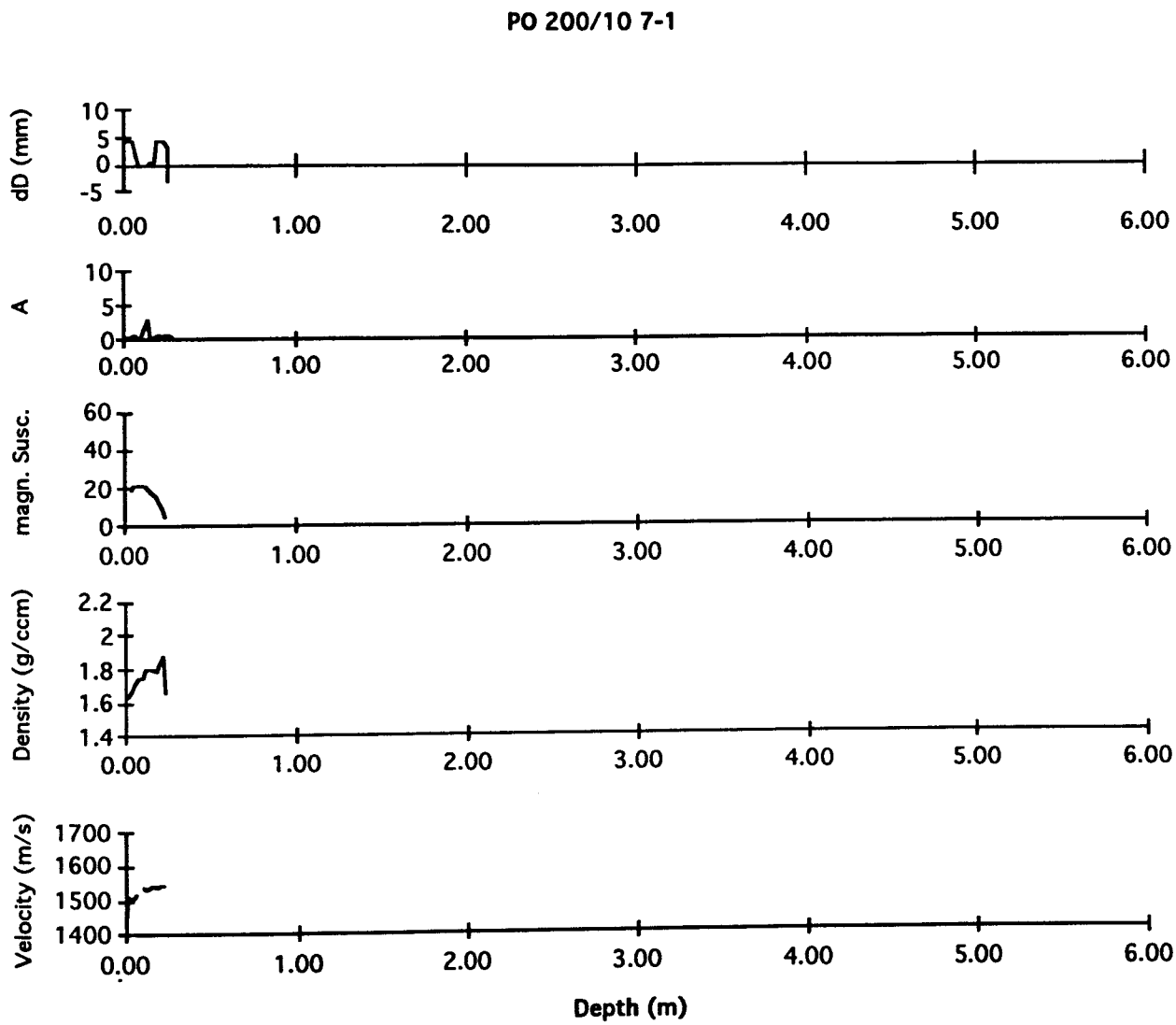

Figure 5e. Physical properties of core 7-1 derived from continous logging. From top to bottom are shown: deviation from standard core diameter, changes in wave amplitude, magnetic suszeptibility (cgs), density (g/cc) and velocity (m/s).

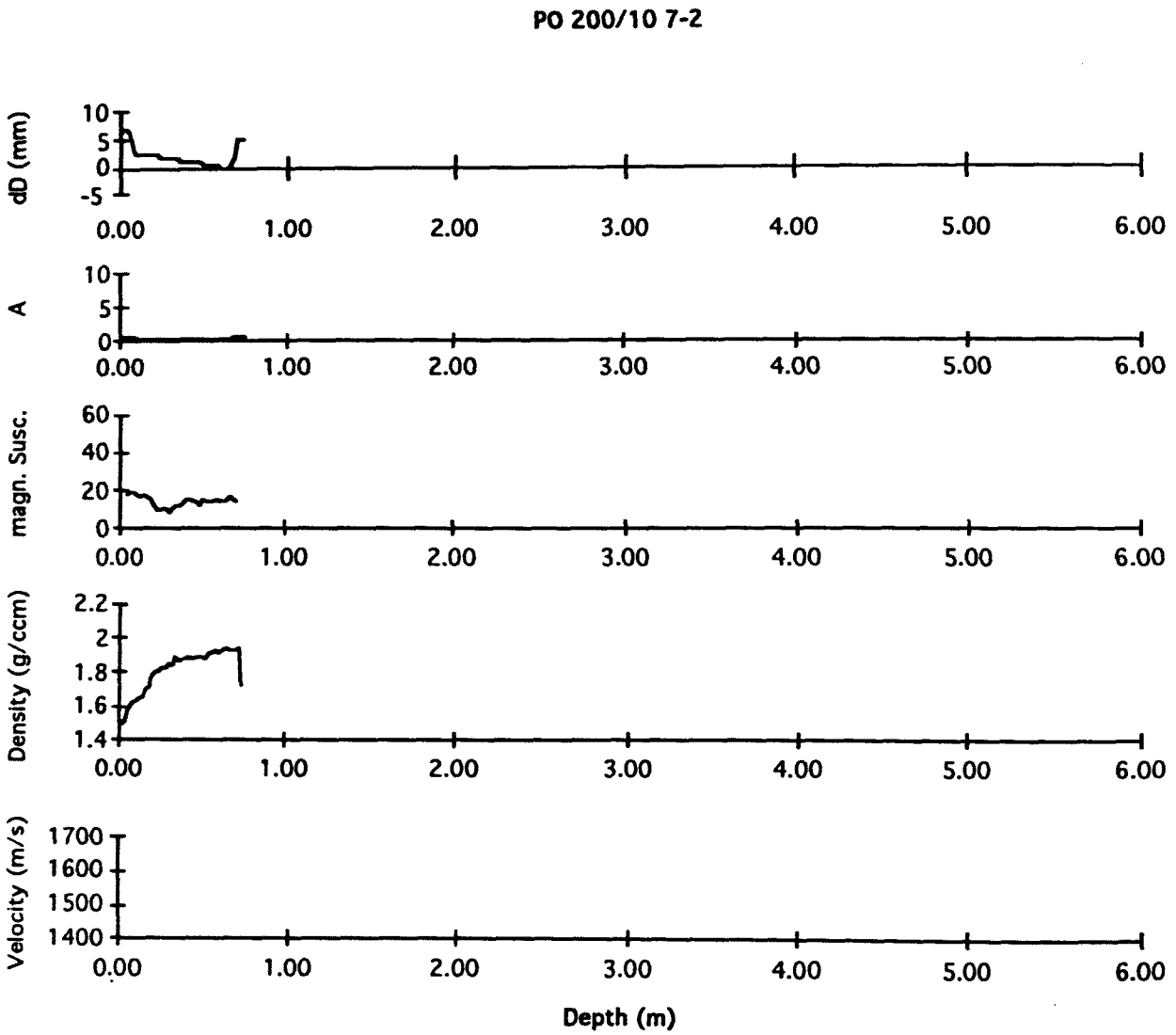

Figure 5f. Physical properties of core 7-2 derived from continous logging. From top to bottom are shown: deviation from standard core diameter, changes in wave amplitude, magnetic suszeptibility (cgs), density (g/cc) and velocity (m/s).

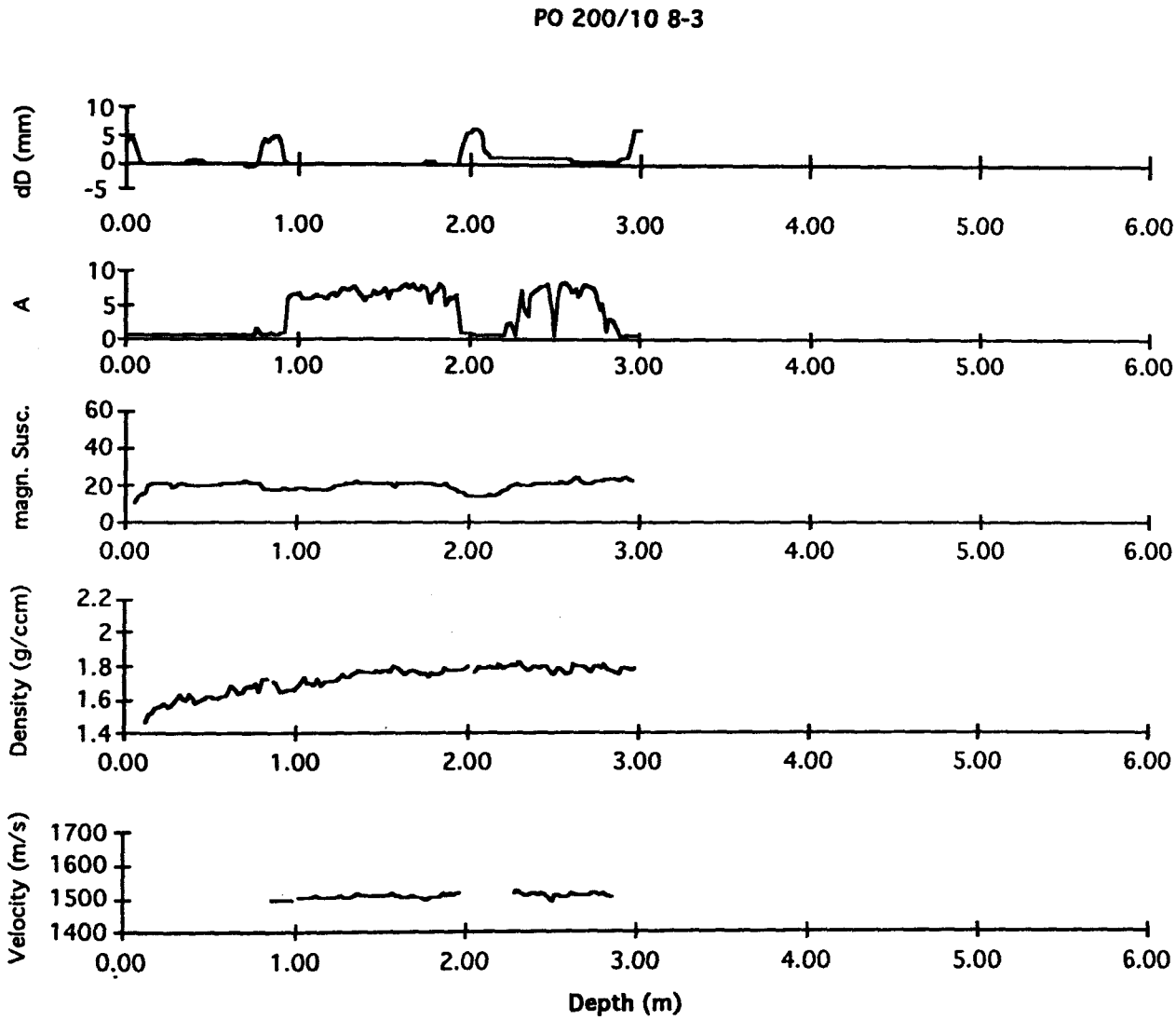

Figure 5g. Physical properties of core 8-3 derived from continous logging. From top to bottom are shown: deviation from standard core diameter, changes in wave amplitude, magnetic suszeptibility (cgs), density (g/cc) and velocity (m/s).

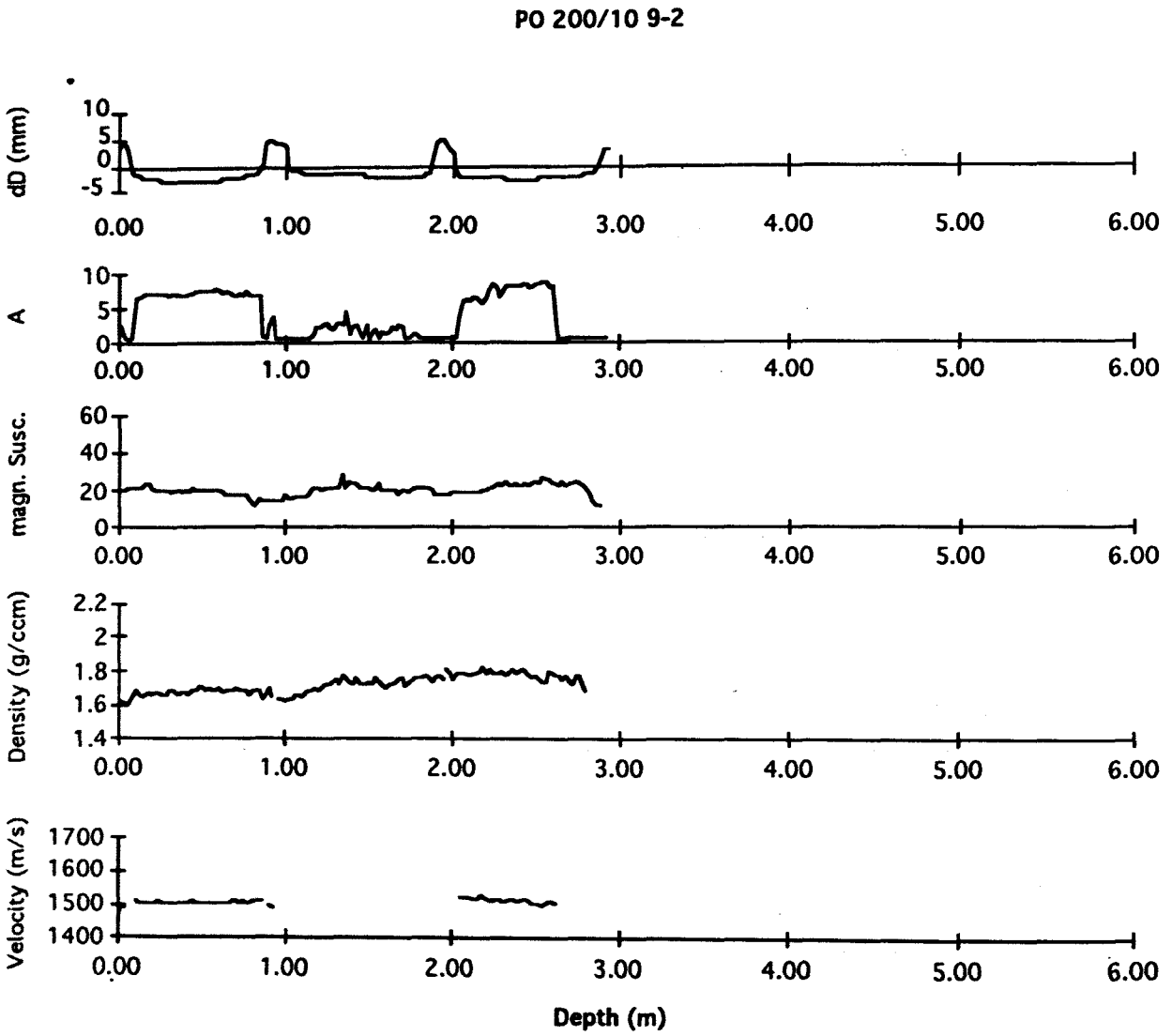

Figure 5h. Physical properties of core 9-2 derived from continous logging. From top to bottom are shown: deviation from standard core diameter, changes in wave amplitude, magnetic suszeptibility (cgs), density (g/cc) and velocity (m/s).

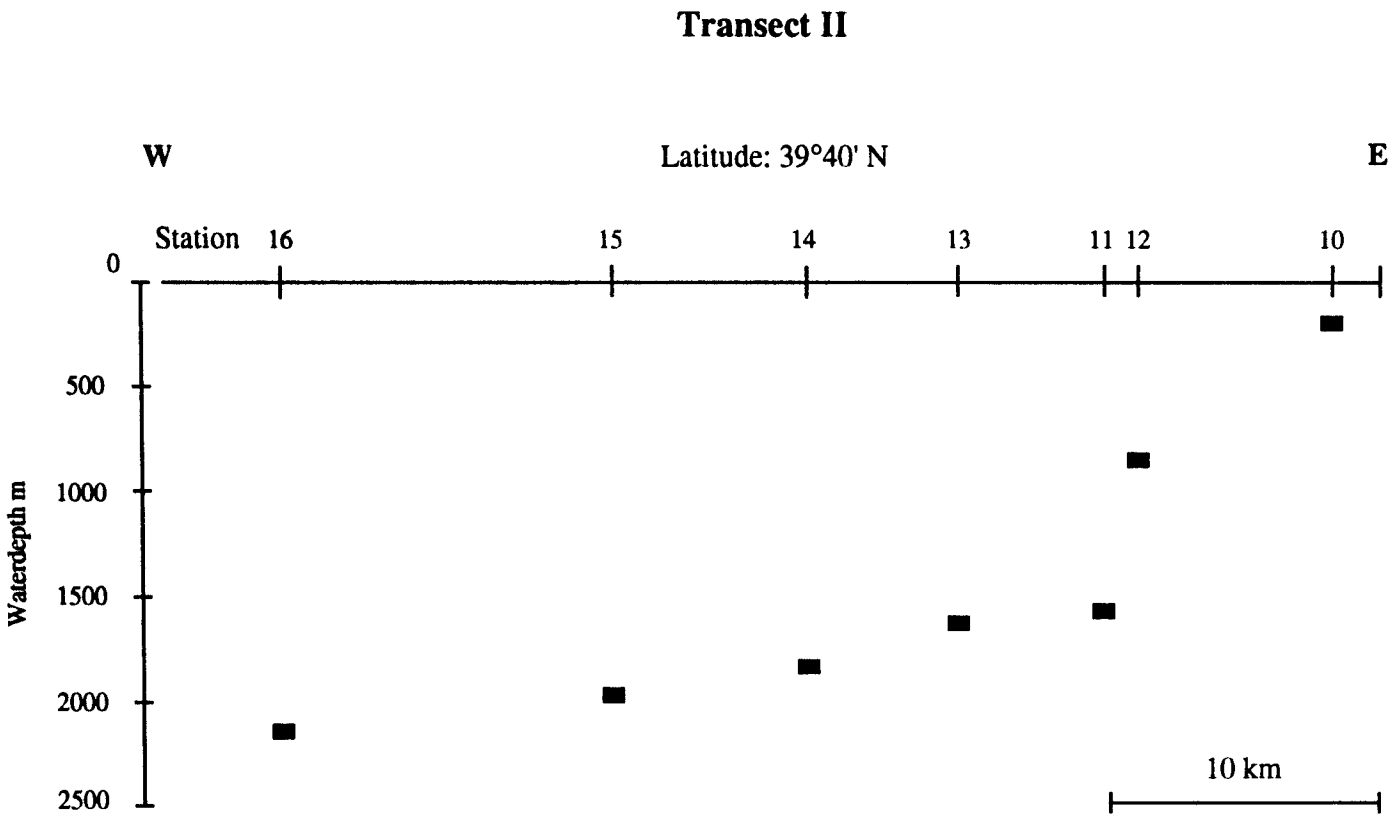

Figure 6. Core stations on transect II, showing waterdepth of core positions projected on 39°40' N Latitude

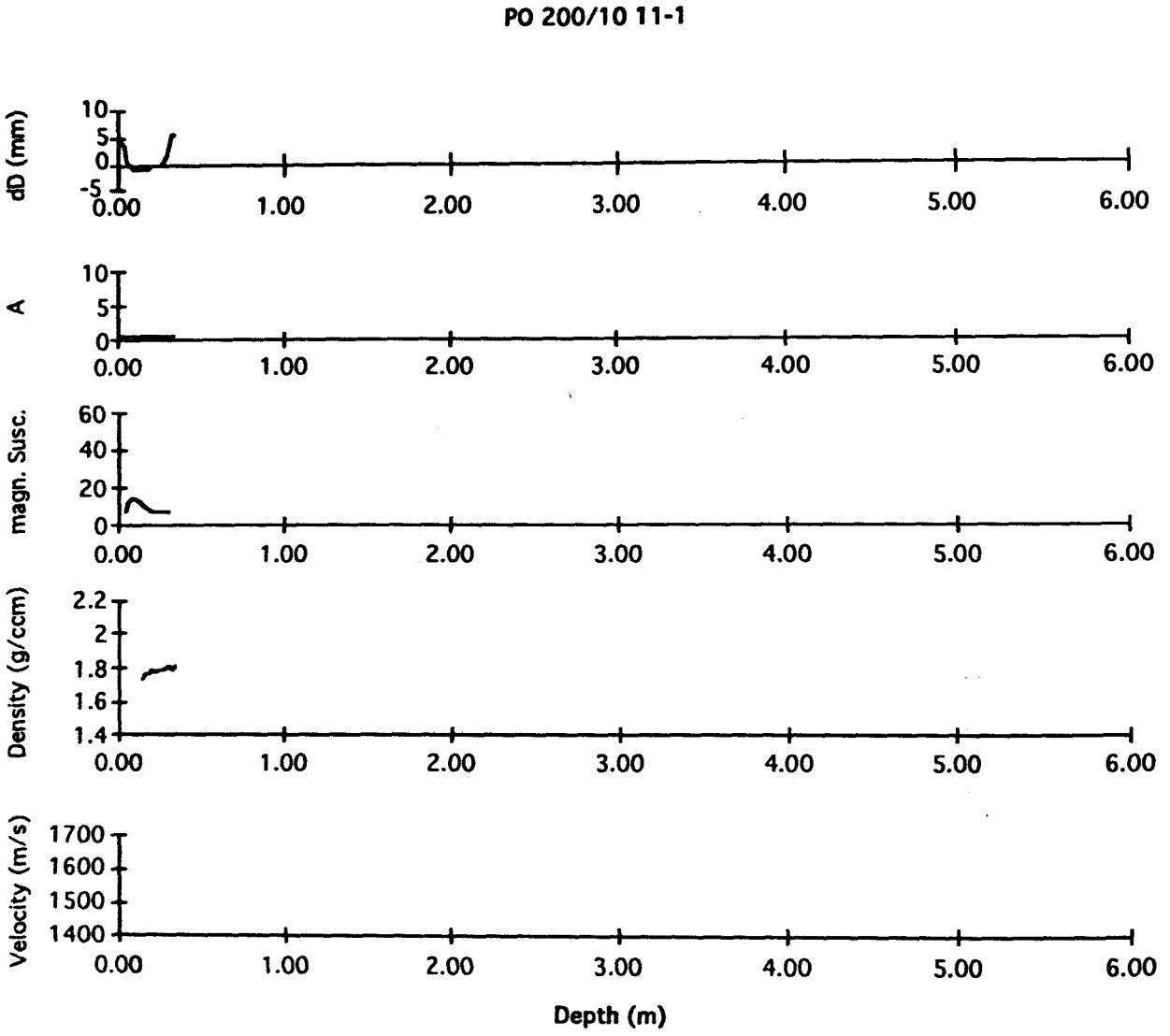

Figure 7a. Physical properties of core 11-1 derived from continous logging. From top to bottom are shown: deviation from standard core diameter, changes in wave amplitude, magnetic suszeptibility (cgs), density (g/cc) and velocity (m/s).

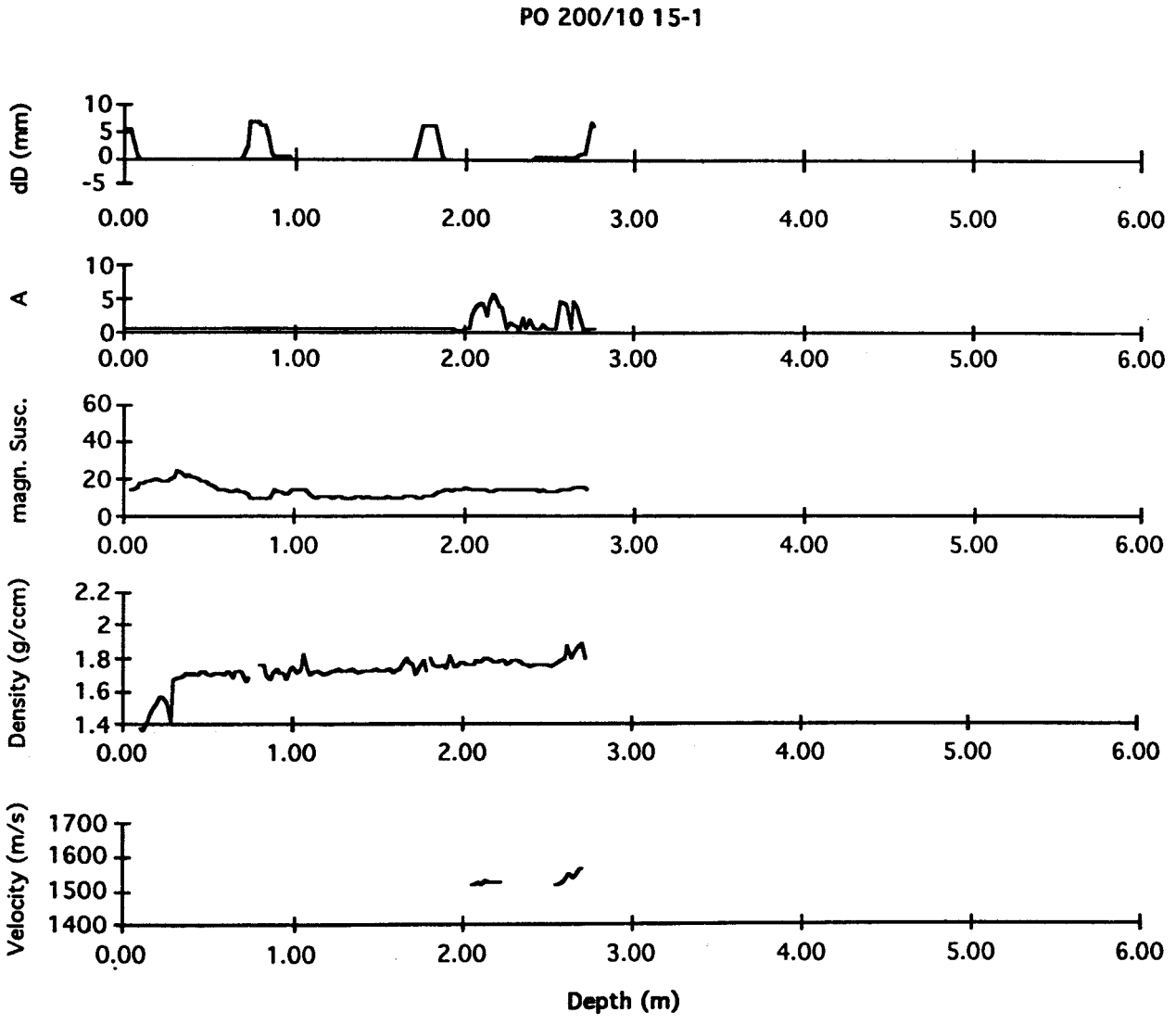

Figure 7b. Physical properties of core 15-1 derived from continous logging. From top to bottom are shown: deviation from standard core diameter, changes in wave amplitude, magnetic suszeptibility (cgs), density (g/cc) and velocity (m/s).

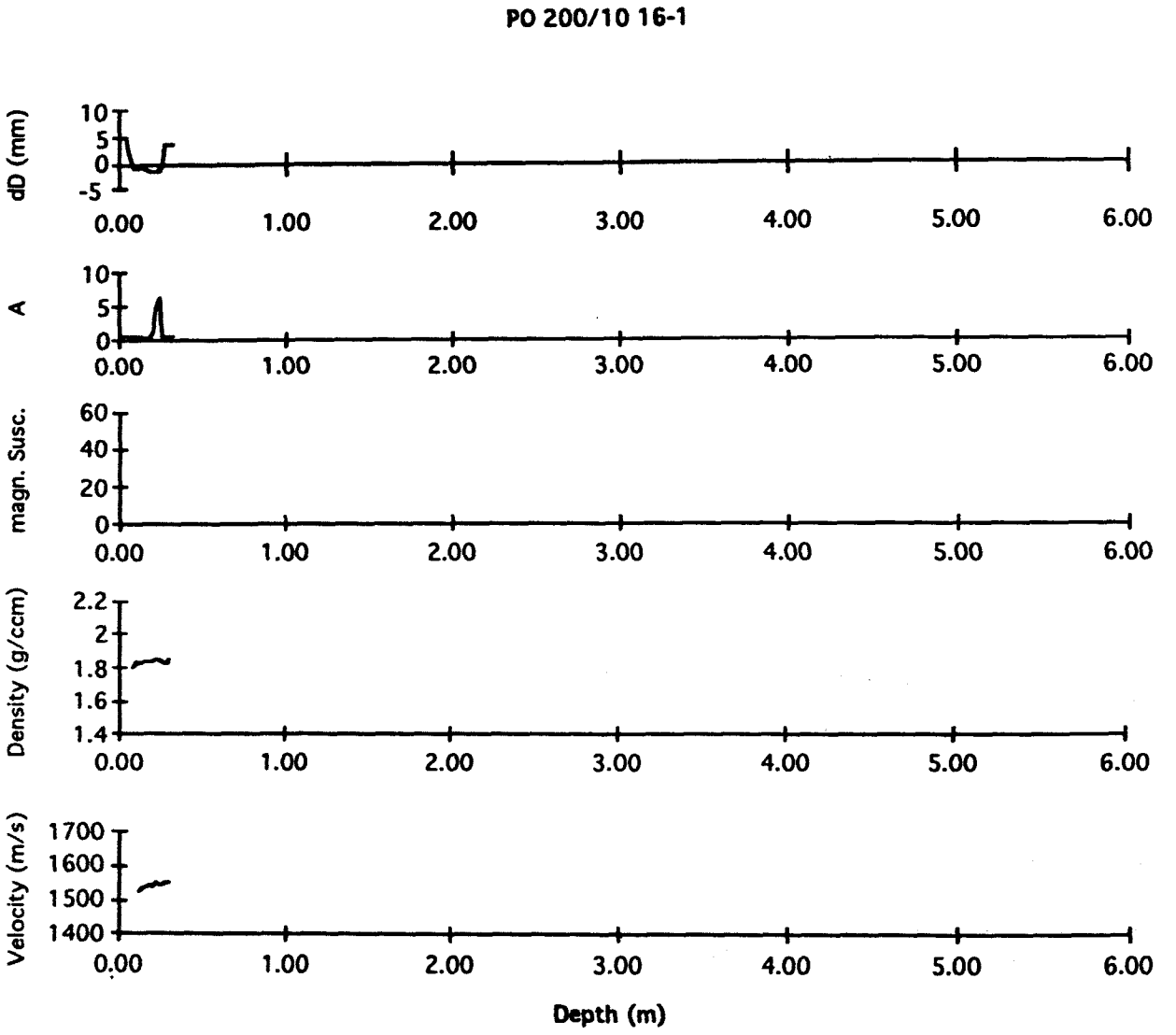

Figure 7c. Physical properties of core 16-1 derived from continous logging. From top to bottom are shown: deviation from standard core diameter, changes in wave amplitude, magnetic suszeptibility (cgs), density (g/cc) and velocity (m/s).

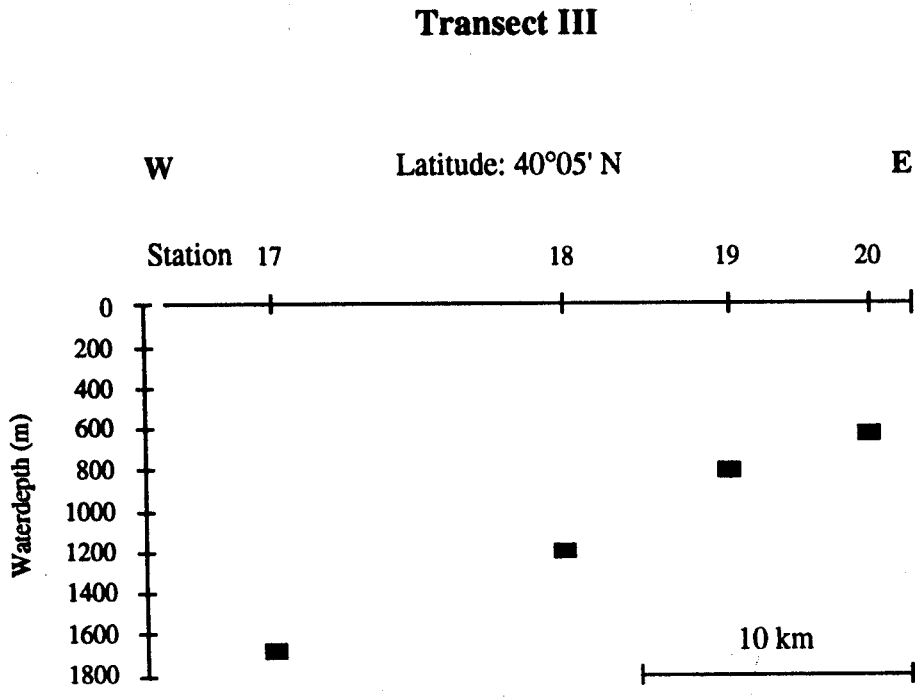

Figure 8. Core stations on transect III, showing waterdepth of core positions projected on 40°05' N Latitude

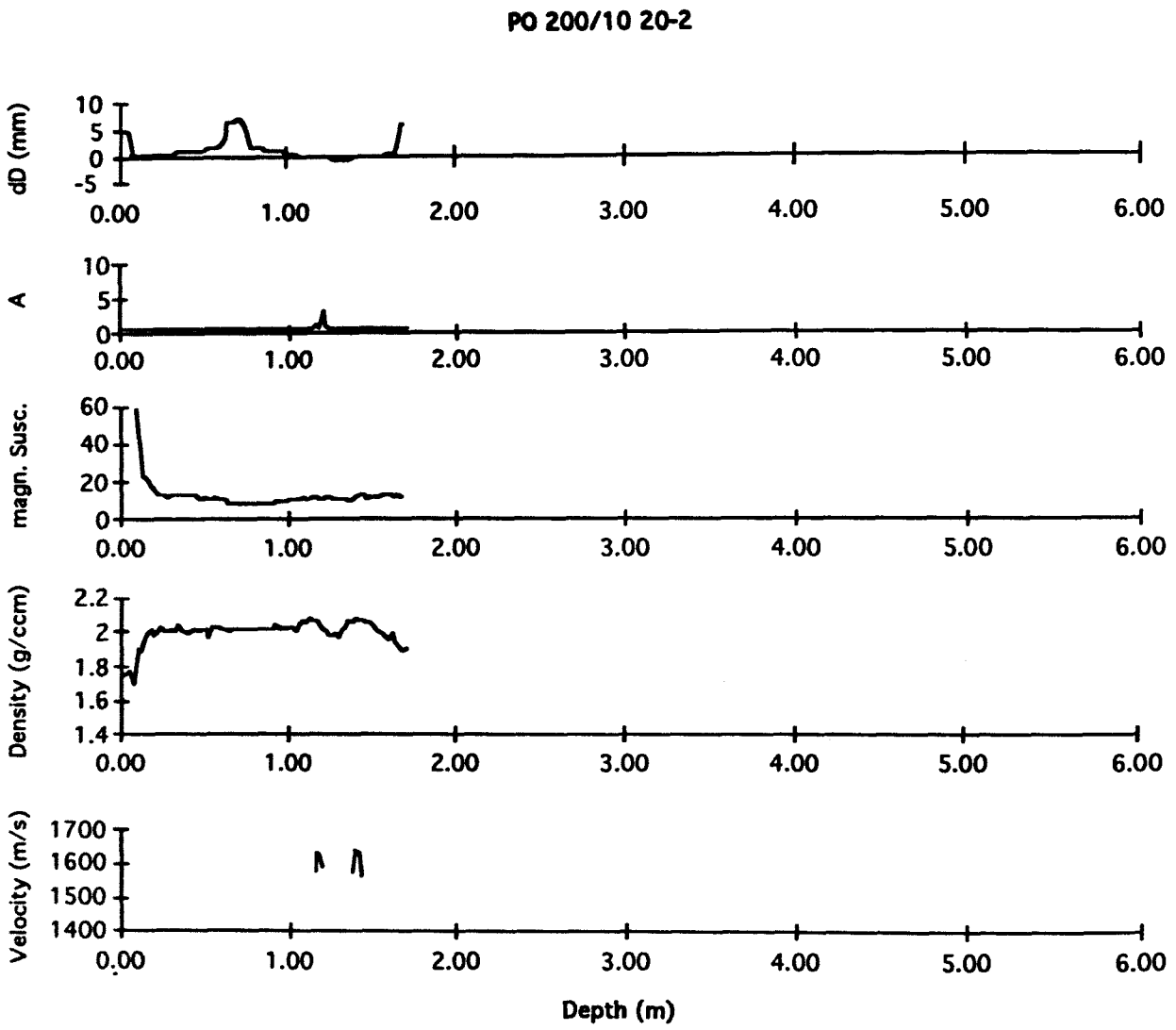

Figure 9a. Physical properties of core 20-2 derived from continous logging. From top to bottom are shown: deviation from standard core diameter, changes in wave amplitude, magnetic suszeptibility (cgs), density (g/cc) and velocity (m/s).

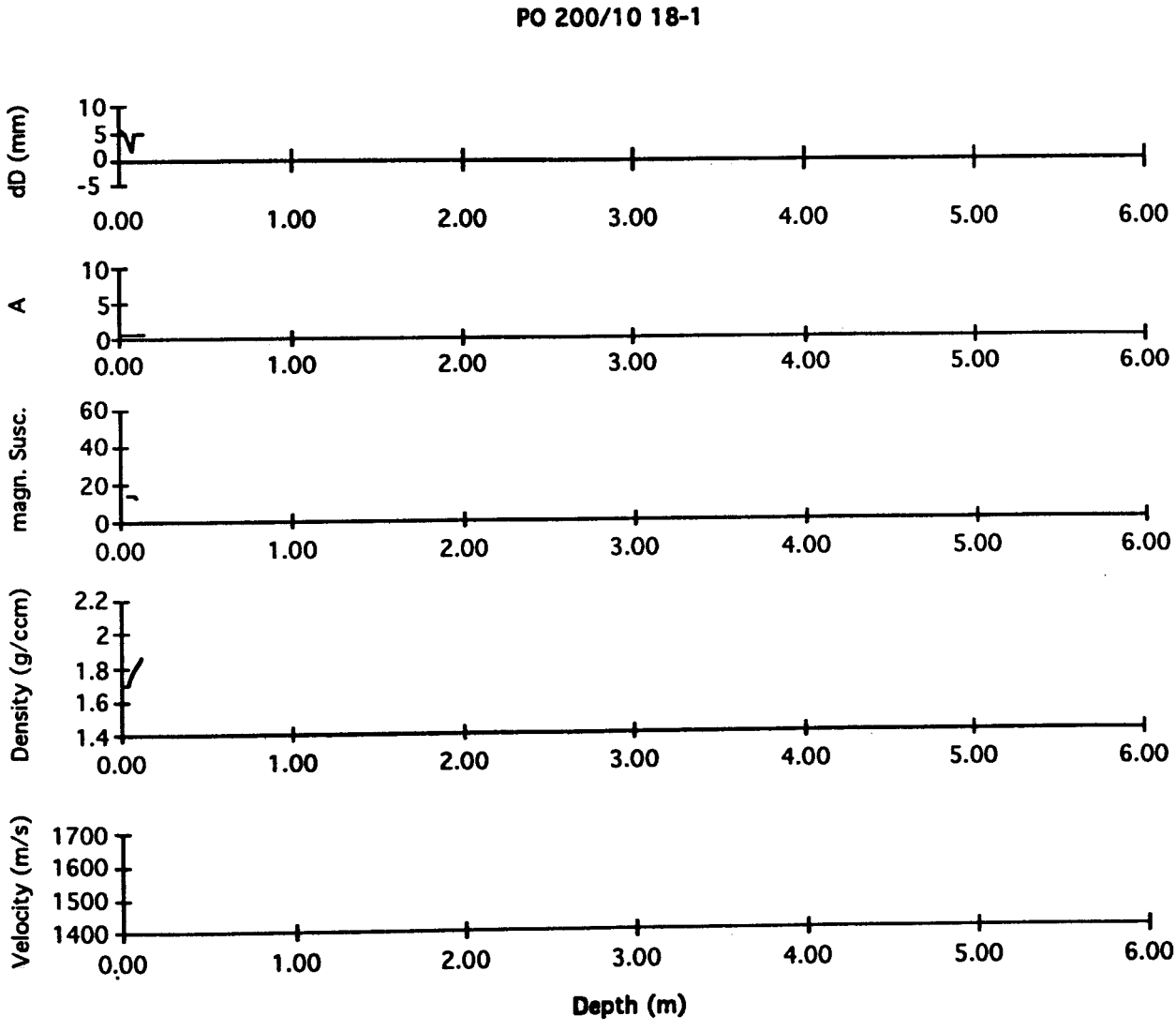

Figure 9b. Physical properties of core 18-1 derived from continous logging. From top to bottom are shown: deviation from standard core diameter, changes in wave amplitude, magnetic suszeptibility (cgs), density (g/cc) and velocity (m/s).

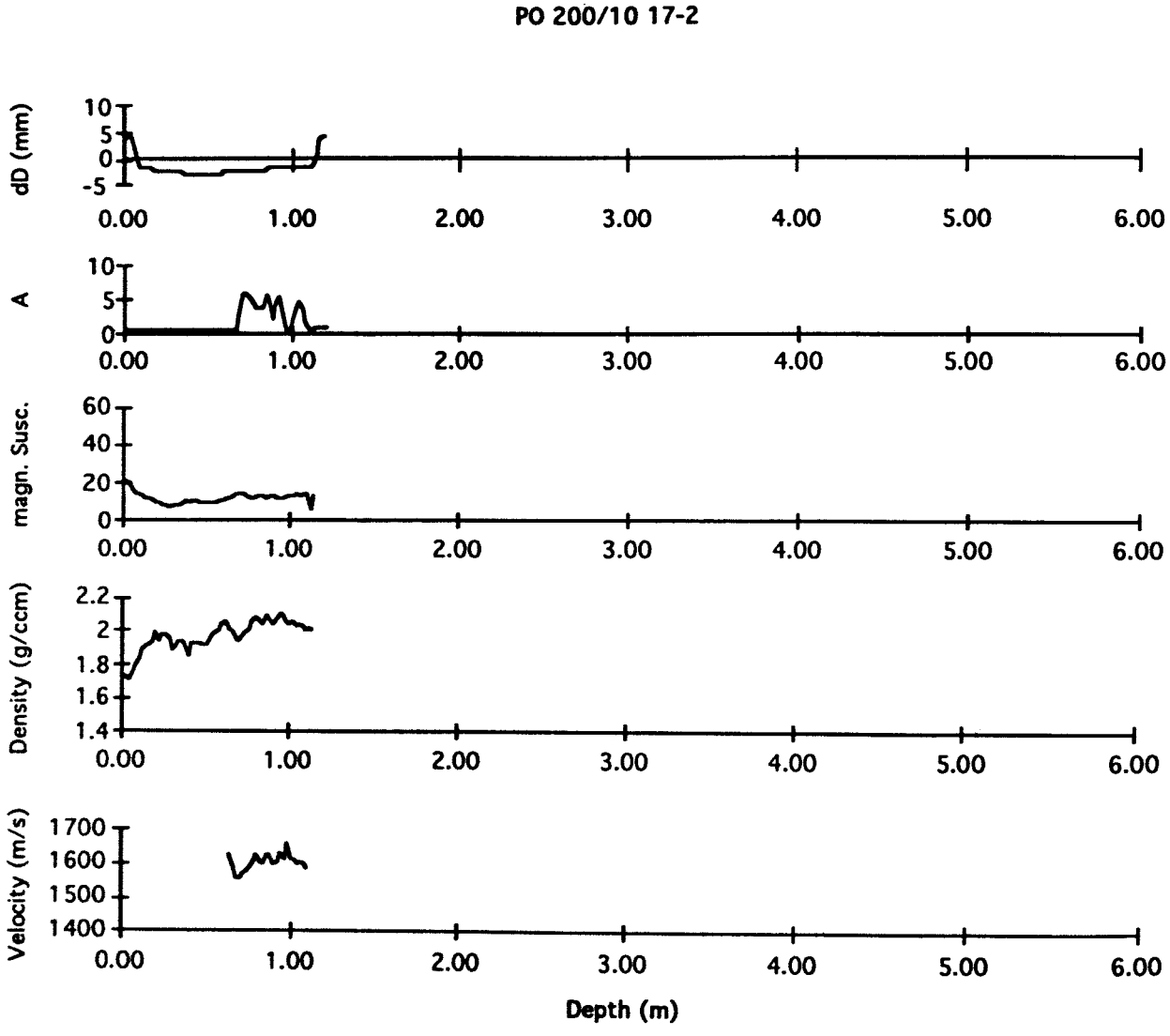

Figure 9c. Physical properties of core 17-2 derived from continous logging. From top to bottom are shown: deviation from standard core diameter, changes in wave amplitude, magnetic suszeptibility (cgs), density (g/cc) and velocity (m/s).

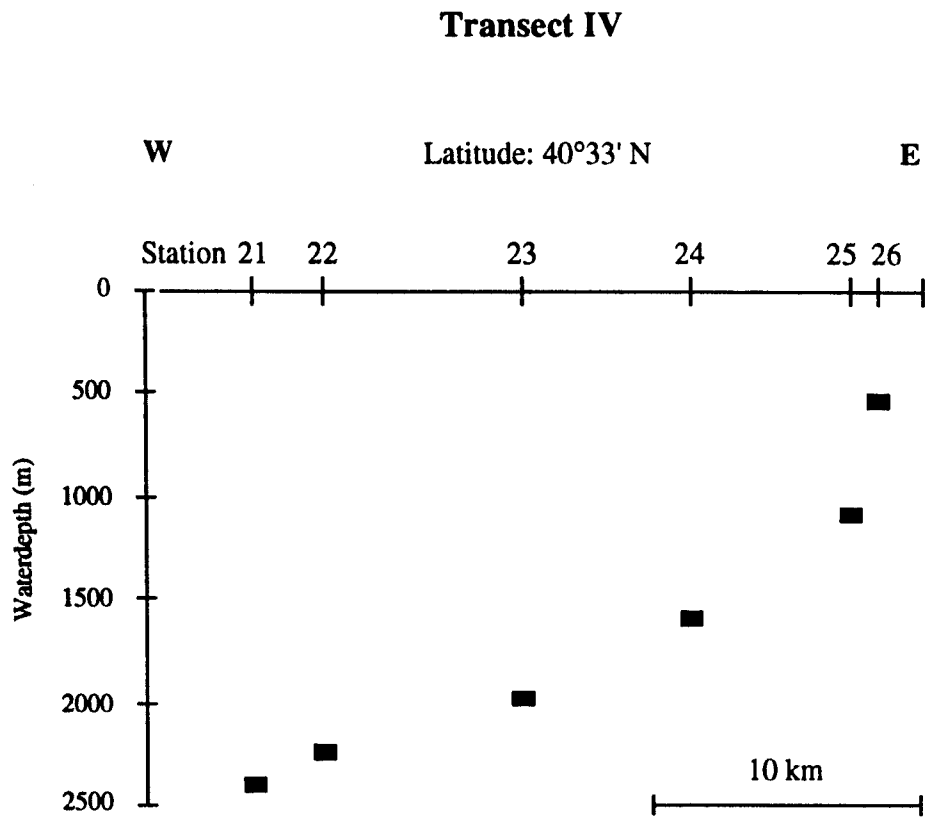

Figure 10. Core stations on transect IV, showing waterdepth of core positions projected on 40°33' N Latitude

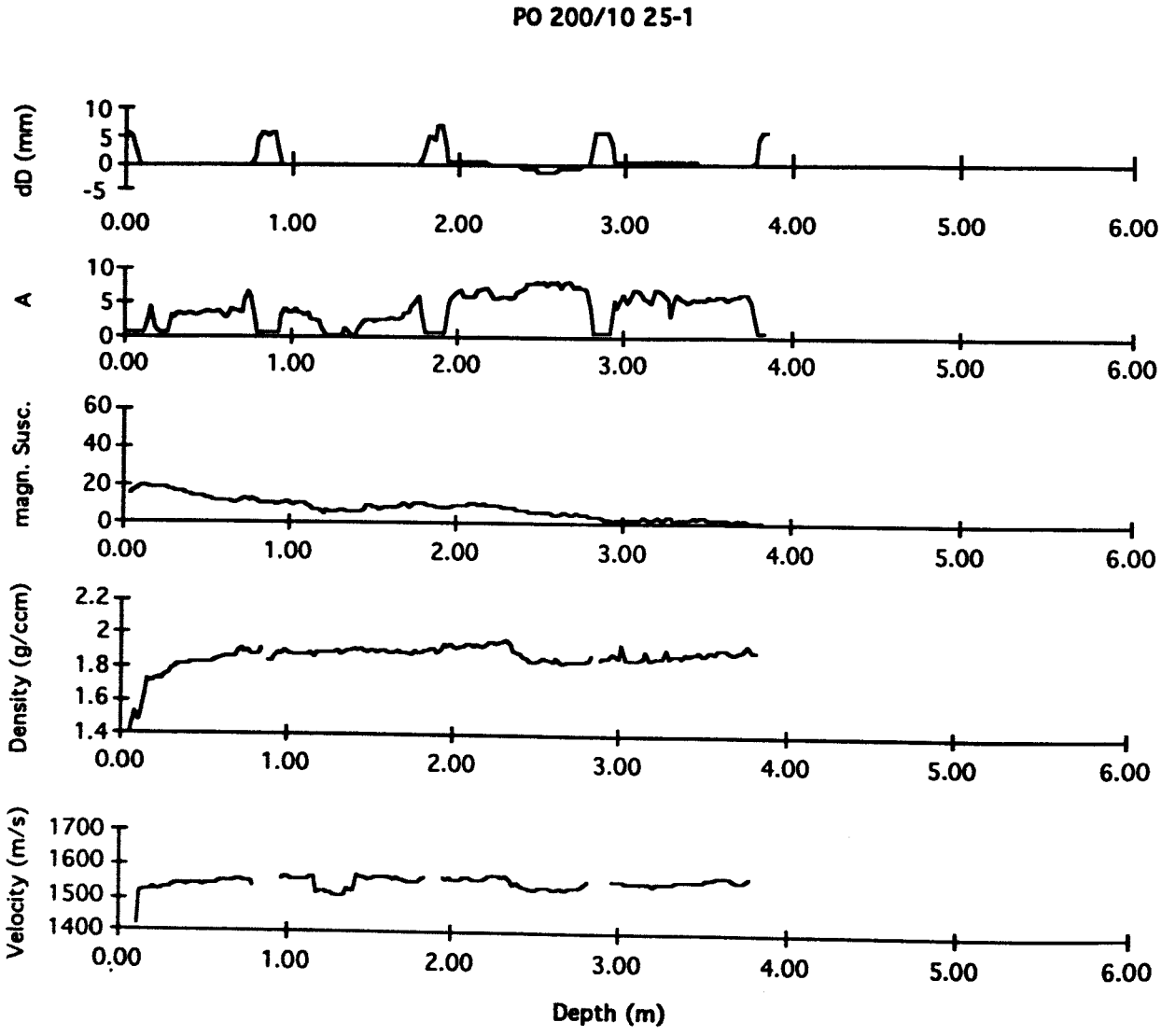

Figure 11a. Physical properties of core 25-1 derived from continous logging. From top to bottom are shown: deviation from standard core diameter, changes in wave amplitude, magnetic suszeptibility (cgs), density (g/cc) and velocity (m/s).

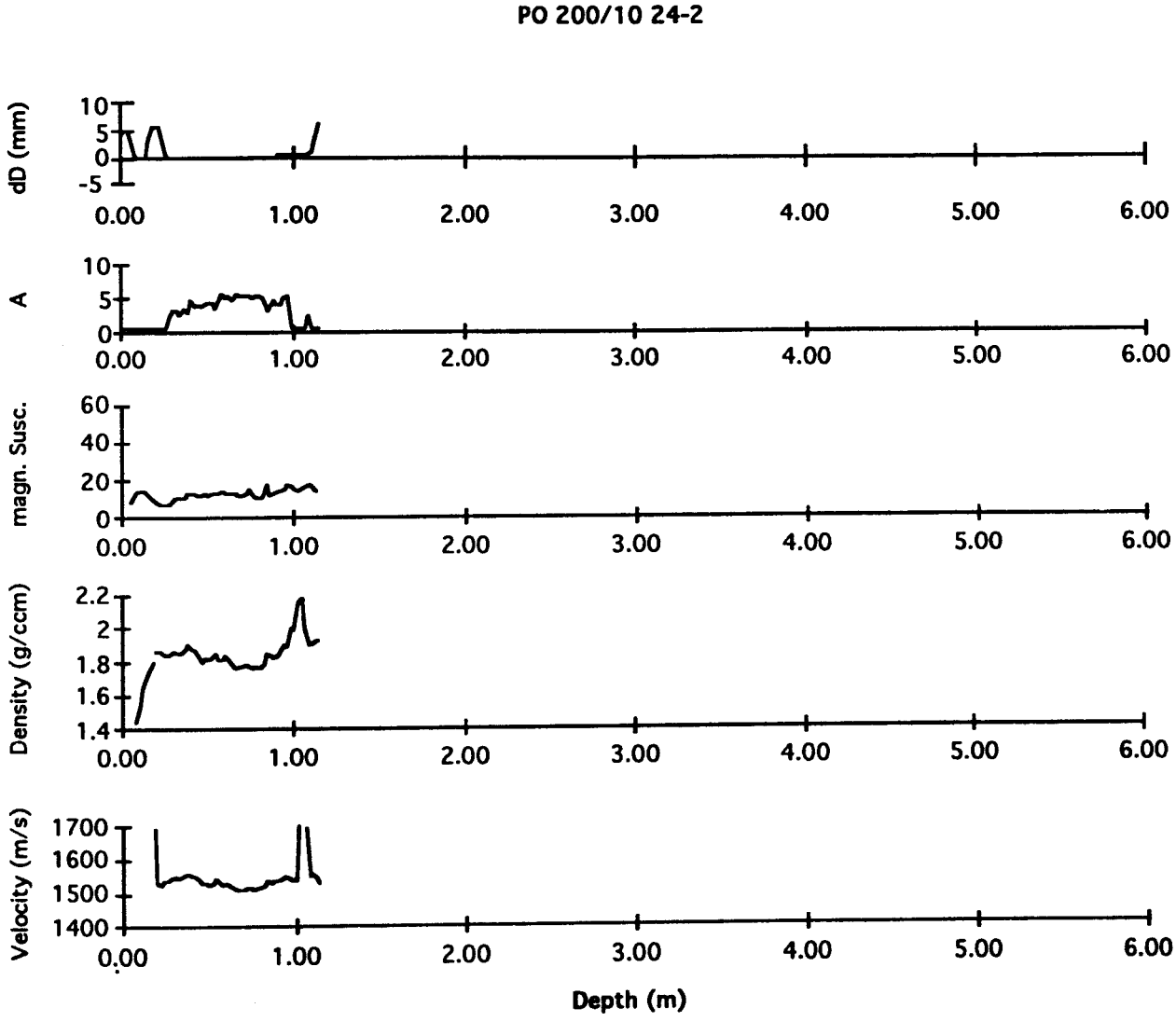

Figure 11b. Physical properties of core 24-2 derived from continous logging. From top to bottom are shown: deviation from standard core diameter, changes in wave amplitude, magnetic suszeptibility (cgs), density (g/cc) and velocity (m/s).

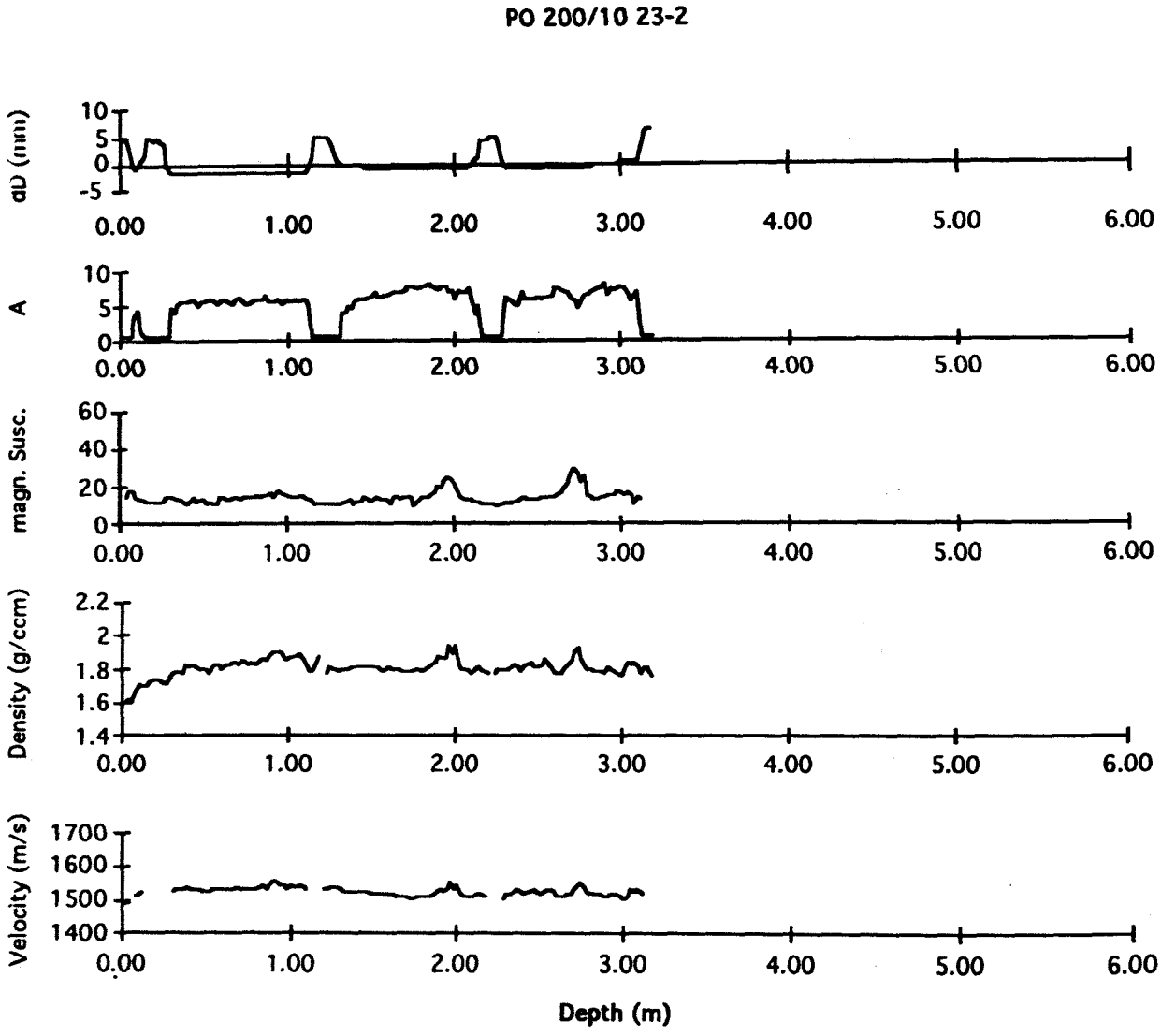

Figure 11c. Physical properties of core 23-2 derived from continous logging. From top to bottom are shown: deviation from standard core diameter, changes in wave amplitude, magnetic suszeptibility (cgs), density (g/cc) and velocity (m/s).

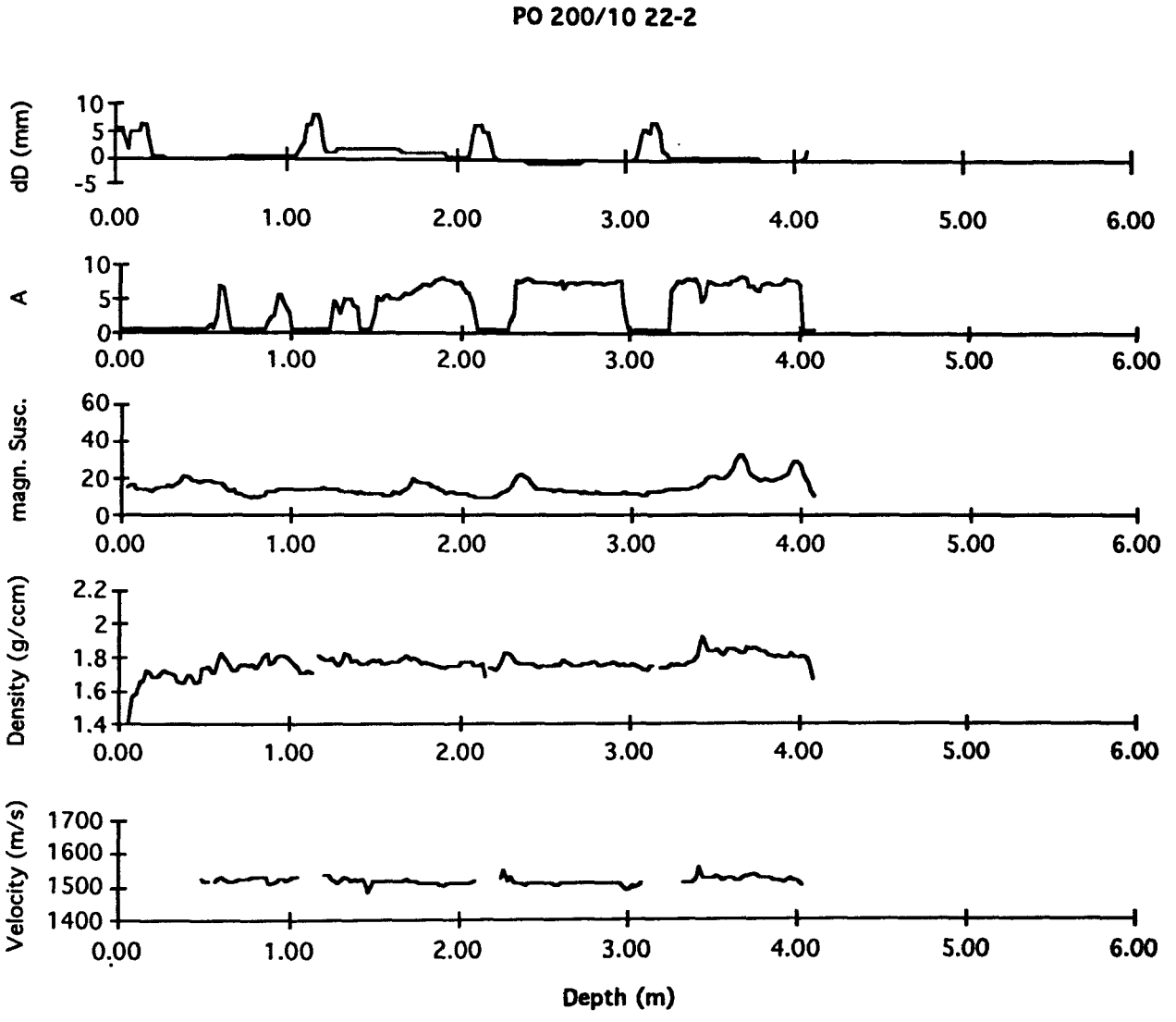

Figure 11d. Physical properties of core 22-2 derived from continous logging. From top to bottom are shown: deviation from standard core diameter, changes in wave amplitude, magnetic suszeptibility (cgs), density (g/cc) and velocity (m/s).

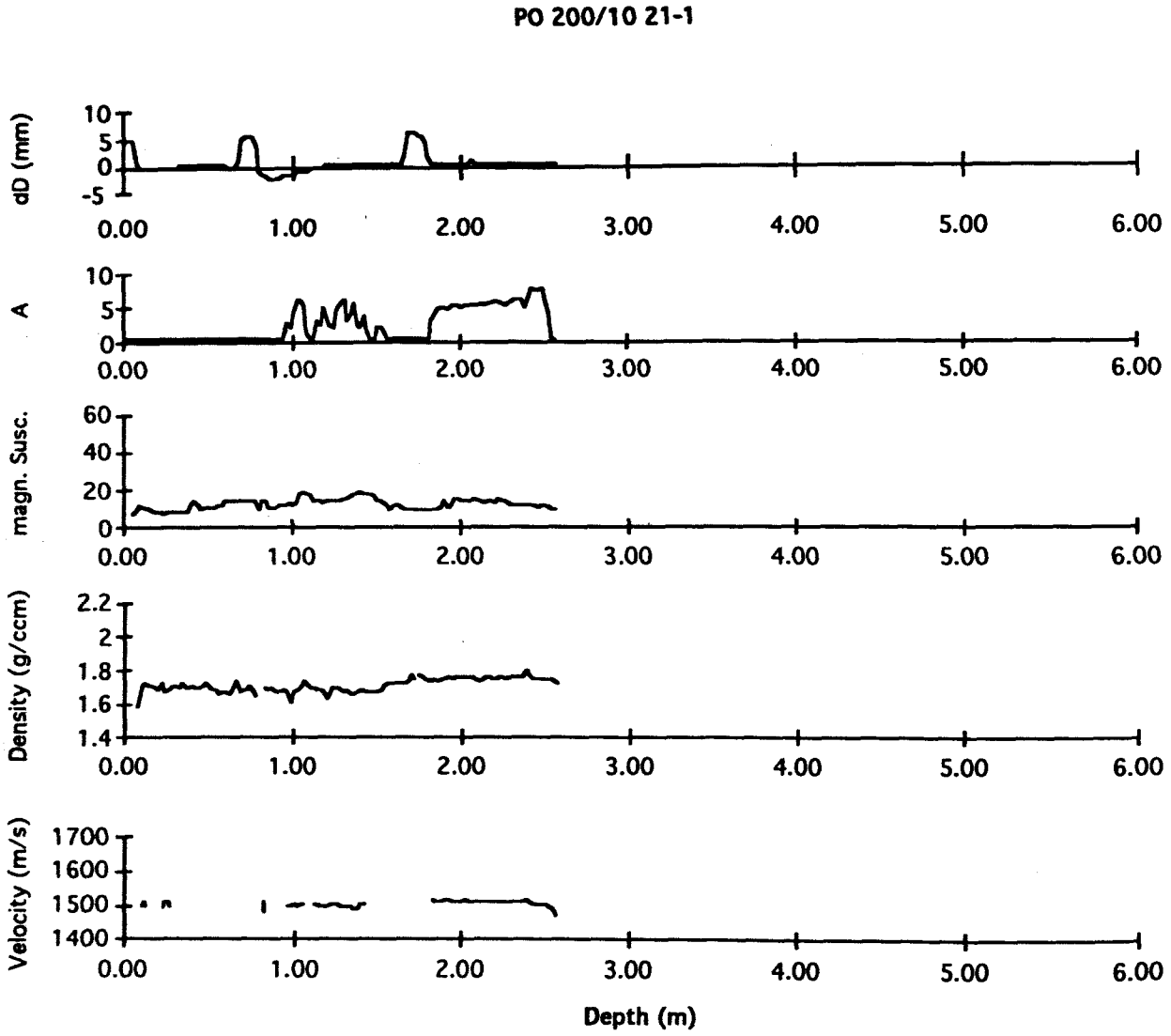

Figure 11e. Physical properties of core 21-1 derived from continous logging. From top to bottom are shown: deviation from standard core diameter, changes in wave amplitude, magnetic suszeptibility (cgs), density (g/cc) and velocity (m/s).

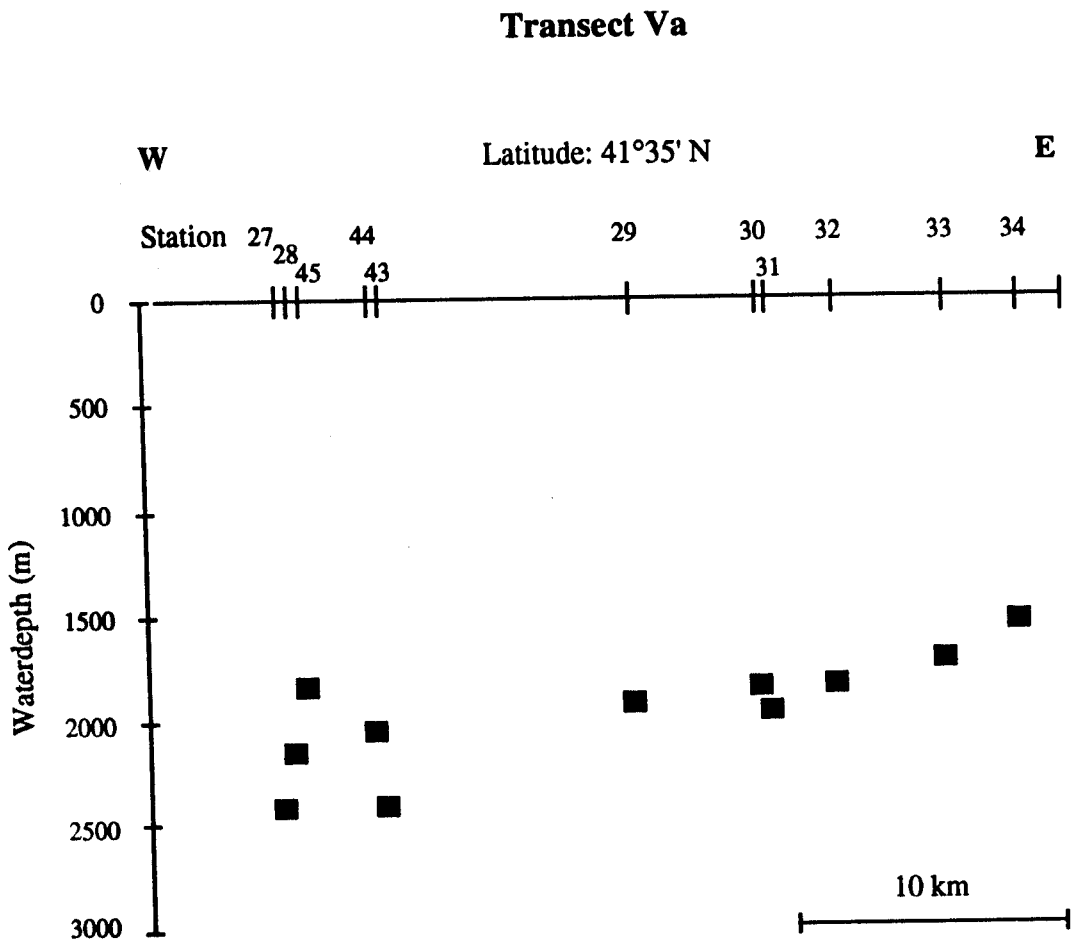

Figure 12. Core stations on transect Va, showing waterdepth of core positions projected on 41°35' N Latitude

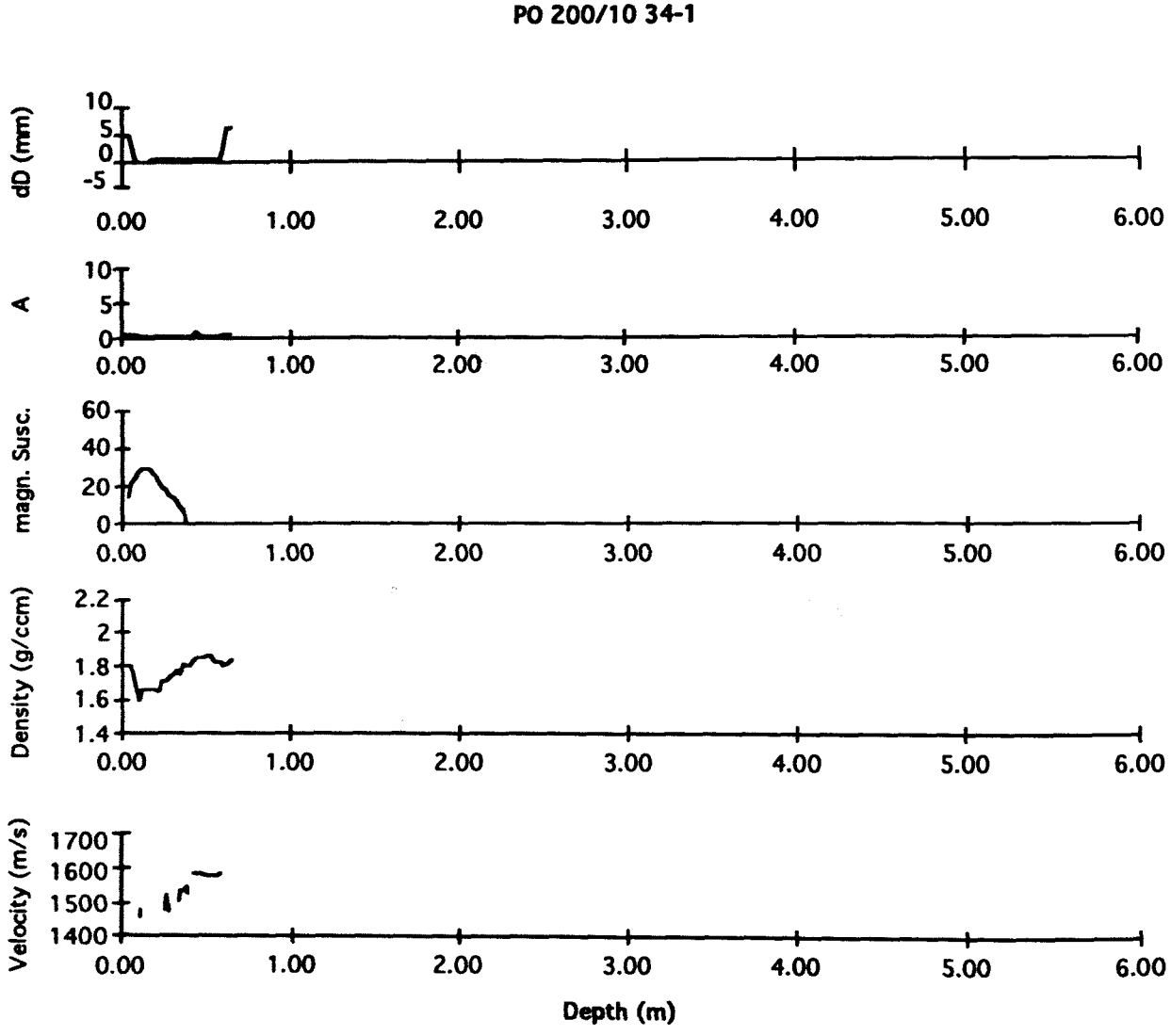

Figure 13a. Physical properties of core 34-1 derived from continous logging. From top to bottom are shown: deviation from standard core diameter, changes in wave amplitude, magnetic suszeptibility (cgs), density (g/cc) and velocity (m/s).

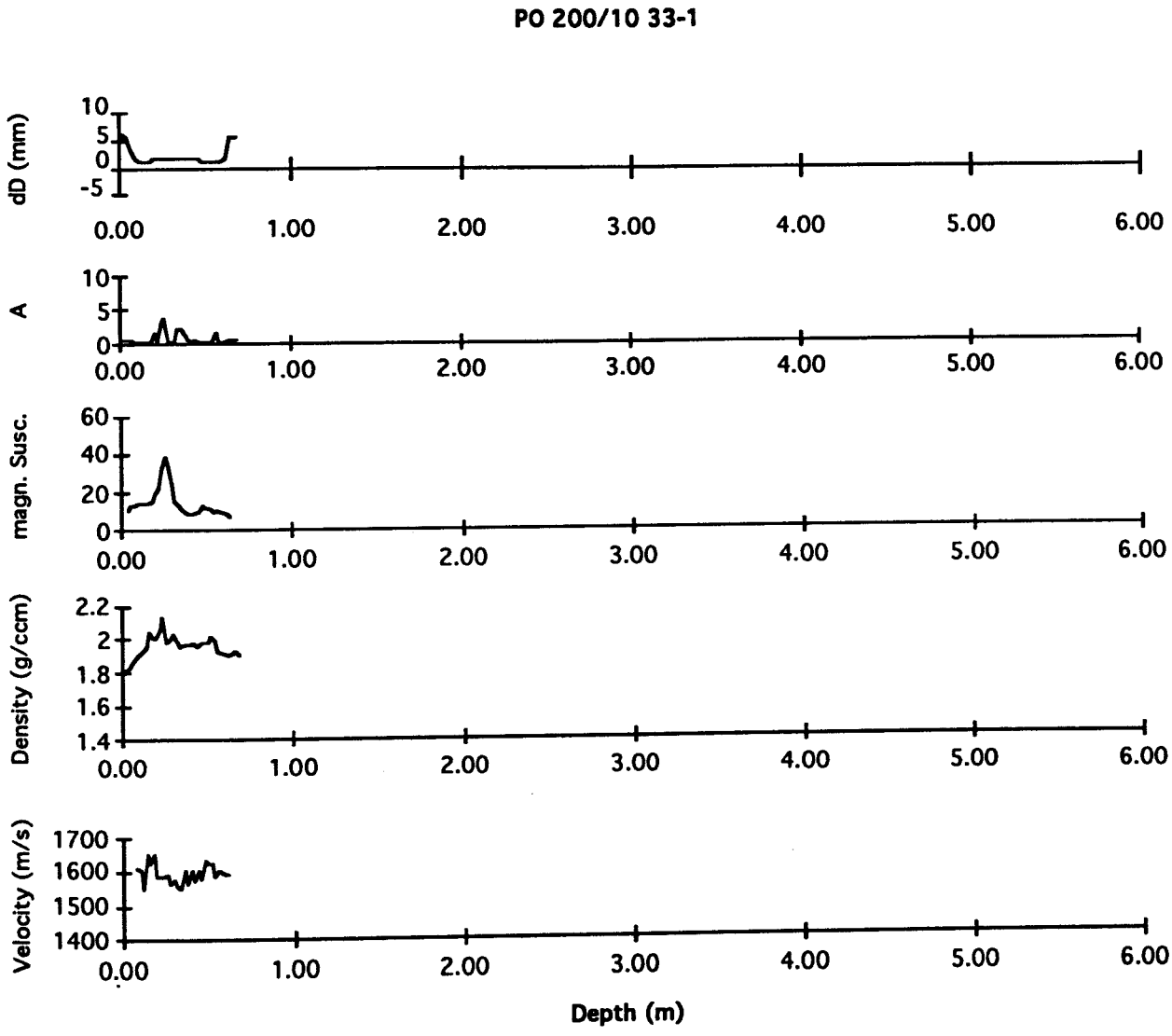

Figure 13b. Physical properties of core 33-1 derived from continous logging. From top to bottom are shown: deviation from standard core diameter, changes in wave amplitude, magnetic suszeptibility (cgs), density (g/cc) and velocity (m/s).

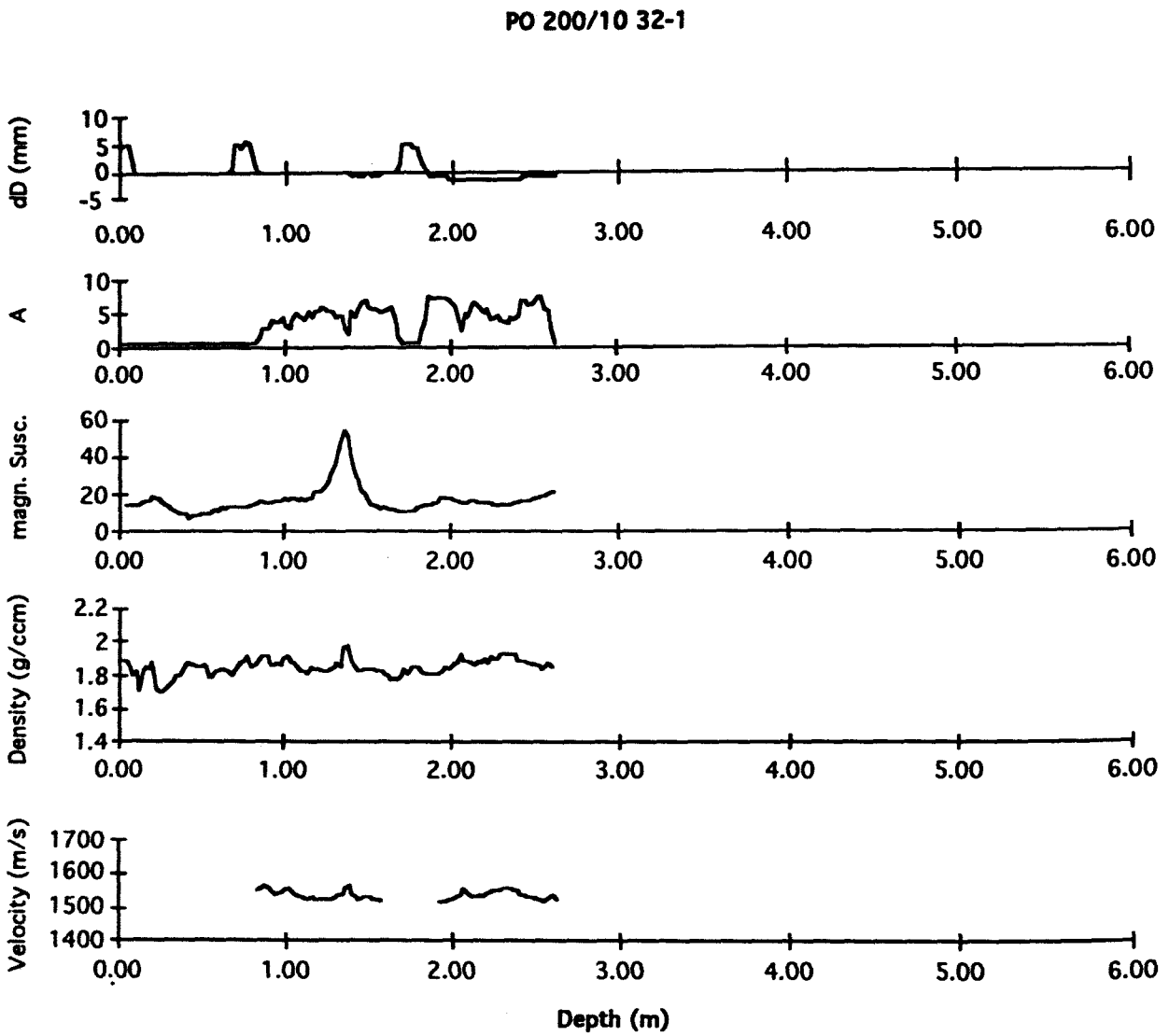

Figure 13c. Physical properties of core 32-1 derived from continous logging. From top to bottom are shown: deviation from standard core diameter, changes in wave amplitude, magnetic suszeptibility (cgs), density (g/cc) and velocity (m/s).

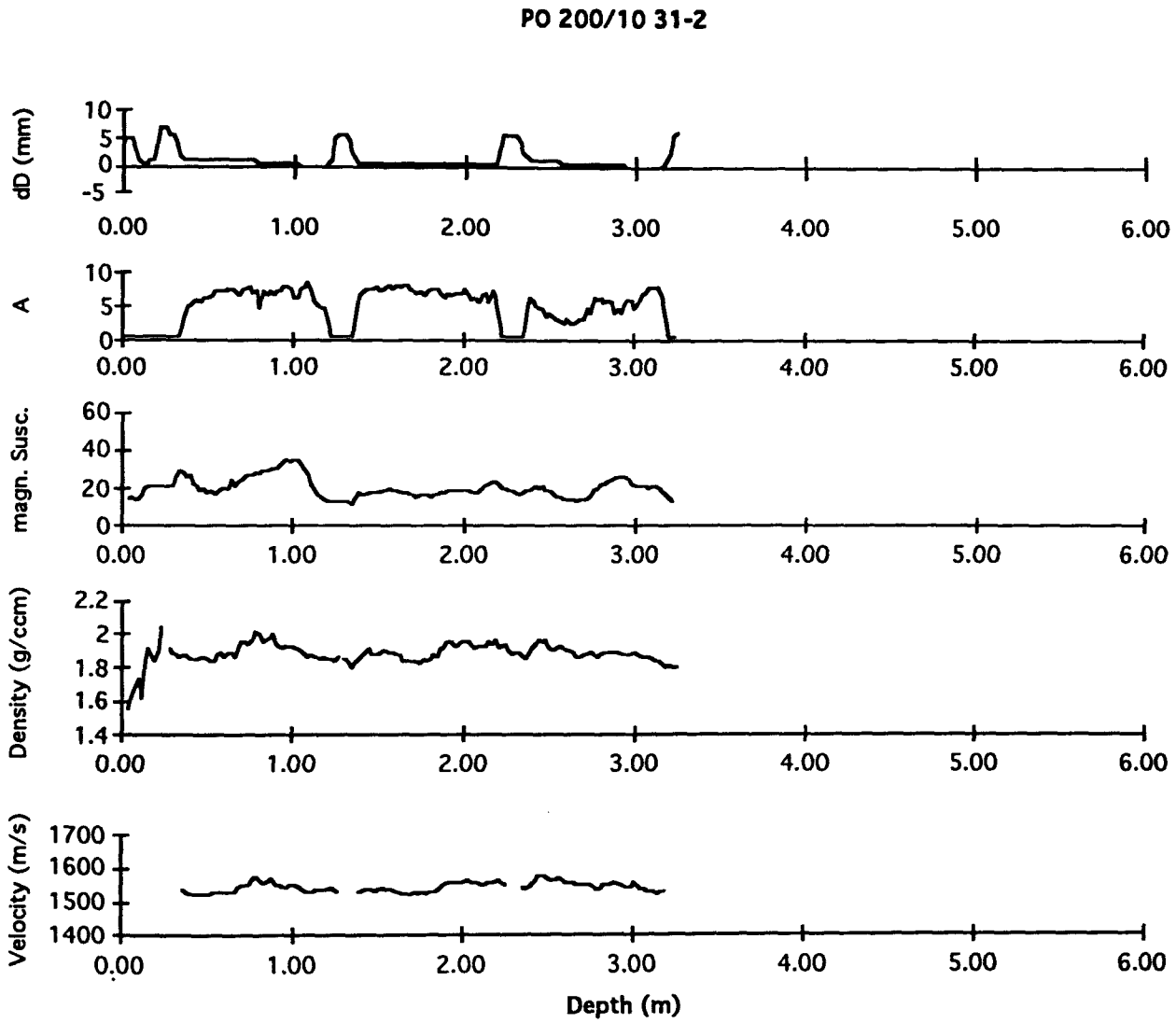

Figure 13d. Physical properties of core 31-2 derived from continous logging. From top to bottom are shown: deviation from standard core diameter, changes in wave amplitude, magnetic suszeptibility (cgs), density (g/cc) and velocity (m/s).

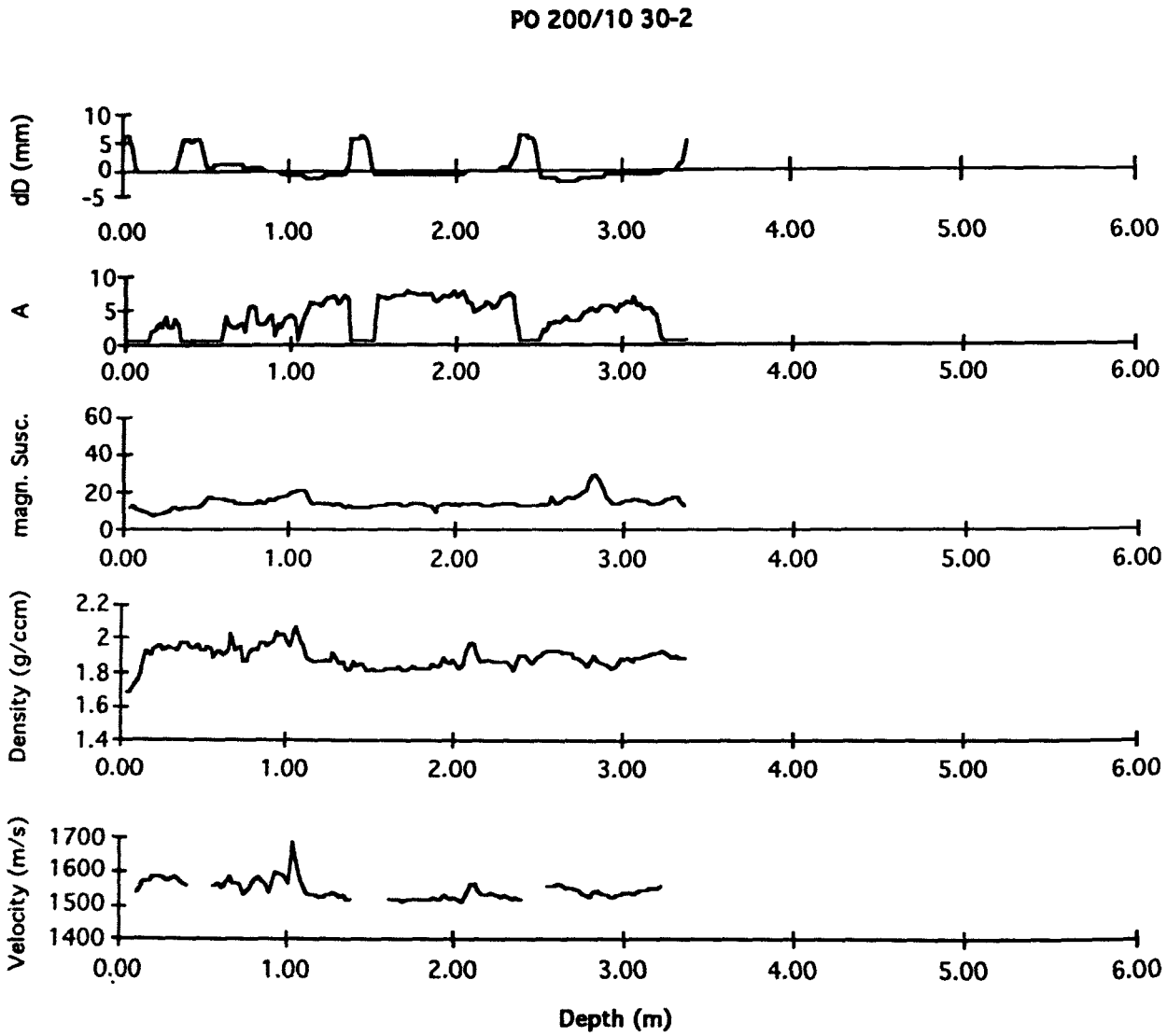

Figure 13e. Physical properties of core 30-2 derived from continous logging. From top to bottom are shown: deviation from standard core diameter, changes in wave amplitude, magnetic suszeptibility (cgs), density (g/cc) and velocity (m/s).

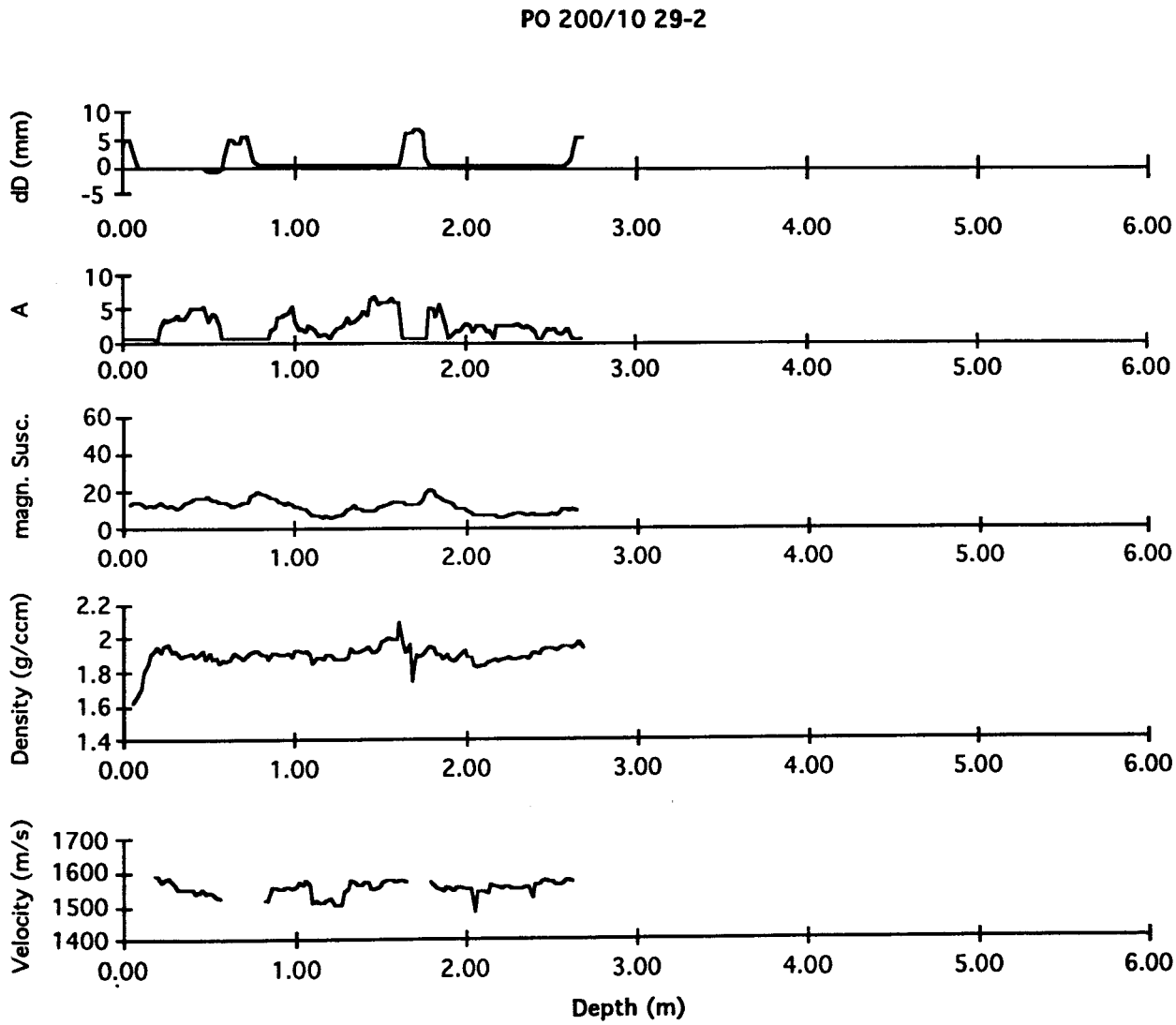

Figure 13f. Physical properties of core 29-2 derived from continous logging. From top to bottom are shown: deviation from standard core diameter, changes in wave amplitude, magnetic suszeptibility (cgs), density (g/cc) and velocity (m/s).

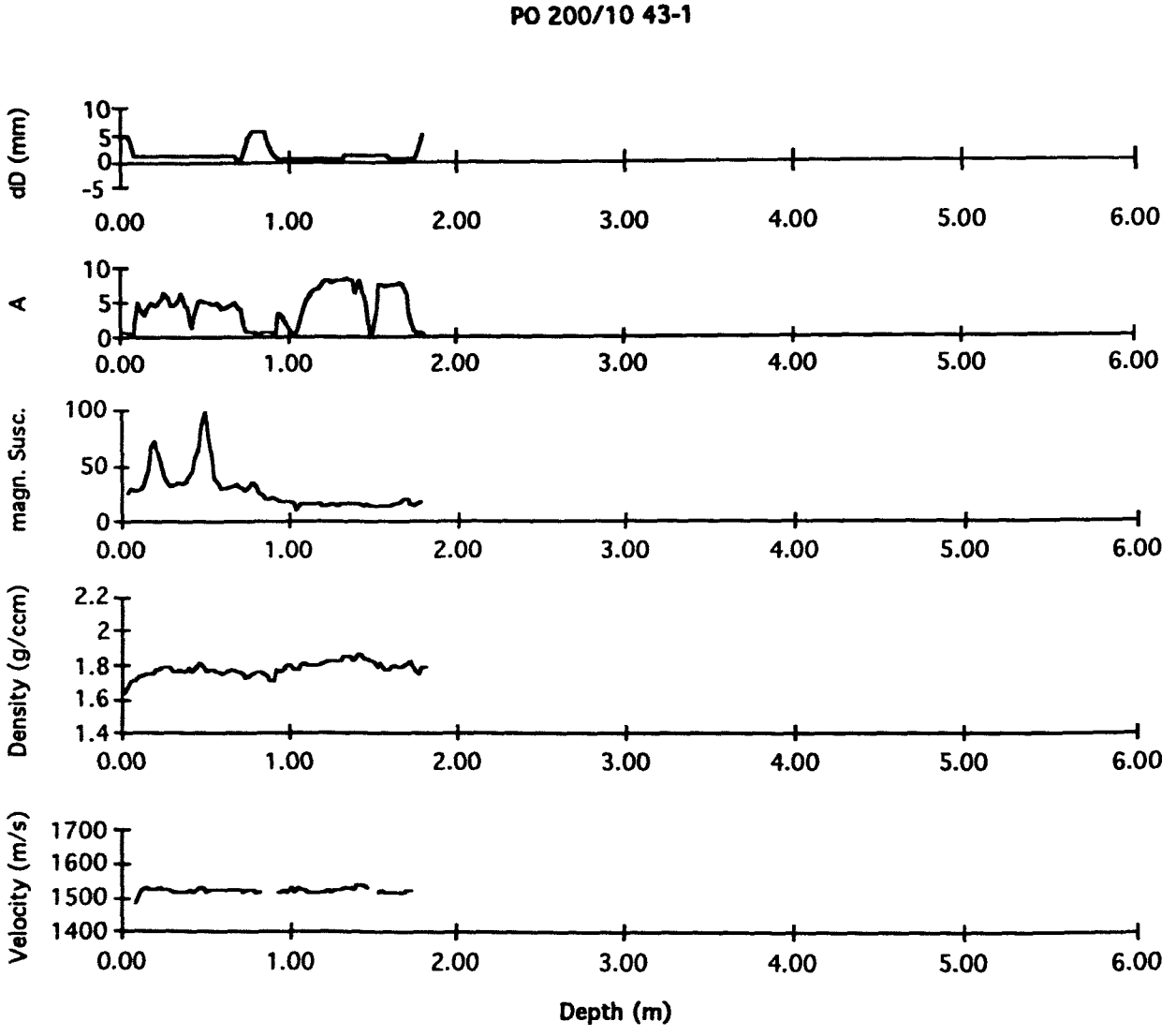

Figure 13g. Physical properties of core 43-1 derived from continous logging. From top to bottom are shown: deviation from standard core diameter, changes in wave amplitude, magnetic suszeptibility (cgs), density (g/cc) and velocity (m/s).

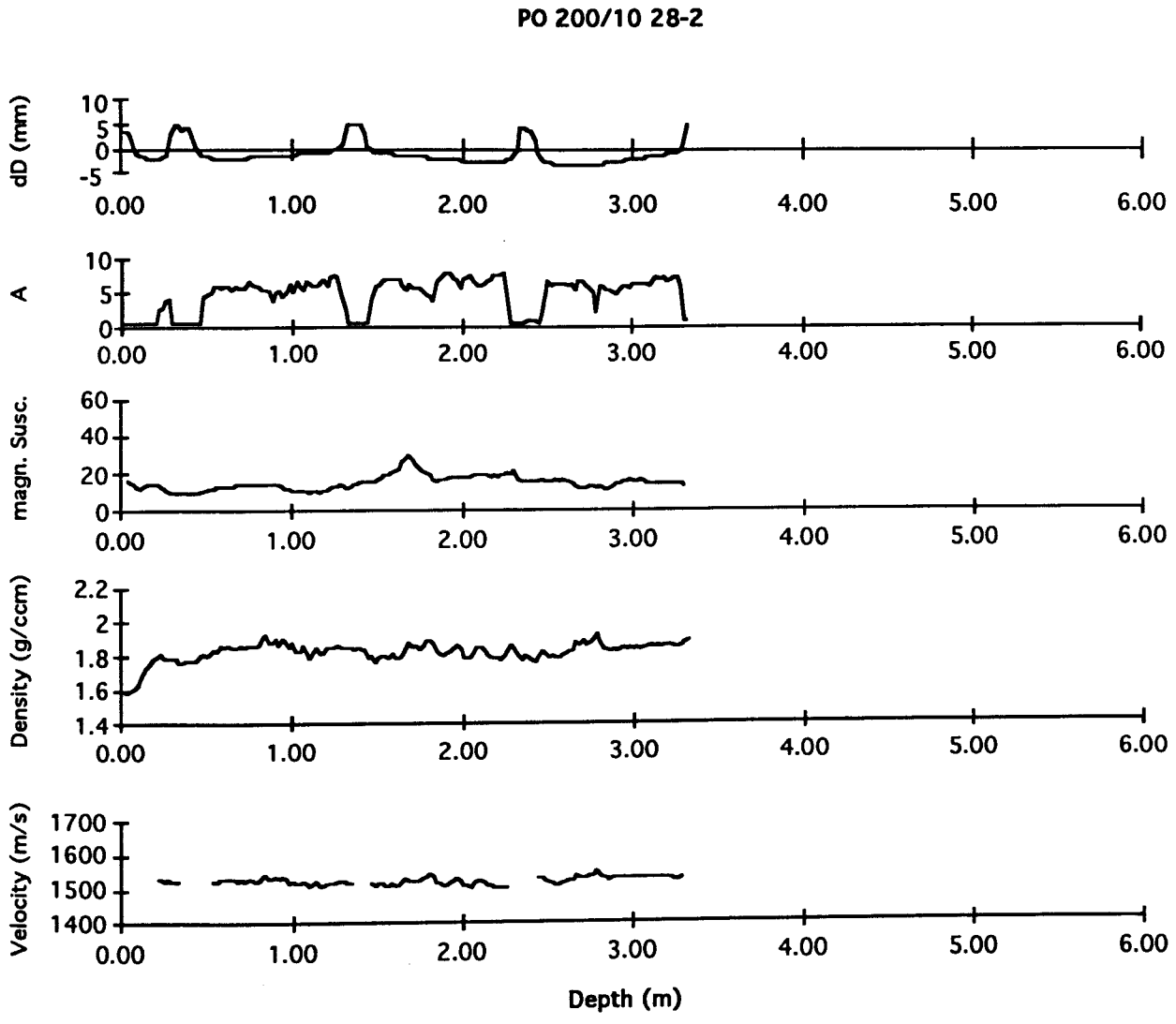

Figure 13h. Physical properties of core 28-2 derived from continous logging. From top to bottom are shown: deviation from standard core diameter, changes in wave amplitude, magnetic suszeptibility (cgs), density (g/cc) and velocity (m/s).

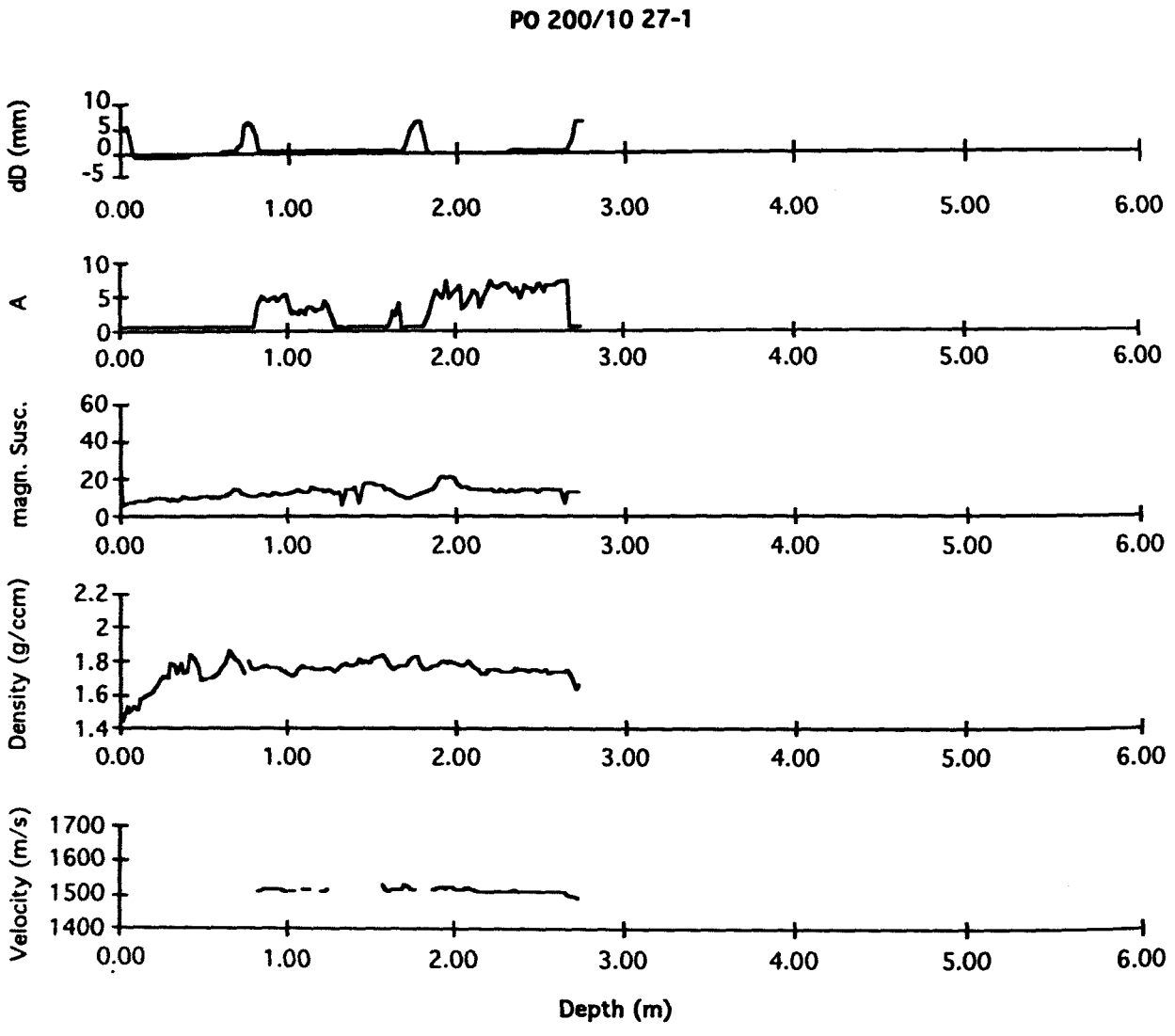

Figure 13i. Physical properties of core 27-1 derived from continous logging. From top to bottom are shown: deviation from standard core diameter, changes in wave amplitude, magnetic suszeptibility (cgs), density (g/cc) and velocity (m/s).

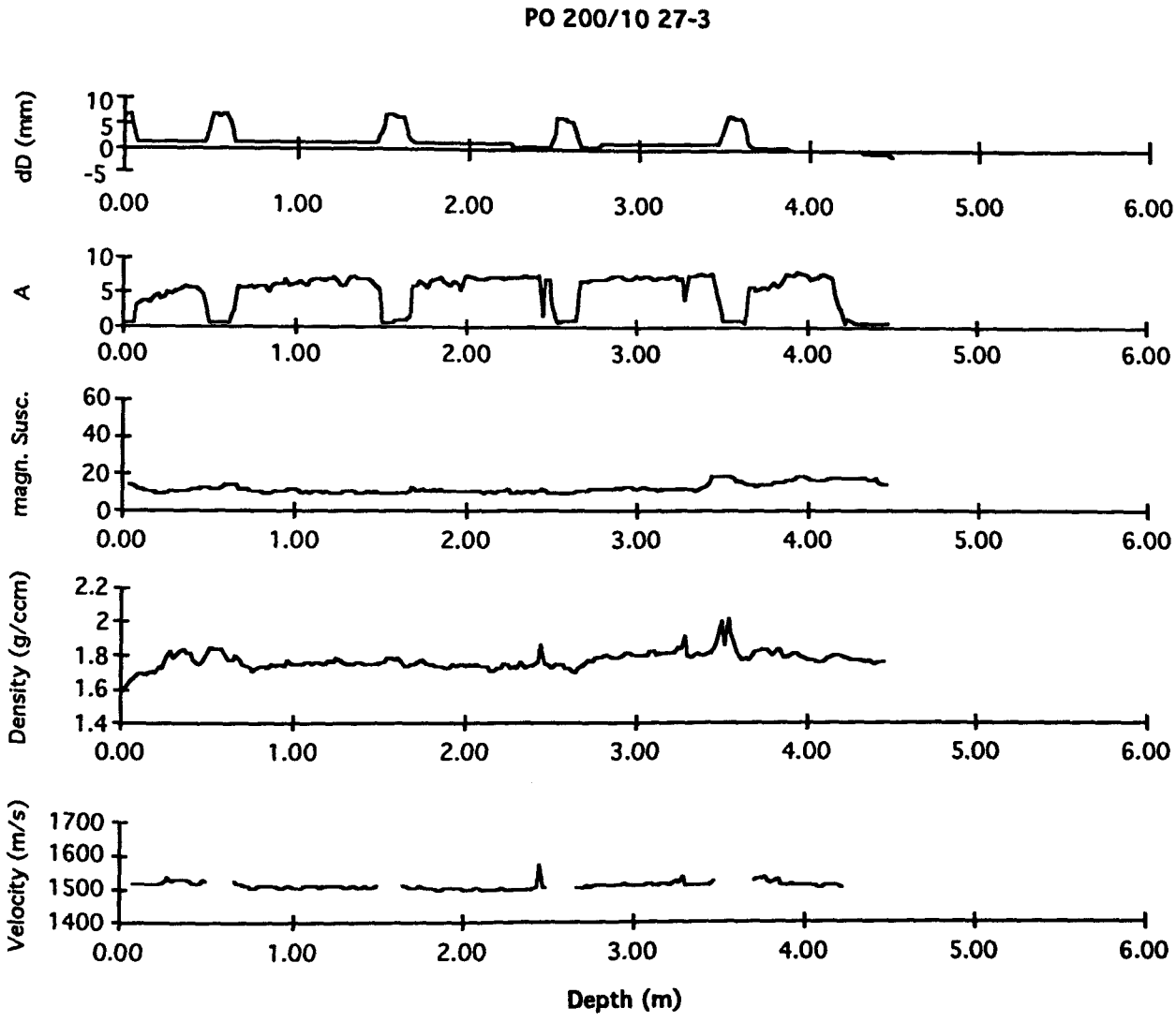

Figure 13j. Physical properties of core 27-3 derived from continous logging. From top to bottom are shown: deviation from standard core diameter, changes in wave amplitude, magnetic suszeptibility (cgs), density (g/cc) and velocity (m/s).

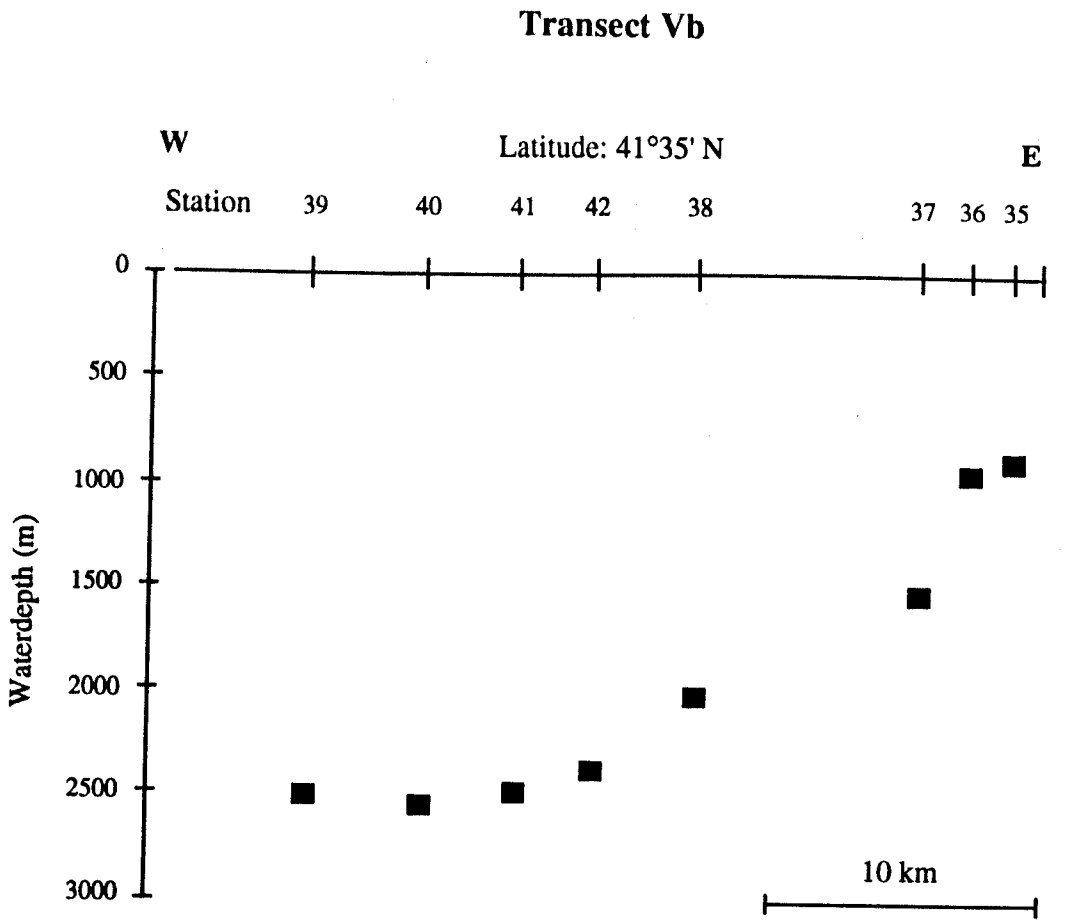

Figure 14. Core stations on transect Vb, showing waterdepth of core positions projected on 41°35' N Latitude

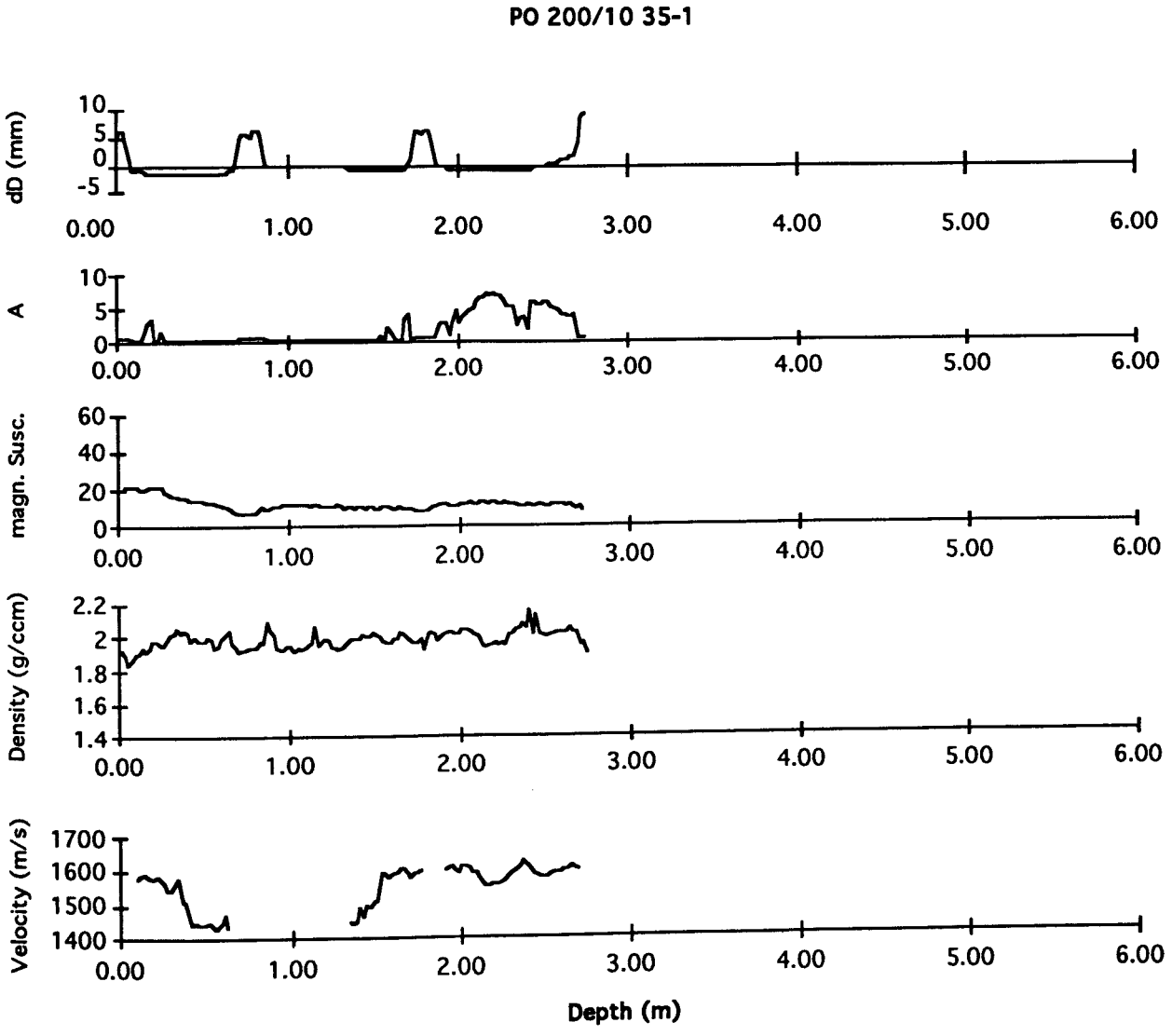

Figure 15a. Physical properties of core 35-1 derived from continous logging. From top to bottom are shown: deviation from standard core diameter, changes in wave amplitude, magnetic suszeptibility (cgs), density (g/cc) and velocity (m/s).

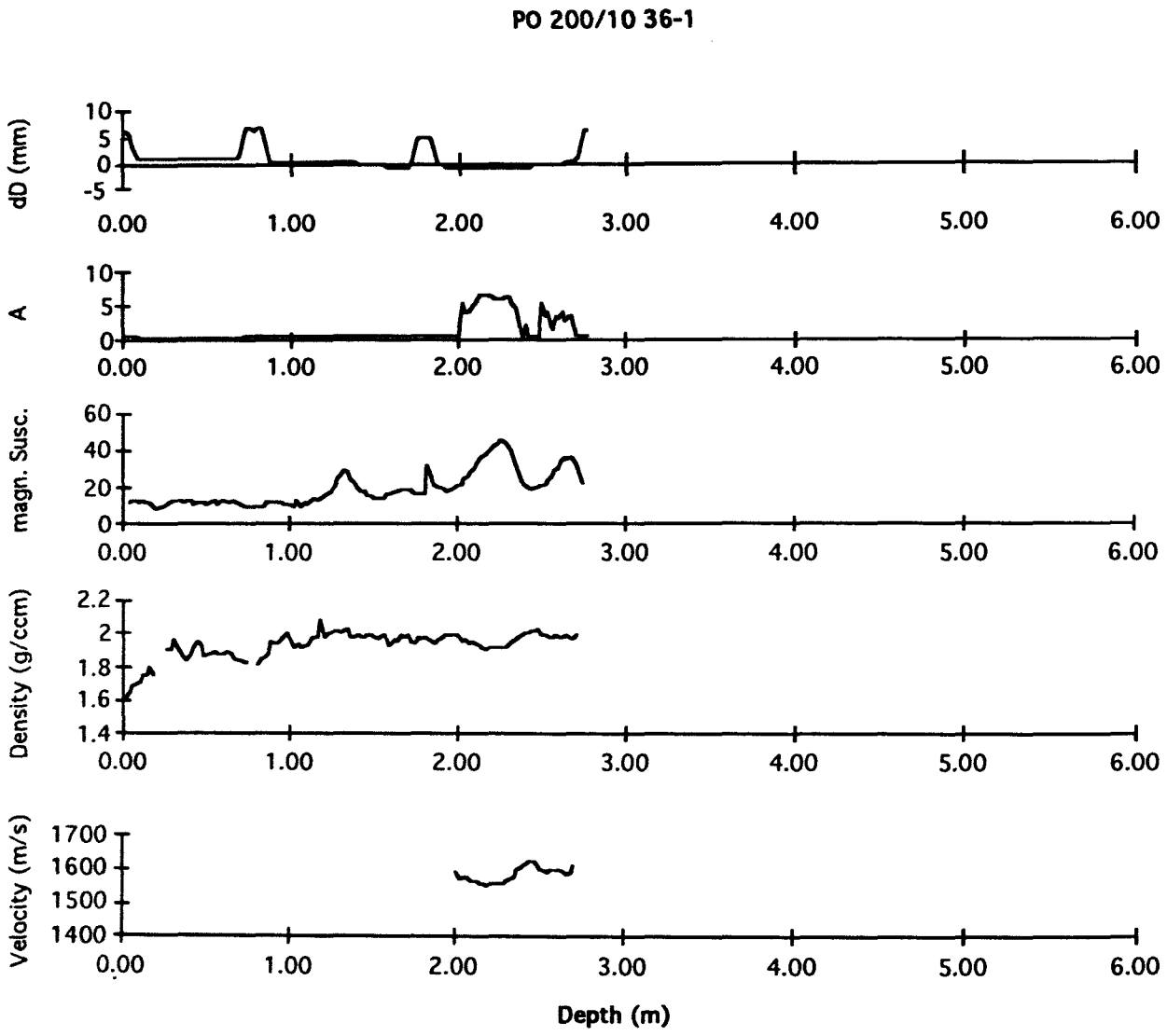

Figure 15b. Physical properties of core 36-1 derived from continous logging. From top to bottom are shown: deviation from standard core diameter, changes in wave amplitude, magnetic suszeptibility (cgs), density (g/cc) and velocity (m/s).

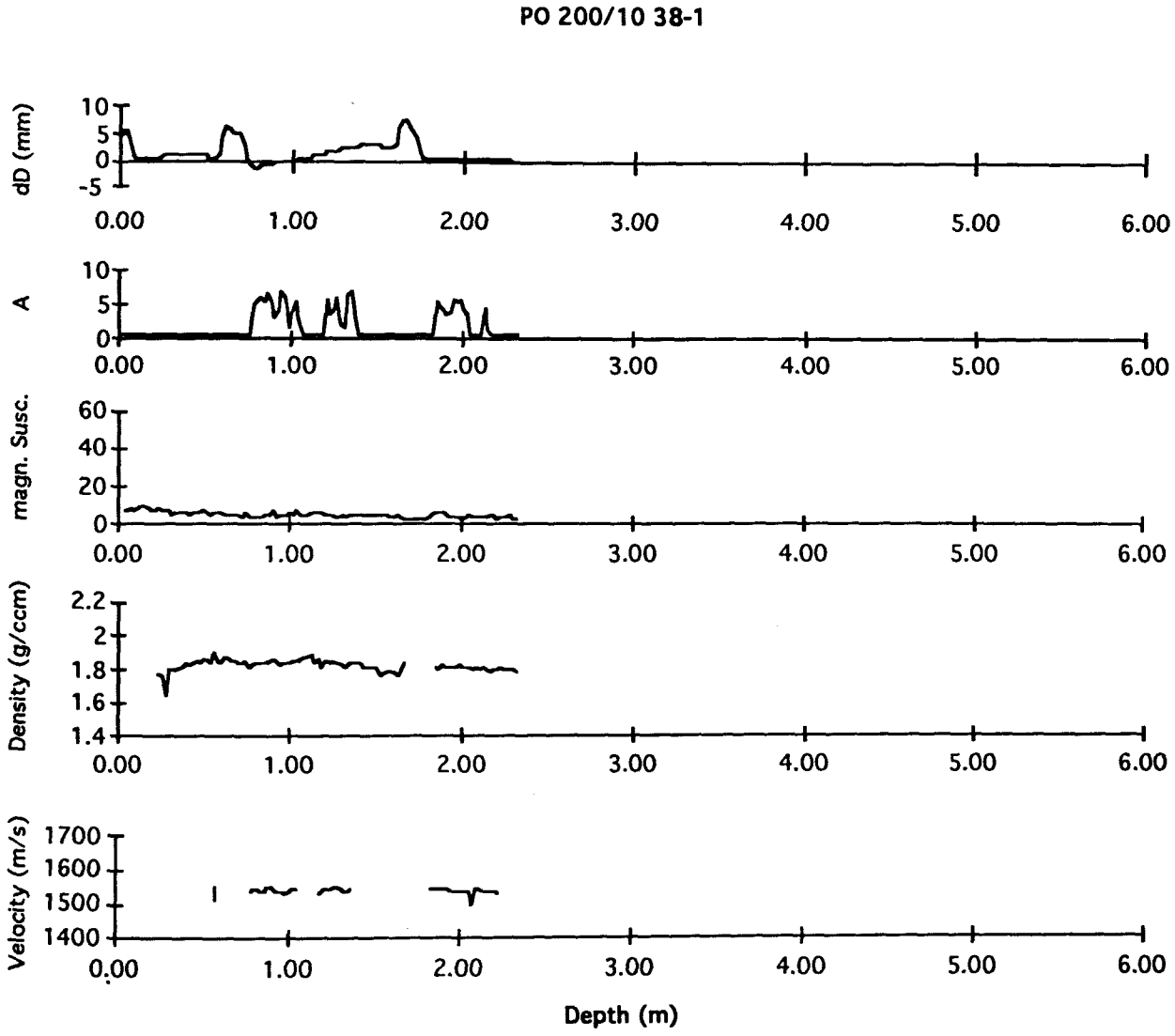

Figure 15c. Physical properties of core 38-1 derived from continous logging. From top to bottom are shown: deviation from standard core diameter, changes in wave amplitude, magnetic suszeptibility (cgs), density (g/cc) and velocity (m/s).

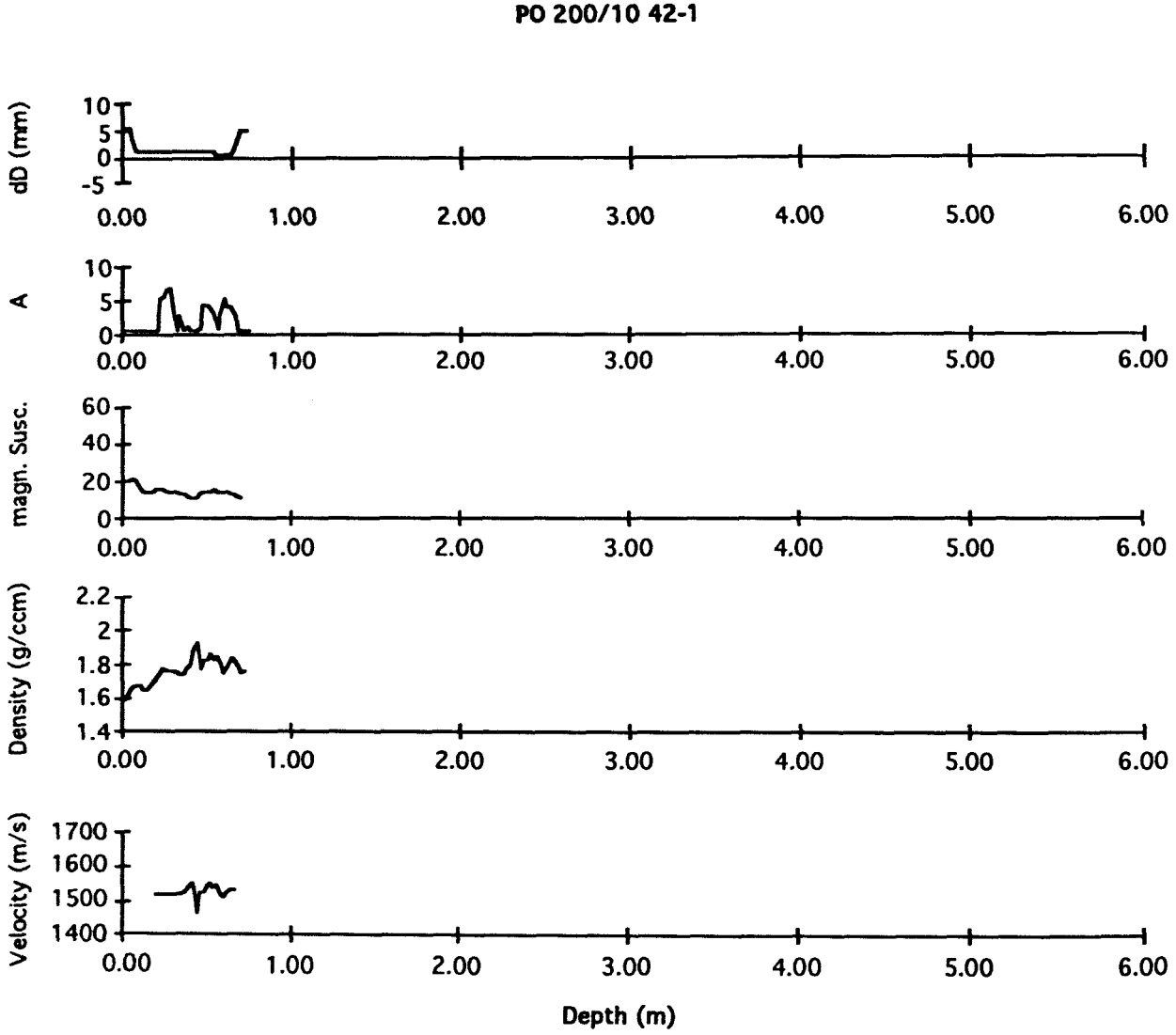

Figure 15d. Physical properties of core 42-1 derived from continous logging. From top to bottom are shown: deviation from standard core diameter, changes in wave amplitude, magnetic suszeptibility (cgs), density (g/cc) and velocity (m/s).

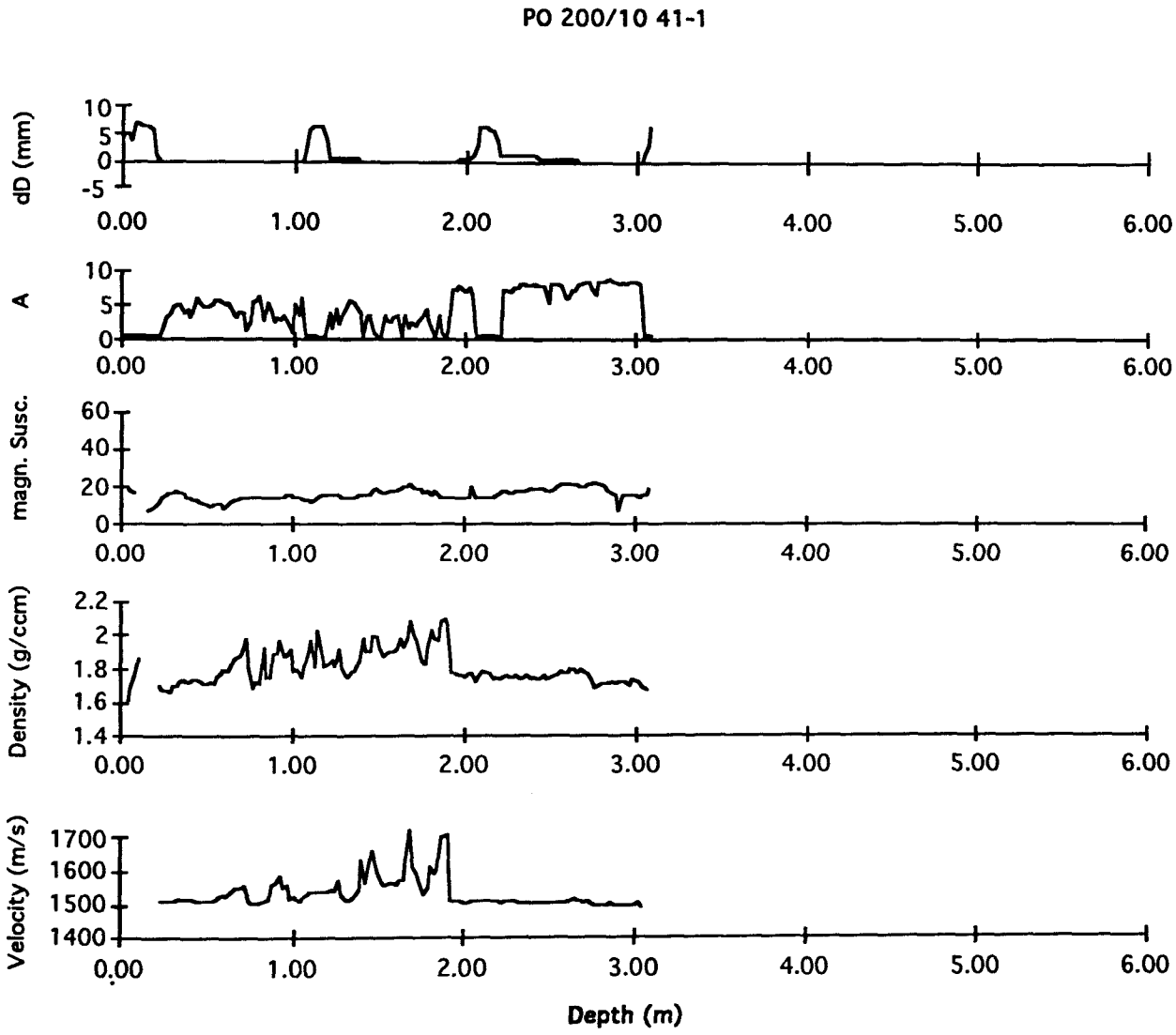

Figure 15e. Physical properties of core 41-1 derived from continous logging. From top to bottom are shown: deviation from standard core diameter, changes in wave amplitude, magnetic suszeptibility (cgs), density (g/cc) and velocity (m/s).

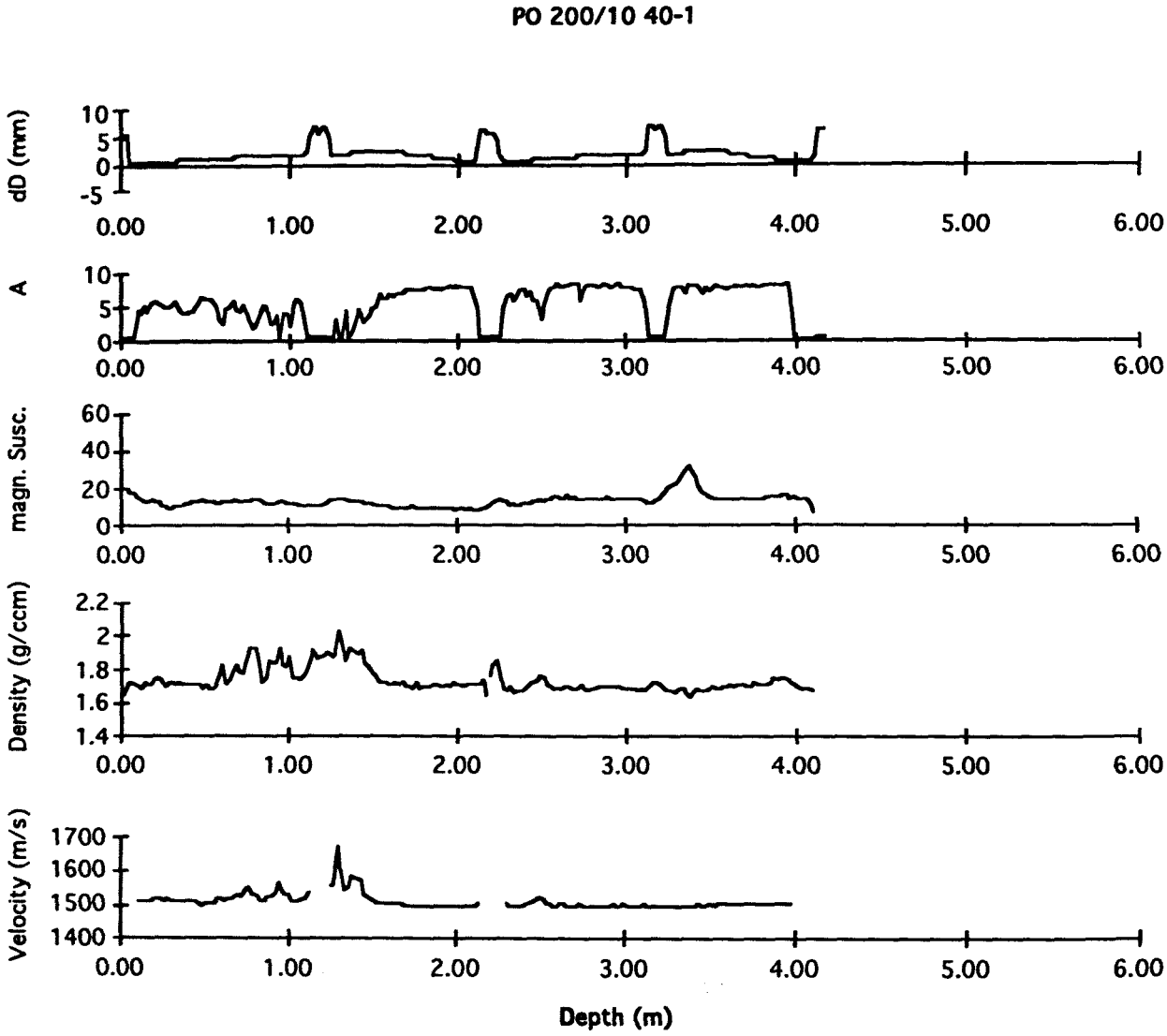

Figure 15f. Physical properties of core 40-1 derived from continous logging. From top to bottom are shown: deviation from standard core diameter, changes in wave amplitude, magnetic suszeptibility (cgs), density (g/cc) and velocity (m/s).

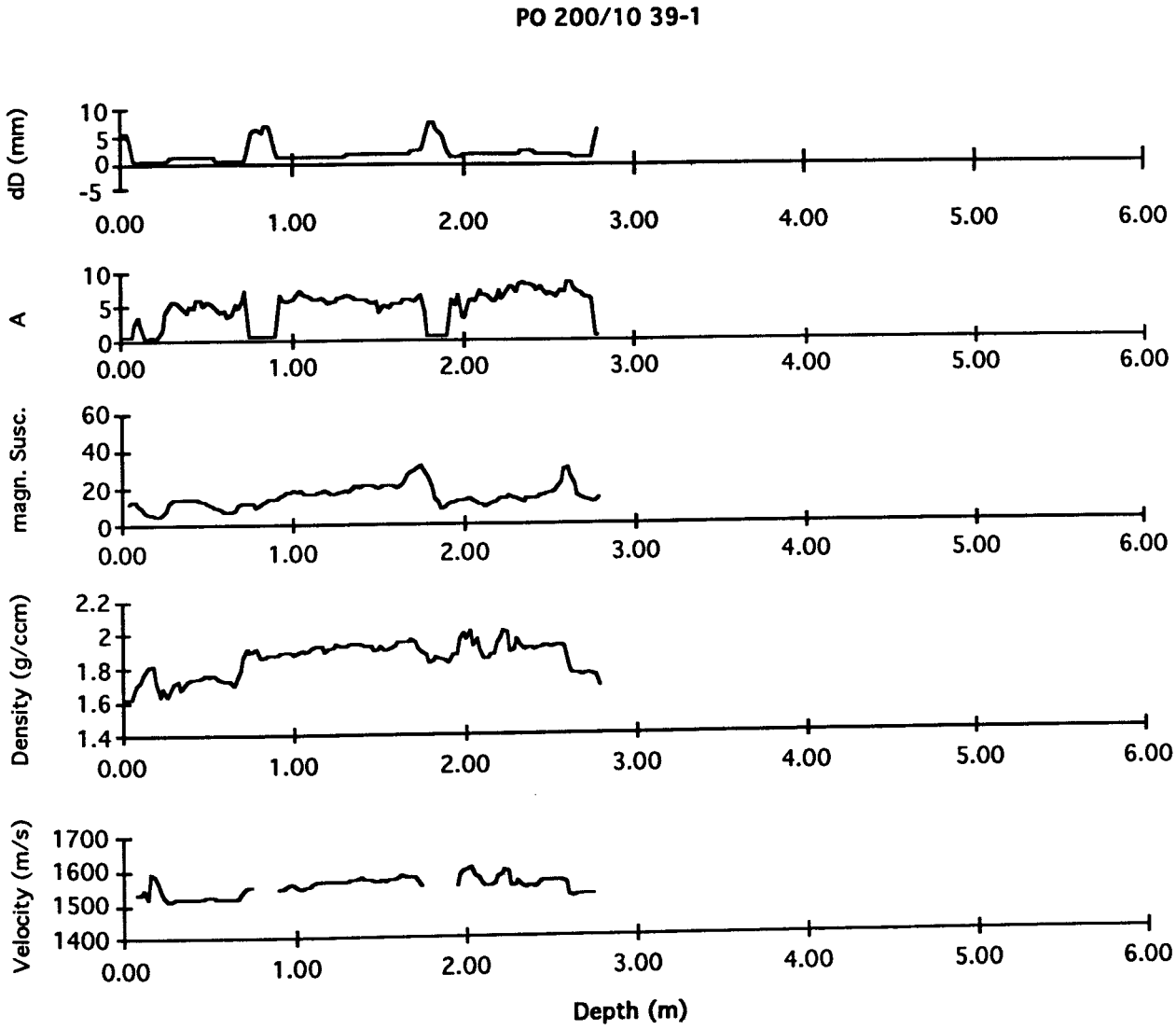

Figure 15g. Physical properties of core 39-1 derived from continous logging. From top to bottom are shown: deviation from standard core diameter, changes in wave amplitude, magnetic suszeptibility (cgs), density (g/cc) and velocity (m/s).

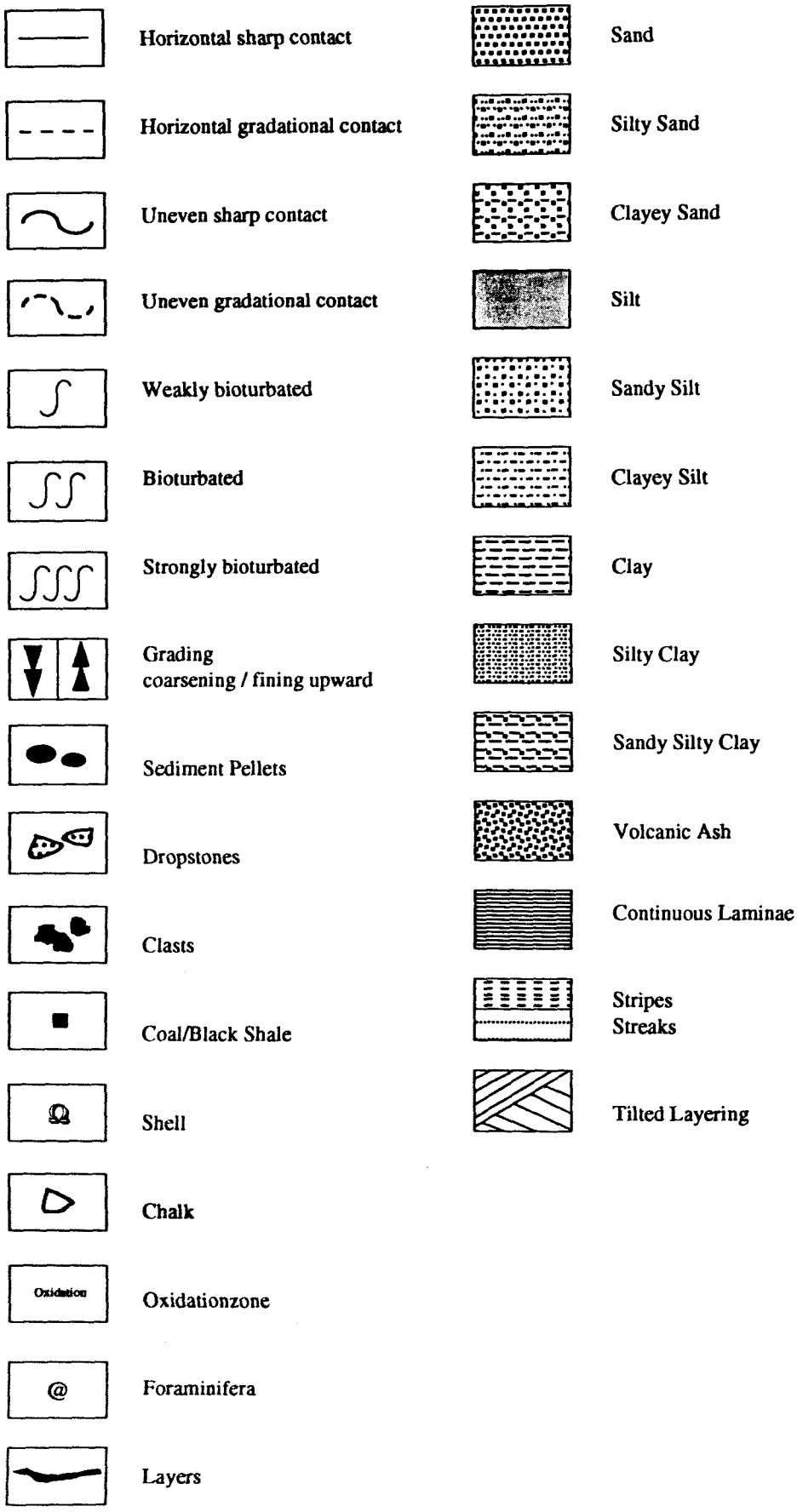

Figure 16. Legend: lithology symbols and symbols used to describe sediments

POSEIDON 200/10 — 07.08.1993 - 23.08.1993
Station: PO 200/10-8 — Date: 09.08.1993
Position: 37° 38,5´ N ; 09° 56,4´ W — Water Depth: 2170 m

Core: PO 200/10-8-2 SL — Core Recovery: 300 cm
Section: 0 - 150 cm

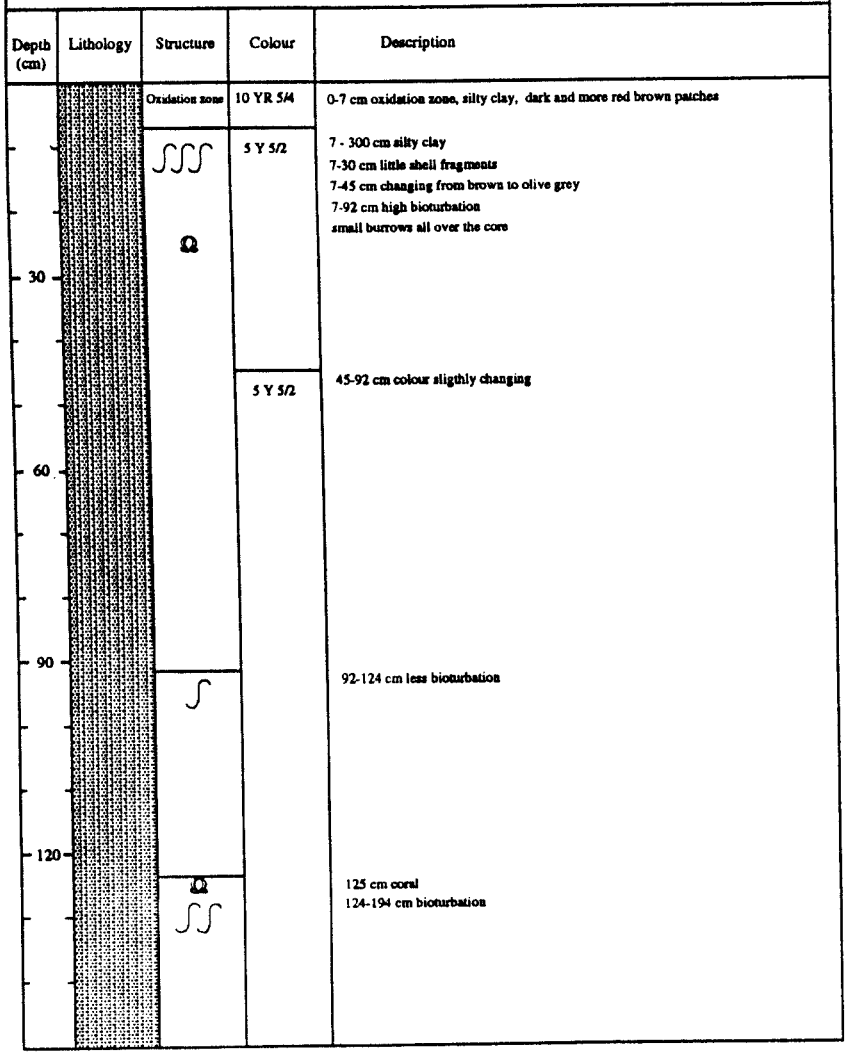

Figure 17a. Description of sediment column of core 8-2

POSEIDON 200/10 — 07.08.1993 - 23.08.1993
Station: PO 200/10-8 — Date: 09.08.1993
Position: 37° 38,5´ N ; 09° 56,4´ W — Water Depth: 2170 m

Core: PO 200/10-8-2 SL — Core Recovery: 300 cm
Section: 150 - 300 cm

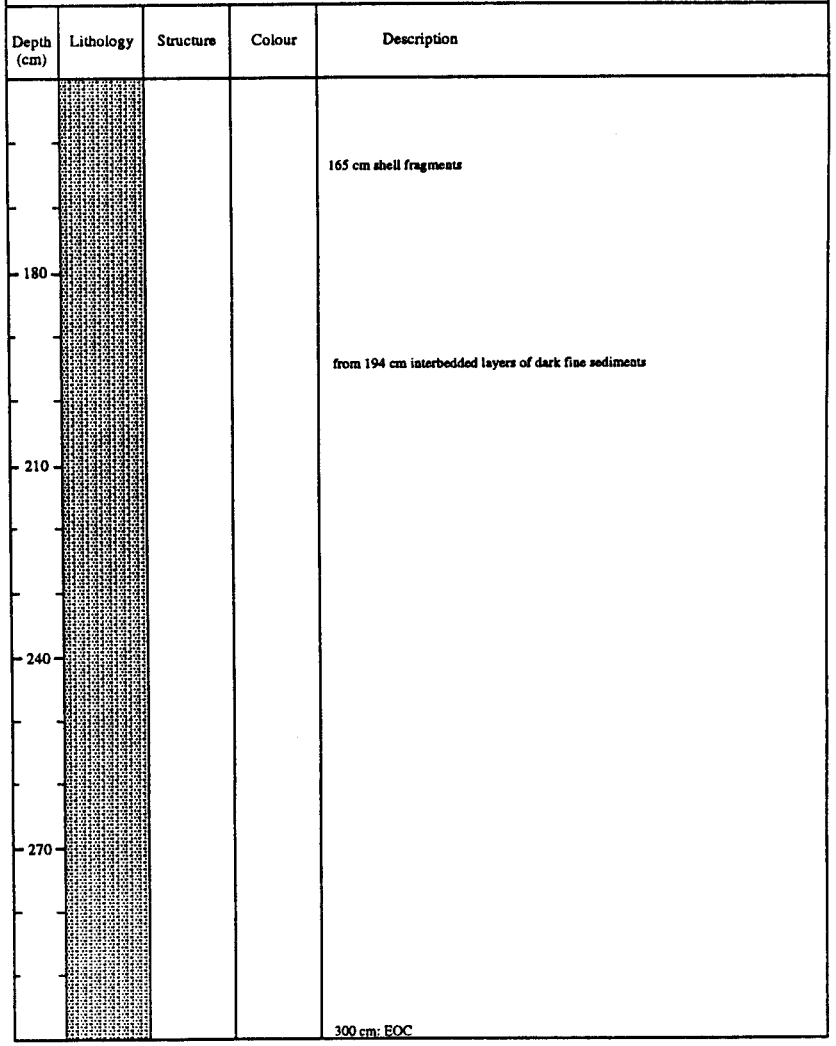

Figure 17a. continued

POSEIDON 200/10 — 07.08.1993 - 23.08.1993
Station: PO 200/10-9 — Date: 09.08.1993
Position: 37° 36,8' N ; 10° 02,6' W — Water Depth: 2320 m

Core: PO 200/10- 9-1 SL — Core Recovery: 300 cm
Section: 0 - 150 cm

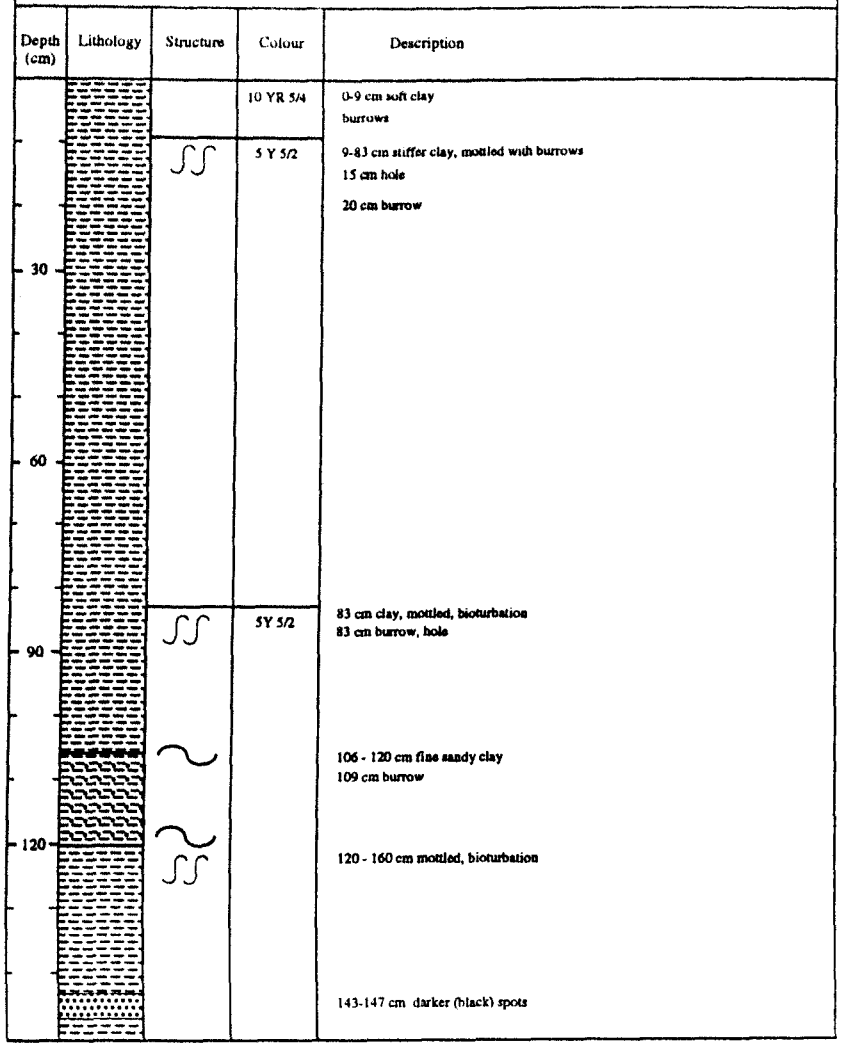

Figure 17b. Description of sediment column of core 9-1

POSEIDON 200/10 — 07.08.1993 -23.08.1993
Station: PO 200/10-9 — Date: 09.08.1993
Position: 37° 36,8' N ; 10° 02,6' W — Water Depth: 2320 m

Core: PO 200/10-9-1 SL — Core Recovery: 300 cm
Section: 150 - 300 cm

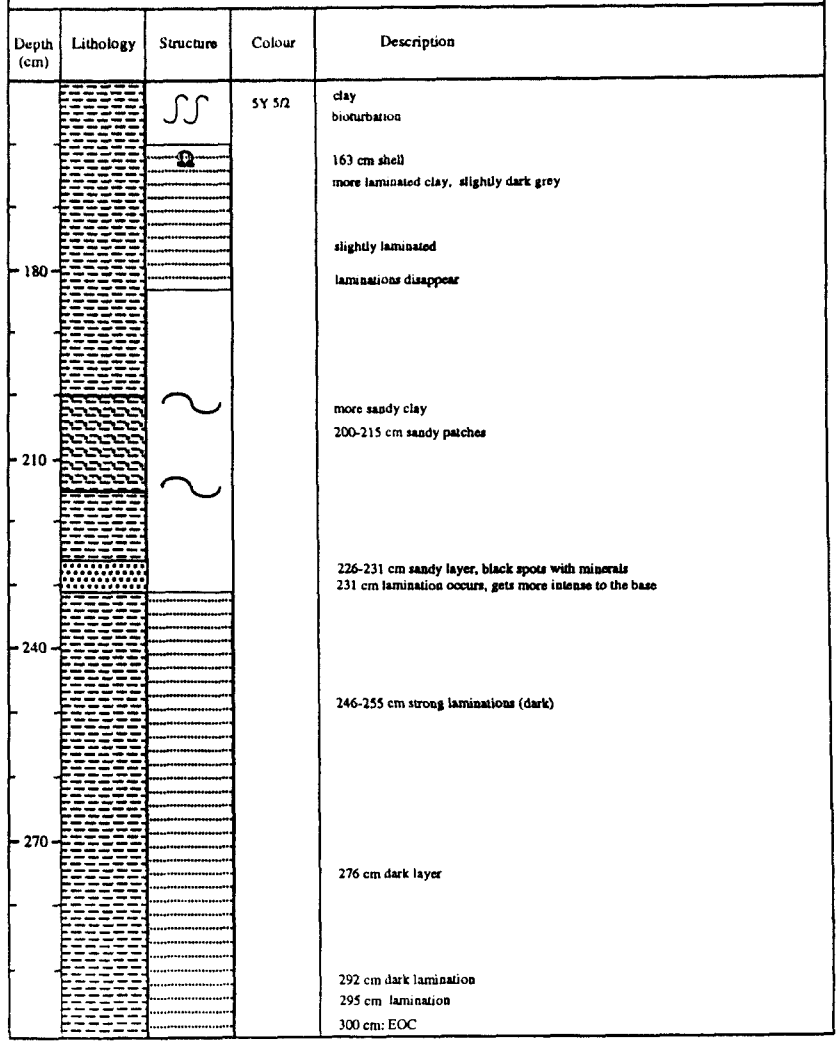

Figure 17b. continued

POSEIDON 200/10
Station: PO 200/10-12
Position: 39° 38,2´ N ; 09° 40,3´ W

07.08.1993 - 23.08.1993
Date: 10.08.1993
Water Depth: 865 m

Core: PO 200/10-12-1 SL
Section: 0 - 150 cm

Core Recovery: 273 cm

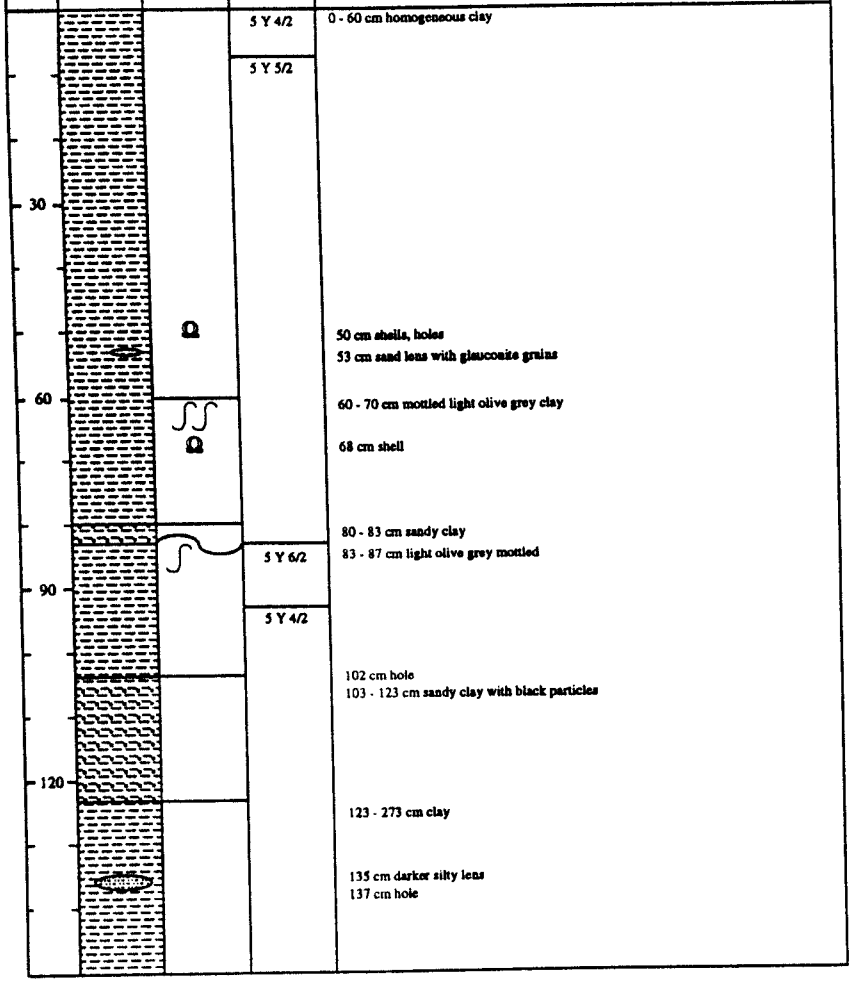

Figure 18a. Description of sediment column of core 12-1

POSEIDON 200/10
Station: PO 200/10-12
Position: 39° 38,2´ N ; 09° 40,3´ W

07.08.1993 - 23.08.1993
Date: 10.08.1993
Water Depth: 865 m

Core: PO 200/10-12-1 SL
Section: 150 - 273 cm

Core Recovery: 273 cm

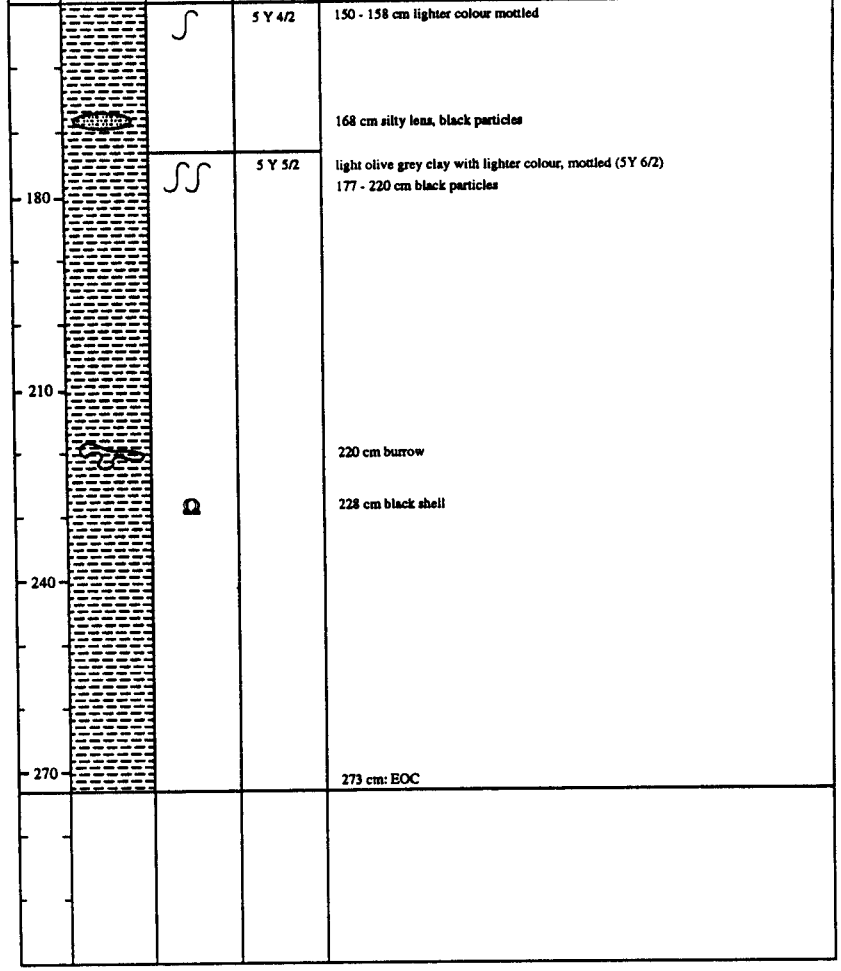

Figure 18a. continued

POSEIDON 200/10
Station: PO 200/10-13
Position: 39° 37,52´ N ; 09° 45,4´ W

07.08.1993 - 23.08.1993
Date: 10.08.1993
Water Depth: 1620 m

Core: PO 200/10-13-1 SL
Section: 0 - 62 cm

Core Recovery: 62 cm

Depth (cm)	Lithology	Structure	Colour	Description
			5 YR 5/6	0 - 50 cm clayey sand, mostly foraminifera, high number of planktonic foraminifera; different colours of red and yellow lines
			5 Y 6/4	
30			10 R 4/6	26 - 35 cm red particles stained sediment
			5 Y 6/4	
			10 R 4/6	
			5 Y 4/2	shell on erosional surface
				50 - 62 cm silty clay with black particles (reducing environment)
60				62 cm : EOC
				first 2 cm in a seperate bag !
				Interpretation: Turbidity sediments over reducing environment. Clay seperated by erosional surface.
90				
120				

Figure 18b. Description of sediment column of core 13-1

POSEIDON 200/10
Station: PO 200/10-14
Position: 39° 37,11´ N ; 09° 50,48´ W

07.08.1993 - 23.08.1993
Date: 10.08.1993
Water Depth: 1824 m

Core: PO 200/10-14-1 SL
Section: 0 - 150 cm

Core Recovery: 172 cm

Depth (cm)	Lithology	Structure	Colour	Description
		Oxidation zone	10 YR 6/6	0 - 5 cm dark yellowish orange soft clay
			5 Y 5/2	5 - 62 cm mottled light olive grey clay with bands of lighter colour
				at 10 cm burrows
			5 Y 5/2	
30				
				48 cm hole
				51 cm shell
60			5 Y 4/2	erosional surface at a slump section beneath
				from 62 cm to bottom darker olive grey stiffer clay, disturbed and with black material
			5 Y 5/2	
				slump probable from top to bottom
				light olive grey sediment
				disturbed mixture of very hard and soft sediment
90				softer clay
120				

Figure 18c. Description of sediment column of core 14-1

POSEIDON 200/10
Station: PO 200/10-14
Position: 39° 37,11´ N ; 09° 50,48´ W

07.08.1993 - 23.08.1993
Date: 10.08.1993
Water Depth: 1824 m

Core: PO 200/10-14-1 SL
Section: 150 - 172 cm

Core Recovery: 172 cm

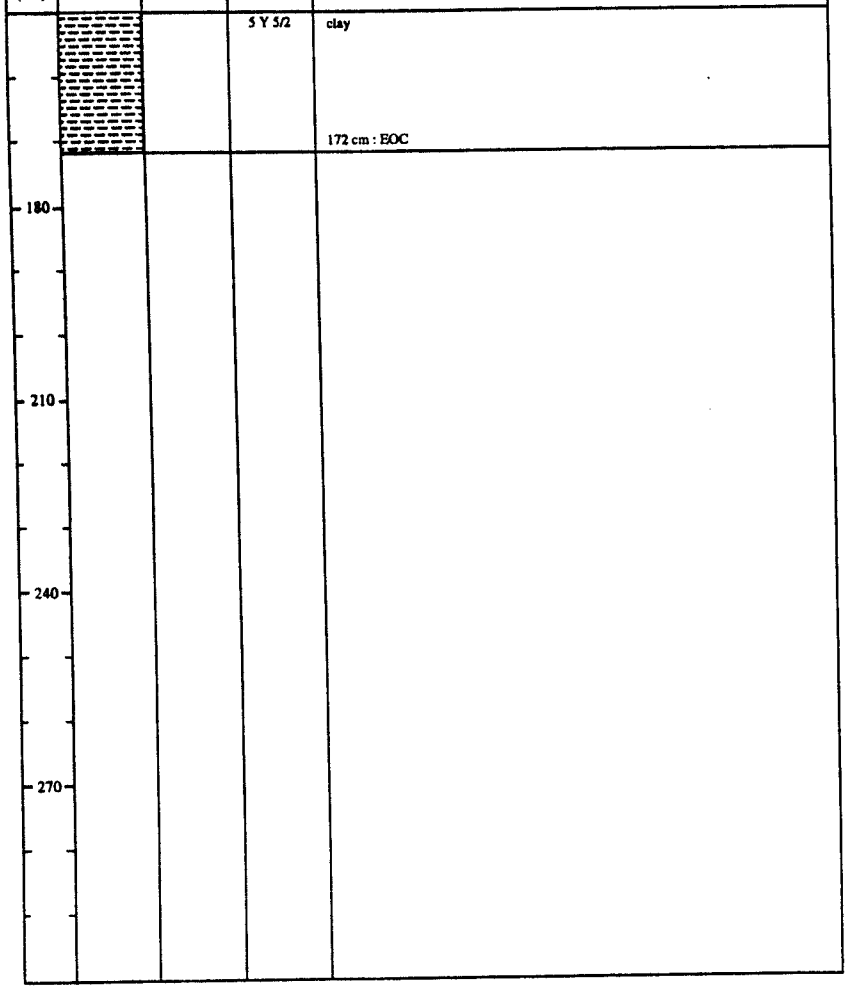

Figure 18c. continued

POSEIDON 200/10
Station: PO 200/10-15
Position: 39° 38´ N ; 09° 55,3´ W

07.08.1993 - 23.08.1993
Date: 10.08.1993
Water Depth: 1940 m

Core: PO 200/10-15-2 SL
Section: 0 - 150 cm

Core Recovery: 343 cm

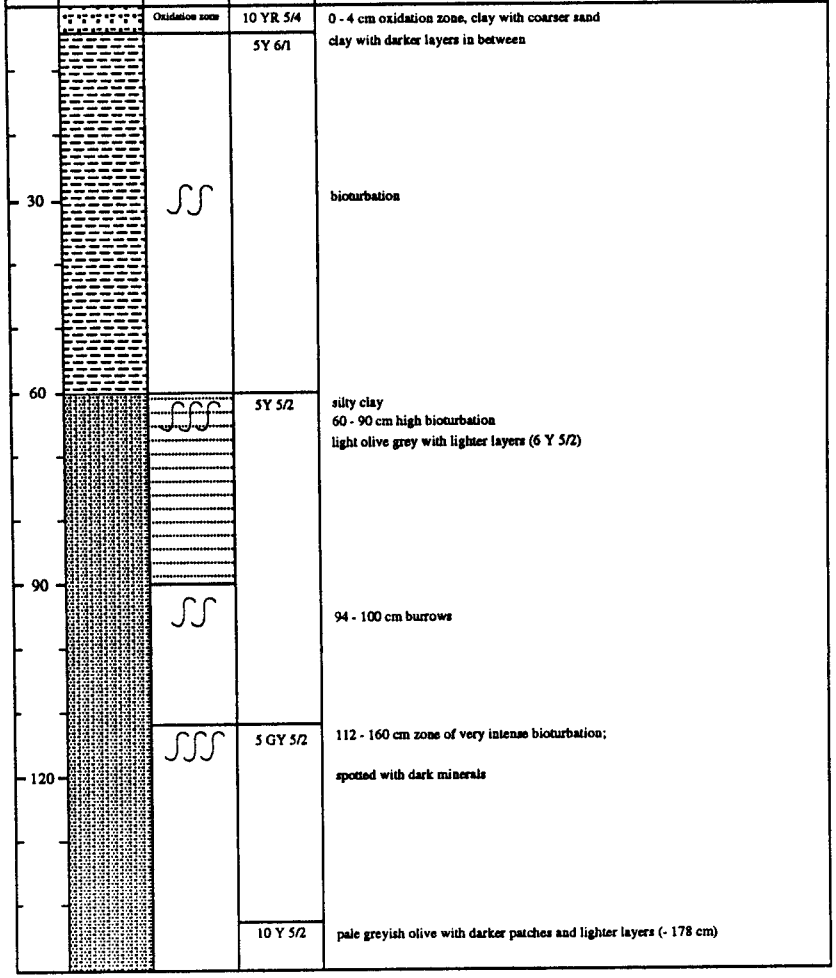

Figure 18d. Description of sediment column of core 15-2

POSEIDON 200/10
Station: PO 200/10-15
Position: 39° 38´ N ; 09° 55,3´ W

07.08.1993 - 23.08.1993
Date: 10.08.1993
Water Depth: 1940 m

Core: PO 200/10-15-2 SL
Section: 150 - 300 cm

Core Recovery: 343 cm

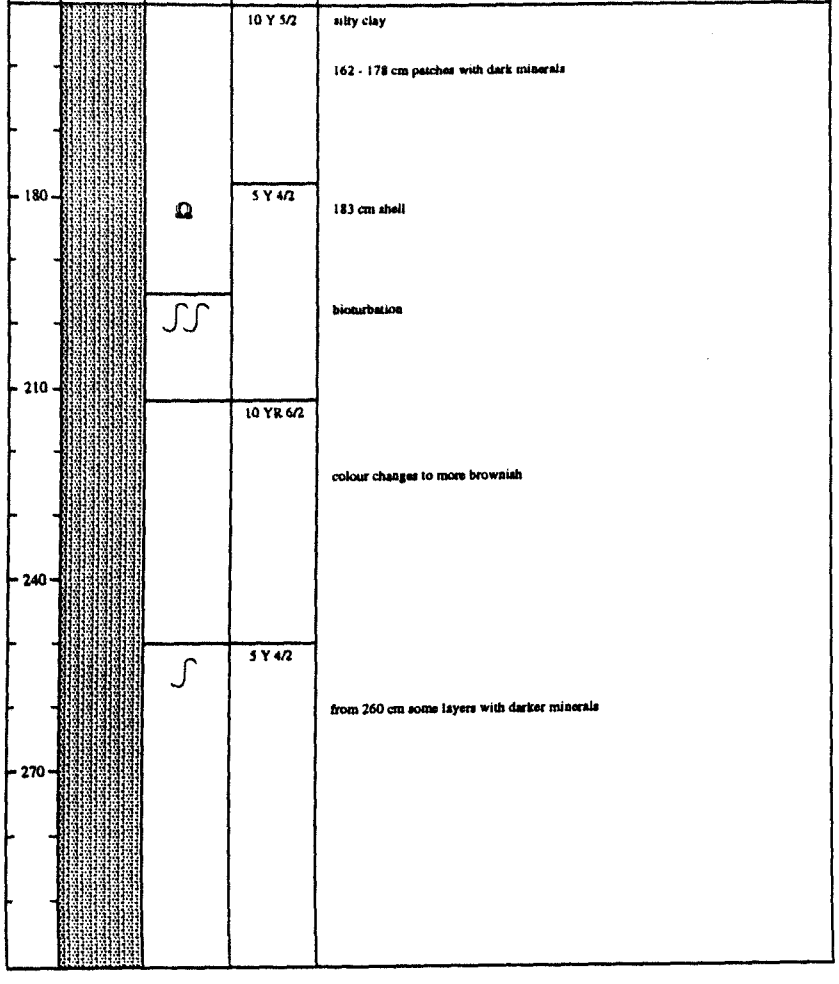

Figure 18d. continued

POSEIDON 200/10
Station: PO 200/10-15
Position: 39° 38´ N ; 09° 55,3´ W

07.08.1993 - 23.08.1993
Date: 10.08.1993
Water Depth: 1940 m

Core: PO 200/10-15-2 SL
Section: 300 - 343 cm

Core Recovery: 343 cm

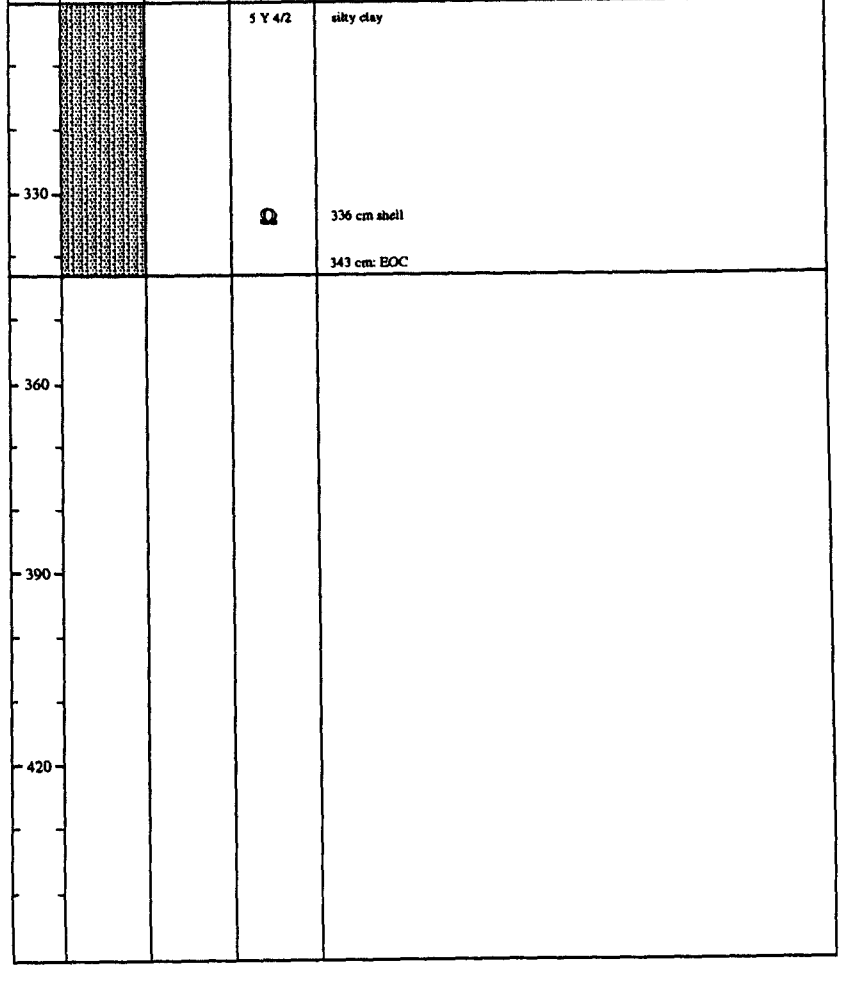

Figure 18d. continued

POSEIDON 200/10
Station: PO 200/10-16
Position: 39° 43,9´ N ; 09° 10,8´ W

07.08.1993 - 23.08.1993
Date: 10.08.1993
Water Depth: 2140 m

Core: PO 200/10-16-2 SL
Section: 0 - 61 cm

Core Recovery: 61 cm

Depth (cm)	Lithology	Structure	Colour	Description
		Oxidation zone	10 YR 7/4	0-5 cm brown foraminiferal clayey sand sharp erosional surface
			5 Y 8/1	5 - 61 cm indurated yellowish grey clay 8 cm burrows near surface
				small yellow sand lens
30				small yellow sand lens
60				61 cm: EOC
90				
120				

Figure 18e. Description of sediment column of core 16-2

POSEIDON 200/10
Station: PO 200/10-20
Position: 40° 05,42´ N ; 09° 42,3´ W

07.08.1993 - 23.08.1993
Date: 11.08.1993
Water Depth: 633 m

Core: PO 200/10-20-1 SL
Section: 0 - 150 cm

Core Recovery: 230 cm

Depth (cm)	Lithology	Structure	Colour	Description
		Ω	5 Y 5/2	clayey fine sand, medium to soft mica flakes, shell debris, foraminifera and quarz sand
		@		
		Ω		more sandy, more shell debris occurs
		Ω		25 cm shell
30				3 cm empty core
			5 Y 5/2	clayey sand, slightly scattered with black spots
		∫∫		sandy clay, mica disappeared, lots of burrows, bioturbation
		∫		50 - 53 cm sandy spot, sand like that at the top
				less but still mottled
60				
				82 - 84 cm sandy spot
90				sandy clay
		∫∫		more burrows, more bioturbation
		Ω		108 cm shell, small shells and debris
		∫∫∫		110 - 116 cm intense bioturbation 112 cm burrows
120				120 - 123 cm dark sandy layer
		Ω		
		Ω		clayey sand, small shells
		∫∫∫		136 - 212 cm bioturbated sediment, with shells and shell debris sandy clay, shells, burrows
		Ω		149 - 154 cm shell (good for double dating 14C)

Figure 19a. Description of sediment column of core 20-1

POSEIDON 200/10
Station: PO 200/10-20
Position: 40° 05,42' N ; 09° 42,3' W

07.08.1993 - 23.08.1993
Date: 11.08.1993
Water Depth: 633 m

Core: PO 200/10-20-1 SL
Section: 150 - 230 cm

Core Recovery: 230 cm

Depth (cm)	Lithology	Structure	Colour	Description
180			5 Y 5/2	sandy clay
				black stains
				large burrows, black bended layers
				sandy spots
				sharp bended black layer
				frequent occurence of bioturbation
210				less bioturbation
				230 cm : EOC
240				+ 15 cm TOP OF THE CORE (stored in a plastic bag), the top material is nearly of the same consistency as the described first 30 cm, a little more sandy at the top and scattered with shells and quarzite sand, same colour: 5 Y 5/2
270				

Figure 19a. continued

POSEIDON 200/10
Station: PO 200/10-17
Position: 40° 02,4' N ; 09° 57,94' W

07.08.1993 - 23.08.1993
Date: 11.08.1993
Water Depth: 1694 m

Core: PO 200/10-17-1 SL
Section: 0 - 58 cm

Core Recovery: 58 cm

Depth (cm)	Lithology	Structure	Colour	Description
		Oxidation zone	10 YR 5/4	0-5 cm slightly s... clay, soft yellowish moderate brown
			10 YR 6/2	0-10 cm slightly stiffer sandy clay, fare yellowish brown
			10 YR 5/4	silty clay, from 10-14 cm increase in sand, yellowish brown
			10 YR 6/2	
			5 YR 5/2	clayey silt, mottled with lighter colour, coarser and darker to the base
30			5 Y 4/4	
			5YR 5/2	silty clay with small fine sandy spots
				35 - 44 cm sand layer
		@	5 Y 3/2	sand, foraminifera and black particles
				soft sandy clay, pale yellowish brown
			5 Y 3/2	sand, olive grey
			10 YR 6/2	soft sandy clay
60				Interpretation: Possible disturbed sand layer at base, inclined brown sediment at the base, can be the result of two touchdowns of the corer??
90				
120				

Figure 19b. Description of sediment column of core 17-1

POSEIDON 200/10 — 07.08.1993 - 23.08.1993
Station: PO 200/10-25 — Date: 12.08.1993
Position: 40° 33,06´ N ; 09° 24,95´ W — Water Depth: 1041 m

Core: PO 200/10-25-2 SL — Core Recovery: 307 cm
Section: 0 - 150 cm

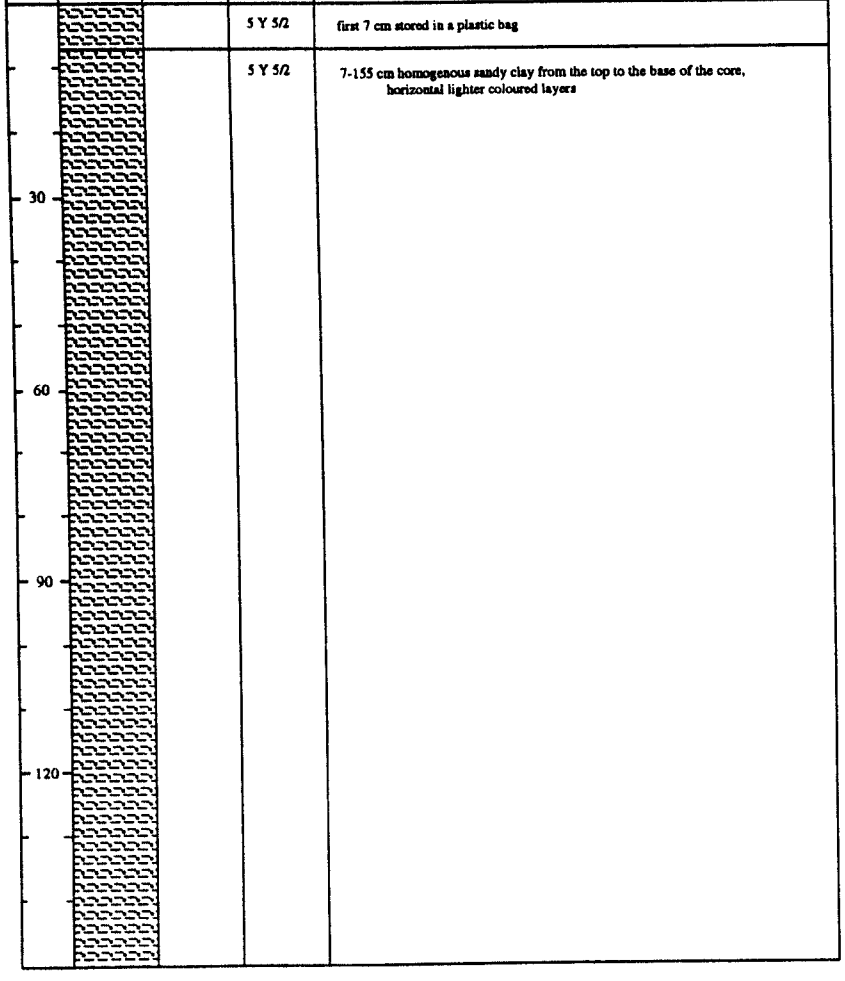

Figure 20a. Description of sediment column of core 25-2

POSEIDON 200/10 — 07.08.1993 - 23.08.1993
Station: PO 200/10-25 — Date: 12.08.1993
Position: 40° 33,06´ N ; 09° 24,95´ W — Water Depth: 1041 m

Core: PO 200/10-25-2 SL — Core Recovery: 307 cm
Section: 150-307 cm

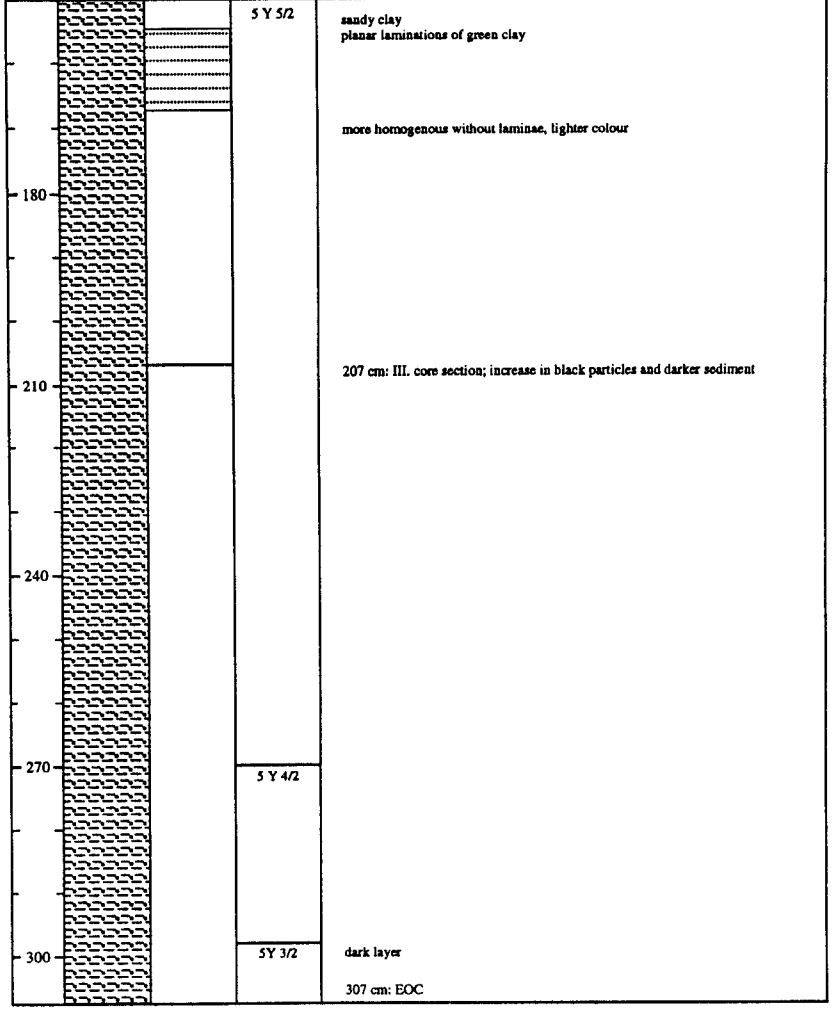

Figure 20a. continued

POSEIDON 200/10
Station: PO 200/10-24
Position: 40° 34,35´ N ; 09° 29,0´ W

07.08.1993 - 23.08.1993
Date: 12.08.1993
Water Depth: 1580 m

Core: PO 200/10-24-1 SL
Section: 0-150 cm

Core Recovery: 273,5 cm

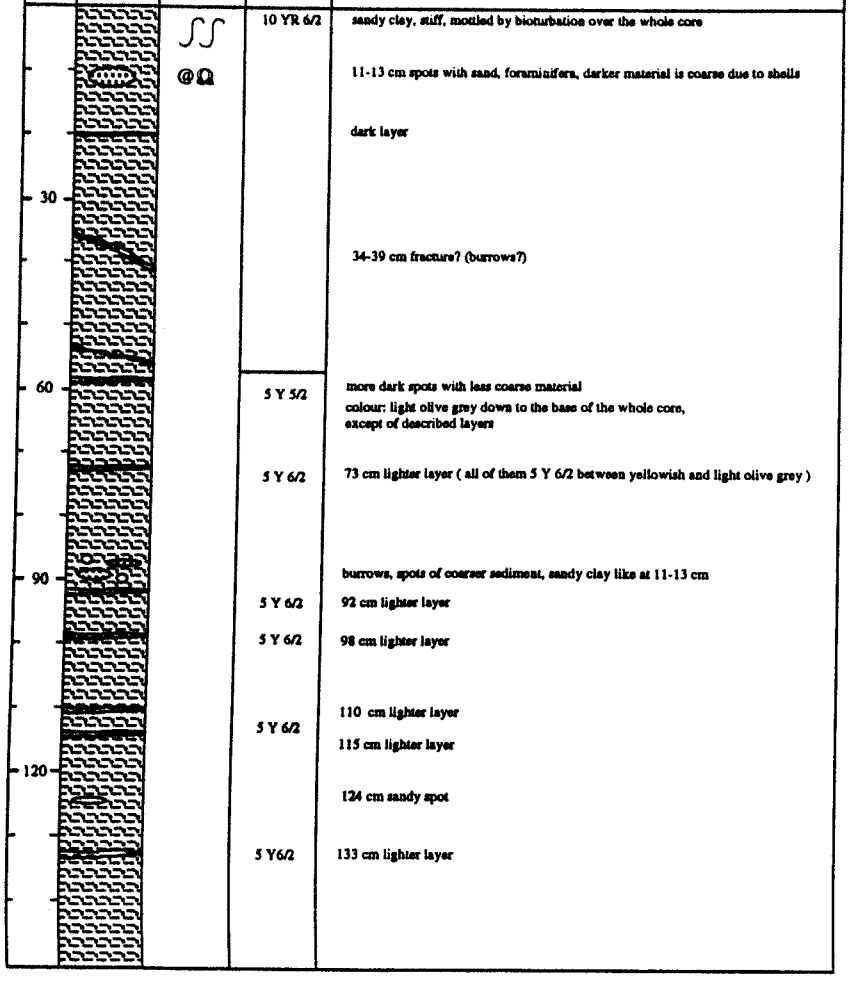

Figure 20b. Description of sediment column of core 24-1

POSEIDON 200/10
Station: PO 200/10-24
Position: 40° 34,35´ N ; 09° 29,0´ W

07.08.1993 - 23.08.1993
Date: 12.08.1993
Water Depth: 1580 m

Core: PO 200/10-24-1 SL
Section: 150-273,5 cm

Core Recovery: 273,5 cm

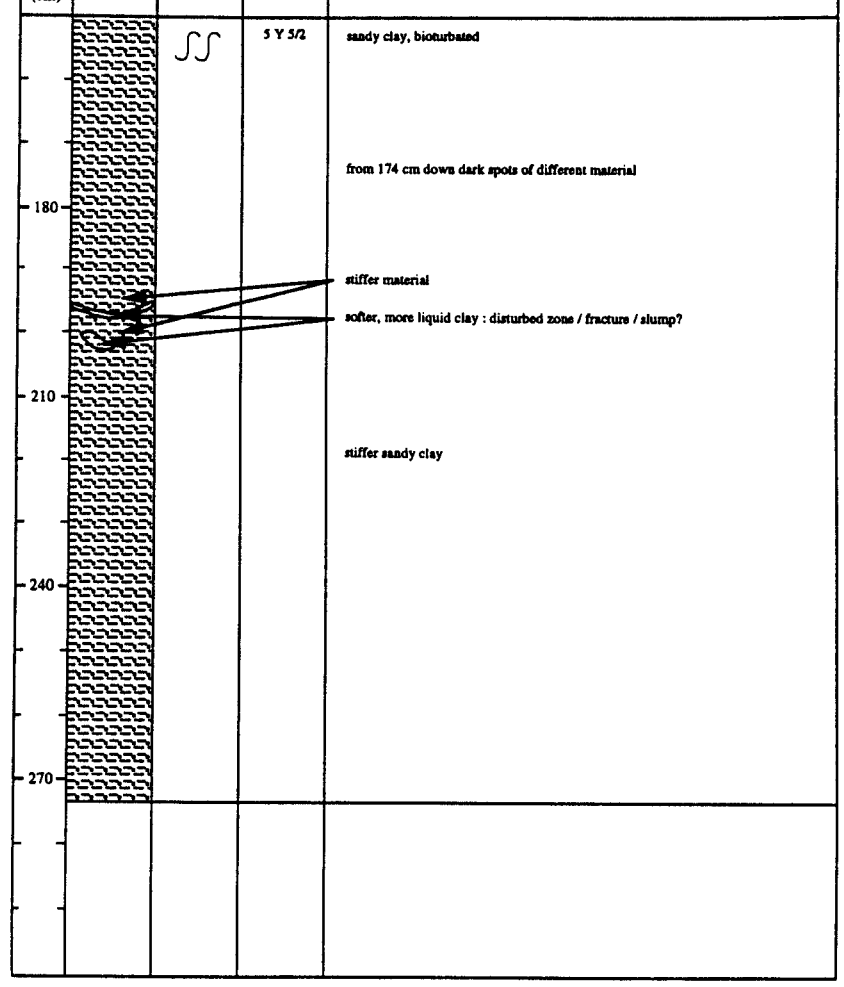

Figure 20b. continued

POSEIDON 200/10 — 07.08.1993 - 23.08.1993
Station: PO 200/10-23 — Date: 12.08.1993
Position: 40° 35,92´ N ; 09° 33,57´ W — Water Depth: 1972 m

Core: PO 200/10-23-1 SL — Core Recovery: 268 cm
Section: 0 - 150 cm

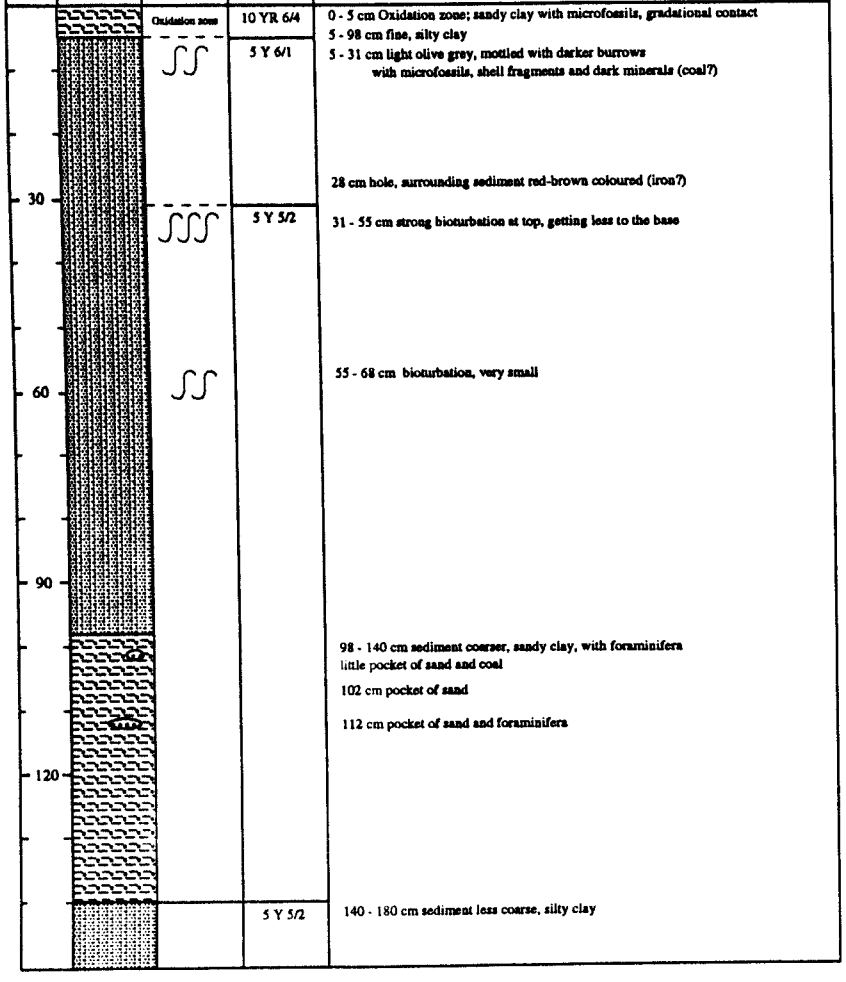

Figure 20c. Description of sediment column of core 23-1

POSEIDON 200/10 — 07.08.1993 -23.08.1993
Station: PO 200/10-23 — Date: 12.08.1993
Position: 40° 35,92' N ; 09° 33,57' W — Water Depth: 1972 m

Core: PO 200/10-23-1 SL — Core Recovery: 268 cm
Section: 150 - 268 cm

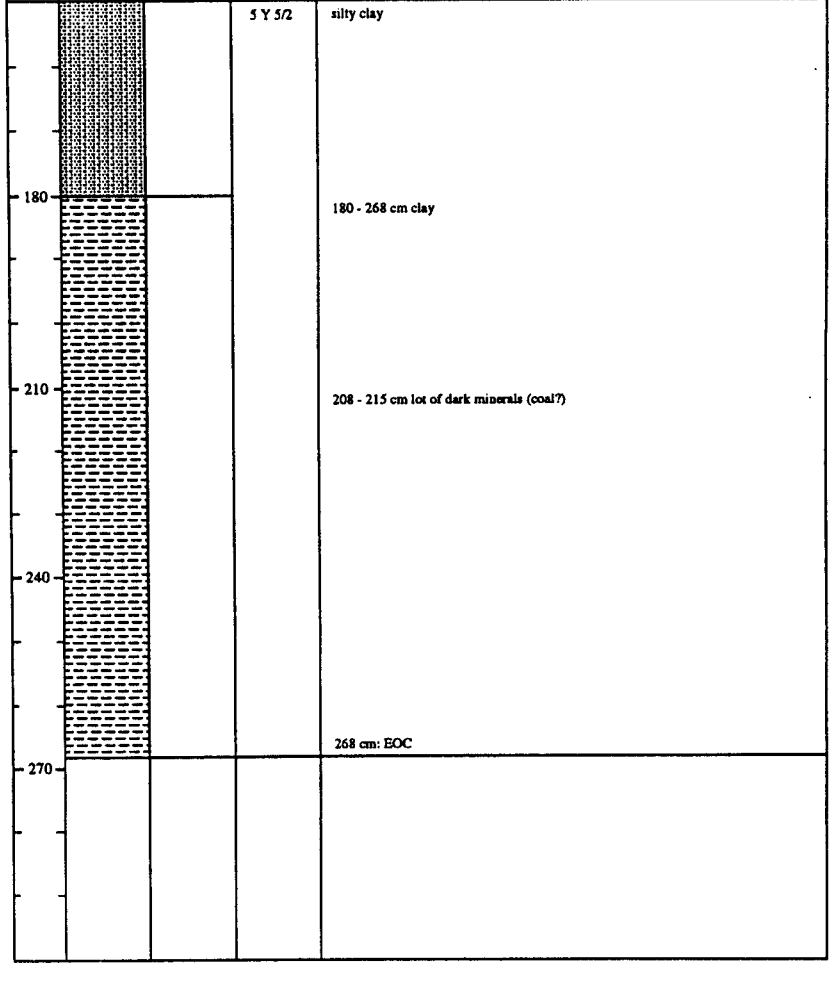

Figure 20c. continued

POSEIDON 200/10 — 07.08.1993 - 23.08.1993
Station: PO 200/10-22 — Date: 12.08.1993
Position: 40° 33,26´ N ; 09° 39,1´ W — Water Depth: 2247 m

Core: PO 200/10-22-1 SL — Core Recovery: 422 cm
Section: 0 - 150 cm

Depth (cm)	Lithology	Structure	Colour	Description
		Oxidation zone	10 YR 5/4	soft sandy clay
			10 YR 6/2	4 cm silty clay, slightly stiffer
		@ ∫	5 Y 5/2	whole sediment consists of silty clay with scattered black dots of sandy (foraminifera) clay, bioturbation and small stones
30			5 Y 6/2	lighter layer
				stiffer silty clay
		~		silty clay, much softer and more liquid than upper and deeper part, seems to be a disturbance zone
		~ ∫	5 Y 6/2	silty clay, slightly mottled and bioturbated
60				53 cm layer
			5 Y 5/2	
90				burrow
				slightly darker spot
				black spots
120		@		sandy clay, black spots of dark minerals and foraminifera and some shell fractures
		Ω		136 cm shell fracture
				135 cm and 138 cm patches of coarser sediment, mostly shell fractures at 142-144 cm

Figure 20d. Description of sediment column of core 22-1

POSEIDON 200/10 — 07.08.1993 - 23.08.1993
Station: PO 200/10-22 — Date: 12.08.1993
Position: 40° 33,26´ N ; 09° 39,1´ W — Water Depth: 2247 m

Core: PO 200/10-22-1 SL — Core Recovery: 422 cm
Section: 150 - 300 cm

Depth (cm)	Lithology	Structure	Colour	Description
		∫	5Y 5/2	silty clay
		@		spots of foraminifera and dark minerals
		@ Ω		170- 173 cm layer of clayey sand with holes full of foraminifera and darker black material, fractures of shells
180		@		slightly sandy clay with foraminifera
210		@	5 Y 3/2	217 cm darker, more silty clay with dark minerals and foraminifera
				220 cm stiff silty clay
			5 Y 4/2	229 cm sandy clay, scattered with black spots
240			5 Y 3/2	240 cm olive grey spot of silty clay
			5 Y 5/2	
270				
				288 cm small stone

Figure 20d. continued

POSEIDON 200/10 — 07.08.1993 - 23.08.1993
Station: PO 200/10-22 — Date: 12.08.1993
Position: 40° 33,26´ N ; 09° 39,1´ W — Water Depth: 2247 m

Core: PO 200/10-22-1 SL — Core Recovery: 422 cm
Section: 300 - 422 cm

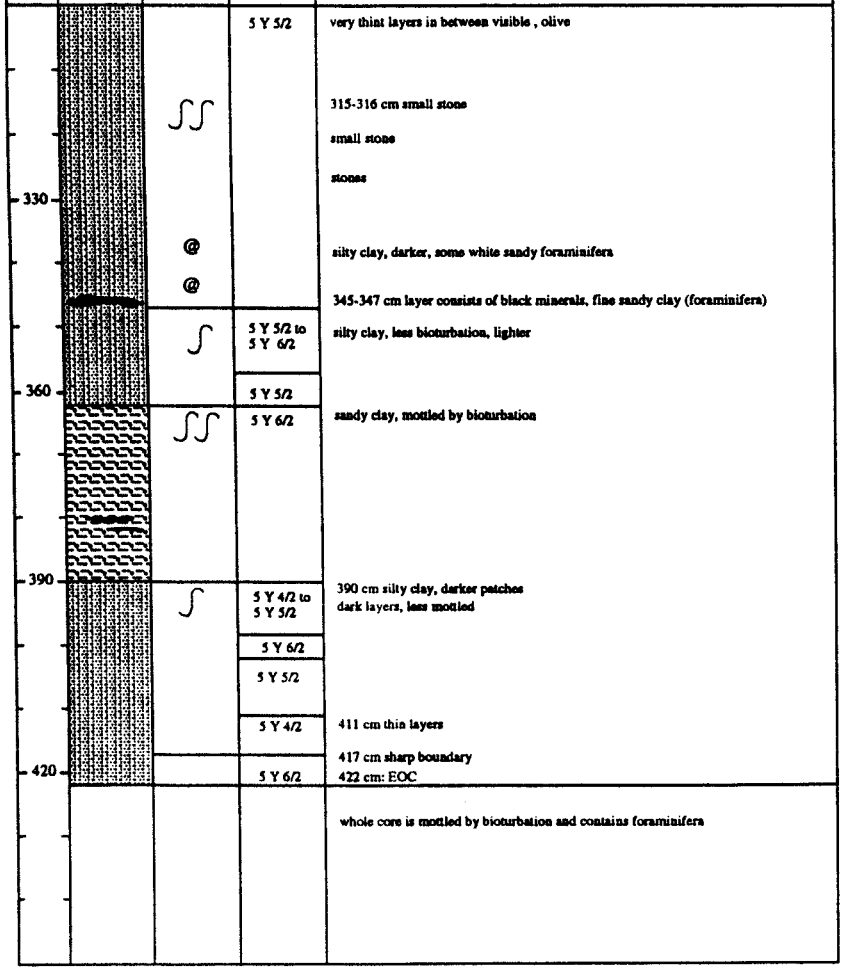

Figure 20d. continued

POSEIDON 200/10 — 07.08.1993 - 23.08.1993
Station: PO 200/10-21 — Date: 12.08.1993
Position: 40° 32,84´ N ; 09° 40,59´ W — Water Depth: 2388m

Core: PO 200/10-21-2 SL — Core Recovery: 367 cm
Section: 0 - 150 cm

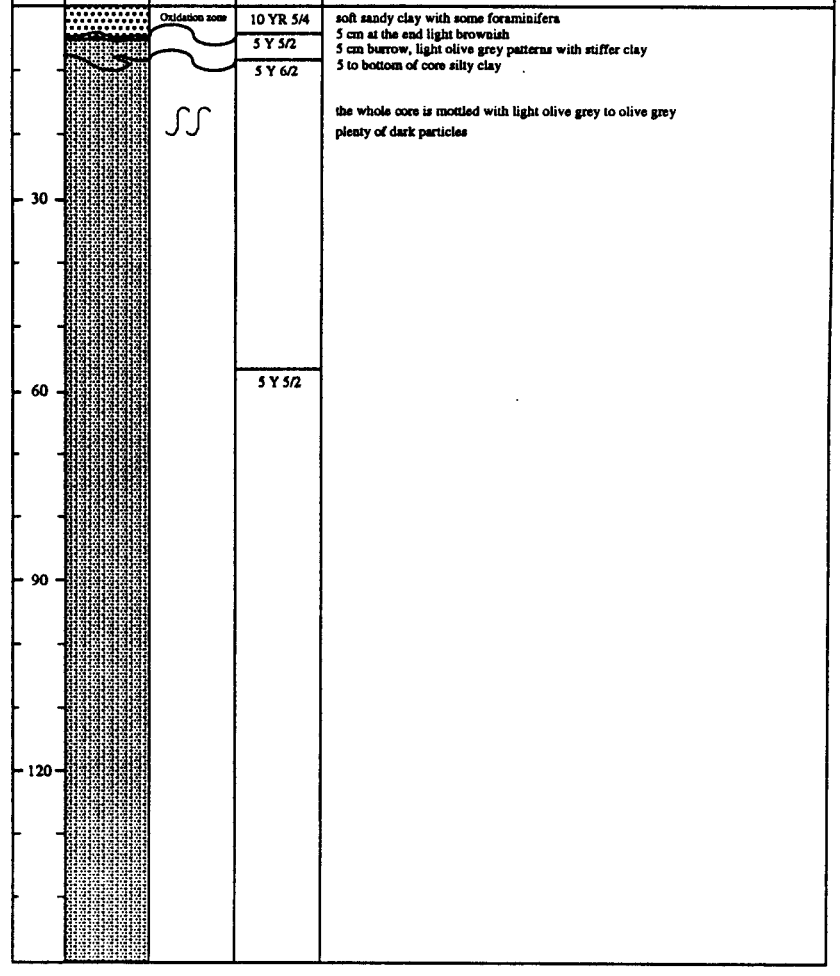

Figure 20e. Description of sediment column of core 21-2

POSEIDON 200/10
Station: PO 200/10-21
Position: 40° 32,84´ N ; 09° 40,59´ W

07.08.1993 - 23.08.1993
Date: 12.08.1993
Water Depth: 2388 m

Core: PO 200/10-21-2 SL
Section: 150 - 300 cm

Core Recovery: 367 cm

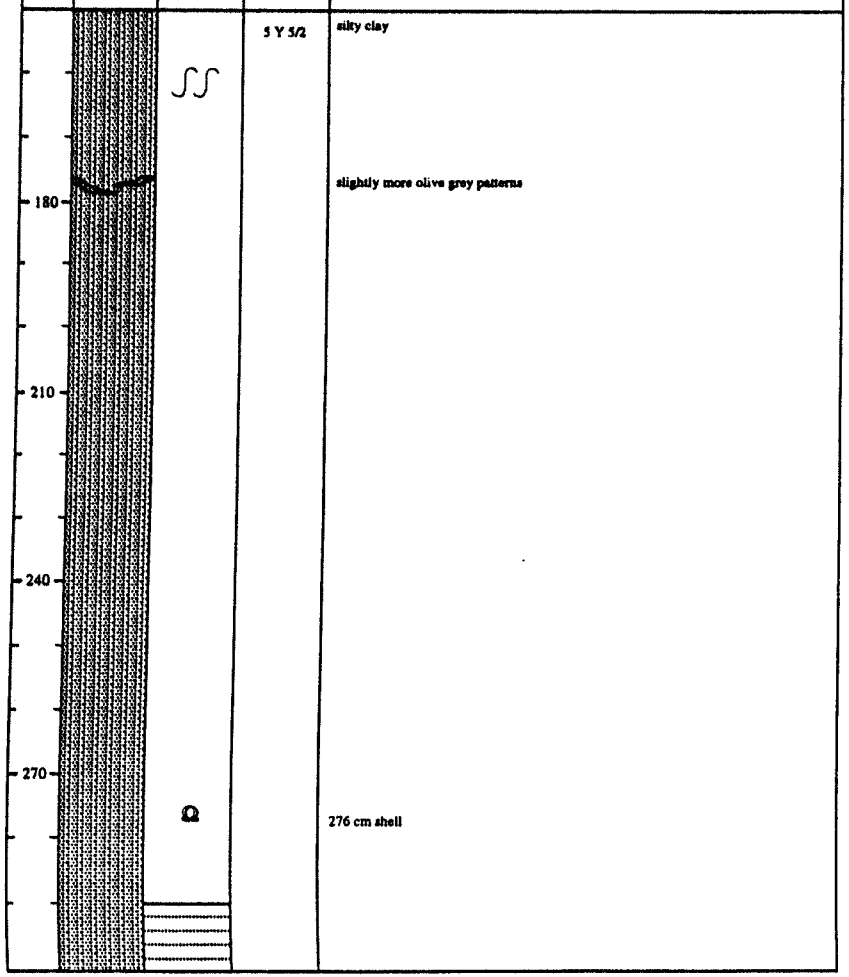

Figure 20e. continued

POSEIDON 200/10
Station: PO 200/10-21
Position: 40° 32,84´ N ; 09° 40,59´ W

07.08.1993 - 23.08.1993
Date: 12.08.1993
Water Depth: 2388 m

Core: PO 200/10-21-2 SL
Section: 300 - 367 cm

Core Recovery: 367 cm

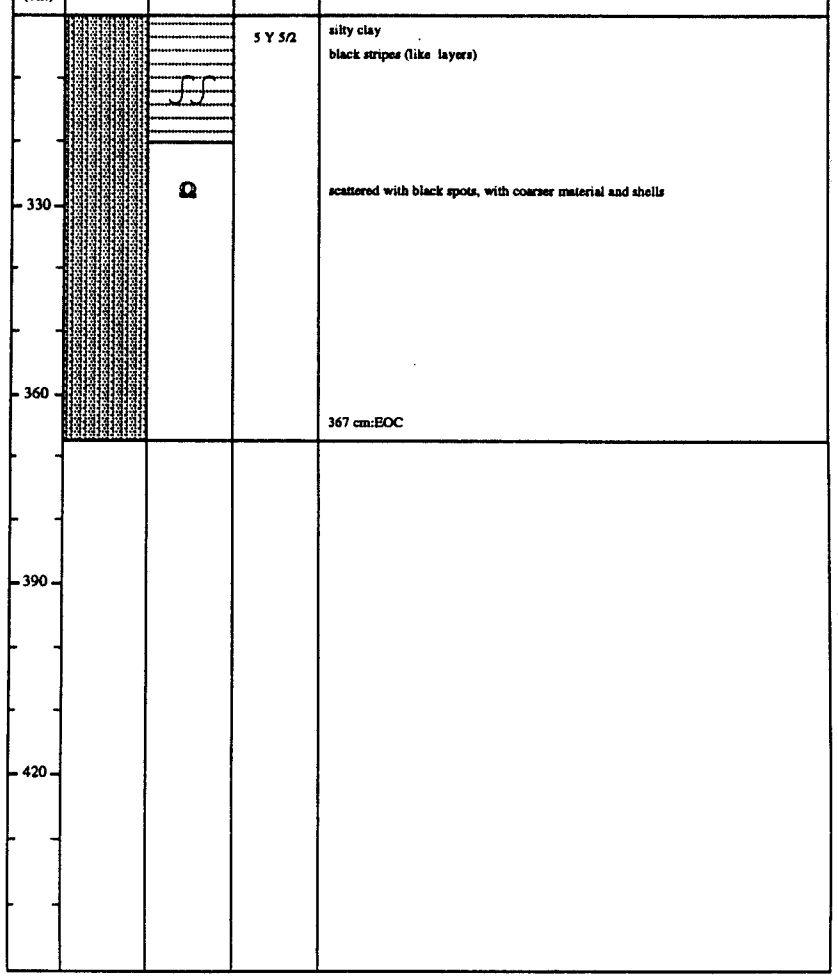

Figure 20e. continued

POSEIDON 200/10 — 07.08.1993 - 23.08.1993
Station: PO 200/10-33 — Date: 13.08.1993
Position: 41° 40,09´ N ; 09° 25,98´ W — Water Depth: 1732 m

Core: PO 200/10-33-2 SL — Core Recovery: 80 cm
Section: 0 - 80 cm

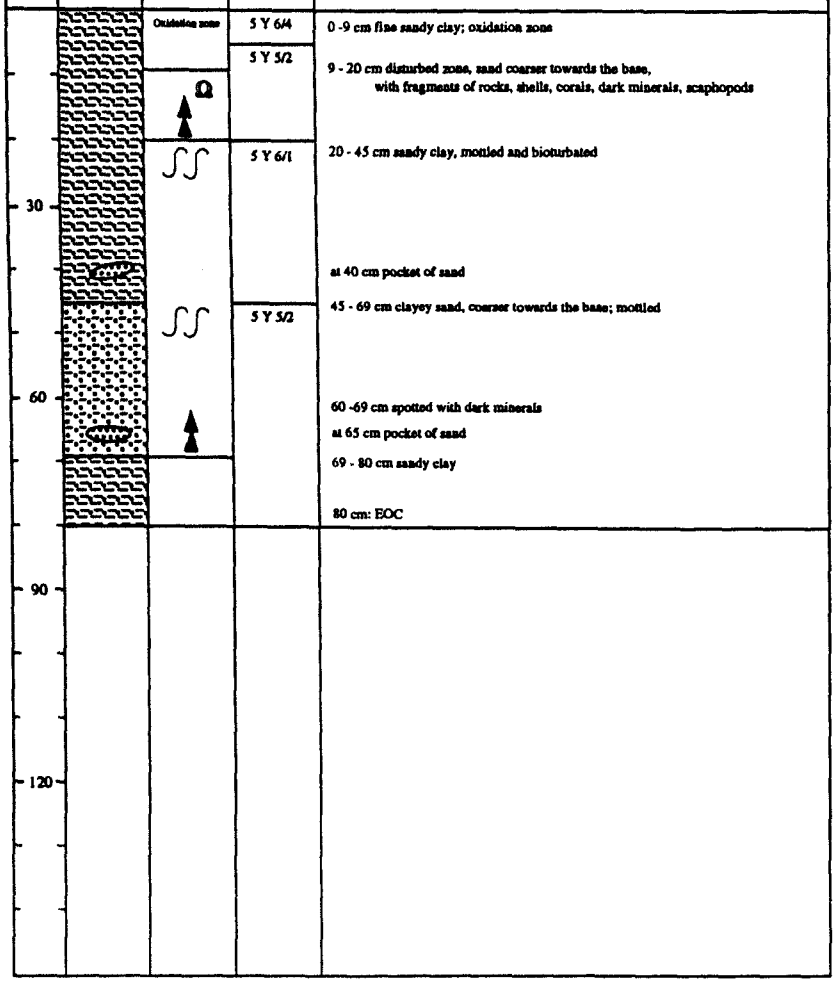

Figure 21a. Description of sediment column of core 33-2

POSEIDON 200/10 — 07.08.1993 - 23.08.1993
Station: PO 200/10-32 — Date: 13.08.1993
Position: 41° 37,99´ N ; 09° 29,01´ W — Water Depth: 1844 m

Core: PO 200/10-32-2 SL — Core Recovery: 415 cm
Section: 0 - 150 cm

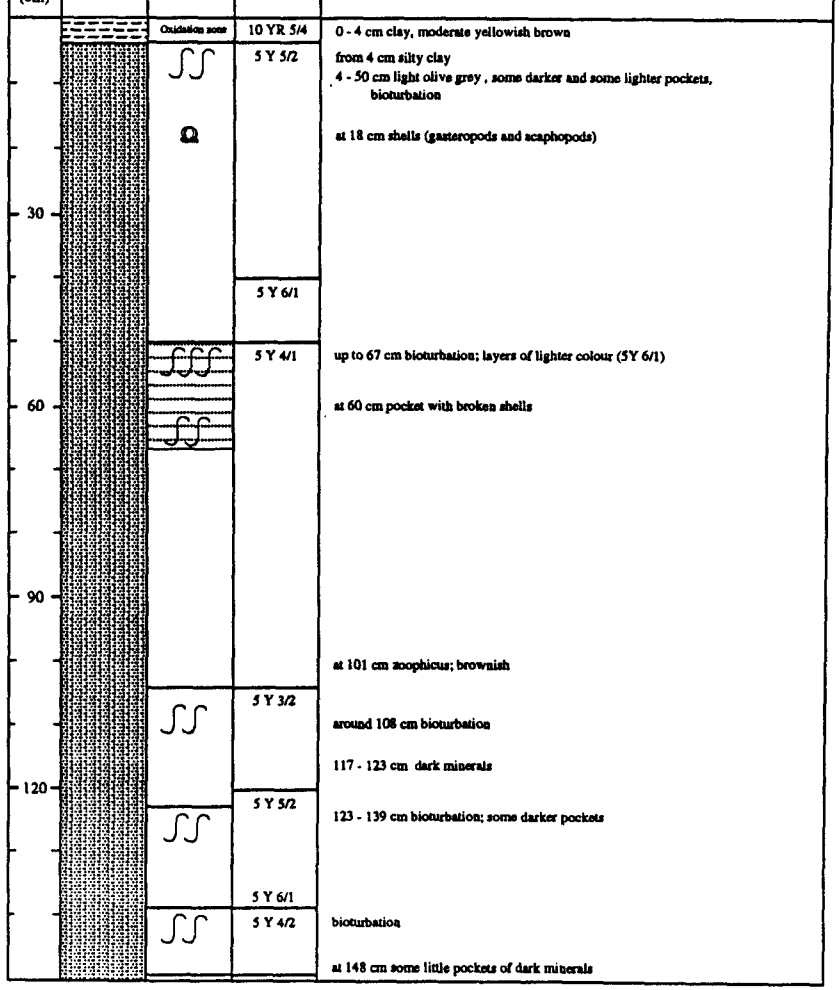

Figure 21b. Description of sediment column of core 32-2

POSEIDON 200/10 — 07.08.1993 - 23.08.1993
Station: PO 200/10-32 — Date: 13.08.1993
Position: 41° 37,99' N ; 09° 29,01' W — Water Depth: 1844 m

Core: PO 200/10-32-2 SL — Core Recovery: 415 cm
Section: 150-300 cm

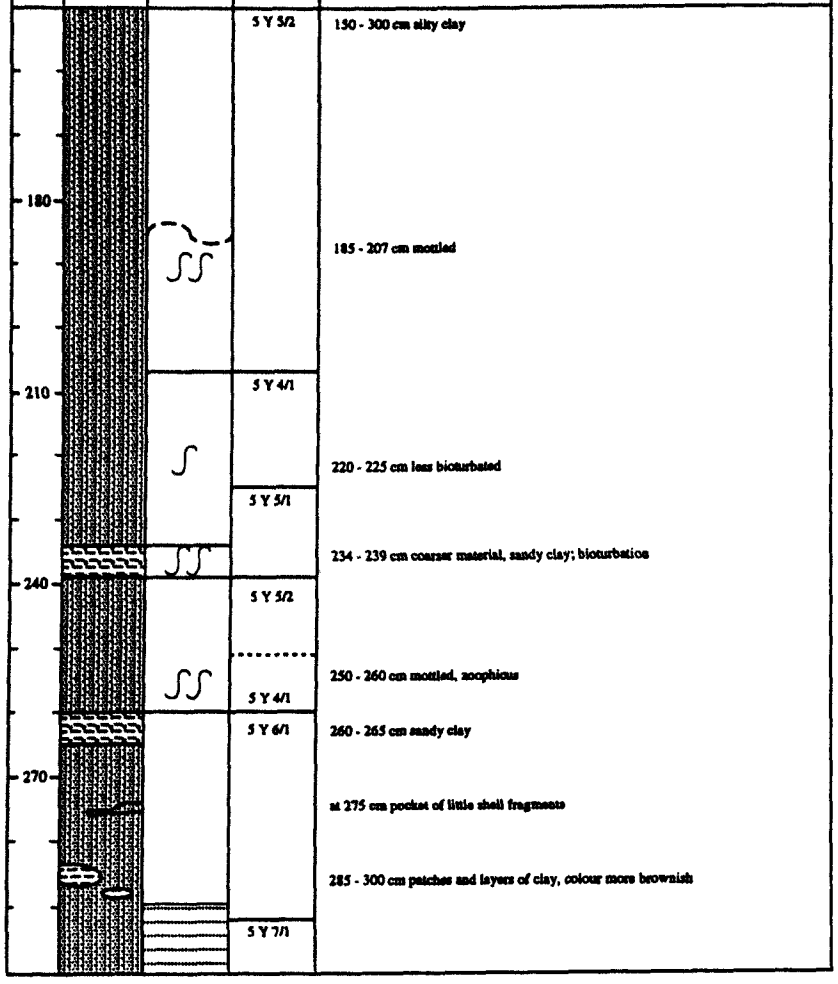

Figure 21b. continued

POSEIDON 200/10 — 07.08.1993 - 23.08.1993
Station: PO 200/10-32 — Date: 13.08.1993
Position: 41° 37,99' N ; 09° 29,01' W — Water Depth: 1844 m

Core: PO 200/10-32-2 SL — Core Recovery: 415 cm
Section: 300 - 415 cm

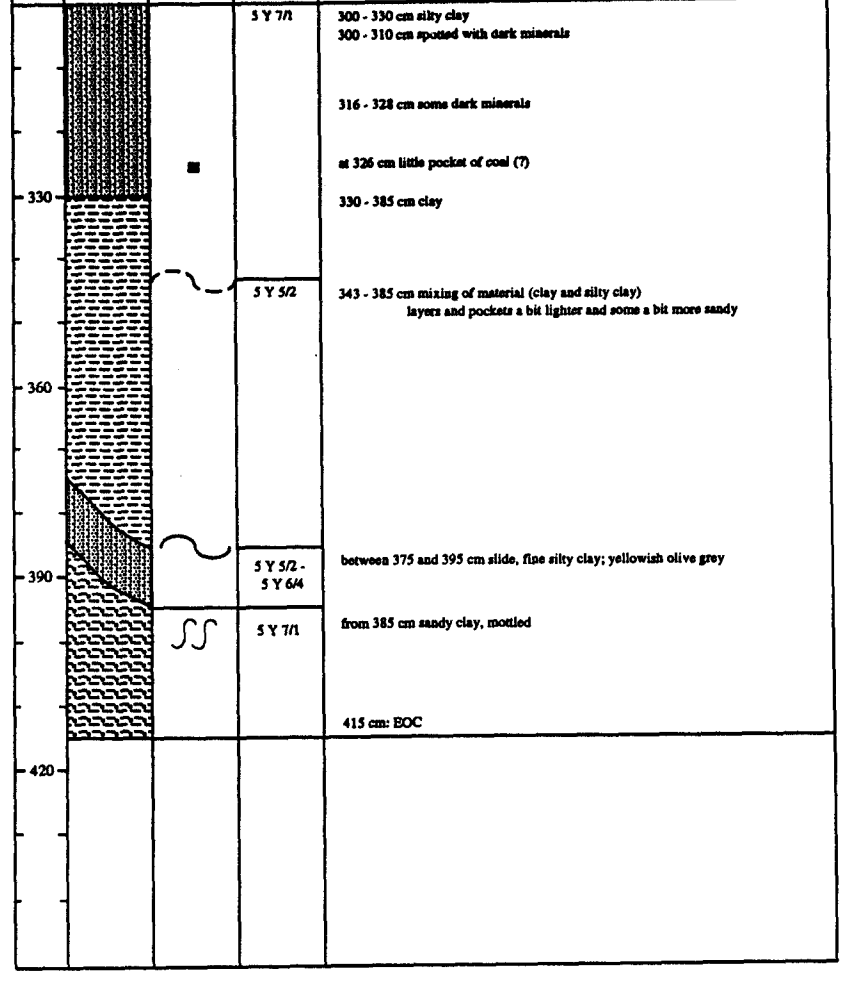

Figure 21b. continued

POSEIDON 200/10 — 07.08.1993 - 23.08.1993
Station: PO 200/10-31 — Date: 13.08.1993
Position: 41° 36,36´ N ; 09° 30,68´ W — Water Depth: 1966 m

Core: PO 200/10-31-1 SL — Core Recovery: 265 cm
Section: 0 - 150 cm

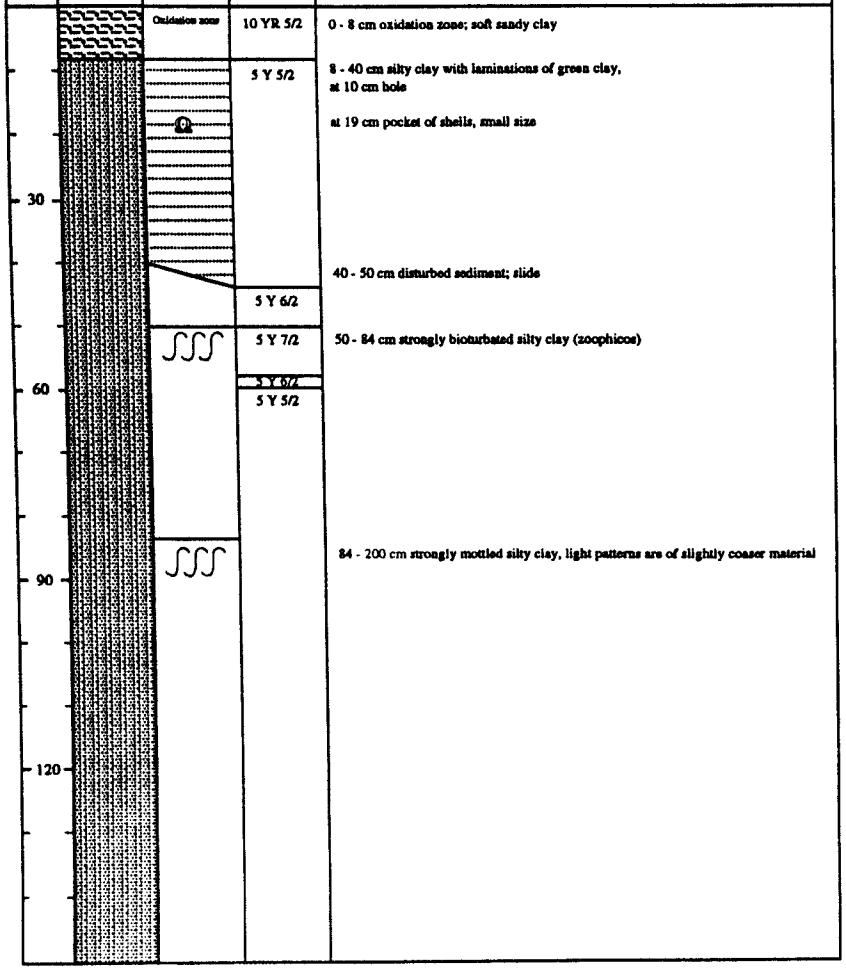

Figure 21c. Description of sediment column of core 31-1

POSEIDON 200/10 — 07.08.1993 - 23.08.1993
Station: PO 200/10-31 — Date: 13.08.1993
Position: 41° 36,36' N ; 09° 30,68' W — Water Depth: 1966 m

Core: PO 200/10-31-1 SL — Core Recovery: 265 cm
Section: 150-265 cm

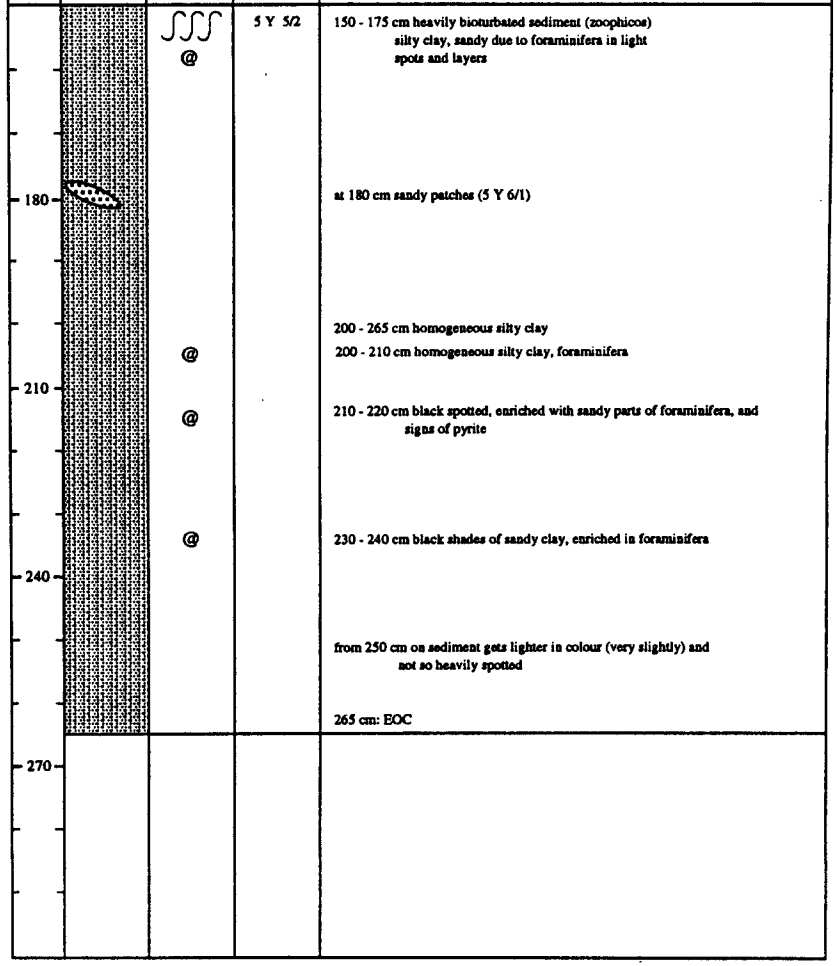

Figure 21c. continued

POSEIDON 200/10
Station: PO 200/10-30
Position: 41° 33,29´ N ; 09° 31,02´ W

07.08.1993 - 23.08.1993
Date: 13.08.1993
Water Depth: 1847 m

Core: PO 200/10-30-1 SL
Section: 0 - 150 cm

Core Recovery: 263 cm

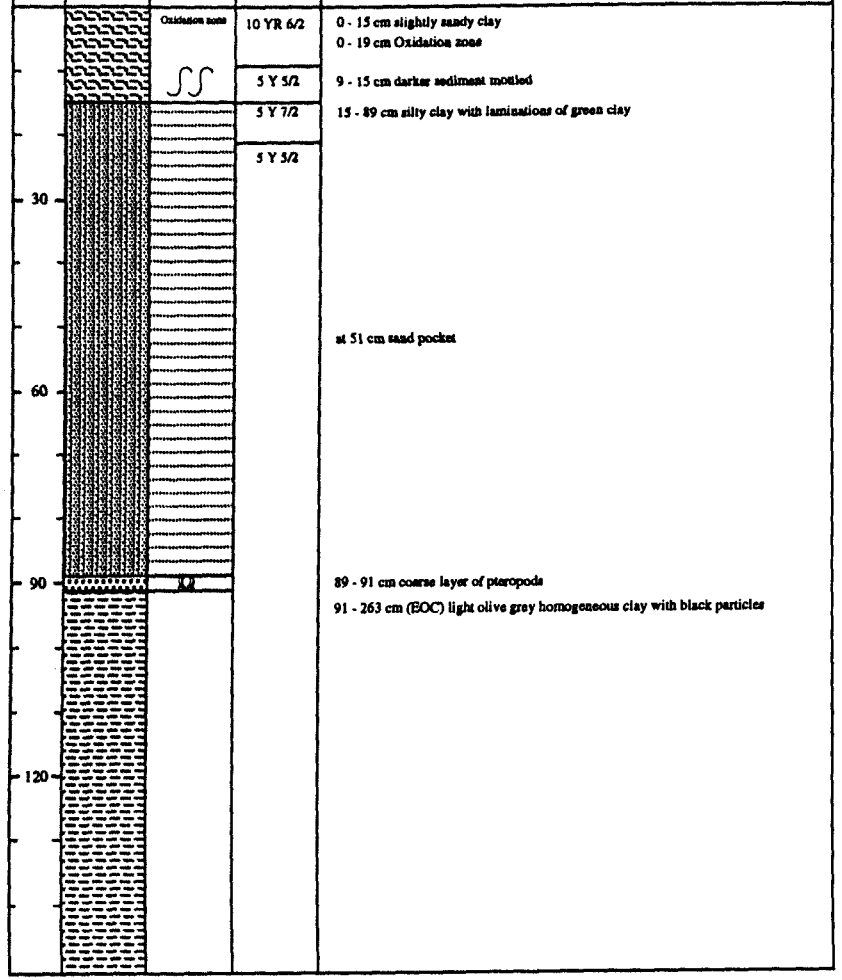

Figure 21d. Description of sediment column of core 30-1

POSEIDON 200/10
Station: PO 200/10-30
Position: 41° 33,29' N ; 09° 31,02 ' W

07.08.1993 - 23.08.1993
Date: 13.08.1993
Water Depth: 1847 m

Core: PO 200/10-30-1 SL
Section: 150-268 cm

Core Recovery: 268 cm

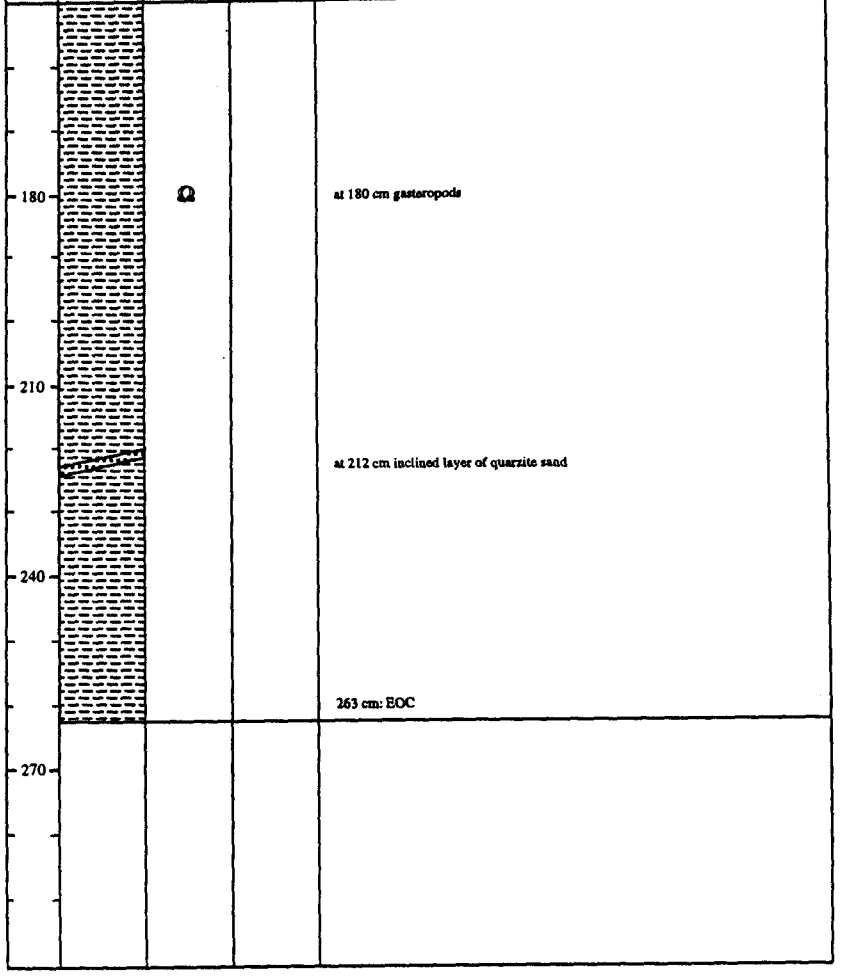

Figure 21d. continued

POSEIDON 200/10	07.08.1993 - 23.08.1993
Station: PO 200/10-29	Date: 13.08.1993
Position: 40° 32,52´ N ; 09° 34,26´ W	Water Depth: 1926 m

Core: PO 200/10-29-1 SL — Core Recovery: 250 cm
Section: 0 - 150 cm

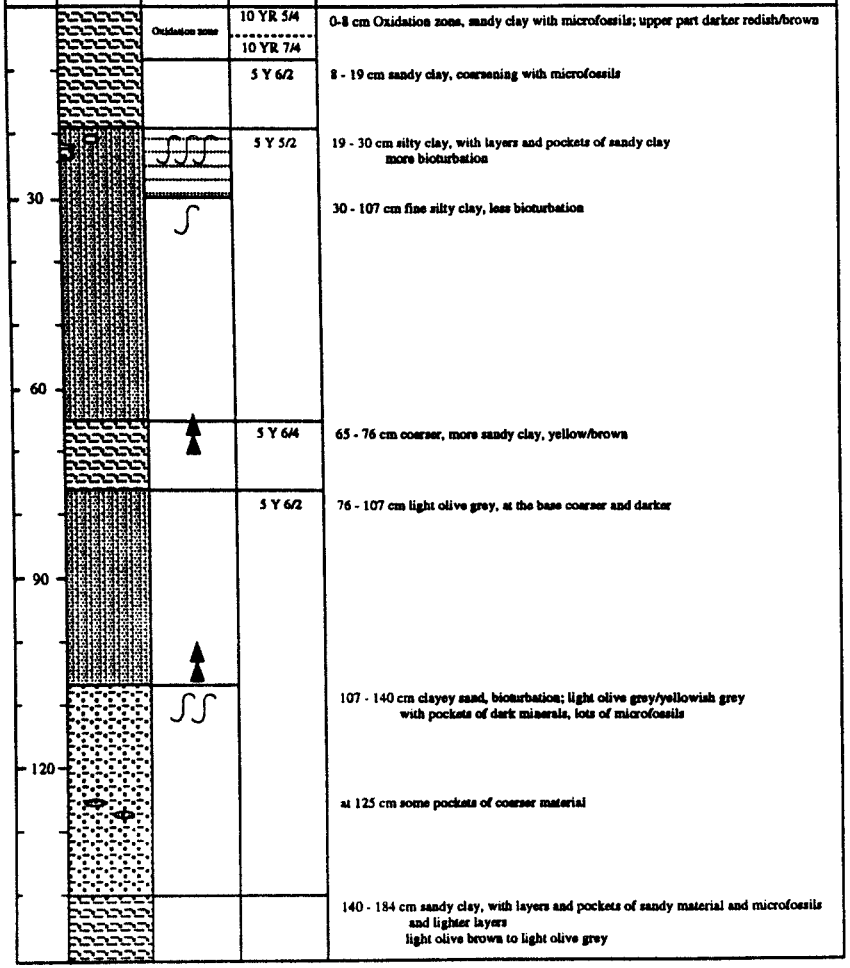

Figure 21e. Description of sediment column of core 29-1

POSEIDON 200/10	07.08.1993 - 23.08.1993
Station: PO 200/10-29	Date: 13.08.1993
Position: 40° 32,52´ N ; 09° 34,26' W	Water Depth: 1926 m

Core: PO 200/10-29-1 SL — Core Recovery: 250 cm
Section: 150-250 cm

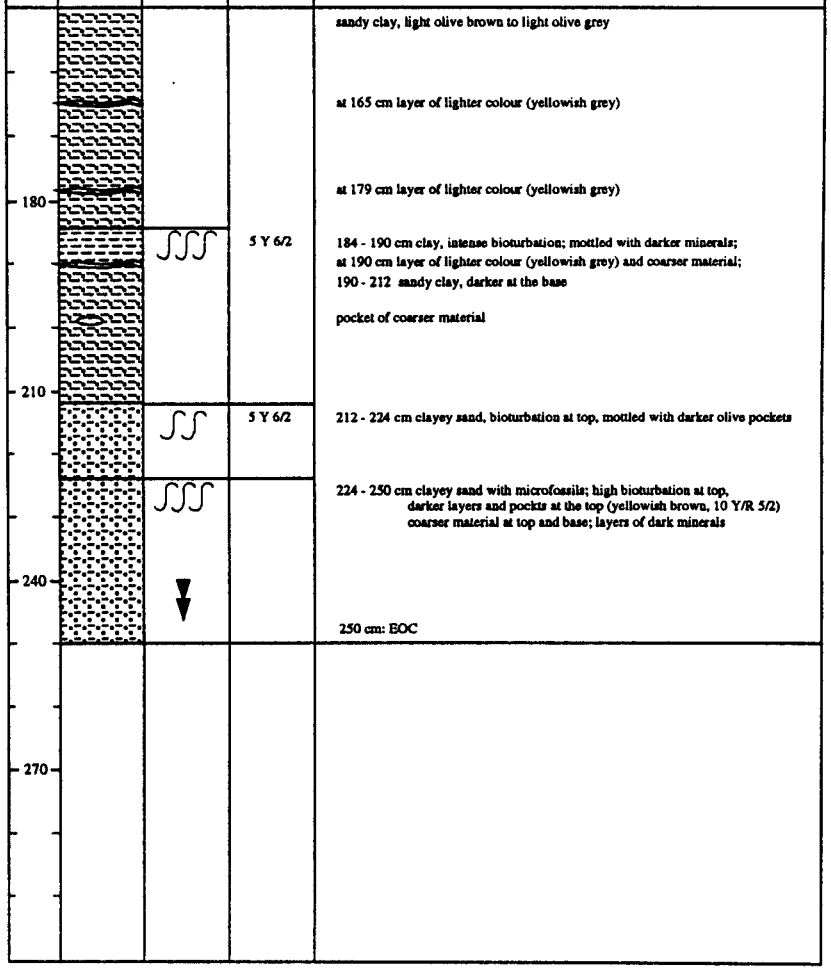

Figure 21e. continued

POSEIDON 200/10 — 07.08.1993 - 23.08.1993
Station: PO 200/10-28 — Date: 13.08.1993
Position: 41° 29,31´ N ; 09° 42,95´ W — Water Depth: 2160 m

Core: PO 200/10-28-1 SL — Core Recovery: 265 cm
Section: 0-150 cm

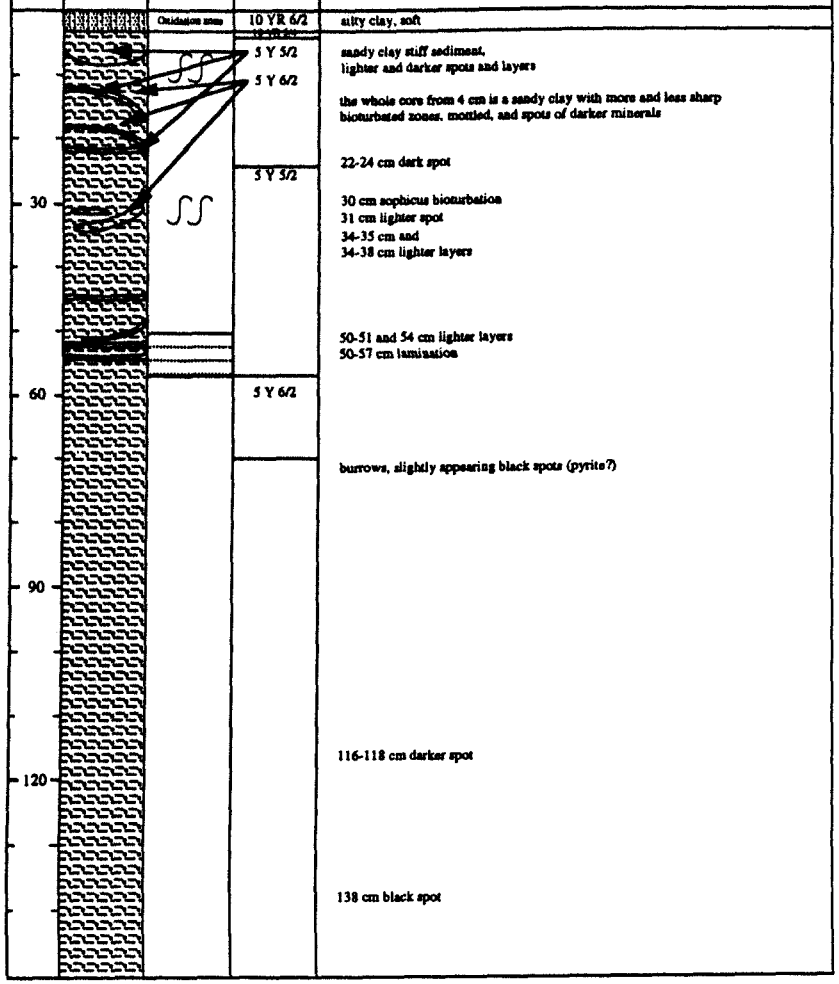

Figure 21f. Description of sediment column of core 28-1

POSEIDON 200/10 — 07.08.1993 - 23.08.1993
Station: PO 200/10-28 — Date: 13.08.1993
Position: 41° 29,31´ N ; 09° 42,95´ W — Water Depth: 2160 m

Core: PO 200/10-28-1 SL — Core Recovery: 265 cm
Section: 150-265 cm

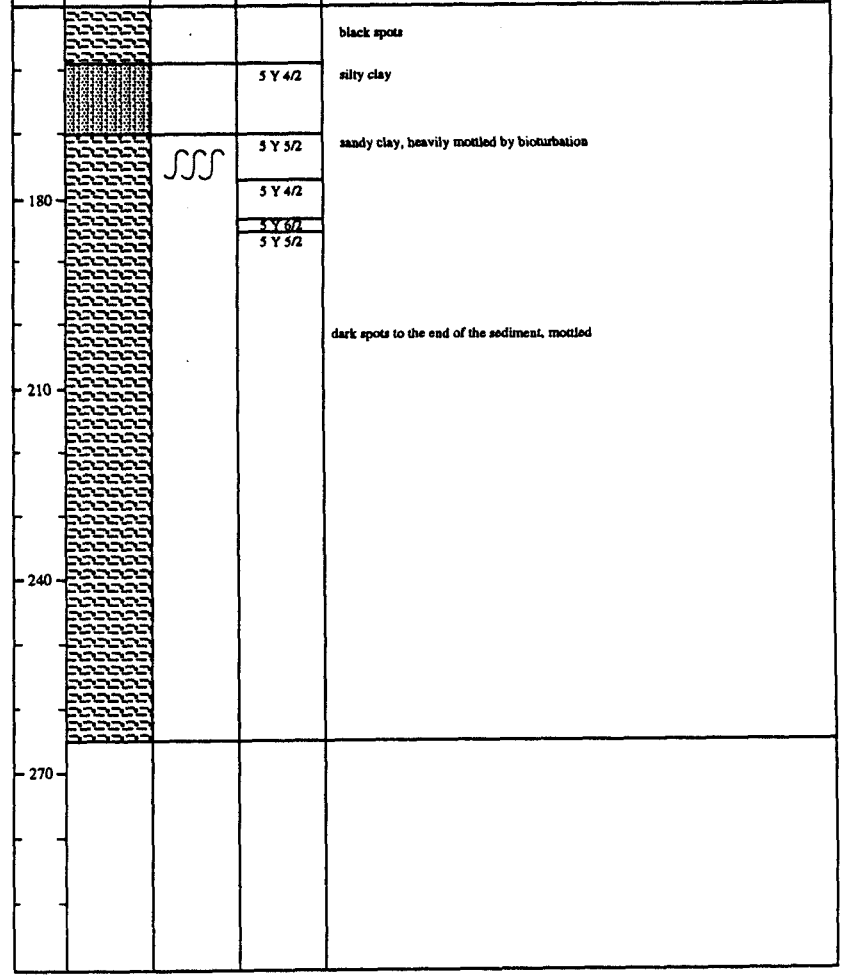

Figure 21f. continued

POSEIDON 200/10 — 07.08.1993 - 23.08.1993
Station: PO 200/10-27 — Date: 13.08.1993
Position: 41° 26,42´ N ; 09° 42,47´ W — Water Depth: 2371 m

Core: PO 200/10-27-2 SL — Core Recovery: 325 cm
Section: 0-150 cm

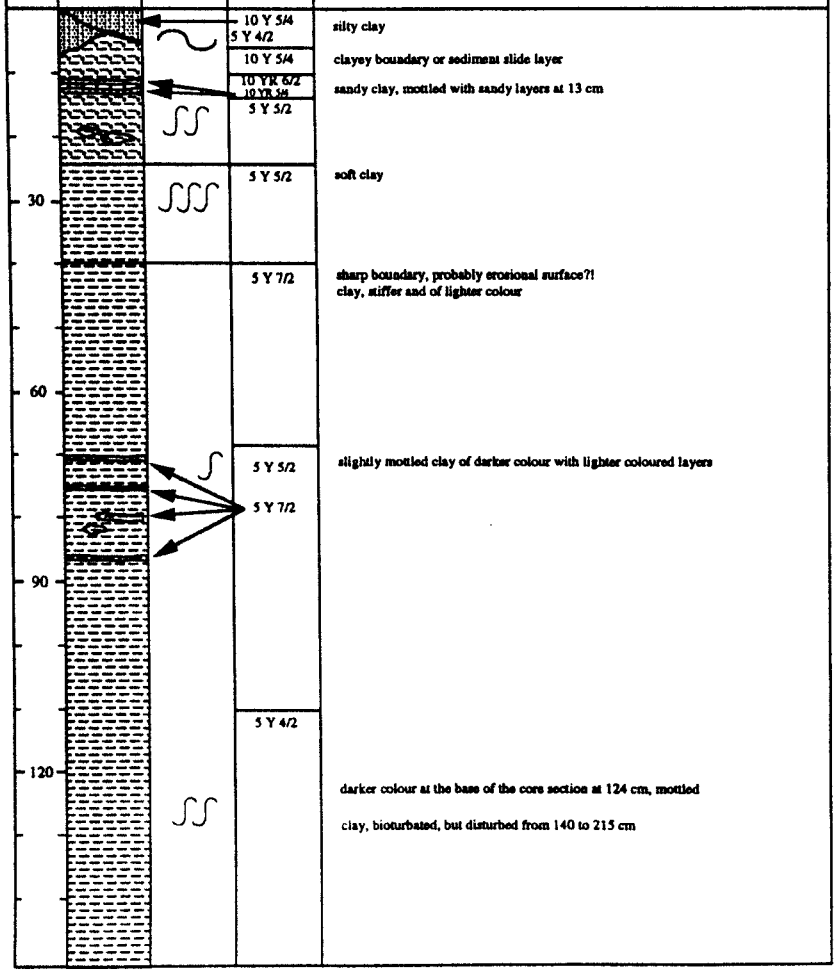

Figure 21g. Description of sediment column of core 27-2

POSEIDON 200/10 — 07.08.1993 - 23.08.1993
Station: PO 200/10-27 — Date: 13.08.1993
Position: 41° 26,42´ N ; 09° 42,47´ W — Water Depth: 2371 m

Core: PO 200/10-27-2 SL — Core Recovery: 325 cm
Section: 150-300 cm

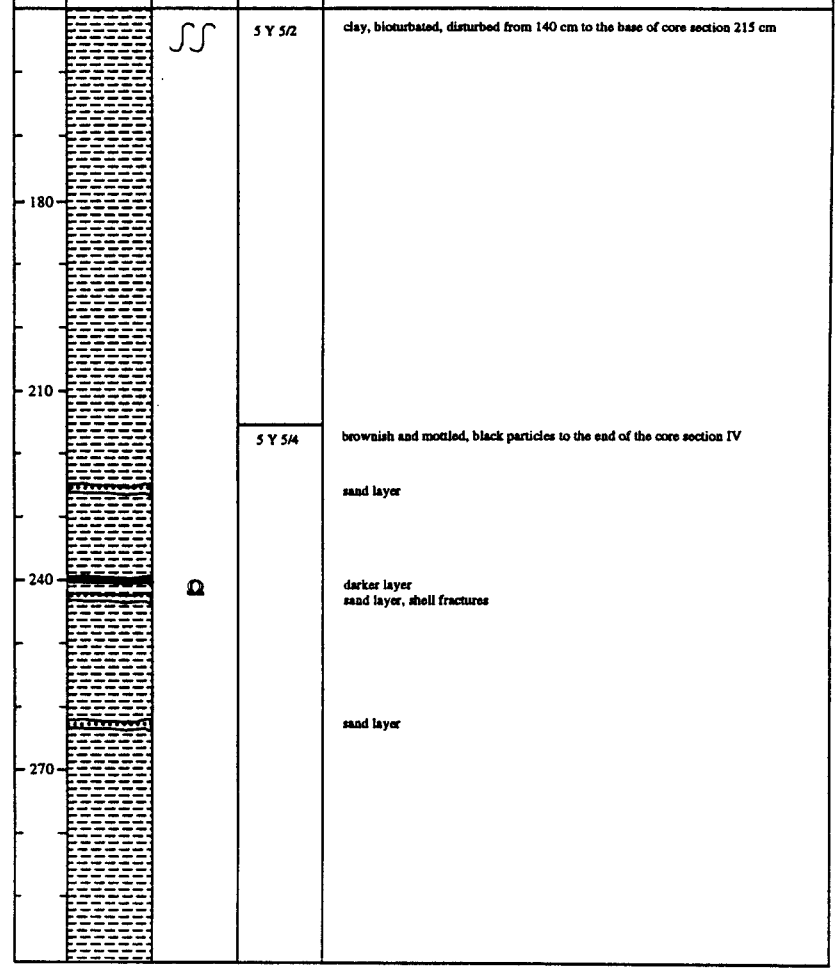

Figure 21g. continued

POSEIDON 200/10 — 07.08.1993 - 23.08.1993
Station: PO 200/10-27 — Date: 13.08.1993
Position: 41° 26,42´ N ; 09° 42,47´ W — Water Depth: 2371 m

Core: PO 200/10-27-2 SL — Core Recovery: 325 cm
Section: 300-325 cm

Depth (cm)	Lithology	Structure	Colour	Description
		∫	5 Y 5/4	clay
				sand layer
				324 cm: EOC
330				
360				
390				
420				

Figure 21g. continued

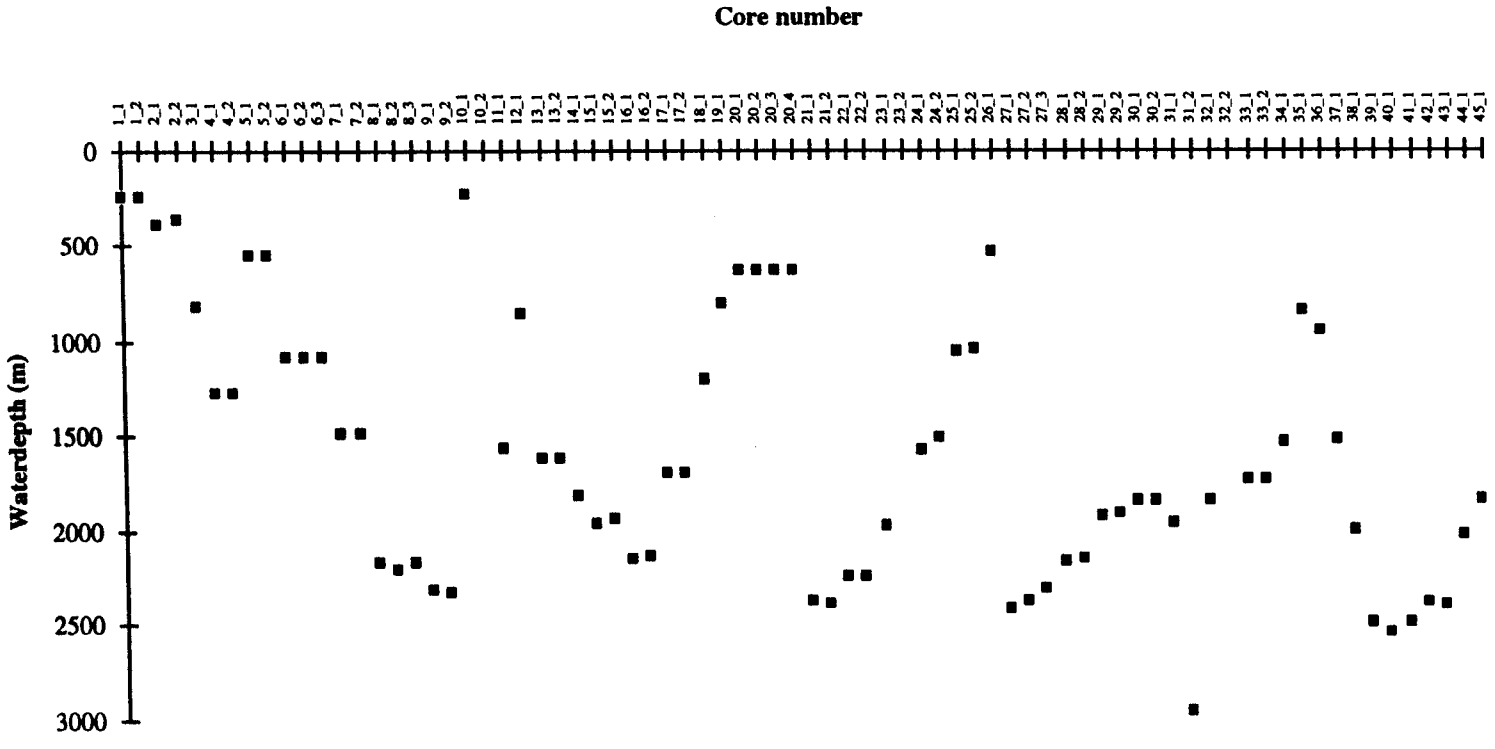

Figure 22. Core transects shown by core number versus waterdepth; type of coring device is listed in table 1.

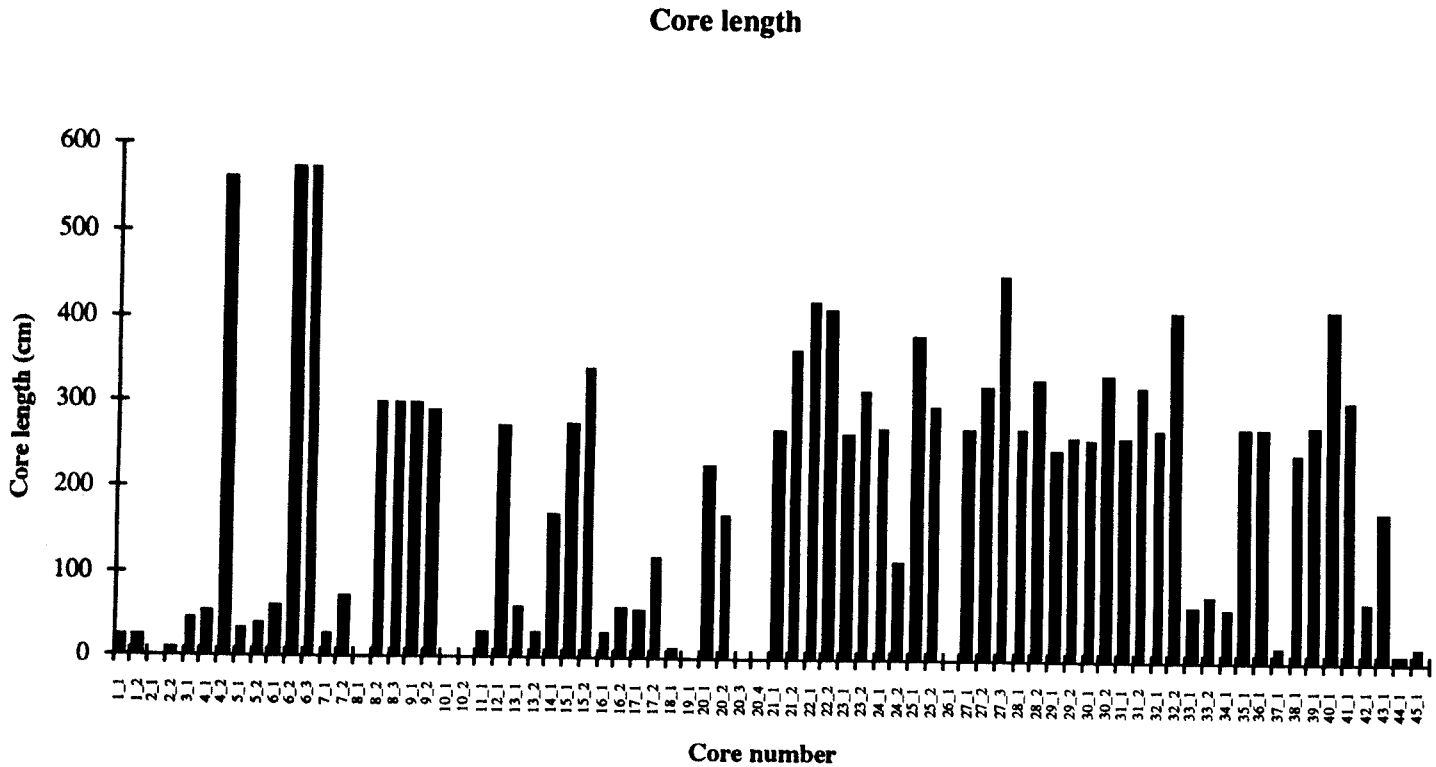

Figure 23. Sediment core recoveries shown by core length versus core number

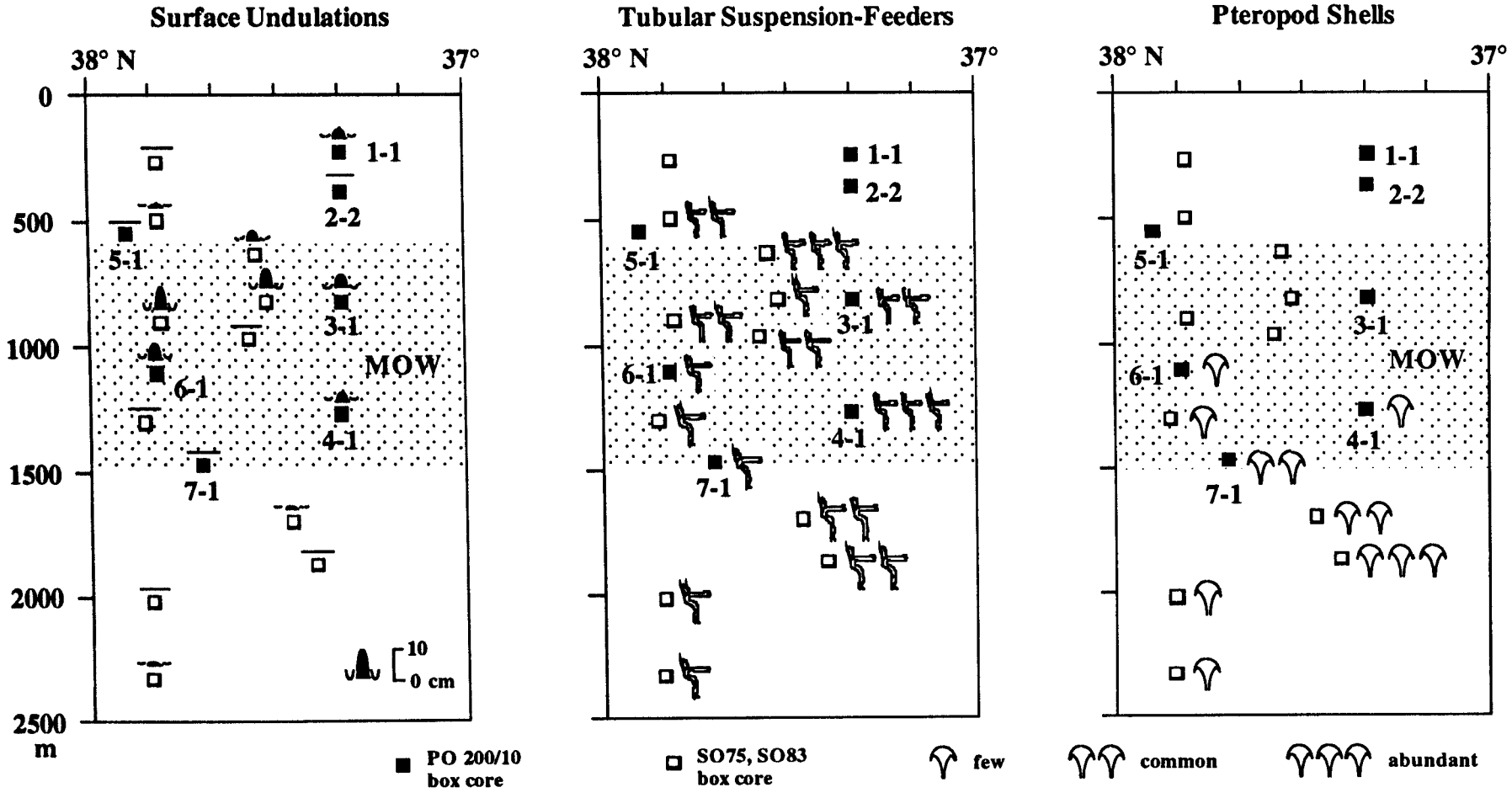

Figure 24. Surface structures observed at the Portuguese Continental margin between 37° and 38°. MOW: Mediterranean Outflow Water

Station Nr. Fahrt PO 200/10	Latitude	Longitude	Water-Depth (m)	Tool	Core Length (cm)	Date 1993	Time [GMT]
1-1	37°19,60' N	9°06,70' W	245	GKG	25	8.8	5:15
1-2			246	GKG	24		6:05
2-1	37°19,50' N	9°12,10' W	389	GKG	0	8.8	9:18
2-2			368	GKG	11		
3-1	37°19,50' N	9°18,60' W	822	GKG	46	8.8	9:28
4-1	37°19,49' N	9°31,10' W	1271	GKG	54	8.8	12:17
4-2			1276	SL	561		13:37
5-1	37°53,91' N	9°15,99' W	550	GKG	34	8.8	20:20
5-2			551	SL	41		21:20
6-1	37°49,30' N	9°30,20' W	1085	GKG	60	8.8	23:30
6-2			1086	SL	573,5	9.8	0:39
6-3			1086	SL	575		1:48
7-1	37°42,10' N	9°38,40' W	1480	GKG	28	9.8	4:28
7-2			1484	SL	74		7:45
8-1	37°38,46' N	9°55,91' W	2168	GKG	0	9.8	9:18
8-2			~2200	SL	300		11:40
8-3			2159	SL	300		13:09
9-1	37°36,60' N	10°02,90' W	2315	SL	302	9.8	15:22
9-2			2320	SL	293		17:07
10-1	39°38,80' N	9°35,60' W	227	SL	0	10.8	10:39
10-2				SL	0		10:57
11-1	39°37,10' N	9°41,60' W	1570	SL	32,5	10.8	12:19
12-1	39°38,17' N	9°40,33' W	865	SL	273	10.8	15:06
13-1	39°37,50' N	9°45,40' W	1620	SL	62	10.8	16:58
13-2			1621	SL	30		18:33
14-1	39°37,00' N	9°50,50' W	1824	SL	171	10.8	21:35
15-1	39°37,70' N	9°55,50' W	1967	SL	278	10.8	21:37
15-2			1940	SL	343		23:01
16-1	39°43,56' N	10°04,70' W	2147	SL	32	11.8	1:32
16-2			2140	SL	61		4:29
17-1	40°02,30' N	9°58,10' W	1694	SL	58	11.8	8:12
17-2			1693	SL	120		9:10
18-1	40°04,90' N	9°50,40' W	1207	SL	13	11.8	11:29
19-1	40°05,80' N	9°46,20' W	809	SL	0	11.8	12:55
20-1	40°05,30' N	9°42,30' W	633	SL	230	11.8	14:19
20-2			627	SL	170		15:17
20-3			637	SL	0		16:37
20-4			636	SL	0		17:11
21-1	40°32,90' N	9°40,65' W	2381	SL	272	12.8	00:04
21-2			2388	SL	367		2:02

Table 1: Core stations from transect Io to Vb

Station Nr. Fahrt PO 200/10	Latitude	Longitude	Water-Depth (m)	Tool	Core Length (cm)	Date 1993	Time [GMT]
22-1	40°33,30' N	9°39,04' W	2247	SL	422,5	12.8	4:04
22-2			2246	SL	414		5:28
23-1	40°35,30' N	9°33,50' W	1972	SL	268	12.8	7:29
23-2				SL	319		8:48
24-1	40°34,12' N	9°28,97' W	1580	SL	274	12.8	10:34
24-2			1509	SL	118		11:58
25-1	40°33,06' N	9°24,90' W	1065	SL	385	12.8	13:25
25-2			1041	SL	300		14:16
26-1	40°32,50' N	9°24,10' W	540	SL	0	12.8	15:05
27-1	41°25,90' N	9°43,50' W	2422	SL	273	12.8	23:16
27-2			2371	SL	325	13.8	1:03
27-3			2306	SL	455		2:50
28-1	41°29,30' N	9°43,26' W	2160	SL	275	13.8	4:59
28-2			2155	SL	335		6:42
29-1	41°32,41' N	9°34,30' W	1926	SL	250	13.8	8:59
29-2			1916	SL	267		11:09
30-1	41°33,00' N	9°30,90' W	1847	SL	263	13.8	11:49
30-2			1842	SL	341		13:11
31-1	41°36,10' N	9°30,90' W	1966	SL	265	13.8	14:46
31-2			1967	SL	325		17:50
32-1	41°38,05' N	9°28,94' W	1844	SL	273	13.8	17:20
32-2			1844	SL	415		18:36
33-1	41°40,01' N	9°25,96' W	1733	SL	68	13.8	20:00
33-2			1732	SL	80		21:05
34-1	41°41,29' N	9°24,40' W	1540	SL	64	13.8	22:00
35-1	41°45,90' N	9°24,30' W	847	SL	277	13.8	23:44
36-1	41°45,90' N	9°25,30' W	950	SL	277	14.8	2:40
37-1	41°45,90' N	9°26,90' W	1528	SL	20	14.8	3:55
38-1	41°46,02' N	9°33,81' W	2002	SL	249	14.8	7:15
39-1	41°40,00' N	9°44,25' W	2502	SL	281	14.8	10:30
40-1	41°40,85' N	9°43,27' W	2551	SL	417	14.8	12:45
41-1	41°41,16' N	9°38,49 W	2492	SL	311	14.8	15:16
42-1	41°41,71' N	9°36,51' W	2390	SL	73	14.8	16:58
43-1	41°36,77' N	9°41,09 W	2407	SL	181	14.8	20:45
44-1	41°34,41' N	9°41,31' W	2028	SL	10	14.8	22:10
45-1	41°31,80' N	9°42,20' W	1840	SL	20	15.8	00:03

Table 1: Core stations from transect Io to Vb

GAS HYDRATES ON THE NORTHERN EUROPEAN CONTINENTAL MARGIN

Kiel-Tromsø

5 - 25 July 1994

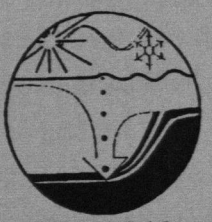

SFB 313

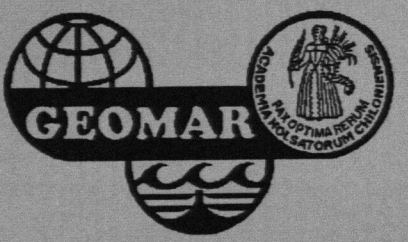

Jürgen Mienert[1,2]
and shipbaord scientific party

[1] GEOMAR, Forschungszentrum für marine Geowissenschaften der Christian-Albrechts-Universität zu Kiel, Wischhofstr. 1-3, 24148 Kiel, F.R.G.

[2] Sonderforschungsbereich 313 (SFB 313) der Christian-Albrechts-Universität zu Kiel, Olshausenstr. 40-60, 24118 Kiel, F.R.G.

Polar Marine Geology Expedition (PMGE), Pobeda St. 24, St. Petersburg - Lomonosov, 189510, RUSSIA

Table of Contents

1. Research Objectives

1.1. Introduction

This study will contribute to the understanding of the distribution of gas hydrate layers in margin sediments and will determine the zones of free gas that could have some influence on slope stabilities of the European continental margin.

Gas hydrates consist of solid phases of gas and water in ice-like crystals. These crystals are stable under low temperature, high pressure and gas saturation. Below this stable gas hydrate layer, the crystals become unstable and release methane gas and fresh water into the surrounding pore fluids. This process creates a zone of high porosity and methane content located below the gas hydrate zone. Changes in the stability field of gas hydrates affect the stability of the continental margins, because the breakdown of gas hydrate layers and the increased porosity of the sediments may create sliding planes and, therefore, finally mass wasting processes of sediments down the margins. Thus it is important to understand the distribution and the history of the gas hydrate layers along the margin and their relationship to the sedimentary processes moulding the margins. In addition, gas hydrate layers do not only influence the stability of margins, but could also contribute to climatic changes, in particular to the greenhouse effect, if the released methane was to escape through the water column into the atmosphere.

Gas hydrates in marine sediments can best be determined by seismic methods because their ice-like crystals cause a strong impedance contrast in sediments. This results in an acoustic horizon known as bottom simulating reflector (BSR). The BSR is characterized by high seismic amplitudes, a phase shift and a reflector running parallel to the sea floor. A phase shift indicates a change from a high velocitiy medium to a medium with low velocity. Within the gas hydrate zone (solid phase) sound velocities could reach values in the range of 2.3 to 3.4 km/s (Max, 1990). Below the BSR (gas phase) sound velocities drop to values well below 1.5 km/s, due to the fact that these gas hydrates may emit free gas. This large detectable change in the vertical sound velocity distribution leads to the positioning of gas hydrate accumulations and could be detected by using acoustic geophysical methods.

1.2. Projects

The SFB 313, funded by the German Science Foundation, investigates the "Environmental Changes in the Northern North Atlantic", while the European Commission funded project ENAM (European North Atlantic Margin: sediment pathways, processes and fluxes) studies the

processes that shape the margins during glacial and interglacial times. During this cruise both programmes were carried out in co-operation with the Institute of Polar Marine Geology Expedition (PMGE) St. Petersburg, Russia. The side-scan sonar and the airgun systems including the research vessels RV Akademik Aleksandr Karpinskiy and RV Professor Logachev had been chartered for a joint expedition to investigate gas hydrates along the European and the Polar margin. The integration of the two research vessels and the collaboration with scientists from neighbouring countries were essential elements during the planning of the voyages (Figures 1-4).

2. Research Programme

2.1. Sonderforschungsbereich 313 (SFB 313)

The objective of project B1 (Marine Geophysics) of the SFB 313 during RV Karpinskiy Leg 20 was to study the formation of geophysical signals in sediment sequences and gassy sediments. Sub-seafloor investigations along the margin were concentrated in areas of gas hydrates and gassy sediments located between Spitsbergen and the Knipovich Ridge (Figure 4).

2.2. European North Atlantic Continental Margin - Sediment Pathways, Processes and Fluxes (ENAM)

During the RV Karpinskiy cruise we studied Quaternary sediment deposits at the Norwegian Trench and Fan, which is one of the major glacially influenced conduits off Norway (Figure 2). Airgun seismic profiling techniques were used to identify the extent of large-scale sediment slide complexes which pre-date the mass wasting event of Storegga Slide (30000-50000yr, Bugge et al., 1988).

At the Storegga Slide airgun profiling and ocean bottom hydrophon deployments were carried out to provide pertinent information about the distribution of gas hydrates and gassy sediments (Figure 3). A detailed study north of the major slide complex may allow to determine whether the sediments there are liable to slide in the future.

3. Narrative of the Cruise

The RV Akademik Aleksandr Karpinskiy departed from Kiel on 5 July 1994 at 17:00 hrs

(UTC) in the afternoon. The ship sailed to the working area 1 of the Norwegian Trench and Fan (Figures 1 and 2). On our way to the working area, we picked up a Norwegian observer from a pilot boat of Stavanger on 7 July, 16:00 hrs. He had been sent to the ship as requested by the fishery directorate in Stavanger.

On the next day (8 July) we started airgun profiling at 22:32 hrs (UTC) in working area 1 of the Norwegian Trench and Fan (Figure 2). The ship`s speed was about 4.5 knts. We used 2 and 3 litres airguns and a 500 m long streamer with an active hydrophone cable of 62.5 m. Six channels (10 hydrophones/channel) actively recorded the acoustic signals. The seismic group adjusted both the towing depth of the streamer and the airgun. While the towing depth of the streamer was about 15 m, the airgun was towed at about 5 m water depth. The frequency filter of the digital recording unit was set from 65 to 500 Hz. During profile 1 (Tables 2 and 3) the airgun malfunctioned on 9 July at 6:02 hrs. Fortunately, we were able to use the 3 ltr instead of the previously used 2 ltr airgun and continued our profiling at 12:38 hrs. The airgun records yielded 1sec (TWT) penetration, good resolution and showed a prograding wedge from the Norwegian outer trough to the fan. In addition, the record showed a sediment slide,which may correlate to the slide that pre-dates the Storegga Slide (NORMAST, 1994).

Seismic work from 9-10 July was favoured by the good weather conditions of Bft 2-3. However, several interruptions due to mechanical and electrical problems with the airguns caused a major setback at the beginning of our seismic work (see Table 3) in the area of the Norwegian Trench. The seismic investigations ended here on 10 July at 07:30 hrs (Figure 2).

On July 11 at 06:25 hrs, we reached the working area 2 at the Storegga Slide (Figure 3) and started profile No. 4 with the 2 ltr airgun. The profile was in the vicinity of our previous deep-tow boomer seismic line (Evans, 1994). Again, the airgun caused severe problems and we interrupted the profile after 3 hours at 09:17 hrs.

Later the ocean bottom hydrophones (OBH) were tested successfully in 600 m water depth at 13:12 hrs. Airgun profiling started on 11 July at 21:33 hrs with profile 5 across the most exciting area of Storegga as it contains over 400 m wide and several metres deep mud volcanoes. The profile ended on 12 July at 05:57 hrs in the early morning. The seismic gear was brought on deck and we sailed to the selected OBH stations which were in the area of mud volcanoes at a water depth of about 870 m.

It was there that we met the second research vessel, Prof. Logachev, on 12 July at 12:00 hrs (64°48,61´N, 04°15,0´E) in order to carry out a two ship operation at Storegga. The chief scientists (Drs. Ivanow on RV Prof. Logachev and Mienert on RV Aleksandr Karpinskiy) met

each other on Prof. Logachev for a 2 hours science meeting about side-scan sonar and seismic investigations at the northern border of Storegga. Mr. Belousov from the Aleksandr Karpinskiy kindly provided his assistance in translating during the discussions. Michail Belousov and Jürgen Mienert returned from Prof. Logachev to Aleksandr Karpinskiy at 15:00 hrs and the ship continued sailing to the selected working areas (Figure 3).

On 12 July at 17:19 hrs and at 18:02 hrs respectively, the OBH platforms were disconnected from the wire of the winch and released to the sea. The platforms settled down on the sea floor after approx. 10 to 20 minutes in a water depth of 870 m and a separation of approx. 500 m. The 6.29 nm long airgun profile 6, which runs directly across the two OBH stations was started at 20:30 hrs and finished at 21:14 hrs. This allowed us to carry out a wide-angle reflection profile. We stopped profiling at a distance of about 3 km from the OBH nearest to the airgun. After having finished the profile, the OBHs were successfully released from the sea floor by an acoustic signal and brought on deck on 13 July at 01:38 hrs.

RV Prof. Logachev was continuing the side-scan sonar survey at Storegga for two more days. The Norwegian observer, who had changed from RV Karpinskiy to RV Prof. Logachev, was picked up by a pilot boat on 16 July. We left the area on 13 July at approx. 02:00 hrs and sailed under a calm sea (2-3 Bft) to the region of the Knipovich Ridge located west of Spitsbergen at 76°47,0´N 8°00,0´E.

Airgun profile No. 7 started immediately after the arrival in working area 3 at the Knipovich Ridge on 16 July (Figure 4, Tables 2 and 3). The weather changed from Bft 2-3 to Bft 6 and the passing of a storm during the day and the night caused wave heights of approx. 5 m. This, in turn, increased ambient noise around the ship, thus decreasing the quality of the seismic records. Profile 8 was interrupted during this storm and was, therefore, continued at a later time when the sea was calmer.

During the following days a calm sea but increasingly cold weather accompanied the profiling work. On 17 July the airgun profiles 9 and 10 (Table 3) showed BSRs in sediments at the margin and the Knipovich Ridge. A high density seismic grid (profiles 11 - 15) indicated the extension and the local distribution of the BSRs. This evidence allowed us to select ideal ocean bottom seismometer stations above a BSR. On 17 July the OBHs were deployed and airgun profile 16 was run across the positions. After having finished the wide-angle acoustic experiment, the OBH deployments 5 and 6 (Tables 2 and 3) were released from the sea floor by an acoustic signal and brought on deck safely in the morning on 18 July at 7:10 and at 8:23 hrs.

The most northern end of the Knipovich Ridge was investigated with the seismic profiles No.

18 to 20 including OBH stations across a BSR. Because we encountered an accumulation of BSRs between 1000 m and 1500 m water depth, a south-north profile was planned to run along the margin into the Arctic Ocean. However, at 79° 27,68´N, 06°23,28´E sea ice hindered the northward extension of profile 21 which ended southwest from the Yermak Plateau (Figure 4). Enhanced reflectors (bright spots) and reflectors crossing bedding planes were observed, that may allow the determination of the north-south extension of the BSRs which accumulate at approx. 240 ms below the sea floor (TWT).

Under continuously calm sea conditions we returned to the south, running at first a west-east profile (No. 22) from the margin onto the shelf, at second a north-south profile along the shelf (No. 23), and at third an east-west seismic line from the shelf across the margin (No. 24). The profile sections across the shelf ran at approx. 300 m water depth and showed a very limited penetration due to an apparently hard sea floor and strong acoustic backscattering. The penetration increased to approx. 1sec (TWT) on the margin, showing reflector patterns which may indicate large sediment waves or contourites. Although it is still not clear to what degree the sediments of the Fram Strait and the Arctic Ocean were dominated by the deep-sea circulation system, these seismic patterns may be interpreted as intense contourites of late Cenozoic paleocurrents (i.e. Eiken & Hinz, 1989).

The last of the OBH stations (No. 7 and 8) were completed at a water depth of 1087 m on 21 July at 20:08 hrs UTC. The scientific work during the RV Aleksandr Karpinskiy cruise was under good weather conditions throughout the voyage. In the morning of 25 July 1994 the ship tied up at Tromsø harbour and the cruise ended as planned.

4. Marine Geophysics

4.1. Airgun Seismic Profiling and Ocean Bottom Hydrophone Investigations

North Sea Fan

Airgun profiles were run over the western end of the Norwegian Trench and Fan (Figure 2) to search for geophysical evidence of past mass wasting processes that may be tied into the events pre-dating the Storegga Slide. The records revealed an acoustic penetration to approx. 800 ms. A cross profile over the Norwegian Fan showed evidence for one widespread slide event at a sub-bottom depth of 400 ms. Above the inferred sediment slide, which was indicated by hyperbolic echoes at its top, a series of distinct reflectors mark a prograding sediment wedge. The survey lines were positioned such that the seismic reflection profiles of the trough and fan

could be tied in to the Troll core (NORMAST, 1994). This profiling work proved to be hampered by several airgun failures which were tried to be overcome by a carefully made major overhaul of the mechanical and electrical parts of the airgun system.

Storegga Slide

Northeast of the Norwegian outer trough and fan lies the Storegga Slide, one of the world's largest slides. It has been described by Bugge et al. (e.g. 1988) who suggested three major events with minor or secondary slides. It is believed that earthquake loading and gas hydrate decomposition caused liquefaction which triggered these catastrophic events. One airgun profile and two OBH stations were deployed to proof the existence of widespread horizons of free gas and gas hydrates. For this aim we operated with two research vessels. The RV Prof. Logachev made a detailed side-scan sonar survey across areas where gas may be emitted through the sea floor, for example in areas of pockmarks and vents. In addition, we surveyed the sub-bottom with acoustic methods based on airgun and OBH wide-angle experiments. At the northern border of Storegga we encountered in our airgun records clear evidence for sub-vertical horizones of "wipe out" zones which are to be named "vents". In some cases they may be associated with large sea floor craters and mud volcanoes encountered on the side-scan sonar records during the RV Prof. Logachev survey. The ocean bottom seismometer stations (Figure 5) which were designed to measure the sound propagation of compressional waves in sediments proved to be the most successful experiment in these areas of gassy sediments.

Spitsbergen - Knipovich Ridge

A major topographic height between the northern plate boundary in the Norwegian Greenland Sea is the Knipovich Ridge (Eiken and Austegard, 1987). Its most northern part is buried under sediments that came from Spitsbergen. The correlation to the seismic profiles is only possible through DSDP Site 344, which encountered approx. 3 Ma sediments at its base at 300 mbsf. The age implies high sedimentation rates of about 10 cm/kyr. In addition to the high sedimentation rates and high organic carbon content, the temperature and pressure conditions at this water depth (approx. 1000 m - 2400 m) provided ideal circumstances for the accumulation of gas hydrates.

Airgun profiling detected the local distribution of BSRs along the eastern part of the ridge and the lower slope of the margin in a water depth of between 1000 m and 3000 m. These profiles and several OBH stations (Figure 4 and Tables 2 and 3) across the BSRs should provide

the evidence for the development and distribution of gas hydrates from the northern mid-oceanic ridge to the margin off Spitsbergen.

5. Preliminary results

The Norwegian margin was surveyed in three locations (Figure 1) to study and determine the distribution of gas hydrates in high latitude margin sediments and its relationships to continental slope instability. These investigations were part of the SFB 313 project B1 (Marine Geophysics) and the ENAM project (MAST II). The three working areas encompassed a transect at (1) the Norwegian Trough and Fan, (2) the Storegga Slide, and (3) the Spitsbergen margin as well as Knipovich Ridge. The results of the airgun seismic profiling were of good quality, owing to the skills of the crew and good weather conditions. The results of the post-processing of the seismic data and the processing of the OBH data will become available after extensive work onshore.

Norwegian Trough and Fan

The seismic reflector sequences at the outer trough and fan show largely parallel reflectors which may indicate undisturbed sedimentary sequences. The sequences appeared to have an almost constant thickness when short intervals of the records were examined. Only one example exists (Figure 6) where a channel cuts into the underlying sediments. This channel reflects erosional processes in a restricted area of the sea floor from past to present times.

Below approx. 400 ms (TWT), there were widespread occurrences of hyperbolic echoes indicating sediment mass flow deposits, i.e. debris flows (Figure 7). This unit of debris flows was overlain by well-stratified reflector sequences. The zone of hyperbolic echoes fades out towards the upper part of the continental slope. Towards the inner part of the Norwegian Trough the debris flows apparently end at a buried scarp which could be the upper, eastern boundary of the slide edge. It is hoped that the dating of the overlying sediments will determine the age of the debris flow and the widespread mass wasting process that pre-dates the Storegga event will be stratigraphically identified.

Storegga Slide

The airgun profiles 4 and 5 (Tables 2 and 3) at the northern border of the Storegga Slide

comprise mainly undisturbed sedimentary sequences. These sequences were shown to be interrupted where vents occur. The vents are recognised as vertical or sub-vertical acoustic "wipe out" zones (Figure 8). The vents have shown to be up to 100 m wide and greater than 500 ms (TWT) deep and are characterised by the upward turning of reflectors at the position of the vents (Figure 8). The evaluation of the side-scan sonar data from the RV Logachev survey will shed light on the question of whether these sub-bottom vents break through the surface. There is evidence for large mud volcanoes which may be connected to some of the vents thus indicating regions of overpressure in the sediments.

Spitsbergen Margin and Knipovich Ridge

Bottom simulating reflectors (BSRs) were observed in many local areas of the continental slope off Spitsbergen in water depths between 1000 m and 1500 m (Figure 9) and at the Knipovich Ridge in a water depth of approx. 2000 m (Figure 10). Also, acoustic "wipe out" zones, previously observed at the northern border of Storegga, were found to be a common feature in study area 3 (Figures 11a and b). The BSRs have a common sub-bottom depth of between 200 ms and 300 ms (TWT) and a patchy distribution. Gas hydrates are usually generated from intensive bacterial alteration of organic matter (Kvenvolden and Barnard, 1982) in areas of high sedimentation rates and high contents of organic carbon. However, because the BSRs occured not only at the eastern flank of the Knipovich Ridge but also at the margin (Figures 9 and 10), the result of two principally different processes of hydrate generation may be observed. Gas hydrates at the Knipovich Ridge may be thermogenic in origin, whilst those from the margin may be the more common microbially produced methane gas hydrates.

Large sediment waves underlie a well-stratified reflector sequence (Figure 12). The sediment waves had amplitudes of 100 ms (TWT) and wavelenghts of several kilometres. One can relate this local distribution of sediment waves at the eastern margin of the Fram Strait can be related to the action of strong paleocurrents. The wavy pattern occurs at about 250 ms below the sea floor indicating times of severe bottom current activity. The change from the wavy pattern to a well-stratified sequence above probably relates to a decrease in bottom water current intensity from Tertiary to Quaternary times. The initiation of these strong currents may be related to late Cenozoic climatic cooling (Eiken and Hinz, 1989).

6. Scientific participants

Name	Speciality	Institute
Dr. Jürgen Mienert (Chief Scientist)	Geophysics	GEOMAR/SFB 313
Michael Bobsien, Dipl. Geophys.	Geophysics	SFB 313
Jörg Posewang, Dipl. Geophys.	Geophysics	SFB 313
Robert Hird, Student	Geotechnics	GTB
Christian Berndt, Student	Geophysics	GEOMAR
Tilmann Steinmetz, Student	Geology	GPIT
Ute Brennwald	Geology	GEOMAR
Anja Wersinski, Student	Geography	GEOMAR
Manon Wilken, Student	Geography	GEOMAR
Mikhail Belousov, Dipl. Geophys.	Geophysics	PMGE
Viktor Gandyuchin, Dipl. Engineer	Geophysics	PMGE
Alexandr Orudshev, Dipl. Engineer	Geophysics	PMGE
Anatoly Berezka, Dipl. Engineer	Geophysics	PMGE
Anatoly Ganschin, Dipl. Engineer	Geophysics	PMGE
Anatoly Borisov, Dipl. Geotechn.	Geophysics	PMGE
Igor Rudnikov, Dipl. Engineer-radiotech.	Geophysics	PMGE
Valery Barinov, Dipl. Mathemat.	Geophysics	PMGE
Nikolay Filimonov, Dipl. Hydrogr.	Hydrography	PMGE
Yury Loginov, Dipl. Hydrogr.	Hydrography	PMGE
Sergey Goryatchich, Dipl. Hydrogr.	Hydrography	PMGE
Nikolay Volkov, Engineer-radiotechn.	Hydrography	PMGE
Alexandr Prischepa, Dipl. Engineer-mech.	Pneumatics	PMGE
Konstantin Spiridonov, Techn.	Pneumatics	PMGE
Vladimir Fedorov, Techn.	Pneumatics	PMGE
Yury Abramov, Techn.	Pneumatics	PMGE

7. References

Bugge, T. Belderson, R.H. &Kenyon, N.H. (1989) The Storeega Slide. Philosiphical Transactions of the Royal Society of London, A, 325, pp. 357-388.

Eiken, O. &Austegard, A. (1987) The Tertiary organic belt of West-Spitsbergen: seismic expressions of the offshores sedimentary basins. Norsk Geologisk Tidsskrift, Vol. 67, pp. 383-394.

Eiken, O. & Hinz, K. (1989) Contourites in the Fram Strait. In: O. Eiken: Aspekter ved refleksjonsseismikk, pp. 93-118.

Evans, D. (1994) British report of ENAM. In: Mienert et al. (eds.) ENAM European North Atlantic Margin: Sediment pathways, processes and fluxes. Progress Report (12 months)

Kvenvolden, K.A. & Barnard, L.A. (1982) Hydrates of Natural Gas in Continental Margins. American Association of Petroleum Geologists Memoir, 34, pp. 631-664.

Max, M.D. (1990) Gas hydrate and acoustically laminated sediments: Potential environmental cause of anamalously low acoustic bottom loss in deep-ocean sediments, NRL report 9235, Washington DC 20375-5000, 68p.

NORMAST (1994) Norwegian Part of ENAM. In: Mienert et al. (eds.) ENAM European North Atlantic Margin: Sediment pathways, processes and fluxes. Progress Report (12 months)

8. Acknowledgement

The expedition was funded by the Deutsche Forschungsgemeinschaft and the European Commision Mast II programme.

Оглавление

1. Цель исследования

1.1. Введение

Это исследование должно внести свой вклад в понимание характера распределения газогидратных слоёв на материковом склоне и определить газонасыщенные зоны, которые влияют на устойчивость материкового склона на европейской окраине материка.

В газогидратном слое газы и вода находятся в твёрдой кристаллической фазе. При низких температурах, высоком давлении и насыщенности газом, газогидраты находятся в устойчивом состоянии. Ниже устойчивых слоёв газогидраты переходят из твёрдой фазы в свободную, т.е. происходит образование высокой пористости за счет расширения газа-метана растворенного в воде. Таким образом ниже зоны газогидратов образуется слой с высокой пористостью и повышенным содержанием метана. Изменение устойчивости газогидратов является решающим для устойчивости окраин материка, потому что при переходе газогидратов в другую фазу и образованию повышенной пористости осадков, возникает возможность перемещения слоёв по плоскостям скольжения, образующиеся в высокопористом слое. Таким образом важно изучить характер распределения и историю формирования газогидратных слоев вдоль материкового склона, чтобы разобраться с процессом осадконакопления в его пределах. Устойчивость материкового склона, насыщенного газогидратными слоями, может оказывать влияние на климат, особенно на возникновение тепличного эффекта.

Газогидратный слой в морских осадках лучше всего можно выделить сейсмическими методами. Газогидратные слои в осадочной толще характеризуются значительным увеличением плотностных параметров по отношению к подстилающим слоям, что приводит к образованию акустического горизонта, называемого BSR. Такой BSR характеризуется высокими сейсмическими амплитудами, инверсией фаз и обычно параллелен морскому дну. Инверсия фаз указывает на переход от среды с высокой скоростью распространения упругих волн над BSR, к среде с более низкими скоростями ниже BSR. В газогидратном слое (твёрдое состояние газа) распространение упругих волн достигает скорость от 2.3 до 3.4 км/с (Max, 1990). А в подстилающих BSR слоях (газовое состояние) скорость уменьшается до 1.5 км/с, потому что газогидратные слои становятся неустойчивыми и свободный газ может существовать. Это изменение распределения скоростей наилучшим образом объясняет, почему можно открывать газогидратные слои наилучше всего сейсмическими методами.

1.2. Проекты

SFB 313, финансируемый Германским Научным Обществом, исследует "Изменении окружающей среды в северной части Северной Атлантики", а проект ENAM (Материковый склон европейской части Северной Атлантики: пути осадконакопления, процессы и потоки), финансируемый Европейской комиссией, исследует процессы, влияющие на форму материкового склона в ледниковый период и последующих периодах. В течение нашего рейса обе программы выполняются в кооперации с Полярной морской геологоразведочной экспедицией (ПМГРЭ), Санкт-Петербург, Россия. Научно-исследовательские суда экспедиции "Академик Александр Карпинский" и "Профессор Логачев" были зафрахтованы для совместных работ по исследованию газогидратов вдоль европейского и полярного материкового склона. Совместная работа обоих судов и сотрудничество со специалистами из разных стран явились существенной основой при планировании рейса (Рис. 1-4).

2. Программа исследовательских работ

2.1. Специальный исследовательский сектор 313 (SFB 313)

Целью проекта B1 (морская геофизика) SFB 313 в рейсе НИС "Академик Александр Карпинский" являлись геофизическая стратификация осадочной толщи и изучение газонасыщенных слоев. Придонные исследования вдоль материкового склона концентрировались в районах развития газогидратов и газонасыщенных осадочных слоев находящиеся между арх. Шпицберген и хребетом Книповича (Рис. 4).

2.2. Материковый склон европейской части Северной Атлантики: пути осадконакопления, процессы и потоки (ENAM)

Во время рейса НИС "Ак. А. Карпинский" мы занимались изучением осадочных отложении четвертичного периода в пределах Норвежского жёлоба и конуса выноса, которые подвергались большому ледниковому влиянию (Рис. 2). В области Норвежского жёлоба использовалась методика непрерывного сейсмоакустического профилирования с пневмоисточниками для оценки размеров обширных скользящих массивов, в ряду которых самым древним является событие по перемещению осадков на массиве Сторегга (30 - 50 тыс. лет, Бугге и др., 1988).

На скользящем массиве Сторегга сейсмоакустическое профилирование и использование донных сейсмометров должны были дать информацию о

распределении газогидратов и газонасыщенных слоёв (Рис. 3). Районы с газонасыщенными слоями имеют мощный сбросовый потенциал. Поэтому нами проводится детальное изучение к северу от одного из главных возможных в будущем сбросов.

3. Ход рейса

НИС "Ак.А. Карпинский" вышел из Киля 5-го июля 1994г. в 19 часов. Судно направилось к 1ой области работ - Норвежскому жёлобу и конусу выноса (Рис. 1 и 2). 7-го июля в 18 часов мы взяли на борт норвежского наблюдателя доставленного на лоцманском боте. Он представлял директорат рыболовства в Ставангере.

В следующуй день мы начали профилирование с источниками возбуждения в 19 часов в 1ой области работ, в районе Норвежского жёлобы и конуса выноса (Рис. 2). Мы использовали 2-х и 3-х литровые излучатели и сейсмоприёмную косу длиной 500м (Таб. 1) с активной частью длиной 62,5м, шесть каналов (10 гидрофонов/канале), активно записывали акустические сигналы.Мы начали профилирование 8-го июля 94г. в 22:32ч. Перед этим мы регулировали глубину буксирования сейсмоприёмной косы и излучателя. Частотный диапазон цифровой записывающей системы был установлен от 65 до 500Гц. Во время 1-го профиля (Таб. 2 и 3) источник возбуждения отказал 9-го июля в 6:02ч. Мы произвели замену на 3-х литровый источник возбуждения вместо 2-х литрового источника и продолжили профилирование в 12:38ч. Излучаемый источником сигнал обеспечил отличное изучение в интервале регистрации 1сек с высокой разрешающей способностью и показал продвигаюшийся клин от наружного Норвежского жёлоба в конус выноса. Кроме того, запись показала скольжение осадков которое может иметь связь со скольжением ранее произошедшем на массиве Сторегга (NORMAST, 1994).

Сейсмические работы с 9-го по 10-ое июля были проведены при хороших погодных условиях (волнение 2-3 балла). Однако некоторые прерывания работы из-за механических и электрических проблем с излучателями, порождали значительное замедление наших сейсмических работ (смотр. Табл. 3) в районе Норвежского жёлоба. Сейсмические исследования здесь закончили 10-го июля в 7:30ч (Рис. 2).

11-го июля в 6:25ч мы достигли область работы 2 на скользящем массиве Сторегга (Рис. 3) и начали профиль 4 с 2-х литровым излучателем. Профиль находился недалеко от нашего ранее выполненного сейсмического профиля (Evans, 1994). Ещё раз возникли проблемы с излучателями и мы прервали профилирование в 9:17ч.

Потом ocean bottom hydrophones (OBH) были успешно подвергнуты испытанию на глубинах 600м в 13:12ч. Сейсмическое профилирование с 2-х литровыми источниками было продолжено 11-го июля в 21:33ч (профиль 5) по самой интересной области Сторегги, где выделена зона распространения mud volcanoes шириной 400м и мощностью несколько метров. Профиль был окончен 12 июля в 5:57ч утра. Сейсмическое оборудование было поднято на палубу и мы совершили переход к месту постановки OBH, которое находится в области развития mud vulcanoes на глубинах около 870м.

Здесь мы встретили второе научно-исследовательское судно, "Профессор Логачев" 12 июля в 12:00ч (64°48,61'С, 04°15,0'В), чтобы провести совместные работы на скользящем массиве Сторегга. Начальники рейсов ("Проф. Логачев" - Господин Иванов и "Александр Карпинский" - Др. Минерт) встретились на борту судна "Проф. Логачев". В течение 2 часов они обменивались опытом исследований звуколокатором бокового обзора и сейсмических исследованиях на северной границе массива Сторегга. Господин Белоусов ("Александр Карпинский") любезно помогал во время переговоров. Др. Минерт и господин Белоусов вернулись на "Александр Карпинский" в 15:00ч, и были продолжены работы (Рис. 3).

12-го июля в 17:19ч и в 18:02ч OBH были отделённы от троса лебёдки и остановлены на дне. Мы начали профиль 6 с пневмоисточником в 20:30ч, который точно проходит через станции OBH. Профиль длиной в 6,29 мили окончен в 21:14ч. Мы окончили профилирование на расстоянии около 3-х милв от того OBH который находился ближайщим к судну. Расстояние между станциями OBH составляло около 870м. По акустическому сигналу OBH успешно оторвались от морского дна и были подняты на палубу 13-го июля в 01:38ч.

"Проф. Логачев" ещё 2 дня продолжал съёмку звуколокатором бокового обзора на массиве Сторегга. Мы вышли из 2ой области работ 13-го июля в 2:00ч и последовали при хорошей погоде (2-3 балла) в район хребта Книповича, находящегося на западе арх. Шпицберген (76°47,0'С 8°00,0В).

После достижения области работы 3, на хребте Книповича, 16-го июля, мы начали профилирование с излучателями N 7 (Рис. 4, Таб. 2 и 3). Погодные условия изменились с 2-3 баллов до 6 баллов и в течение суток, проходящий шторм порождал волны высотой до 5м. Поэтому качество записей ухудшилось из-за увеличения шумов. Профиль 8 был прерван во время шторма и был продолжен когда шторм закончился.

При работе на профилях в последуюшие дни море было спокйно, но температура понизилась. 17-го июля на профилях 9 и 10 (Таб. 3) обнаружен BSR в осадках

материкового склона и на хребте Книповича. Детальная сейсмическая съёмка (профиль 11 - 15) показала расширение и местное разпределение BSR. Это послужило доказательством идеального места для выбора постановки ОВН над BSR. 17-го июля ОВН были выставлены и над ними был выполнен сейсмический профиль 16. После окончания широкоугольного акустического эксперимента ОВН 5 и 6 (Таб. 2 и 3) были подняты с морскового дна акустическим сигналом и приняты на борту судна утром 18-го июля в 7:10ч и 8:23ч.

Самый северный конец хребта Книповича был исследован сейсмическими профилями 18 и 19 включительно, постановками ОВН через BSR. Мы определили аккумуляцию BSR на глубинах между 1000 и 1500м. Поэтому мы запланировали выполнить профиль направлением S-N вдоль окраины материка в Северный Ледовитый Океан. Однако на широте 79°27,68'С, и долготе 06°23,28'В мы встретили поле морского льда который препятствовал продолжению профиля 21 на север, профиль был закончен югозападнее от Плато Ермак (Рис. 4). Были замечены границы с повышенным отражением (яркие пятна) и границы отражения, пересекающие плоскости напластования, что позволило определить направление BSR севера на юг, аккумулируещегося примерно в 240мс ниже уровня морского дна.

При хороших гидрометеорологических условиях мы вернулись на юг. Мы выполнили первый профиль направлением W-E (номер 22) с материкового склона на шельф, второй профиль направлением N-S вдоль шельфа (номер 23), и третий направлением E-W с шельфа через материковый склон (номер 24). На части профилей проходящих через шельф, отмечались глубины до 300м, а проникновение было очень ограниченно, обычно из-за жёсткого морского дна и сильного акустического обратного рассеяния. Проникновение повысилась на материковом склоне примерно на 1сек, при этом выявилась группа границ отражающих длинные осадочные образование или контуры течений. Не смотря на то, что точно не определено влияние системы циркуляции глубиных вод на осадки в районах Fram Strait и Северного Ледовитого Океана, эти сейсмические схемы могут быть интерпретированны как отчетливые контуриты древнего течения из позднего Кайнозоя (на пр. Eiken & Hinz, 1989).

Последние постановки ОВН (номера 7 и 8) была осушествленна на глубине 1087м 21-го июля в 20:08ч по Гринвичу. Научные работы во время рейса НИС "Александр Карпинский" сопровождались хорошими погодными условиями. Утром 25-го июля судна отшвартовалось в п. Тромсё и рейс закончился, как планировалось.

4. Морская Геофизика

4.1. Сейсмическое профилирование с источниками возбуждения и исследования с донными регистраторами

4.1.1. Конус Северного Моря

Профили записанные с источниками возбуждения были выполнены через западное окончание Норвежского жёлоба и конуса выноса (Рис. 2), чтобы найти геофизические доказательства прошедщих процессов перемещения слоёв, которые можно связать с событиями предшествовавшими образованию массива Сторегга. Записи показали акустическое проникновение до 800м. Секущий профиль через Норвежский конус выноса подтвердил наличие растянутого скольжения на глубине 400м от дна. Над предполагаемой границей скольжения осадков, которая обозначена гиперболическими отражёнными волнами, серия различных отражающих границ отмечает смещённый клин осадков. Профили съёмки были расположены так, чтобы сейсмические отражённые волны в жёлобе и конусе, можно связывать с керном Тролл (NORMAST, 1994). Профилирование было осложнено некоторыми перерывами в работе излучателей. Эта ситуация была устранена текущим ремонтом механической и электрической части системы излучателей.

4.1.2. Скользящий Массив Сторегга

На северо-востоке Норвежского внешнего жёлоба и конуса находится массив Сторегга, один из самых больших в мире скользящих массивов. Он был описан Бугге и др. (на пр. 1988), который различает три главные события с меньшими или второстепенными скольжениями. Предполагается что землетрясения и разложение газогидратов вызвали сжижение, которое было причиной этих катастрофических событий. Один профиль с излучателями и две постановки ОВН были произведены чтобы проверить существование обширного горизонта свободного газа и газогидратов. Поэтому НИС "Профессор Логачев" сделал детальную съёмку гидролокатором бокового обзора (ГБО) через области, где газ может выходить сквозь морское дно, например в районах, где находятся pockmarks и vents. Более того мы применили придонные акустические методы базирующие на широкоугольных экспериментах с источниками возбуждения и ОВН. На северной границе массива Сторегга мы установили в наших записях излучателей надежное доказательство суб-вертикальных горизонтов wipe out зоны которые могут быть названы "vents". В некоторых случаях их можно связать с большими кратерами морского дна и mud vulcanoes встречаемых на записях гидролокатора бокового обзора. Постановки ОВН (Рис. 5), созданные чтобы

измерить распространение звука продольних волн в осадках, явились самым успешным экспериментом в этих районах газонасыщенных осадков.

4.1.3. Шпицберген - Хребет Книповича

Одной из главных топографических высот между северной пластинчатой границой в Норвежском Гренландском море является хребет Книповича (Eiken & Austegard, 1987). Его самая северная часть покрыта осадками вынесеными из Шпицбергена. Степень изученности района можно оценить по сейсмическим профилям программы DSDP Site 344 которая обнаружила около 3Ма осадков на его основе на 300mbsf. О возрасте говорят большие объёмы осадконакопления в размере около 10см/тыс. лет. Кроме мощного осадконакопления и высокого содержания органического карбона, температура и давление на этой глубине воды (около 1000-2400м) создают идеальное условие для накоплении газогидратов.

Профилирование с излучателями обнаружило местное распределение BSR вдоль восточной части гребня и нижнего склона окраины материка. Эти профили и несколько постановок OBH (Рис. 4, Таб. 2 и 3) через BSR дают представление о развитии и распределении газогидратов вдоль северного срединноокеанского хребта до окраины материка перед Шпицбергеном.

5. Предварительные результаты

Норвежская окраина материка была исследована в 3-х областях (Рис. 1) чтобы изучить и определить распределение газогидратов в материковых осадках с большой мощностью и их влияние на неустойчивость материкового склона. Эти исследования были частью проекта B1 (морскя геофизика) SFB 313 и проекта ENAM (MAST II). Три области исследований охватали район на (1) Норвежском жёлобе и конусе, (2) на Массиве Сторегга и окраине материка перед Шпицбергеном, а также хребет Книповича. Слажённое действие русского персонала и хорошие погодные условия позволили получиь на сейсмических профилях материали высокого качества. Результаты дополнительной обработки сейсмических данных и обработка данных OBH будут получены после интенсивных работ на суше.

Норвежский жёлоб и конус выноса

Последовательности отражающих границ на внешнем жёлобе и конусе отмечены параллельными отражающими границами которые могут указывать на

неразрушенные последовательности осадков. Когда короткие интервалы были исследованы, слои оказались почти одинаковой мощностью. Существует только один пример (Рис. 6), где канал пересекает подстилающие осадки. Этот канал указывает на процессы эрозии на небольшом участке морского дна происходившие с древнего времени по настоящее время.

Ниже на глубине, примерно, 400мс находятся обширные отложения mass flow deposits на пр. depris flows, фиксируемые гиперболическим отражённым сигналом (Рис. 7). Этот щебенчатый слой образует хорошо слоистые последовательности отражающих границ. Район, где отмечается гиперболические отражения, заканчивается в верхней части континентального склона. Внутренняя часть Норвежского жёлоба, по-видимому, заканчивается заглублённым склоном, верхная часть которого, может быть верхней восточной границей щебенчатого слоя. Надеемся, что определение возраста поверхностных осадков путём стратиграфического сравнения, позволит определить возраст щебенчатого слоя и процессы перемещения осадков предшествовавшие образованию массива Сторегга.

Массив Сторегга

Профили с пневмоисточниками (4 и 5, -Таб. 2 и 3) на северной границе массива Сторегга охватывают, в основном, неразрушенные осадочные последовательности. Профили показали, что эти последовательности были прерванны там где сушествуют vents, которые в свою очередь опознаются как вертикальные или субвертикальные акустические wipe out зоны (Рис. 8). Vents имеют ширину до 100м и глубину более чем 500мс и имеются признаки, которые указывают, что положение отражающих границ перевернуто (Рис. 8). Использование данных сьёмки гидролокатора бокового обзора НИС "Проф. Логачев" прольют свет на вопрос, выходят ли vents на поверхность морского дна. Сушествует доказательство для больших mud vulcanoes, которые могут быть связанны с некоторыми vents, указывая таким образом на районы повышенного давления в осадках.

Материковый склон Шпицбергена и хребет Книповича

BSR были обнаруженны во многих локальных районах континентального склона Шпицбергена на глубинах между 1000м и 1500м (Рис. 9) и на хребте Книповича на глубинах примерно 2000м (Рис. 10). Для акустические wipe out зоны обнаруженных ранее на северной границе массива Сторегга, найдены общие черты в изучаемом районе 3 (Рис. 11а и 11б). BSR разположены под дном на глубине 200мс и 300мс и распространены неравномерно. Газогидраты обычно возникают в связи с

интенсивным бактериальным изменением органического материала (Квенволден и Нарнард, 1982) в районах с большой мощностью осадков и высоким содержанием органических карбонов. Однако, в связи с тем, что BSR не только существовал на восточном фланге хребета Книповича, но также и на окраине материка (Рис. 9 и 10), мож :о наблюдать результаты двух различных процессов генерации газогидратов. Газогидраты на хребте Книповича могут быть термогенного происхождения, в то время как газогидраты окраины материка могут быть более общими метановыми газогидратами, биогенного происхождения.

Хорошо прослеживаемую слоистую осадочную толщу подстилают мощные волнообразные осадочные образования (Рис. 12). Эти осадочные образования имеют амплитуду от 100мс, а протяженность волн до нескольких километров. Можно связать локальное распространение осадочных волн на восточной части материкового склона Fram Strait с действием сильных палео-течений. Пример волнистого образования сушествует на глубинах 250мс, что указывает на время активности сильных донных течений. Переход от волнистого образования к хорошо слоистой последовательности связан, вероятно, с затуханием интенсивных донных течений от Третичного к Четвертичному периоду. Начало этих сильных течений может быть связанно с климатическим охлаждением позднего Cenozoic (Eiken & Hinz, 1989).

6. Участники рейса

Имя, Фамилия	Специализ.	Институт
Др. Юрген Минерт (начальник рейса)	геофизика	SFB313/GEOMAR
Михаел Бобсин, Дипл. геофизик	геофизика	SFB 313
Ёрг Позеванг, Дипл. геофизик	геофизика	SFB 313
Роберт Хирд, студент	геотехника	GTB
Кристиан Берндт, студент	геофизика	GEOMAR
Тилманн Стейнмец, студент	геология	GPIT
Аня Верзински, студентка	география	GEOMAR
Манон Вилькен, студентка	география	GEOMAR
Уте Бреннвальд	геология	GEOMAR
Михайл Белоусов, Дипл. геофизик (руководитель российских специалистов)	геофизика	ПМГРЭ
Виктор Гандюхин, Дипл. геофизик	геофизика	ПМГРЭ
Александр Оруджев, Дипл. инженер	геофизика	ПМГРЭ
Анатолий Березка, Дипл. инженер	геофизика	ПМГРЭ
Анатолий Ганшин, Дипл. инженер	геофизика	ПМГРЭ
Анатолий Борисов, Дипл. геотехник	геофизика	ПМГРЭ
Игорь Рудников, Дипл. инженер-радиотехник	геофизика	ПМГРЭ
Валерий Баринов, Дипл. математик	геофизика	ПМГРЭ
Николай Филимонов, Дипл. гидрограф	гидрография	ПМГРЭ
Юрий Логинов, Дипл. гидрограф	гидрография	ПМГРЭ
Сергей Горячих, Дипл. гидрограф	гидрография	ПМГРЭ
Николай Волков, инженер-радиотехник	гидрография	ПМГРЭ
Александр Прищепа, Дипл. инженер-механик	пневматика	ПМГРЭ
Константин Спиридонов, техник	пневматика	ПМГРЭ
Владимир Федоров, техник	пневматика	ПМГРЭ
Юрий Абрамов, техник	пневматика	ПМГРЭ

7. Литература

Bugge, T. Belderson, R.H. &Kenyon, N.H. (1989) The Storeega Slide. Philosiphical Transactions of the Royal Society of London, A, 325, pp. 357-388.

Eiken, O. &Austegard, A. (1987) The Tertiary organic belt of West-Spitsbergen: seismic expressions of the offshores sedimentary basins. Norsk Geologisk Tidsskrift, Vol. 67, pp. 383-394.

Eiken, O. & Hinz, K. (1989) Contourites in the Fram Strait. In: O. Eiken: Aspekter ved refleksjonsseismikk, pp. 93-118.

Evans, D. (1994) British report of ENAM. In: Mienert et al. (eds.) ENAM European North Atlantic Margin: Sediment pathways, processes and fluxes. Progress Report (12 months)

Kvenvolden, K.A. & Barnard, L.A. (1982) Hydrates of Natural Gas in Continental Margins. American Association of Petroleum Geologists Memoir, 34, pp. 631-664.

Max, M.D. (1990) Gas hydrate and acoustically laminated sediments: Potential environmental cause of anamalously low acoustic bottom loss in deep-ocean sediments, NRL report 9235, Washington DC 20375-5000, 68p.

NORMAST (1994) Norwegian Part of ENAM. In: Mienert et al. (eds.) ENAM European North Atlantic Margin: Sediment pathways, processes and fluxes. Progress Report (12 months)

8. Признание

Европейская комиссия (программа MAST II) и Deutsche Forschungsgemeinschaft финанцировали рейсу.

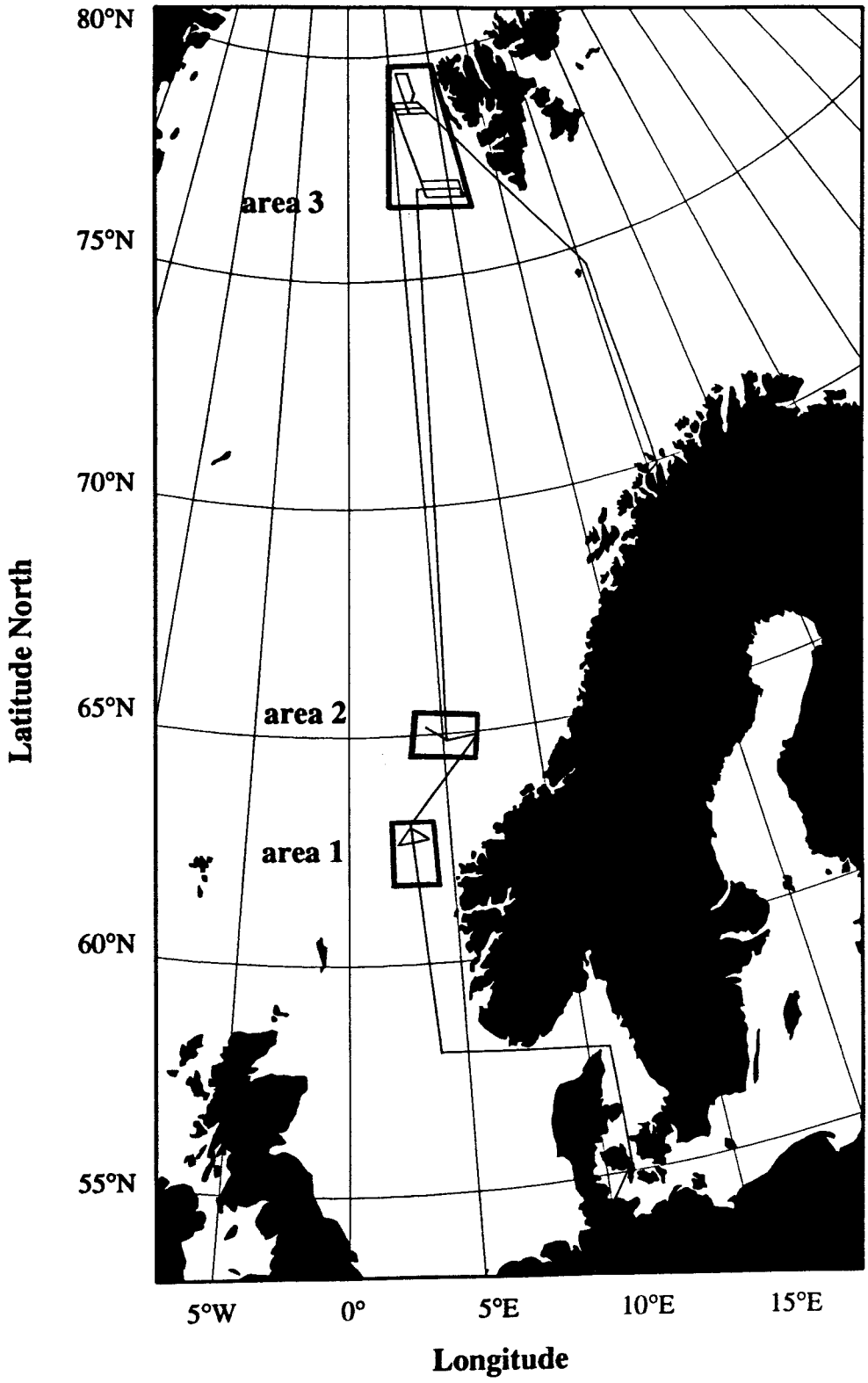

Figure 1: Cruise track and working areas of FV Aleksandr Karpinskiy

Рисунок 1: Схема рейса и области работ НИС Ак. Александр Карпинский и НИС Проф. Логачев

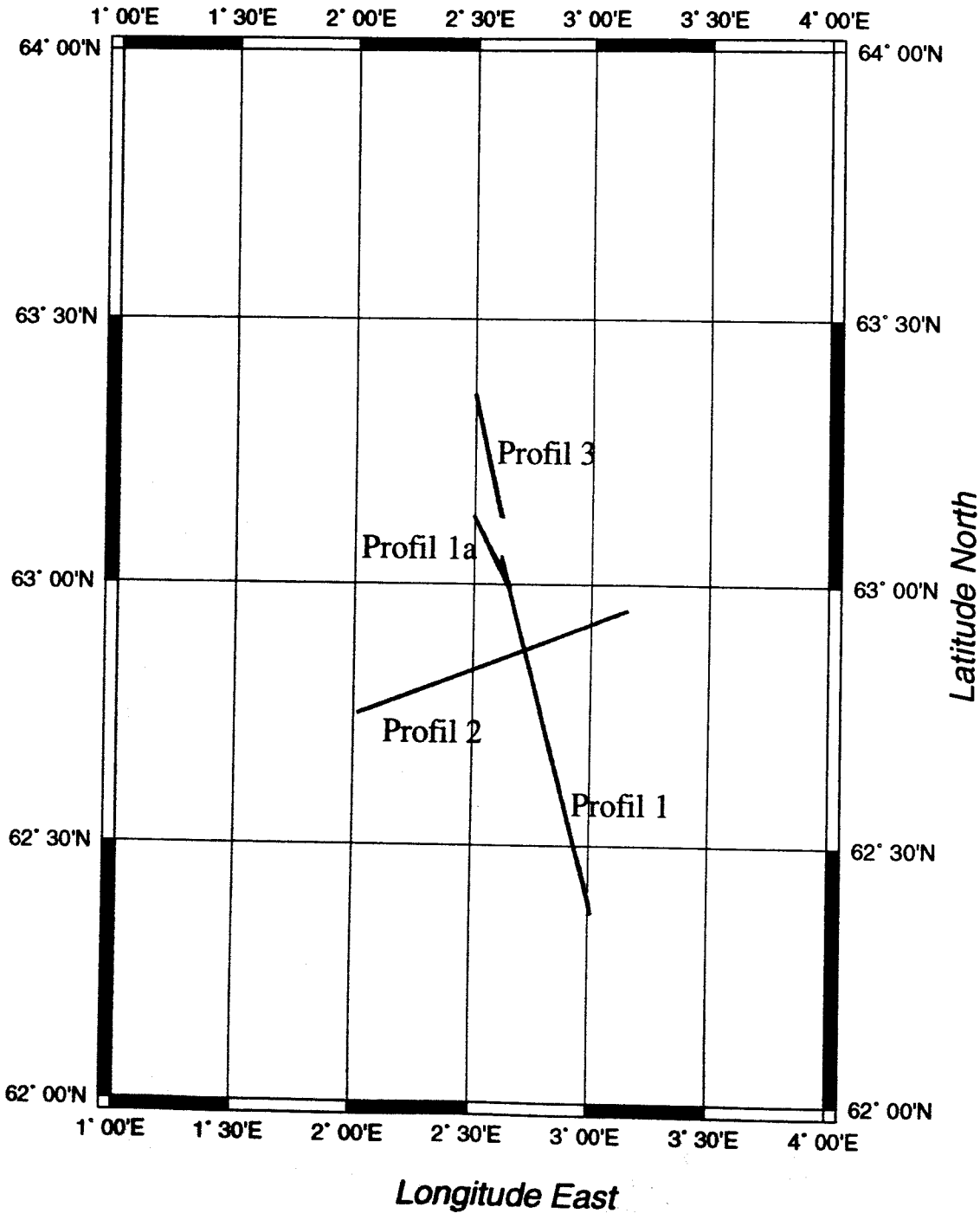

Figure 2: Cruise track in working area 1 at the Norwegian Trench and Fan

Рисунок 2: Схема рейса в области работ 1 на Норвежском жёлобе и конусе выноса

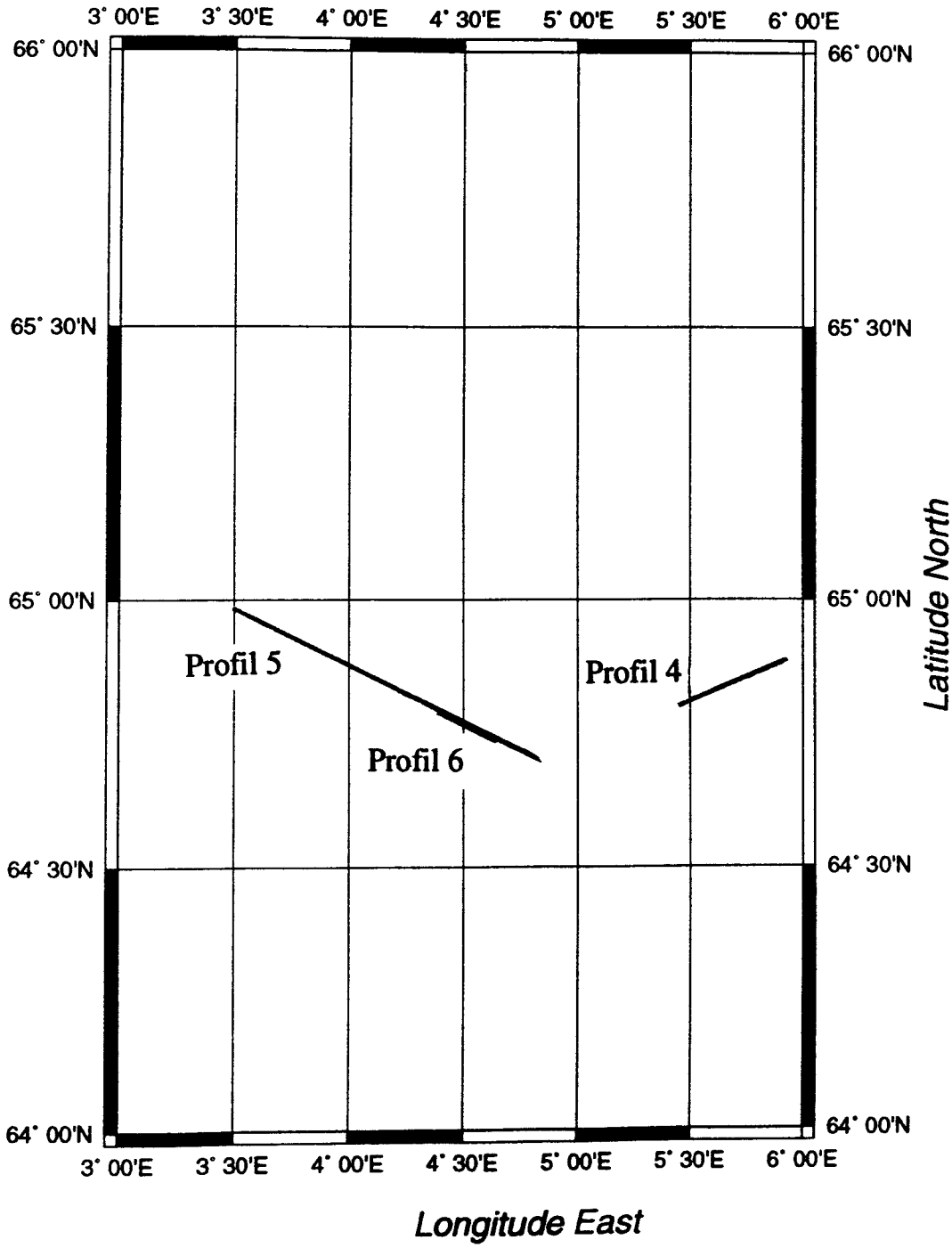

Figure 3: Cruise track in working area 2 at the Storegga Slide

Рисунок 3: Схема рейса в области работ 2 на массиве Сторегга

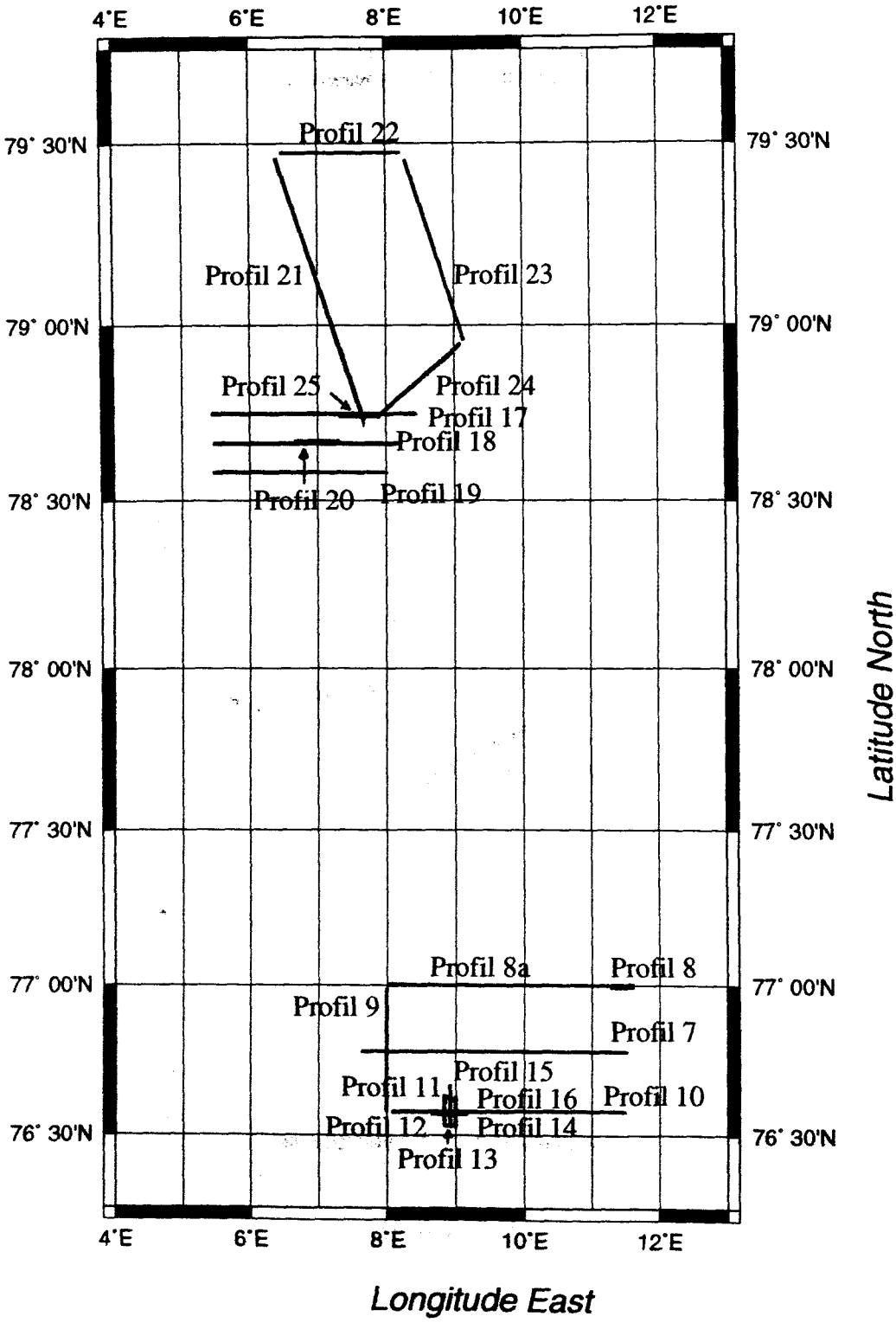

Figure 4: Cruise track in working area 3 between Spitsbergen and Knipovich Ridge

Рисунок 4: Схема рейса в области работ 3 между Шпицбергеном и хребтом Книповича

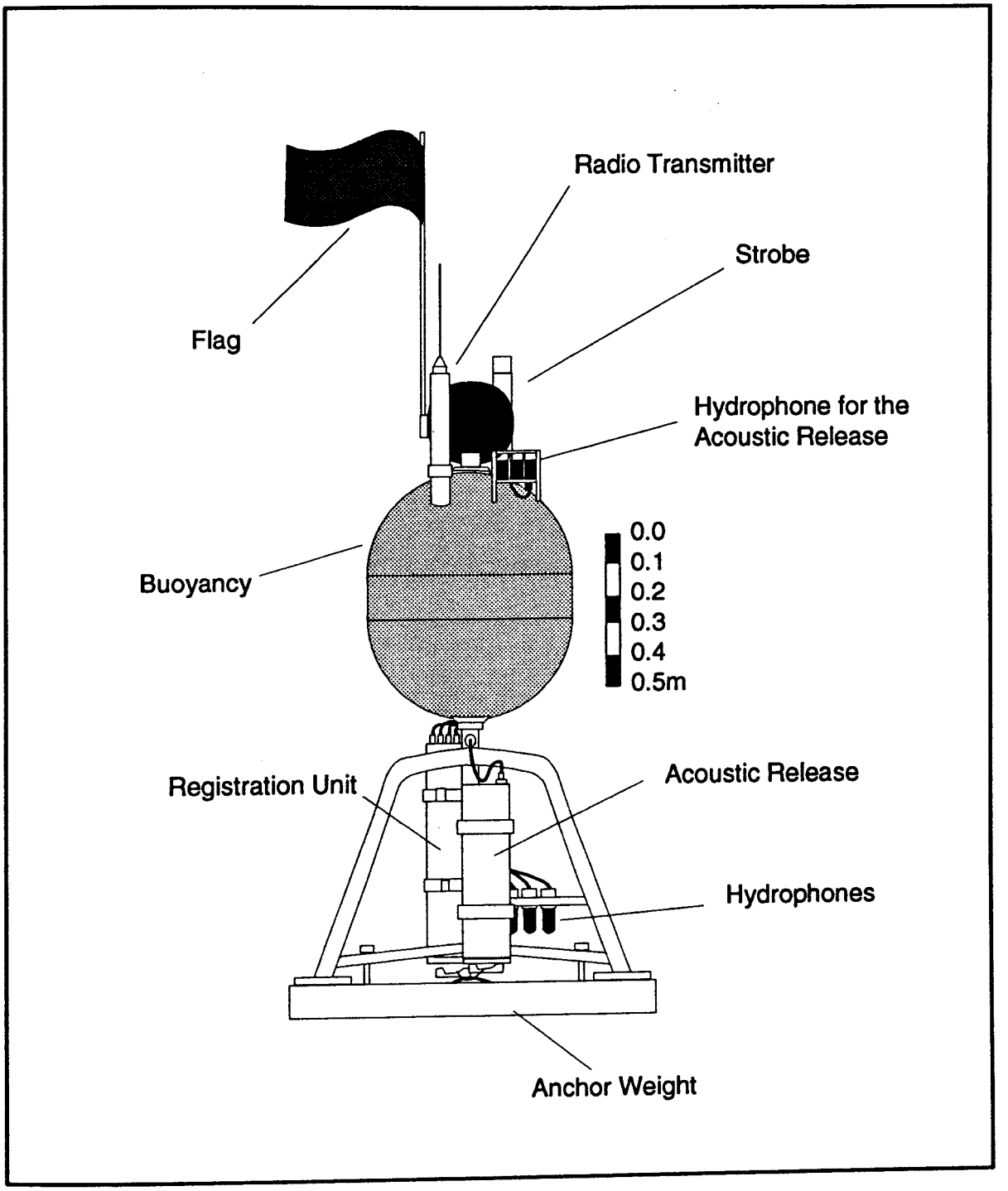

Figure 5: High-Frequency Ocean-Bottom-Hydrophone employed on the cruise of RV Aleksandr Akademik Karpinskyi

Рисунок 5: Платформа ОВН включая различные компоненты акустической системы

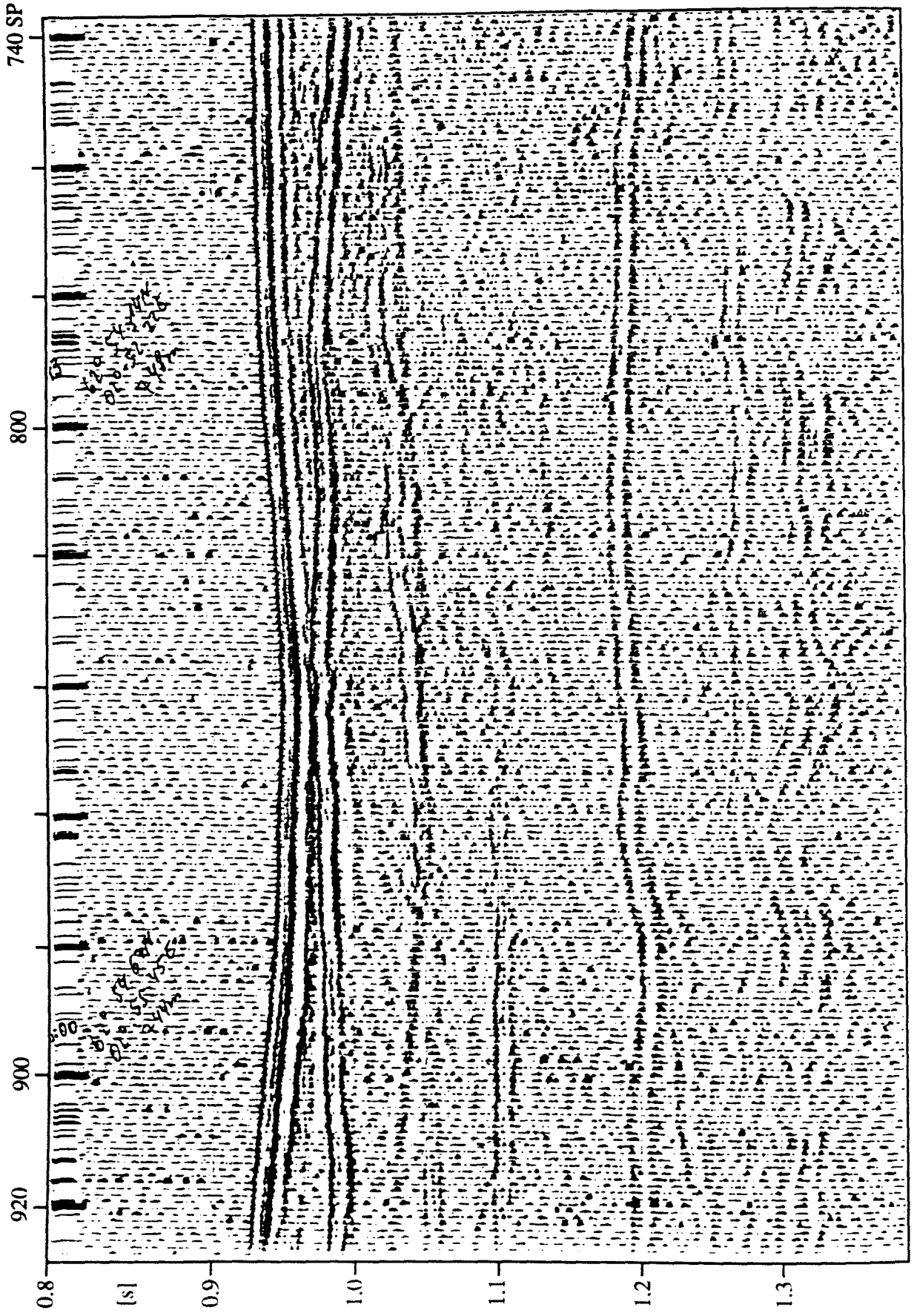

Figure 6: Airgun record from the outer Norwegian Trough showing an erosional channel. For loaction see Figure 2.

Рисунок 6: Запись излучателей от внешнего Норвежского жёлоба указывающий на канал эрозии (см. рис. 2).

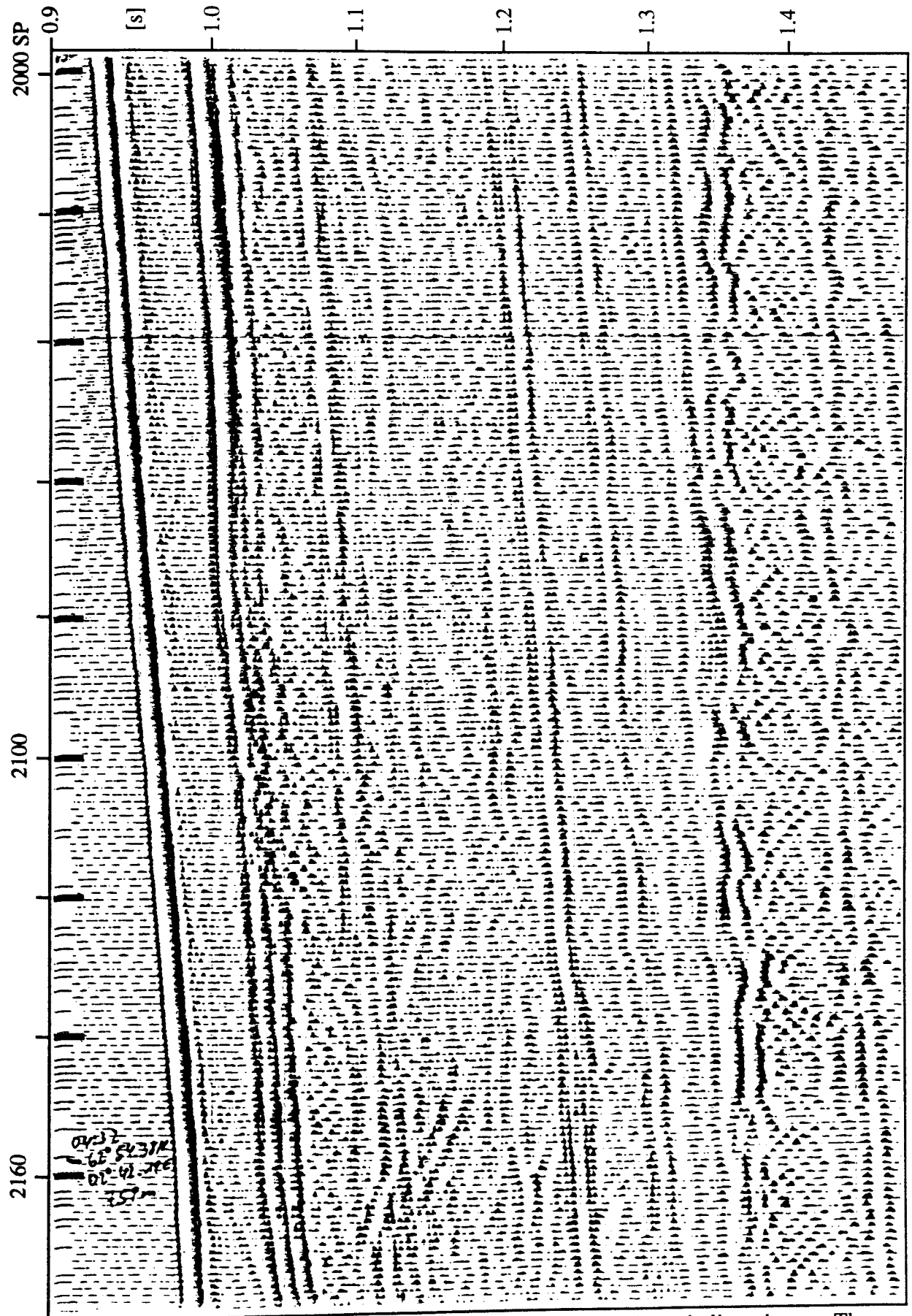

Figure 7: Airgun record from the Norwegian Fan showing hyperbolic echoes. The hyperbolic echoes are believed to indicate debris flows. For loaction see Figure 2

Рисунок 7: Запись излучателей от Норвежского Конуса с гиперболическим отражением. Предполагается, что гиперболическое отражение указывает на щебенчатый слой (см. рис. 2).

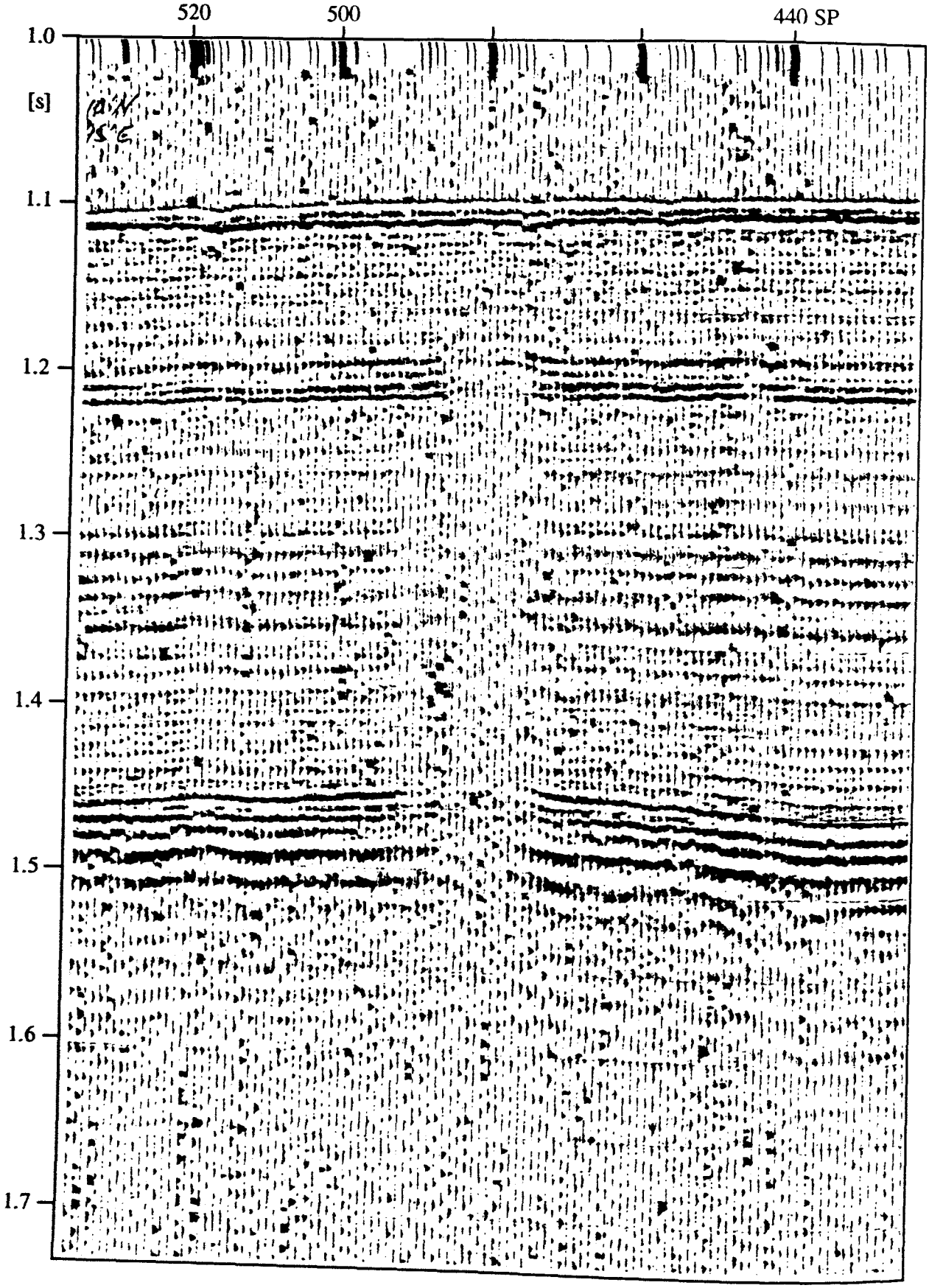

Figure 8: Airgun record from the Storegga slide showing acoustic "wipe out" zones which are interpreted as vents. Note the upward turning of the reflectors towards the vent. For location see Figure 3.

Рисунок 8: Запись излучателей от массива Сторегга указывающий на акустические "wipe out" зоны, интерпретируемые, как "vents". Отражающие границы перевернуты направлением "vents" (см. рис. 3).

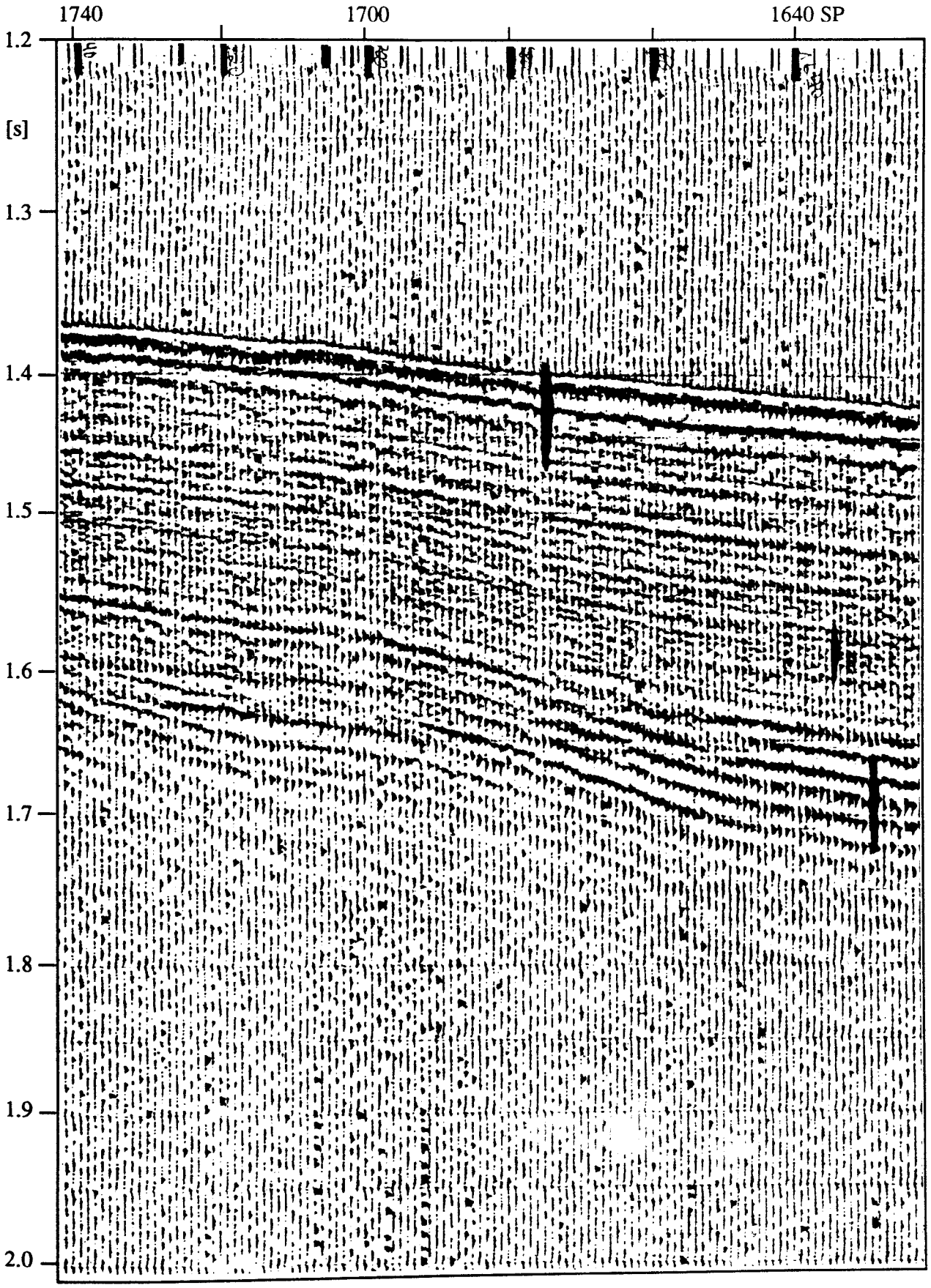

Figure 9: Airgun record from the Spitsbergen continental margin showing a bottom simulating reflector (BSR). For location see Figure 4.
Рисунок 9:Профиль излучателей от материкового склона Шпицбергена указывающий на BSR (см. рис. 4).

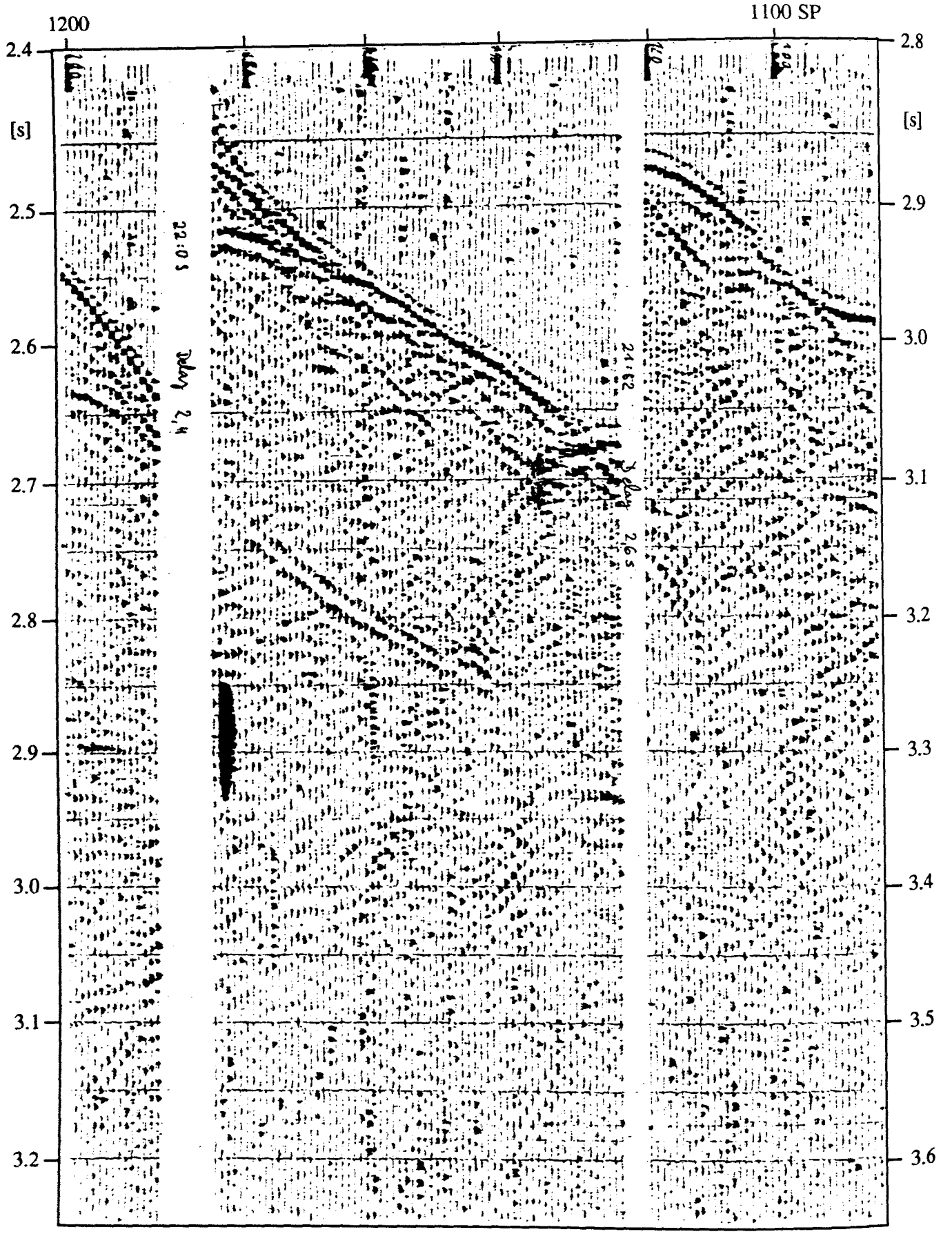

Figure 10: Airgun record from the eastern flank of the Knipovich Ridge showing a bottom simulating reflector (BSR). For location see Figure 4.

Рисунок 10: Профиль излучателей от восточной фланге хребета Книповича указывающий на BSR. (см. рис. 4)

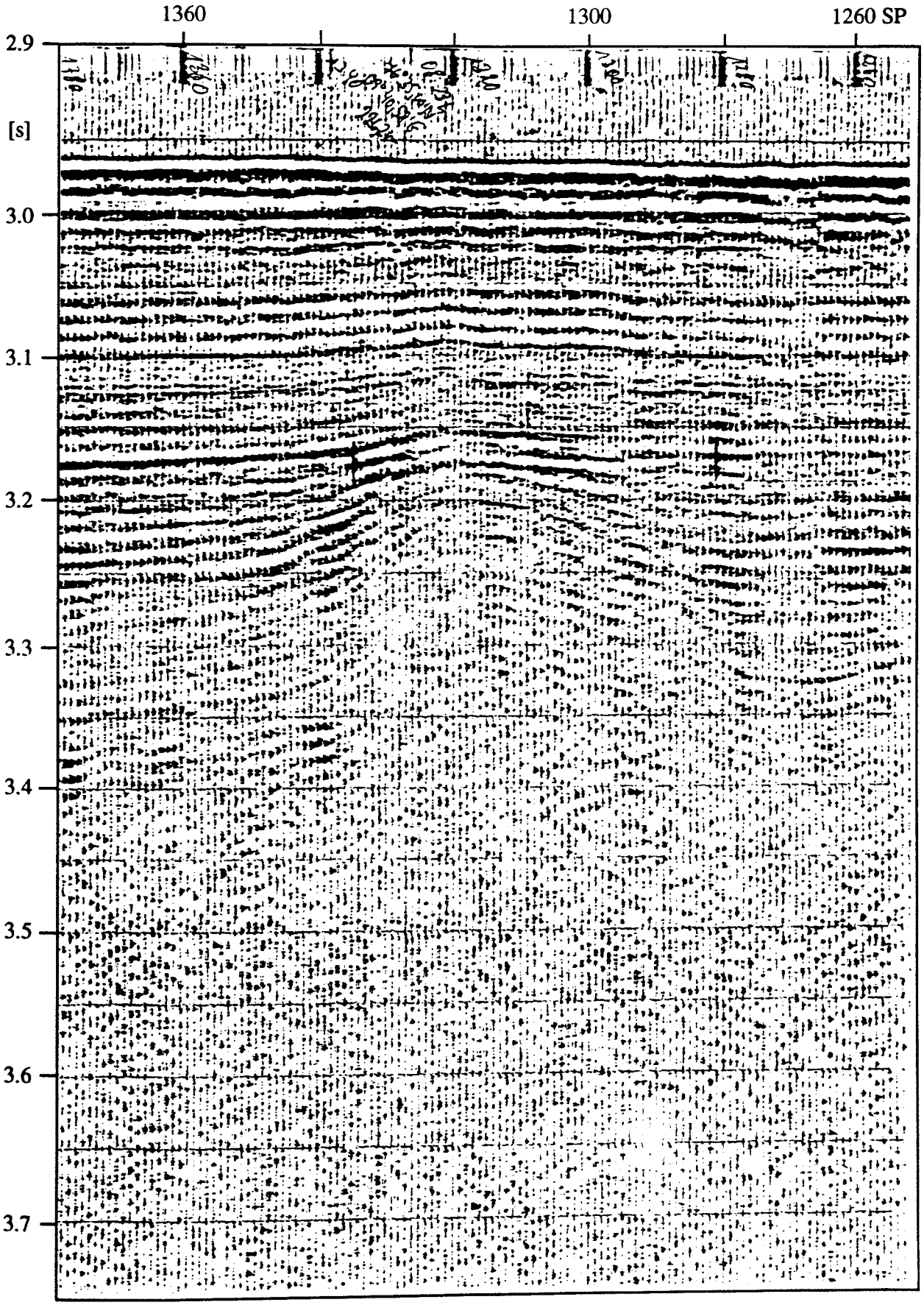

Figure 11a: Airgun record from the Spitsbergen continental margin showing an acoustic "wipe out" zone. For location see Figure 4.

Рисунок 11а: Профиль излучателей от окраины материка Шпицбергена указывающий на акустические "wipe out" зоны (см. рис. 4).

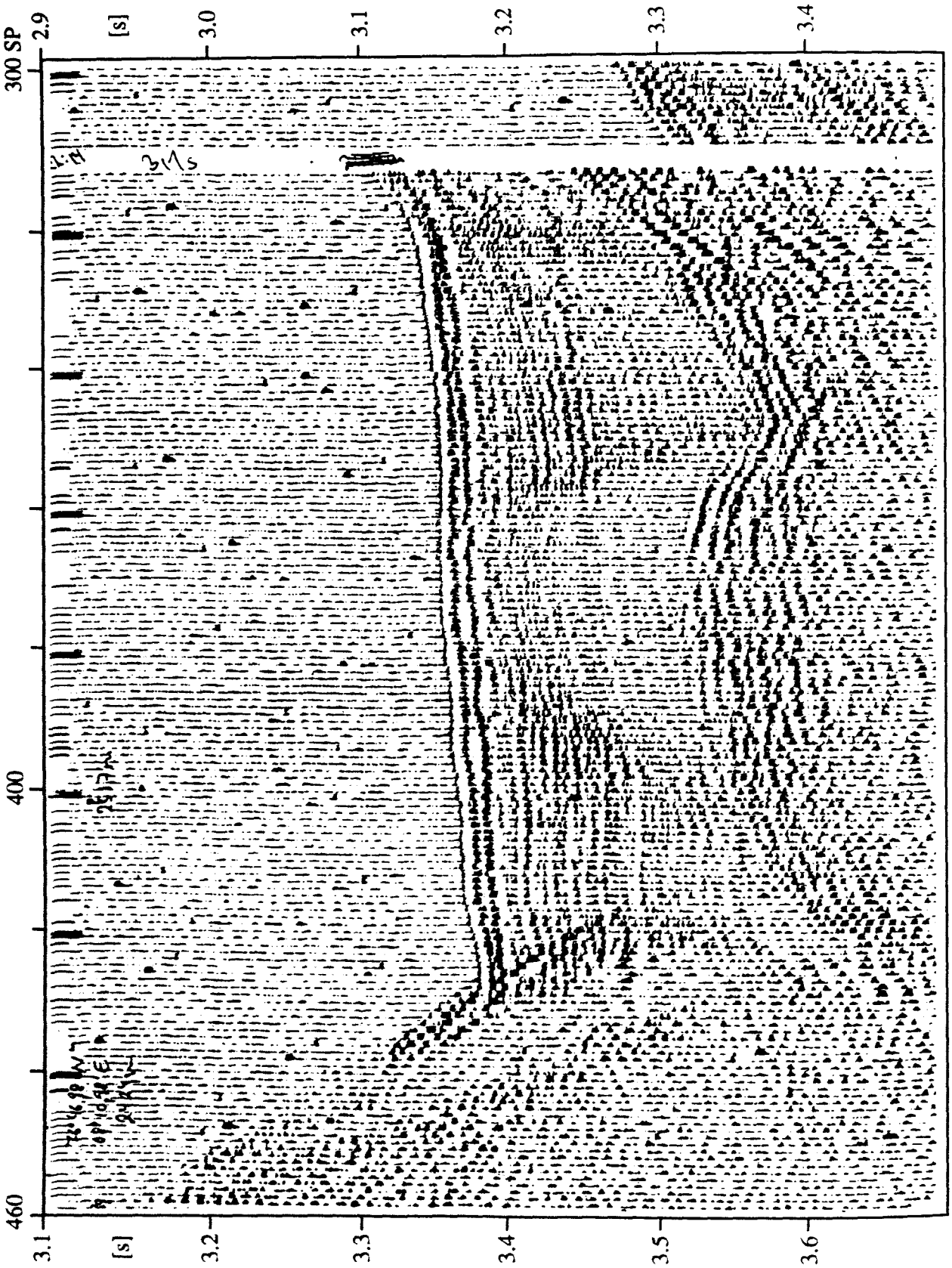

Figure 11b: Airgun record from a basin of the eastern flank of the Knipovich Ridge showing an acoustic "wipe out"zone. For location see Figure 4.

Рисунок 11б: Профиль излучателей от одного бассейна восточного фланга хребета Книповича указывающий на акустические "wipe out" зоны (см. рис.4).

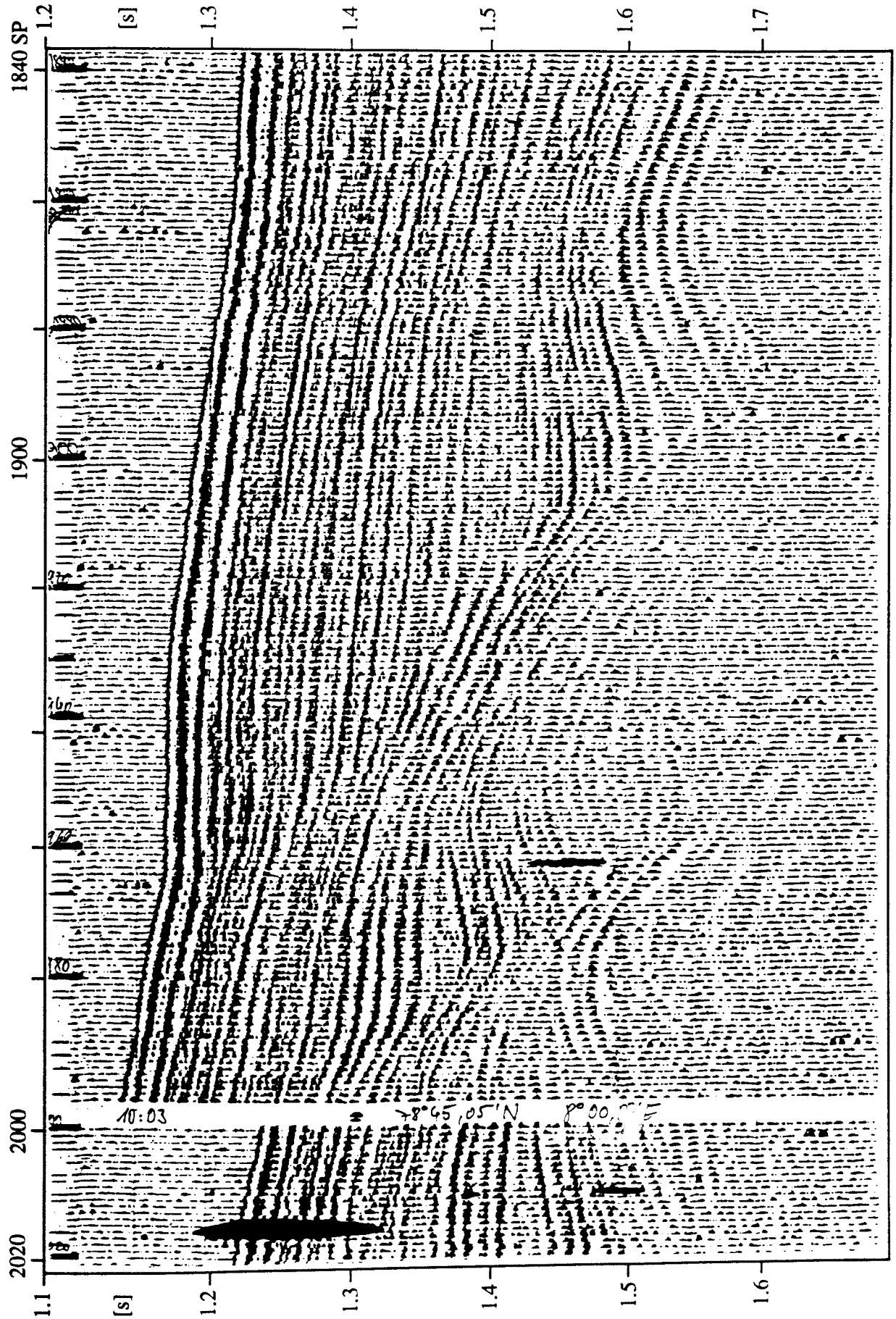

Figure 12: Airgun record from the Spitsbergen margin showing large sediment waves. For location see Figure 4.

Рисунок 12: Профиль излучателей от окраины материка Шпицбергена указывающий на большие осадочные волны (см. рис. 4).

Working area 1: Seismic profiling (2 ltr airgun) in the Norwegian trench

Test of airgun-system: 7.7.94 - 8.7.94

Seismic profiling: 8.7.94 - 9.7.94

Start of Profile		End of Profile		distance	ship speed	time	Profile Nr.
Latitude	Longitude	Latitude	Longitude	sm/km	kn	h	
62°22,12'N	3°00,83'E	63°02,94'N	2°36,88'E	42/78	4,5	9,4	1 (!)
62°45,16'N	2°00,97'E	62°57,04'N	3°09,14'E	33/61	4,5	7,4	2
62°59,19'N	2°39,38'E	63°07,73'N	2°34,28'E	9/16	4,5	2,0	1a
63°07,73'N	2°37,08'E	63°21,56'N	2°29,91'E	14/26	4,5	3,1	3
63°21,56'N	2°29,91'E	64° 53,31'N	5°55,77'E	128/237	11,5	11,2	Transit

working area 2: OBS- deployment an seismic profiling at the northern rim of Storrega slide. Water depth ranges from 400-1500m.

OBS-deployment and seismic profiling (2 ltr airgun): 11.7.94 - 12.7.94

Start of Profile		End of Profile		distance	ship speed	time	Profile Nr.
Latitude	Longitude	Latitude	Longitude	sm/km	kn	h	
64° 53,31'N	5°55,77'E	64°46,78'N	5°16,00'E	18/34	4,5	4,0	4
64°47,41'N	5°28,05'E					5,0	OBS-Test
64°42,41'N	4°48,40'E	64°59,10'N	3°29,89'E	37/69	4,5	8,3	5 (!)
64°46,09'N	4°30,28'E	1 OBS deployment					OBS 1 (II)
64°46,29'N	4°29,71'E	2 OBS deployment					OBS 2 (I)
64°47,60'N	4°23,92'E	64°44,39'N	4°38,75'E	7/13	2,5	2,8	6
64°44,39'N	4°38,75'E	76°47,0'N	8°00,0'E	725/1342	11,5	63	Transit

Airgun profile 6 runs at a speed of 2,5 knts within a 2,5 hrs time window across the two OBS stations.
Meeting with RV Prof. Logachov at Storegga (64°48,61'N, 04°15,0'E) on 12 July at 12:00. Visit of Dr. Ivanow on board Prof. Logachev and discussion of science plan.

Table 1: List of working areas with profiles and OBS station

working area 3: OBS- deployment and seismic profiling west of Spitzbergen. Water depth ranges from 1000m to 3000m.

Seismic profiling: 15.7.94

OBS-deployment and seismic profiling: 16.7.94 - 23.7.94

Start of Profile		End of Profile		distance	ship speed	time	Profile Nr.
Latitude	Longitude	Latitude	Longitude	sm/km	kn	h	
76°46,97'N	07°37,52'E	76°47,01'N	11°31,94'E	53/99	4,5	11,9(7)	7
77°00,04'N	11°36,76'E	77°00,02'N	11°16,77'E	5/8	4,5	1	8
77°00,09'N	11°36,66'E	76°59,99'N	07°59,98'E	49/90	4,5	11	8a
76°59,52'N	07°59,59'E	76°34,82'N	08°00,15'E	25/46	4,5	5,5	9
76°34,75'N	08°04,03'E	76°35,02'N	11°29,98'E	48/88	4,5	10,6	10
76°35,00'N	11°29,98'E	76°37,97'N	09°01,69'E	35/64	6	5,7	Transit
76°37,97'N	09°01,69'E	76°38,01'N	08°49,40'E	3/5	4,5	0,6	11
76°38,34'N	08°50,07'E	76°31,81'N	08°50,08'E	7/12	4,5	1,5	12
76°32,13'N	08°49,80'E	76°32,01'N	09°01,26'E	3/5	4,5	0,6	13
76°31,61'N	09°00,02'E	76°38,06'N	08°59,99'E	7/12	4,5	1,5	14
76°40,46'N	08°55,23'E	76°31,69'N	08°55,24'E	9/16	4,5	2,0	15
76°34,50'N	08°53,91'E			3 OBS deployment			OBS 1
76°34,52'N	08°56,01'E			4 OBS deployment			OBS 2
76°34,64'N	08°38,33'E	76°34,51'N	09°10,85'E	8/14	OBS profile	1,6	16
				OBS 1 (07:10) and OBS 2 (08:23) on board			
76°34,51'N	09°10,85'E	78°44,96'N	05°25,81'E	139/257	11,5	12	Transit
78°44,96'N	05°25,81'E	78°45,00'N	08°28,04'E	36/66	4,5	7,9	17
78°40,09'N	08°13,15'E	78°39,97'N	05°28,00'E	33/60	4,5	7,,2	18
78°34,92'N	05°27,60'E	78°35,00'N	08°01,34'E	30/56	4,5	6,8	19
78°35,00'N	08°01,34'E	78° 40,00'N	06°49,18'E	15/28	11,5	1,3	Transit
78° 40,00'N	06°49,18'E			5 OBS deployment			OBS 1
78° 40,00'N	06°51,69'E			6 OBS deployment			OBS 2

Table 1: List of working areas with profiles and OBS station

78°39,95'N	6°38,51'E	78°40,00'N	7°20,25'E	8/15	OBS profile	1,8	20
78°45,00'N	07°59,00'E	79°27,68'N	06°23,28'E	46/86	4,5	10,3	21
79°28,50'N	06°29,04'E	79°28,44'N	08°14,06'E	19/36	4,5	4,3	22
79°27,19'N	08°17,50'E	79°24,95'N	08°20,59'E	2/4	4,5	0,5	23
79°23,71'N	08°23,80'E	78°57,42'N	09°09,05'E	28/52	4,5	6,1	23a
78°56,98'N	09°05,88'E	78°56,96'N	06°38,53'E	28/51	4,5	6,3	24
78°45,00'N	07°40,00'E			OBS test with deep-frozen fish			
78°45,00'N	07°37,00'E			7 OBS deployment			OBS 1
78°45,00'N	07°37,39'E			8 OBS deployment			OBS 2
78°45,00'N	07°20,00'E	78°45,00'N	07°55,00'E	7/13	OBS profile	1,5	25
				OBS 1 ( ) and OBS 2 ( ) on board.			
78°45'N	8°00'E	70°00'N	20°00'E	557/1030		58	Transit

Total legth of seismic profiles (km) : 1131

Total number of successful OBS deployments : 8

Equipment loss : -

End of programme

Departure on 22 July 1994.

Arrival in TROMSØ 25.7.94

Table 1: List of working areas with profiles and OBS station

Station/ Profile No.	Date	Time UTC (h)	Geographical Position Latitude Longitude	Depth uncorr. (m)	Comments Start/End, Tape No. etc.
1	08.07.94	22:32	62°22,12'N 03°00,83'E	391	Start of profile1, tape 1, delay 0,4s
		23:17	62°26,10'N 02°58,67'E	384	Tape 2, SP 270
	09.07.94	00:02	62°30,00'N 02°56,30'E	390	Tape 3, SP 541
		00:46	62°33,96'N 02°54,20'E	416	Tape 4, SP 808
		01:32	62°38,17'N 02°51,55'E	483	Tape 5, delay 0,5s, SP 1080
		02:16	62°42,56'N 02°48,87'E	585	Tape 6, delay 0,6s, SP 1349
		03:02	62°45,75'N 02°47,12'E	640	Tape 7, delay 0,7s, SP 1619
		03:46	62°50,43'N 02°44,48'E	714	Tape 8, delay 0,9s, SP 1885
		04:32	62°54,38'N 02°42,19'E	759	Tape 9, SP 2158
		05:12	62°57,79'N 02°39,34'E	840	Tape 10, SP 2401
		05:16	62°58,23'N 02°39,59'E	835	Delay 1,0s, Sp 2427
		06:02	63°02,94'N 02°36,88'E	900	End of profile 1 (airgun breakdown)
					Restart with SP 2400 on tape 20
					as profile 1a
		11:30	62°44,46'N 02°58,98'E		Start of test
2	09.07.94	12:38	62°45,16'N 02°00,97'E	742	Start of profile 2, tape 11, delay 0,8s
		13:21	62°46,60'N 02°09,10'E	750	Tape 12, SP 262
		14:07	62°47,96'N 02°17,14'E	741	Change of amplification, SP 520
		14:08	62°48,10'N 02°17,77'E	750	Tape 13, SP 535
		14:31	62°48,84'N 02°22,13'E	744	Tape 14, SP 797
		15:07	62°50,02'N 02°29,12'E	746	Problems with the airgun, no shots, SP 897
		15:16	62°50,30'N 02°30,79'E	747	Airgun fixed, restart, SP 940
		15:25	62°50,59'N 02°32,43'E	747	Breakdown of airgun, end of tape 14, 2h loss, SP 1000
2a	09.07.94	17:30	62°49,55'N 02°26,24'E	748	Start of profile 2a, tape 15, delay 0,8s
		18:14	62°51,13'N 02°35,18'E	752	Tape 16, SP 266
		18:59	62°52,58'N 02°43,61'E	744	Tape 17, SP 534, crossing point of profiles 1 and 2
		19:43	62°54,14'N 02°52,22'E	748	Tape 18, SP 799
		20:29	62°55,65'N 03°01,42'E	735	Tape 19, SP 1072
		21:07	62°57,08'N 03°09,14'E	763	End of profile 2a, end of tape 19, SP 1300
	10.7.94	00:08	63°01,89 N 02°37,50'E		Test of airguns, breakdown
1a	10.07.94	03:24	62°59,19'N 02°39,38'E	848	Start of profile 1a, tape 20, delay 1,0s
		04:10	63°03,34'N 02°36,49'E	919	Tape 21, delay 1,1s, SP 274
		04:55	63°07,73'N 02°34,28'E	979	End of profile 1a, end of tape 21, SP 540
3	10.07.94	04:55	63°07,73'N 02°37,08'E	978	Start of profile 3, tape 22, SP 543
		05:08	63°08,88'N 02°33,78'E	997	Delay 1,2s, SP 621

Table 2: List of airgun profiles including magnetic tapes and shot points

Station/ Profile No.	Date	Time UTC (h)	Geographical Position Latitude Longitude	Depth uncorr. (m)	Comments Start/End, Tape No. etc.
		05:39	63°11,85'N 02°34,89'E	1033	Tape 23, SP 812
		06:25	63°16,07'N 02°31,43'E	1100	Tape 24, delay 1,3s, SP 1086
		07:04	63°19,64'N 02°30,51'E	1141	Change of airgun: 3ltr. volume
		07:10	63°20,13'N 02°30,38'E	1152	End of tape 24, SP 1356
		07:13	63°20,37'N 02°30,31'E	1157	Tape 25, SP 1375
		07:30	63°21,56'N 02°29,91'E		End of profile 3, from SP 1266 on no clear signal
4	11.07.94	06:25	64°53,31'N 05°55,77'E	363	Start of profile 4, tape 26, delay 0,4s
		06:34	64°52,98'N 05°53,72'E	368	Change of amplification from 5/0 to 5/1, SP 60
		06:48	64°52,51'N 05°51,15'E	395	SP 140, amplification back to 5/0
		07:10	64°51,77'N 05°46,63'E	431	Tape 27, SP 276
		07:56	64°50,31'N 05°37,26'E	551	Tape 28, delay 0,6s, SP 548
		08:40	64°48,77'N 05°27,85'E	626	Tape 29, delay 0,7s, SP 816
		09:17	64°47,51'N 05°20,44'E	672	SP 1035, failure of data (analogue+digital) transmission (airgun breakdown)
		09:26	64°47,18'N 05°18,61'E	677	Tape 30, SP 1090
		09:40	64°46,78'N 05°16,00'E	684	End of profile 4, SP 1171, tape 30 cancelled because of bad transmission
	11.07.94	13:12	64°47,41'N 05°28,05'E	600	Test OBH 1 and OBH 2
5	11.07.94	23:11	64°42,41N 04°48,40'E	857	Start of profile 5, tape 30, delay 1s
		23:56	64°44,27'N 04°39,09'E	857	Tape 31, SP 274
	12.7.94	00:41	64°46,04'N 04°30,99'E	872	Tape 32, SP 544
		01:27	64°48,00'N 04°21,94'E	924	Tape 33, delay 1,1s, SP 816
		02:11	64°49,90'N 04°13,15'E	983	Tape 34, delay 1,2s, SP 1082
		02:23	64°50,47'N 04°10,63'E	993	Middle of profile, SP 1159
		02:56	64°51,96'N 04°03,66'E	1025	Tape 35, delay 1,3s, SP 1355
		03:42	64°53,60'N 03°55,39'E	1122	Tape 36, delay 1,4s, SP 1628
		04:27	64°55,48'N 03°46,83'E	1199	Tape 37, delay 1,5s, SP 1900
		04:36	64°55,78'N 03°45,41'E	1310	SP 1948, streamer comes up to 7m depth due to heavy sea
		05:13	64°57,37'N 03°38,76'E		Tape 38, delay 1,6s, SP 2172
		05:29	64°58,04'N 03°35,06'E	1366	SP 2313, bad transmission
		05:57	64°59,13'N 03°29,89'E	1421	End of Profile 5, end of tape 38, SP 2436
	12.07.94	17:19	64°46,093'N 04°30,281'E		OBH 1 (II) deployment
		18:02	64°46,286'N 04°29,714'E		OBH 2 (I) deployment
6	12.07.94	20:30	64°47,60'N 04°23,92'E	905	Start of profile 6
		21:10	64°46,32'N 04°29,79'E	905	Crossing OBH 2, SP 240
		21:14	64°46,21'N 04°30,41'E	905	Crossing OBH 1, SP 265
		22:15	64°44,39'N 04°38,75'E	905	End of profile 6, SP 630

Table 2: List of airgun profiles including magnetic tapes and shot points

Station/ Profile No.	Date	Time UTC (h)	Geographical Position Latitude Longitude	Depth uncorr. (m)	Comments Start/End, Tape No. etc.
	13.07.94	00:25			OBH 2 acoustically released
		00:52			OBH 2 on board
		01:10			OBH 1 acoustically released
		01:38			OBH 1 on board
7	15.07.94	21:23	76°46,97'N 07°37,52'E	2900	Start of profile 7, tape 39, delay 3,5s
		21:33	76°46,98'N 07°42,63'E	2672	Delay 3,3s, SP 64
		21:39	76°46,99'N 07°44,86'E	2530	Delay 3,1s, SP 95
		21:47	76°46,99'N 07°47,95'E	2398	Delay 2,9s, SP 145
		21:51	76°47,03'N 07°50,40'E	2198	Delay 2,7s, SP 171
		21:55	76°47,03'N 07°52,21'E	2118	Delay 2,5s, SP 194
		22:01	76°47,03'N 07°55,02'E	2294	Delay 2,7s, SP 231
		22:06	76°47,05'N 07°56,95'E	2409	Delay 2,9s, SP 258
		22:08	76°47,03'N 07°58,24'E	2465	Tape 40, SP 276
		22:14	76°47,04'N 08°00,87'E	2549	Delay 3,1s, SP 311
		22:39	76°46,98'N 08°10,98'E	2424	Delay 2,9s, SP 459
		22:42	76°46,94'N 08°13,05'E	2212	Delay 2,7s, SP 477
		22:53	76°46,97'N 08°17,68'E	2163	Tape 41, SP 537
		23:10	76°46,96'N 08°25,29'E	2201	SP 636
		23:36	76°46,97'N 08°37,68'E	2247	Tape 42, SP 803
		23:53	76° 46,98'N 08°44,05'E	2245	Delay 2,8s, SP 901
		23:58	76°46,96'N 08°46,18'E	2046	Delay 2,6s, SP 932
	16.07.94	00:00	76°46,96'N 08°47,00'E	1841	Delay 2,4s, SP 941
		00:03	76°46,92'N 08°48,43'E	1852	Delay 2,2s, SP 961
		00:10	76°46,93'N 08°52,52'E	2244	Delay 2,4s, SP 1006
		00:13	76°46,92'N 08°52,90'E	2252	Delay 2,6s, SP 1022
		00:22			Tape 43, delay 2,5s, SP 1073
		00:22	76°46,92'N 08°57,97'E	2260	Delay 2,7s, SP 1076
		00:44	76°46,97'N 09°07,03'E	2266	Delay 2,8s, SP 1211
		01:06	76°46,97'N 09°17,03'E	2277	Tape 44, SP 1341
		01:52	76°46,99'N 09°38,59'E	2258	Tape 45, SP 1615
		02:04	76°46,99'N 09°44,47'E	2266	SP 1688
		02:36	76°47,01'N 09°59,85'E	2248	Tape 46, SP 1879
		02:57	76°46,98'N 10°10,28'E	2232	SP 2005
		03:21	76°46,97'N 10°22,04'E	2156	Tape 47, delay 2,7s, SP 2151
		03:36	76°46,98'N 10°33,46'E	2070	Delay 2,5s, SP 2240
		04:05	76°47,04'N 10°43,60'E	1945	Tape 48, delay 2,3s, SP 2418
		04:35	76°47,03'N 10°58,86'E	1792	Delay 2,1s, SP 2598
		04:50	76°47,02'N 11°05,96'E	1740	Tape 48 until SP ~2683, begin of tape 49 not clear, definitely from SP 2700
		05:16	76°46,99'N 11°19,12'E	1655	Delay 2,0s, SP 2841
		05:36	76°47,00'N 11°29,06'E	1573	Tape 50, data due to SP 2962
		05:38	76°46,99'N 11°29,96'E	1570	Delay 1,9s, SP 2973
		05:43	76°47,01'N 11°31,94'E	1554	End of profile 7, SP 2998

Table 2: List of airgun profiles including magnetic tapes and shot points

Station/ Profile No.	Date	Time UTC (h)	Geographical Position Latitude Longitude	Depth uncorr. (m)	Comments Start/End, Tape No. etc.
8	16.07.94	08:22	77°00,04'N 11°36,76'E	1004	Start of profile 8, tape 51, delay 1,1s
		08:43	77°00,15'N 11°28,23'E	1092	Delay 1,3s, SP 121
		08:46	77°00,15'N 11°27,22'E	1100	SP 135, depth of streamer only 8-9m, bad transmission
		09:01	77°00,00'N 11°21,22'E	1169	SP 228, reduced ship speed to 3,5kn, recording is good
		09:09	77°00,01'N 11°18,97'E	1187	Tape 52, SP 273
		09:16	77°00,02'N 11°16,77'E	1218	SP 316, break of recording, depth of streamer not sufficient Restart at SP 200 with tape 52
8a	16.07.94	11:53	77°00,09'N 11°36,66'E	1007	Start of profile 8a, tape 52, delay 1,2s
		12:19	77°00,04'N 11°27,21'E	1101	Delay 1,3s, SP 160
		12:38	77°00,01'N 11°20,95'E	1168	Tape 53, delay 1,4s, SP 270
		13:00	76°59,98'N 11°13,38'E	1243	Delay 1,5s, SP 400
		13:22	76°59,99'N 11°05,79'E	1320	Tape 54, delay 1,6s, SP 537
		13:47	77°00,00'N 10°57,64'E	1410	Delay 1,7s, SP 685
		14:06	77°00,00'N 10°51,96'E	1460	Tape 55, SP 802
		14:10	77°00,01'N 10°50,76'E	1475	Delay 1,8s, SP 827
		14:36	76°59,91'N 10°43,00'E	1566	Delay, 1,9s, SP 981
		14:51	76°59,98'N 10°38,85'E	1612	Tape 56, delay 2,0s, SP 1069
		15:13	76°59,95'N 10°32,28'E	1684	Delay 2,1s, SP 1202
		15:36	76°59,92'N 10°25,53'E	1755	Tape 57, delay 2,2s, SP 1343
		16:03	76°59,99'N 10°17,70'E	1842	Delay 2,3s, SP 1510
		16:21	77°00,04'N 10°13,12'E	1879	Tape 58, delay 2,4s, SP 1613
		17:06	76°59,97'N 10°00,62'E	2015	Tape 59, delay 2,5s, SP 1882
		17:29	76°59,93'N 09°54,09'E	2065	Delay 2,6s, SP 2021
		17:51	76°59,97'N 09°47,86'E	2095	Tape 60, SP 2151, ship speed 3-4kn
		18:09	77°00,03'N 09°43,36'E	2123	SP 2254, amplification increased
		18:36	76°59,95'N 09°35,25'E	2160	Tape 61, SP 2419
		18:49	76°59,99'N 09°31,57'E	2183	Delay 2,7s, SP 2500
		19:21	77°00,01'N 09°22,14'E	2208	Tape 62, SP 2691
		20:06	76°59,98'N 09°08,92'E	2219	Tape 63, SP 2960
		20:30	76°59,99'N 09°01,71'E	2213	SP 3100
		20:51	76°59,92'N 08°55,22'E	2216	Tape 64, SP 3232
		21: 36	77°00,06'N 08°40,65'E	2202	Tape 65, SP 3502
		22:02	76°59,96'N 08°32,62'E	2138	Delay 2,8s, SP 3655
		22:03	76°59,98'N 08°32,59'E	2123	Delay 2,6s, SP 3661
		22:18	76°59,96'N 08°27,60'E	2068	Delay 2,5s, SP 3751
		22:22	76°59,98'N 08°26,71'E	2101	Tape 66, SP 3774
		23:07	76°59,97'N 08°12,23'E	2563	Delay 2,7s, SP 4046
		23:08	76°59,96'N 08°11,80'E	2607	Tape 67, delay 2,7s, SP 4053
		23:13	76°59,95'N 08°10,43'E	2627	Delay 3,0s, SP 4048
		23:15	76°59,96'N 08°09,65'E	2630	Delay 3,3s, SP 4095
		23:46	77°00,00'N 07°59,47'E	2604	End of profile 8a, SP 4275

Table 2: List of airgun profiles including magnetic tapes and shot points

Station/ Profile No.	Date	Time UTC (h)	Geographical Position Latitude Longitude	Depth uncorr. (m)	Comments Start/End, Tape No. etc.
9	16.07.94	23:53	76°59,52'N 07°59,59'E	2592	Start of profile9, tape 68, delay 3,2
	17.07.94	00:23	76°57,44'N 08°00,01'E	2596	SP 170
		00:40	76°55,58'N 07°59,88'E	2600	Tape 69, SP 271
		01:15	76°52,68'N 07°59,59'E	2518	Delay 3,1s, SP 480
		01:25	76°51,30'N 07°59,85'E	2502	Tape 70, SP 544
		02:10	76°47,90'N 08°00,07'E	2519	Tape 71, SP 812
		02:38	76°45,54'N 08°00,13'E	2417	Delay 3,0s, SP 984
		02:55	76°44,16'N 08°00,02'E	2406	Tape 72, Delay 2,9s, SP 1081
		03:13	76°42,46'N 08°00,05'E	2291	Delay 2,8s, SP 1191
		03:17	76°42,18'N 07°59,99'E	2198	Delay 2,7s, SP 1213
		03:20	76°41,87'N 08°00,01'E	2054	Delay 2,5s, SP 1232
		03:25	76°41,48'N 07°59,95'E	1934	Delay 2,3s, SP 1262
		03:29	76°41,11'N 07°59,87'E	1825	Delay 2,1s, SP 1285
		03:39	76°40,08'N 07°59,76'E	1771	Tape 73, SP 1350
		03:51	76°38,79'N 07°59,81'E	1837	Delay 2,3s, SP 1421
		04:04	76°37,67'N 08°00,26'E	1971	Delay 2,5s, SP 1497
		04:23	76°35,94'N 08°00,36'E	1941	Delay 2,3s, SP 1613
		04:24	76°35,51'N 08°00,22'E	1831	Tape 74, SP 1620
		04:26	76°35,56'N 08°00,26'E	1784	Delay 2,1s, SP 1625
		04:28			Delay 1,9s, SP 1644
		04:31	76°34,82'N 08°00,15'E	1473	End of profile 9, SP 1660
10	17.07.94	04:42	76°34,77'N 08°04,30'E	1417	Start of profile 10, tape 75, delay 1,7s
		04:43	76°34,79'N 08°04,97'E	1308	Delay 1,5s, SP 11
		04:50	76°34,90'N 08°08,04'E	1477	Delay 1,7s, SP 49
		04:58	76°35,01'N 08°11,75'E	1622	Delay 1,9s, SP 101
		05:04	76°35,02'N 08°14,40'E	1733	Delay 2,1s, SP 134
		05:10	76°35,04'N 08°16,92'E	1879	Delay 2,3s, SP 172
		05:17	76°35,07'N 08°19,56'E	1925	Delay 2,5s, SP 210
		05:18	76°35,10'N 08°20,15'E	1889	Delay 2,3s, SP 219
		05:26	76°35,13'N 08°23,83'E	2108	Tape 76, delay 2,5s, SP 265
		05:32	76°35,09'N 08°26,37'E	2214	Delay 2,7s, SP 304
		05:40	76°35,08'N 08°29,69'E	2278	Delay 2,9s, SP 351
		06:08	76°34,94'N 08°42,08'E	2274	Amplification increased
		06:11	76°34,93'N 08°42,24'E	2275	Tape 77, SP 534
		06:35	76°34,93'N 08°53,65'E	2270	SP 679
		06:55	76°34,94'N 09°02,51'E	2274	Tape 78, SP 804
		07:25	76°35,00'N 09°14,89'E	2270	SP 979
		07:40	76°35,00'N 09°21,54'E	2268	Tape 79, SP 1069
		07:55	76°34,97'N 09°28,49'E	2272	SP 1158
		08:23	76°35,00'N 09°40,58'E	2262	Tape 80, SP 1326
		08:52	76°35,00'N 09°53,21'E	2256	SP 1500
		09:07	76°35,01'N 10°00,11'E	2244	Tape 81, delay 2,8s, SP 1593
		09:42	76°34,99'N 10°15,40'E	2221	SP 1800
		09:52	76°34,99'N 10°19,90'E	2209	Tape 82, SP 1864
		10:15	76°34,99'N 10°30,18'E	2181	Delay 2,7s, SP 2000

Table 2: List of airgun profiles including magnetic tapes and shot points

Station/ Profile No.	Date	Time UTC (h)	Geographical Position Latitude Longitude	Depth uncorr. (m)	Comments Start/End, Tape No. etc.
		10:37	76°34,99'N 10°39,40'E	2156	Tape 83, SP 2130
		11:02	76°34,99'N 10°50,38'E	2120	Delay 2,6s, SP 2281
		11:21	76°35,00'N 10°59,90'E	2098	Tape 84
		11:51	76°35,05'N 11°10,65'E	2068	SP 2580
		12:06	76°34,98'N 11°16,35'E	2048	Tape 85, delay 2,5, SP 2664
		12:36	76°35,01'N 11°27,60'E	1994	SP 2842
		12:42	76°35,02'N 11°29,98'E	1986	End of profile 10, SP 2879
11	17.07.94	17:53	76°37,97'N 09°02,57'E	2271	Start of profile 11, tape 86, delay 2,8s
		18:22	76°38,01'N 08°49,40'E	2273	End of profile 11, SP 180
12	17.07.94	18:50	76°38,34'N 08°50,07'E	2270	Start of profile 12, tape 87, delay 2,8s
		19:16	76°35,83'N 08°49,97'E		SP 157
		19:34	76°34,09'N 08°50,26'E	2272	Tape 88, SP 269
		19:56	76°31,92'N 08°50,07 E	2267	SP 403
		19:57	76°31,81'N 08°50,08'E	2267	End of profile 12, SP 410
13	17.07.94	20:27	76°32,13'N 08°49,80'E	2267	Start of profile 13, tape 89, delay 2,8 s
		20:52	76°32,01'N 09°01,26'E	2263	End of profile 13, SP 150
14	17.07.94	21:23	76°31,62'N 09°00,02'E	2271	Start of profile 14, tape 90, delay 2,8s
		22:25	76°38,06'N 08°59,99'E	2271	End of profile 14, SP 370
15	17.07.94	23:04	76°40,46'N 08°55,23'E	2267	Start of profile 15, tape 92, delay 2,8s
		23:48	76°36,32'N 08°55,07'E	2272	Tape 93, SP 266
	18.07.94	00:33	76°32,53'N 08°55,10'E	2264	Tape 94, SP 543
		00:44	76°31,69'N 08°55,24'E	2264	End of profile15, SP 600
	17.07.94	02:32	76°34,50'N 08°53,91'E	2271	OBH 3 (I) deployment
		03:08	76°34,52'N 08°56,01'E	2269	OBH 4 (II) deployment
16	18.07.94	04:07	76°34,64'N 08°38,33'E	2272	Start of profile 16
		04:44	76°34,50'N 08°54,00'E	2269	Crossing OBH 3
		04:49	76°34,50'N 08°56,00'E	2269	Crossing OBH 4
		05:22	76°34,51'N 09°10,85'E	2277	End of profile 16
		06:19			OBH 1 acoustical released
		07:10			OBH 1 on board
		07:35			OBH 2 acoustical released
		08:23			OBH 2 on board
17	19.07.94	04:30	78°44,96'N 05°25,81'E	2459	Start of profile 17, tape 95, delay 3,0s
		04:45	78°45,01'N 05°32,52'E	2343	Delay 2,8s, SP 92
		04:59	78°45,01'N 05°38,70'E	2191	Delay 2,6s, SP 171
		05:15	78°44,96'N 05°45,66'E	2177	Tape 96, SP 271
		05:26	78°44,96'N 05°50,82'E	2247	Delay 2,7s, SP 339
		05:42	78°44,96'N 05°58,00'E	2274	Delay 2,8s, SP 433

Table 2: List of airgun profiles including magnetic tapes and shot points

Station/ Profile No.	Date	Time UTC (h)	Geographical Position Latitude Longitude	Depth uncorr. (m)	Comments Start/End, Tape No. etc.
		06:00	78°45,00'N 06°06,18'E	2259	Tape 97, SP 542
		06:17	78°45,00'N 06°13,87'E	2170	Delay 2,6s, SP 641
		06:33	78°45,02'N 06°21,80'E	1999	Delay 2,4s, SP 741
		06:45	78°45,04'N 06°27,63'E	1882	Tape 98, delay 2,2s, SP 813
		07:03	78°44,99'N 06°36,76'E	1735	Delay 2,0s, SP 921
		07:24	78°44,92'N 06°46,74'E	1557	Delay 1,8s, SP 1042
		07:30	78°44,94'N 06°50,27'E	1510	Tape 99, SP 1082
		07:52	78°44,94'N 07°00,75'E	1406	Delay 1,6s, SP 1216
		08:16	78°44,96'N 07°11,96'E	1283	Tape 100, SP 1356
		08:20	78°44,97'N 07°13,68'E	1262	Delay 1,4s, SP 1381
		08:57	78°44,99'N 07°30,64'E	1130	Delay 1,2s, SP1601
		09:01	78°44,96'N 07°32,38'E	1132	Tape 101, SP 1625
		09:43	78°45,01'N 07°51,60'E	1021	Tape 102, SP 1882
		10:03	78°45,05'N 08°00,87'E	974	Delay 1,1s, SP 2000
		10:20	78°45,02'N 08°09,04'E	911	Delay 1,0s, SP 2100
		10:28	78°45,06'N 08°12,95'E	882	Tape 103, SP 2150
		10:38	78°45,04'N 08°17,97'E	831	Delay 0,9s, SP 2210
		10:53	78°45,00'N 08°25,08'E	738	Delay 0,8s, SP 2300
		11:01	78°45,00'N 08°28,04'E	698	End of profile 17, SP 2340
18	19.07.94	12:38	78°40,09'N 08°13,15'E	907	Start of profile 18, tape 104, delay 1,0s
		12:34	78°39,99'N 08°08,10'E	954	Delay 1,1s, SP60
		12:48	78°40,00'N 08°00,93'E	1001	Delay 1,2s, SP 151
		13:05	78°40,04'N 07°52,00'E	1048	SP 260 airgun break down
		13:08	78°40,04'N 07°51,11'E	1056	Tape 105, delay 1,3s, SP270
		13:10	78°40,02'N 07°49,30'E	1056	SP 280 airgun restart
		13:44	78°39,97'N 07°33,20'E	1167	Delay 1,4s, SP 485
		13:52	78°40,02'N 07°28,45'E	1193	Tape 106, SP 538
		14:07	78°39,83'N 07°20,18'E	1284	Delay 1,5s, SP 624
		14:21	78°39,86'N 07°12,00'E	1342	Delay 1,6s, SP 712
		14:37	78°39,46'N 07°03,00'E	1407	Tape 107, delay 1,7s, SP 808
		14:55	78°40,00'N 06°52,90'E	1490	Delay 1,8s, SP 911
		15:09	78°40,03'N 06°45,56'E	1584	Delay 1,9s, SP 995
		15:15	78°40,04'N 06°42,60'E	1598	SP 1032 airgun breakdown
		15:19	78°40,01'N 06°40,24'E	1620	SP 1055 airgun restart
		15:22	78°39,98'N 06°38,44'E	1627	Tape 108, delay 2,0s, SP 1074
		15:36	78°40,04'N 06°30,10'E	1724	Delay 2,1s, SP1161
		15:47	78°40,00'N 06°24,54'E	1827	Delay2,2s, SP 1228
		15:53	78°40,00'N 06°21,00'E	1910	Delay 2,4s, SP 1264
		16:07	78°39,95'N 06°13,60'E	2110	Tape 109, delay 2,7s, SP1343
		16:19	78°39,96'N 06°07,39'E	2305	Delay 2,9s, SP 1420
		16:36	78°39,94'N 05°58,61'E	2413	Delay 3,1s, SP 1520
		16:40	78°39,95'N 05°56,56'E	2359	Delay 3,0s, SP1544
		16:46	78°39,95'N 05°53,47'E	2359	Delay 2,9s, SP 1576
		16:50	78°39,94'N 05°50,34'E	2346	Tape 110, SP 1607
		17:33	78°39,97'N 05°28,00'E	2308	End of profile 18, SP 1860

Table 2: List of airgun profiles including magnetic tapes and shot points

Station/ Profile No.	Date	Time UTC (h)	Geographical Position Latitude Longitude	Depth uncorr. (m)	Comments Start/End, Tape No. etc.
19	19.07.94	18:46	78°34,92'N 05°27,60'E	2116	Start of profile 19, tape 111, delay 2,6s
		19:02	78°35,00'N 05°35,54'E	2006	Delay 2,4s, SP 111
		19:30	78°34,98'N 05°48,30'E	2114	Tape 112, SP 269
		19:34	78°34,97'N 05°49,96'E	2198	Delay 2,6s, SP291
		19:39	78°35,01'N 05°52,13'E	2249	Delay 2,8s, SP 321
		20:15	78°35,00'N 06°06,60'E	2185	Tape 113, SP 539
		20:19	78°35,02'N 06°07,77'E	2159	Delay 2,6s, SP 561
		20:37	78°34,99'N 06°13,40'E	2267	Delay 2,8s, SP 671
		20:52	78°35,00'N 06°19,55'E	2384	Delay 2,9s, SP 761
		21:00	78°35,03'N 06°23,45'E	2346	Tape 114, SP 807
		21:16	78°34,96'N 06°31,17'E	2462	Delay 3,0s, SP 901
		21:39	78°34,96'N 06°40,47'E	2361	Delay 2,8s, SP 1014
		21:45	78°34,95'N 06°45,43'E	2269	Tape 115, SP 1076
		21:52	78°34,98'N 06°49,26'E	2174	Delay 2,6s, SP 1121
		22:03	78°34,98'N 06°54,90'E	2002	Delay 2,4s, SP 1186
		22:12	78°34,98'N 06°59,43'E	1854	Delay 2,3s, SP 1241
		22:22	78°34,98'N 07°03,65'E	1800	Delay 2,2s, SP 1300
		22:31	78°35,01'N 07°07,83'E	1752	Tape 116, SP 1350
		22:39	78°35,01'N 07°11,36'E	1725	Delay 2,1s, SP 1400
		22:54	78°35,05'N 07°19,1'E	1643	Delay 2,0s, SP 1490
		23:11	78°35,03'N 07°26,60'E	1572	Delay 1,9s, SP 1592
		23:16	78°35,01'N 07°28,82'E	1533	Tape 116, SP 1624
		23:19	78°35,02'N 07°29,62'E	1522	Delay 1,7s, SP 1642
		23:49	78°35,00'N 07°43,53'E	1361	Delay 1,6s, SP 1821
	20.07.94	00:03	78°34,99'N 07°49,12'E		Break of recording, no signal
		00:08	78°34,99'N 07°51,75'E	1293	Tape 118, SP 1892, signal back
		00:11	78°35,01'N 07°52,90'E	1264	Delay 1,5s, SP 1906
		00:28	78°35,00'N 08°01,34'E	1203	End of profile 19, SP 2015
	20.07.94		78°40,00'N 06°49,18'E		OBH 5 deployment
			78°40,00'N 06°51,69'E		OBH 6 deployment
20	20.07.94	05:35	78°39,95'N 06°38,51'E	1629	Start of profile 20
		07:13	78°40,00'N 07°20,25'E	1277	End of profile 20, SP 588
		08:11			OBH 1 acoustical released
		08:45			OBH 1 on board
		09:03			OBH 2 acoustical released
		09:43			OBH 2 on board
21	20.07.94	12:25	78°43,33'N 07°42,86'E	1072	Start of profile21, tape 112, delay 1,2s
		13:15	78°47,65'N 07°35,31'E	1117	Delay 1,3s, SP 240
		13:21	78°48,42'N 07°34,50'E	1125	Tape 120, Sp 273
		14:06	78°52,13'N 07°27,60'E	1147	Tape 121, SP 547
		14:51	78°56,08'N 07°20,62'E	1183	Tape 122, delay 1,4s, SP 814

Table 2: List of airgun profiles including magnetic tapes and shot points

Station/ Profile No.	Date	Time UTC (h)	Geographical Position Latitude Longitude	Depth uncorr. (m)	Comments Start/End, Tape No. etc.
		15:36	79°00,00'N 07°13,35'E	1264	Tape 123, delay 1,5s, SP 1083
		16:21	79°04,28'N 07°06,00'E	1324	Tape 124, SP 1349
		16:21	79°04,28'N 07°06,00'E	1323	Delay 1,6s, SP 1350
		17:05	79°08,54'N 06°58,46'E	1359	Tape 125, SP 1618
		17:50	79°12,94'N 06°50,20'E	1357	Tape 126, SP 1888
		18:35	79°17,17'N 06°42,70'E	1355	Tape 127, SP 2157
		19:20	79°21,29'N 06°34,94'E	1388	Tape 128, SP 2425
		19:49	79°24,14'N 06°29,22'E	1451	Delay 1,7s, SP 2601
		20:05	79°25,70'N 06°27,14'E	1477	Tape 129, SP 2695
		20:13	79°26,46'N 06°25,59'E	1498	Delay 1,8s, SP 2741
		20:25	79°27,66'N 06°23,35'E	1507	End of profile 21, SP 2821
22	20.07.94	20:40	79°28,50'N 06°27,85'E	1438	Start of profile 22, tape 130, delay 1,7s
		20:57	79°28,47'N 06°36,96'E	1338	Delay 1,5s, SP 101
		21:24	79°28,49'N 06°51,15'E	1201	Delay 1,3s, SP 261
		21:26	79°28,50'N 06°52,29'E	1189	Tape 131, SP 273
		21:57	79°28,47'N 07°09,34'E	1048	Delay 1,1s, SP 461
		22:11	79°28,48'N 07°16,05'E	978	Tape 132, SP 542
		22:27	79°28,49'N 07°24,87'E	914	Delay 0,9s, SP 640
		22:56	79°28,52'N 07°39,50'E	772	Tape 133, SP 812
		23:00	79°28,50'N 07°41,50'E	752	Delay 0,7s, SP 840
		23:30	79°28,49'N 07°56,38'E	579	Delay 0,5s, SP 1016
		23:40	79°28,50'N 08°01,69'E	462	Tape 134, SP 1081
		23:48	79°28,50'N 08°05,65'E	439	Delay 0,4s, SP1125
	21.07.94	00:03	79°28,46'N 08°13,24'E	312	End of profile 22, SP 1215
23		00:20	79°27,37'N 08°17,28'E	284	Start of profile 23, tape 135, delay 0,4s
		00:32	79°26,19'N 08°18,65'E	227	Delay 0,3s, SP 76
		00:45	79°25,16'N 08°20,31'E	161	Adjustment of Echo sounder necessary, SP 152, profile delay
23a	21.07.94	01:00	79°23,76'N 08°22,33'E	200	Start of profile 23a, tape 136, delay 0,2s
		01:17	79°22,13'N 08°25,44'E	169	Delay 0,1s, SP 100
		01:34	79°20,62'N 08°28,49'E	172	Delay 0,2s, SP 200
		01:47	79°19,34'N 08°30,86'E	175	Tape 137, SP 279
		02:33	79°14,77'N 08°38,20'E	191	Tape 138, SP 554
		03:19	79°10,41'N 08°45,92'E	195	Tape 139, SP 831
		03:47	79°08,15'N 08°50,40'E	206	Tape 140, SP 1000
		04:52	79°02,27'N 09°00,71'E	184	Tape 141, SP 1390
		05:38	78°57,67'N 09°08,65'E	222	Tape 142, SP 1668
		05:44	78°57,49'N 09°08,88'E	207	End of profile 23a, SP 1700
24	21.07.94	05:54	78°56,98'N 09°06,03'E	219	Start of profile 24, tape 143,delay 0,2s
		06:39	78°56,98'N 08°41,27'E	247	Tape 144, SP 273
		07:04	78°57,00'N 08°28,25'E	544	Delay 0,5s, SP 421

Table 2: List of airgun profiles including magnetic tapes and shot points

Station/ Profile No.	Date	Time UTC (h)	Geographical Position Latitude Longitude	Depth uncorr. (m)	Comments Start/End, Tape No. etc.
		07:14	78°56,99'N 08°23,05'E	698	Delay 0,7s, SP 481
		07:24	78°57,00'N 08°18,02'E	809	Delay 0,9s, SP 541
		07:25	78°57,00'N 08°17,39'E	835	Tape 145, SP 548
		07:44	78°56,95'N 08°07,92'E	974	Delay 1,1s, SP661
		08:04	78°56,95'N 07°57,10'E	1085	Delay 1,3s, SP781
		08:10	78°56,98'N 07°53,71'E	1102	Tape 146, SP 821
		08:55	78°56,97'N 07°30,58'E	1194	Tape 147, SP 1091
		09:40	78°57,01'N 07°07,56'E	1202	Tape 148, SP 1358
		09:50	78°56,99'N 07°02,75'E	1248	Delay 1,5s, SP 1422
		10:20	78°56,95'N 06°47,46'E	1410	Delay 1,7s, SP 1600
		10:25	78°56,99'N 06°44,28'E	1438	Tape 149, SP 1631
		10:37	78°56,95'N 06°39,10'E	1483	End of profile 24, SP 1700
	21.07.94	14:55	78°45,00'N 07°37,00'E	1097	OBH 7 deployment
		15:59	78°45,03'N 07°39,03'E	1087	OBH 8 deployment
25		16:44	78°45,02'N 07°18,43'E	1227	Start of profile 25
		18:02	78°45,02'N 07°54,97'E	1006	End of profile 25
	21.07.94	18:54			OBH 1 acoustical released
		19:20			OBH 1 on board
		19:34			OBH 2 acoustical released
		19:45			OBH 2 on board

Table 2: List of airgun profiles including magnetic tapes and shot points

GEOMAR REPORTS

1 GEOMAR FORSCHUNGSZENTRUM FÜR MARINE GEOWISSENSCHAFTEN DER CHRISTIAN-ALBRECHTS-UNIVERSITÄT ZU KIEL
BERICHT FÜR DIE JAHRE 1987 UND 1988. 1989. 71 + 6 pp.
In German

2 GEOMAR FORSCHUNGSZENTRUM FÜR MARINE GEOWISSENSCHAFTEN DER CHRISTIAN-ALBRECHTS-UNIVERSITÄT ZU KIEL
JAHRESBERICHT / ANNUAL REPORT 1989. 1990. 96 pp.
In German and English

3 GEOMAR FORSCHUNGSZENTRUM FÜR MARINE GEOWISSENSCHAFTEN DER CHRISTIAN-ALBRECHTS-UNIVERSITÄT ZU KIEL
JAHRESBERICHT / ANNUAL REPORT 1990. 1991. 212 pp.
In German and English

4 ROBERT F. SPIELHAGEN
DIE EISDRIFT IN DER FRAMSTRASSE WÄHREND DER LETZTEN 200.000 JAHRE. 1991. 133 pp.
In German with English summary

5 THOMAS C. W. WOLF
PALÄO-OZEANOGRAPHISCH-KLIMATISCHE ENTWICKLUNG DES NÖRDLICHEN NORDATLANTIKS SEIT DEM SPÄTEN NEOGEN
(ODP LEGS 105 UND 104, DSDP LEG 81). 1991. 92 pp.
In German with English summary

6 SEISMIC STUDIES OF LATERALLY HETEROGENOUS STRUCTURES - INTERPRETATION AND MODELLING OF SEISMIC DATA.
Edited by ERNST R. FLUEH
Commission on Controlled Source Seismology (CCSS), Proceedings of the 8th Workshop Meeting, held at
Kiel - Fellhorst (Germany), August 27-31, 1990. 1991. 359 pp.
In English

7 JENS MATTHIESSEN
DINOFLAGELLATEN-ZYSTEN IM SPÄTQUARTÄR DES EUROPÄISCHEN NORDMEERES: PALÖKOLOGIE UND PALÄO-OZEANOGRAPHIE. 1991. 104 pp.
In German with English summary

8 DIRK NÜRNBERG
HAUPT- UND SPURENELEMENTE IN FORAMINIFERENGEHÄUSEN - HINWEISE AUF KLIMATISCHE UND OZEANOGRAPHISCHE ÄNDERUNGEN
IM NÖRDLICHEN NORDATLANTIK WÄHREND DES SPÄTQUARTÄRS. 1991. 117 pp.
In German with English summary

9 KLAS S. LACKSCHEWITZ
SEDIMENTATIONSPROZESSE AM AKTIVEN MITTELOZEANISCHEN KOLBEINSEY RÜCKEN (NÖRDLICH VON ISLAND). 1991. 133 pp.
In German with English summary

10 UWE PAGELS
SEDIMENTOLOGISCHE UNTERSUCHUNGEN UND BESTIMMUNG DER KARBONATLÖSUNG IN SPÄTQUARTÄREN SEDIMENTEN DES ÖSTLICHEN
ARKTISCHEN OZEANS. 1991. 106 pp.
In German with English summary

11 FS POSEIDON - EXPEDITION 175 (9.10.-1.11.1990)
175/1: OSTGRÖNLÄNDISCHER KONTINENTALRAND (65° N)
175/2: SEDIMENTATION AM KOLBEINSEYRÜCKEN (NÖRDLICH VON ISLAND)
Hrsg. von J. MIENERT und H.-J. WALLRABE-ADAMS. 1992. 56 pp. + app.
In German with some English chapters

12 GEOMAR FORSCHUNGSZENTRUM FÜR MARINE GEOWISSENSCHAFTEN DER CHRISTIAN-ALBRECHTS-UNIVERSITÄT ZU KIEL
JAHRESBERICHT / ANNUAL REPORT 1991. 1992. 152 pp.
In German and English

13 SABINE E. I. KÖHLER
SPÄTQUARTÄRE PALÄO-OZEANOGRAPHISCHE ENTWICKLUNG DES NORDPOLARMEERES UND EUROPÄISCHEN NORDMEERES ANHAND VON
SAUERSTOFF- UND KOHLENSTOFF- ISOTOTPENVERHÄLTNISSEN DER PLANKTISCHEN FORAMINIFERE
Neogloboquadrina pachyderma (sin.). 1992. 104 pp.
In German with English summary

14 FS SONNE - FAHRTBERICHT SO 78 PERUVENT: BALBOA, PANAMA - BALBOA, PANAMA, 28.2.1992-16.4.1992
Hrsg. von ERWIN SUESS. 1992. 120 pp.
In German with some English chapters

15 FOURTH INTERNATIONAL CONFERENCE ON PALEOCEANOGRAPHY (ICP IV): SHORT- AND LONG-TERM GLOBAL CHANGE:
RECORDS AND MODELLING 21-25 SEPTEMBER 1992, KIEL/GERMANY
PROGRAM & ABSTRACTS. 1992. 351 pp.
In English

16 MICHAELA KUBISCH
DIE EISDRIFT IM ARKTISCHEN OZEAN WÄHREND DER LETZTEN 250.000 JAHRE. 1992. 100 pp.
In German with English summary

17 PERSISCHER GOLF: UMWELTGEFÄHRDUNG, SCHADENSERKENNUNG, SCHADENSBEWERTUNG AM BEISPIEL DES MEERESBODENS: ERKENNEN
EINER ÖKOSYSTEMVERÄNDERUNG NACH ÖLEINTRÄGEN. Schlußbericht zu den beiden BMFT-Forschungsvorhaben 03F0055 A+B. 1993. 108 pp.
In German with English summary

18 TEKTONISCHE ENTWÄSSERUNG AN KONVERGENTEN PLATTENRÄNDERN / DEWATERING AT CONTINENTAL MARGINS.
Hrsg. von / ed. by ERWIN SUESS. 1993. 106+32+68+16+22+38+4+19 pp.
Some chapters in English, some in German

19 THOMAS DICKMANN
DAS KONZEPT DER POLARISATIONSMETHODE UND SEINE ANWENDUNGEN AUF DAS SEIMISCHE VEKTORWELLENFELD IM WEITWINKELBEREICH. 1993. 121 pp.
In German with English summary

20 GEOMAR FORSCHUNGSZENTRUM FÜR MARINE GEOWISSENSCHAFTEN DER CHRISTIAN-ALBRECHTS-UNIVERSITÄT ZU KIEL
JAHRESBERICHT / ANNUAL REPORT 1992. 1993. 139 pp.
In German and English

21 KAI UWE SCHMIDT
PALYNOMORPHE IM NEOGENEN NORDATLANTIK - HINWEISE ZUR PALÄO-OZEANOGRAPHIE UND PALÄOKLIMATOLOGIE. 1993. 104+7+41 pp.
In German with English summary

22 UWE JÜRGEN GRÜTZMACHER
DIE VERÄNDERUNGEN DER PALÄOGEOGRAPHISCHEN VERBREITUNG VON *BOLBOFORMA* - EIN BEITRAG ZUR REKONSTRUKTION UND DEFINITION VON WASSERMASSEN IM TERTIÄR.1993. 104 pp.
In German with English summary

23 RV PROFESSOR LOGACHEV - Research Cruise 09 (August 30 - September 17, 1993): SEDIMENT DISTRIBUTION ON THE REYKJANES RIDGE NEAR 59°N
Edited by H.-J. WALLRABE-ADAMS & K.S. LACKSCHEWITZ. 1993. 66+30 pp.
In English

24 ANDREAS DETTMER
DIATOMEEN-TAPHOZÖNOSEN ALS ANZEIGER PALÄO-OZEANOGRAPHISCHER ENTWICKLUNGEN IM PLIOZÄNEN UND QUARTÄREN NORDATLANTIK. 1993. 113+10+25 pp.
In German with English summary

25 GEOMAR FORSCHUNGSZENTRUM FÜR MARINE GEOWISSENSCHAFTEN DER CHRISTIAN-ALBRECHTS-UNIVERSITÄT ZU KIEL
JAHRESBERICHT / ANNUAL REPORT 1993. 1994.
In German and English

26 JÖRG BIALAS
SEISMISCHE MESSUNGEN UND WEITERE GEOPHYSIKALISCHE UNTERSUCHUNGEN AM SÜD-SHETLAND TRENCH UND IN DER BRANSFIELD STRASSE - ANTARKTISCHE HALBINSEL. 1994. 113 pp.
In German with English summary

27 JANET MARGARET SUMNER
THE TRANSPORT AND DEPOSITIONAL MECHANISM OF HIGH GRADE MIXED-MAGMA IGNIMBRITE TL, GRAN CANARIA: THE MORPHOLOGY OF A LAVA-LIKE FLOW. 1994. 224 pp.
In English with German summary

28 GEOMAR LITHOTHEK. Edited by JÜRGEN MIENERT. 1994. 12 pp + app.
In English

29 FS SONNE - FAHRTBERICHT SO 97 KODIAK-VENT: KODIAK - DUTCH HARBOR - TOKYO - SINGAPUR, 27.7. - 19.9.1994
Hrsg. von ERWIN SUESS. 1994.
Some chapters in German, some in English

30 CRUISE REPORTS:
RV LIVONIA CRUISE 92, KIEL-KIEL, 21.8.-17.9.1992: GLORIA STUDIES OF THE EAST GREENLAND CONTINENTAL MARGIN BETWEEN 70° AND 80°N
RV POSEIDON PO200/10, LISBON-BREST-BREMERHAVEN, 7.-23.8.1993: EUROPEAN NORTH ATLANTIC MARGIN: SEDIMENT PATHWAYS, PROCESSES AND FLUXES
RV AKADEMIK ALEKSANDR KARPINSKIY, KIEL-TROMSØ, 5.-25.7.1994: GAS HYDRATES ON THE NORTHERN EUROPEAN CONTINENTAL MARGIN
Edited by JÜRGEN MIENERT. 1994.
In English; report of RV AKADEMIK ALEKSANDR KARPINSKIY cruise in English and Russian

31 MARTIN WEINELT
BECKENENTWICKLUNG DES NÖRDLICHEN WIKING-GRABENS IM KÄNOZOIKUM - VERSENKUNGSGESCHICHTE, SEQUENZSTRATIGRAPHIE, SEDIMENTZUSAMMENSETZUNG. 1994. 85 pp.
In German with English summary

32 GEORG A. HEISS
CORAL REEFS IN THE RED SEA: GROWTH, PRODUCTION AND STABLE ISOTOPES. 1994. 141 pp.
In English with German summary

33 JENS A.HÖLEMANN
AKKUMULATION VON AUTOCHTHONEM UND ALLOCHTHONEM ORGANISCHEM MATERIAL IN DEN KÄNOZOISCHEN SEDIMENTEN DER NORWEGISCHEN SEE (ODP LEG 104). 1994. 78 pp.
In German with English summary

34 CHRISTIAN HASS
SEDIMENTOLOGISCHE UND MIKROPALÄONTOLOGISCHE UNTERSUCHUNGEN ZUR ENTWICKLUNG DES SKAGERRAKS (NE NORDSEE) IM SPÄTHOLOZÄN. 1994.
In German with English summary

35 BRITTA JÜNGER
TIEFENWASSERERNEUERUNG IN DER GRÖNLANDSEE WÄHREND DER LETZTEN 340.000 JAHRE.
DEEP WATER RENEWAL IN THE GREENLAND SEA DURING THE PAST 340,000 YEARS.1994. 6+109 pp.
In German with English summary

36 JÖRG KUNERT
UNTERSUCHUNGEN ZU MASSEN- UND FLUIDTRANSPORT ANHAND DER BEARBEITUNG REFLEXIONSSEISMISCHER DATEN AUS DER KODIAK-SUBDUKTIONSZONE, ALASKA. 1995. 129 pp.
In German with English summary

37 CHARLOTTE M. KRAWCZYK
DETACHMENT TECTONICS DURING CONTINENTAL RIFTING OFF THE WEST IBERIA MARGIN: SEISMIC REFLECTION AND DRILLING CONSTRAINTS. 1995. 133 pp.
In English with German summary